

# **Pipe-Jacked Tunnelling: Jacking Loads and Ground Movements**

**by**

**Mark Marshall**

*Thesis submitted for the  
degree of Doctor of Philosophy  
at the University of Oxford*

Magdalen College

Trinity Term 1998

# **Pipe-Jacked Tunnelling: Jacking Loads and Ground Movements**

**Mark Andrew Marshall**

**Magdalen College, University of Oxford**

*A thesis submitted for the Degree of Doctor of Philosophy  
Trinity Term, 1998.*

## **ABSTRACT**

The reported work constituted the third phase of a programme of research into the performance of concrete pipes during installation by the pipe-jacked tunnelling technique. This third stage was a continuation of the on-site monitoring of full-scale pipe jacks during construction. Four schemes were monitored in different ground conditions: London clay, dense fine sand below the water table, stiff glacial till and soft alluvial clay. Pipe sizes ranged from 1000mm to 1800mm internal diameter and excavation methods included hand tools, slurry machines and an open face tunnel boring machine.

The main objective was to collect information on jacking loads and stresses at the pipe-soil interface to provide a better basis for future designs. This was achieved by building twelve stress cells - capable of measuring total normal stresses, shear stresses and pore pressures - into the wall of a standard concrete jacking pipe that could be inserted anywhere in the pipe string. Jacking loads and forward movement of the pipe string were simultaneously recorded and the results were correlated against site activities, including lubrication operations, and tunnel alignment surveys.

Another objective was to monitor the ground response by measuring displacements around the tunnel and ground pressures above and perpendicular to the intended line. Ground movements were measured using conventional surveying techniques for surface settlements, and inclinometer access tubes for sub-surface deformation. On one scheme, electro-levels were employed in a near-horizontal tube to measure centre line settlement as the tunnel bore advanced. Push-in spade cells and pneumatic piezometers were installed on two schemes to measure the change in horizontal pressures with the passage of the shield.

Because of the myriad data collected, it has only been possible to present a summary of the results obtained. Jacking force records from all the monitored schemes - including the previous fieldwork stage - are presented. The pattern of jacking load build up and the magnitude of frictional resistance can differ significantly according to the type of ground and use of lubricants. Stress measurements at the pipe-soil interface show that the interaction between jacking loads, pipeline misalignment, stoppages, lubrication, excavation technique etc, is highly complex.

Ground movement measurements compared to well established empirical predictive methods show that short-term displacements are related to ground losses caused by closure of the overbreak void between shield and pipe.

## Contents

<b>ABSTRACT</b>		
Contents		i
Acknowledgements		vi
Publications		vii
Principal Symbols		viii
<b>CHAPTER 1</b>	<b>INTRODUCTION</b>	<b>1.1</b>
1.1	Pipe jacking	1.1
1.2	The research programme	1.3
1.3	Stage 3 research	1.4
<b>CHAPTER 2</b>	<b>LITERATURE REVIEW</b>	<b>2.1</b>
2.1	Introduction	2.1
2.2	Summary of related work	2.2
2.2.1	Oxford research	2.2
2.2.1.1	Stage 1	2.2
2.2.1.2	Stage 2	2.2
2.2.1.3	Stage 4	2.5
2.2.2	Pipe jacking and microtunnelling in Europe	2.6
2.2.3	Microtunnelling in the United States	2.6
2.2.4	Research in Japan	2.7
2.2.5	Pipe barrel and pipe joint behaviour	2.7
2.3	Jacking loads	2.8
2.3.1	Penetration resistance	2.8
2.3.2	Frictional resistance	2.9
2.3.3	Factors influencing jacking loads	2.10
2.3.3.1	Soil stability	2.10
2.3.3.2	Overbreak	2.12
2.3.3.3	Lubrication	2.13
2.3.3.4	Pipeline misalignment	2.15
2.3.3.5	Stoppages	2.16
2.3.4	Theoretical models	2.17
2.4	Contact stresses	2.19
2.5	Ground movements	2.20
2.6	Instrumentation and fieldwork	2.22
2.6.1	Pipe jacking instrumentation	2.22
2.6.2	Measurement of ground movements	2.22
2.6.2.1	Surface settlements	2.22
2.6.2.2	Subsurface movements	2.23
2.6.3	Execution of the fieldwork	2.24

CHAPTER 3	INSTRUMENTATION	3 1
3.1	Introduction	3.1
3 2	Pipe jacking instruments	3 1
3.2.1	Contact stress cells	3 2
3.2.1.1	Cell modification	3 2
3.2.1.2	Calibration	3 5
3 2 1.3	Installation and retrieval	3 7
3.2.2	Jacking forces	3.9
3.2.3	Instrumented pipe movement	3.11
3 2 3.1	Electromagnetic distance measurement	3.11
3.2.3.2	Linear displacement units	3.13
3.2.4	Misalignment angle	3 14
3.2.5	Joint pressures	3.15
3.2.6	Line and level	3 15
3.2.7	Data acquisition	3.15
3.3	Ground instrumentation	3 17
3 3 1	Inclinometer	3.17
3.3.2	Settlement plates	3 18
3.3 3	Electro-levels	3 18
3 3 4	Push-in pressure cells	3 21
3.3.5	Self-boring pressuremeter	3.21
CHAPTER 4	FIELDWORK	4.1
4.1	Introduction	4 1
4.2	Site selection	4.1
4.2.1	Ideal sites	4.1
4.2.2	Available sites	4.3
4 3	Scheme details	4.5
4.3.1	Scheme 6 – Fillebrook Surface Water Sewer Relief Scheme	4.6
4.3.1.1	Background	4.6
4.3.1.2	Ground conditions	4.6
4.3.1.3	Monitoring work	4.9
4.3.2	Scheme 7 – Southport Coastal Waters Interceptor Tunnel	4.13
4.3.2.1	Background	4.13
4.3.2 2	Ground conditions	4.14
4.3.2.3	Monitoring work	4.15
4.3.3	Scheme 8 – Seaham Bathing Water Scheme	4.18
4.3.3.1	Background	4.18
4 3.3.2	Ground conditions	4.18
4.3.3.3	Monitoring work	4.20
4.3.4	Scheme 9 – Thurrock Southern Trunk Sewer	4.23
4 3 4.1	Background	4.23
4.3.4.2	Ground conditions	4 24
4 3 4.3	Monitoring work	4 24
4.4	Instrumentation	4 25
4.4.1	Installation	4 25
4 4.2	Protection	4 28

4.4.3	Performance	4.29
4.4.3.1	Jacking pit	4.29
4.4.3.2	Instrumented pipe	4.31
4.4.3.3	Ground instrumentation	4.31
4.4.4	Retrieval	4.32
4.5	Data handling	4.33
<b>CHAPTER 5</b>	<b>JACKING LOADS</b>	<b>5.1</b>
5.1	Introduction	5.1
5.1.1	General information	5.1
5.1.2	Penetration resistance	5.1
5.1.3	Frictional resistance	5.1
5.2	Jacking records	5.2
5.2.1	Scheme 6	5.2
5.2.2	Scheme 7	5.3
5.2.3	Scheme 8	5.3
5.2.4	Scheme 9	5.4
5.2.5	Summary of all monitored schemes	5.4
5.3	The influence of construction-related factors	5.10
5.3.1	Lubrication	5.10
5.3.1.1	Types of lubricant	5.10
5.3.1.2	Injection arrangement	5.11
5.3.1.3	Lubricant effectiveness	5.14
5.3.1.4	Reduction in frictional resistance	5.16
5.3.1.5	Buoyancy	5.17
5.3.2	Pipeline alignment	5.17
5.3.2.1	Significance of pipeline alignment	5.17
5.3.2.2	Alignments achieved in practice	5.18
5.3.3	Stoppages	5.27
5.3.3.1	London clay	5.27
5.3.3.2	Stiff glacial clay	5.29
5.3.3.3	Soft clay	5.33
5.4	Conclusions	5.35
<b>CHAPTER 6</b>	<b>PIPE-SOIL INTERACTION</b>	<b>6.1</b>
6.1	Introduction	6.1
6.2	Interface stress records	6.1
6.2.1	Scheme 6	6.1
6.2.2	Scheme 7	6.7
6.2.3	Scheme 8	6.14
6.2.4	Scheme 9	6.19
6.2.5	Stage 2 schemes	6.25
6.3	Ground related factors	6.26
6.3.1	Cohesionless soils	6.26
6.3.2	Cohesive soils	6.30
6.4	Effects of stoppages	6.40
6.4.1	Introduction	6.40
6.4.2	London clay	6.40
6.4.3	Stiff glacial clay	6.45

6.4.4	Soft peaty clay	6.46
6.5	Misalignment effects	6.50
6.6	Lubrication effects	6.56
6.6.1	Introduction	6.56
6.6.2	Scheme 7	6.57
6.6.3	Scheme 8	6.63
6.6.4	Scheme 9	6.64
6.7	Conclusions	6.71
6.7.1	Introduction	6.71
6.7.2	Interface stress records	6.71
6.7.3	Ground related factors	6.72
6.7.4	Effects of stoppages	6.72
6.7.5	Misalignment effects	6.73
6.7.6	Lubrication effects	6.73
<b>CHAPTER 7</b>	<b>GROUND RESPONSE</b>	<b>7.1</b>
7.1	Introduction	7.1
7.2	Prediction of settlements	7.1
7.3	Field measurements	7.6
7.3.1	Pressure cell readings	7.6
7.3.2	Surface settlements	7.11
7.3.2.1	Scheme 6	7.11
7.3.2.2	Scheme 7	7.12
7.3.2.3	Scheme 8	7.13
7.3.2.4	Scheme 9	7.14
7.3.3	Subsurface movements	7.15
7.3.3.1	Scheme 6	7.15
7.3.3.2	Scheme 7	7.19
7.3.3.3	Scheme 8	7.19
7.3.3.4	Scheme 9	7.30
7.4	Conclusions	7.35
<b>CHAPTER 8</b>	<b>CONCLUSIONS AND RECOMMENDATIONS</b>	<b>8.1</b>
8.1	Fieldwork	8.1
8.2	Jacking loads	8.3
8.2.1	Face loads	8.3
8.2.2	Lubrication	8.3
8.2.3	Misalignment	8.5
8.2.4	Stoppages	8.5
8.3	Pipe-soil interaction	8.6
8.3.1	Pipe-soil contact	8.6
8.3.2	Stoppages	8.8
8.3.3	Misalignment	8.9
8.3.4	Lubrication	8.9
8.4	Ground response	8.10
8.4.1	Ground movements	8.10
8.4.2	Ground stresses	8.11
8.5	Further work	8.11
8.6	Concluding remarks	8.12

REFERENCES		R.1
APPENDIX A	Australian CPA analysis	A.1
APPENDIX B	Equipment inventory	B.1
APPENDIX C	Evaluation of joint angular deviation from line and level information	C.1
APPENDIX D	Derivation of Milligan and Norris (1998) half-wave model	D.1

## **Acknowledgements**

The author is wholly indebted to Dr George Milligan for his patience, encouragement and invaluable advice during the long, hard course of this work.

The financial and technical support of the Pipe Jacking Association, EPSRC and Northumbrian, North West, Severn Trent, Thames and Yorkshire Water Companies is gratefully acknowledged special thanks are particularly due to the members of the Pipe Jacking Research Group. The pipe manufacturers, for providing the special pipes, and the staff of the various Contractors and Engineers involved in the monitored schemes are also acknowledged for their co-operation and kind help leading into, and during the fieldwork

Mr Bob Sawala provided invaluable assistance during the manufacture of instruments and also during the fieldwork. Thanks are also due to Mr Ron Morton, electronics consultant, who helped modify and repair the data acquisition system The advice and assistance of Mr Clive Dalton and others at Cambridge Insitu Ltd was invaluable in the modification of instruments

The author is very grateful to Dr Harvey Burd and Mr Jonathan Morris for reading the manuscript and for their helpful comments.

Special thanks go to Mr Ken Hosie, Consultant Surgeon in Sheffield, for making me well after a long and debilitating illness.

I wish to express my sincere thanks to the Directors of Charles Haswell and Partners, in particular Mr Geoff Bateman, for their support and the leave of absence to complete the preparation of this thesis.

To my partner, Lynne, and our expected child – I can now look forward to devoting more of my spare time to them.



## Publications

The following conference papers have been published as a result of this research

Milligan, G.W E and Marshall, M A , (1995) *Ground movements due to construction of pipe-jacked tunnels* Proc. XIth Eur Conf. on Soil Mech. and Foundn Engng., Copenhagen

Marshall, M.A and Milligan, G.W.E , (1996). *A case study of an instrumented microtunnel in fine sand*. Proc. Int. Conf on Trenchless Technology, No-Dig '96, New Orleans

Marshall, M.A., Milligan, G W.E. and Mair R.J., (1996) *Movements and stress changes in London Clay due to the construction of a pipe jack*. Proc Int. Symp on Geotech. Aspects of Underground Construction in Soft Ground, London.

Milligan, G W E. and Marshall, M A , (1998) *The functions and effects of lubrication in pipe jacking*. Proc. Int Conf. on Tunnels and Metropolises, World Tunnel Congress, Sao Paulo.

Milligan, G W E. and Marshall, M A., (1998) *The influence of lubrication on jacking loads from six monitored pipe jacks/microtunnels*. Proc. Int. Conf on Trenchless Technology, No-Dig 98, Lausanne.

Marshall, M A and Milligan, G.W E , (1998) *Geotechnical aspects of pipe-jacked tunnelling* Proc. Int Conf on Urban Ground Engng., Hong Kong.

## Principal Symbols

$b$	Contact width between pipe and ground
$D_e$	Diameter of excavation
$D_p$	External diameter of pipe
$d$	Internal diameter of pipe
$E_p$	Elastic modulus of pipe
$E_s$	Elastic modulus of soil
$F$	Frictional resistance
$H$	Ground cover
$i$	Trough width parameter
$k$	Lateral earth pressure coefficient
$K_0$	Coefficient of earth pressure at rest
$K_a$	Coefficient of active earth pressure
$K_p$	Coefficient of passive earth pressure
$L$	Length of pipe
$P$	Unsupported length of excavation
$P_u$	Contact force per unit length
$p$	Internal support pressure (bentonite pressure)
$R$	External radius of pipe
$r$	Internal radius of pipe
$S$	Surface settlement
$s_u$	Undrained shear strength
$S_{max}$	Maximum surface settlement
$T_c$	Stability ratio (cohesive soils)
$T_s$	Stability number (cohesionless soils)
$T_\gamma$	Stability number (cohesionless soils)
$V$	Transverse distance from centre line
$V_s$	Settlement volume
$W$	Unit weight of pipe
$z$	Depth of tunnel axis
$\alpha s_u$	Adhesion between pipe and clay

$\beta$	Angular deflection at pipe joints
$\gamma$	Unit weight of soil
$\gamma_s$	Saturated weight of soil
$\gamma_w$	Unit weight of water
$\delta$	Angle of friction (total stress)
$\delta'$	Angle of friction (effective stress)
$\delta_h$	Reduction in horizontal diameter
$\theta$	Angle
$\sigma$	Total radial stress
$\sigma'$	Effective radial stress
$\sigma_h$	Total horizontal stress
$\sigma_r$	Radial stress at tunnel surface
$\sigma_s$	Surcharge pressure
$\sigma_T$	Pressure required for face stability (cohesive soils)
$\sigma_v$	Total vertical stress
$\sigma_{\max}$	Maximum circumferential stress
$\sigma'_h$	Effective horizontal stress
$\sigma'_v$	Effective vertical stress
$\tau$	Shear stress
$\phi$	Undrained friction angle of soil
$\phi'$	Drained friction angle of soil

---

## chapter one

---

### introduction

#### 1.1 PIPE JACKING

Pipe jacking is the name given to a technique used to form man-entry size diameter tunnels by pushing a 'string' of pipes through the ground from a thrust (or jacking) pit to a receiving pit. Man-entry diameters vary between countries but 900mm is widely accepted as the lower limit; diameters less than 900mm are generally categorised as microtunnels. Hydraulic rams in the thrust pit jack the pipes forward as the ground in front of the pipeline is mined, Figure 1.1. Methods of excavation can range from hand digging within a simple shield, Figure 1.2, to highly sophisticated machinery as illustrated in Figure 1.3. Like conventional tunnelling, slurry pressure machines or earth pressure balance machines can be used in poor ground to support the tunnel face. The external diameter of a cutting shield will conform closely to the size of the jacking pipe reducing the annular space, or overbreak, to a minimum (typically less than 20mm on the diameter). This overbreak can be filled with pressurised lubricant to support the ground and reduce frictional resistance.

Thompson (1993) reports some of the earliest concrete pipe jacks as being carried out in the United States and Europe in the 1930s. In Japan, a market leader in developing microtunnelling technology, concrete pipes were first jacked in the late 1950s. When first introduced the technique was seen principally as a method for short straight crossings (through soft ground or weak rock) of roads, railways and waterways. Advances in operative skills and jacking equipment, gained more from experience than scientific understanding, saw pipe jacking increasingly being used for many sewer installations by the 1980s. Longer drives, greater depths and unstable ground conditions prompted mechanical developments in equipment for excavation and spoil removal and improvements in surveying equipment for alignment control.

The many developments in pipe jacking in recent years include the injection of bentonite or similar grouts into the overbreak to decrease skin friction; the use of intermediate jacking stations (Figure 1.4) to reduce jacking loads; and pipe joints with increased bearing areas to reduce joint stresses. Although the method is now acceptable to many engineers, in the 1980s some specifying authorities had little

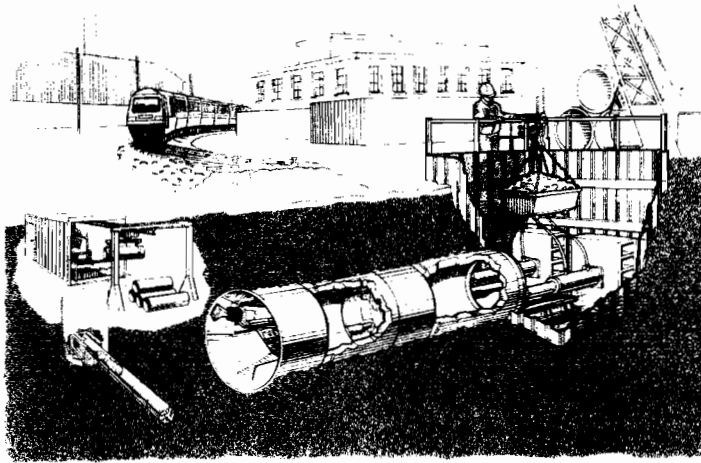


**Figure 1.1** Typical arrangement of pipe jacking and microtunnelling equipment (courtesy the PJA).

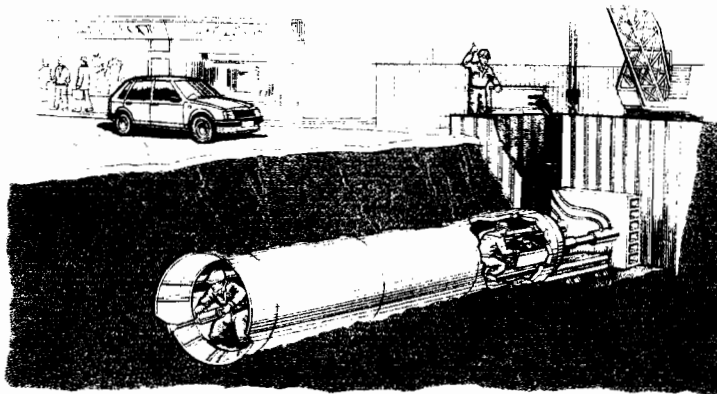


**Figure 1.2** Hand excavation within a simple shield (courtesy the PJA).

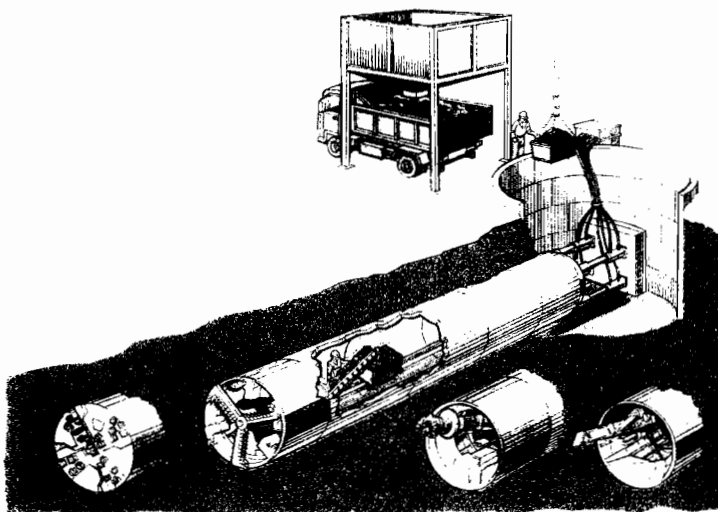


**Figure 1.3** Typical mechanised excavation methods (courtesy the PJA).

confidence in the technique due to some unexpected failures (Shullock, 1982) and the high cost and difficulty of the remedial work. It became evident that there was a need for research into the technique and a programme in the U K. was initiated

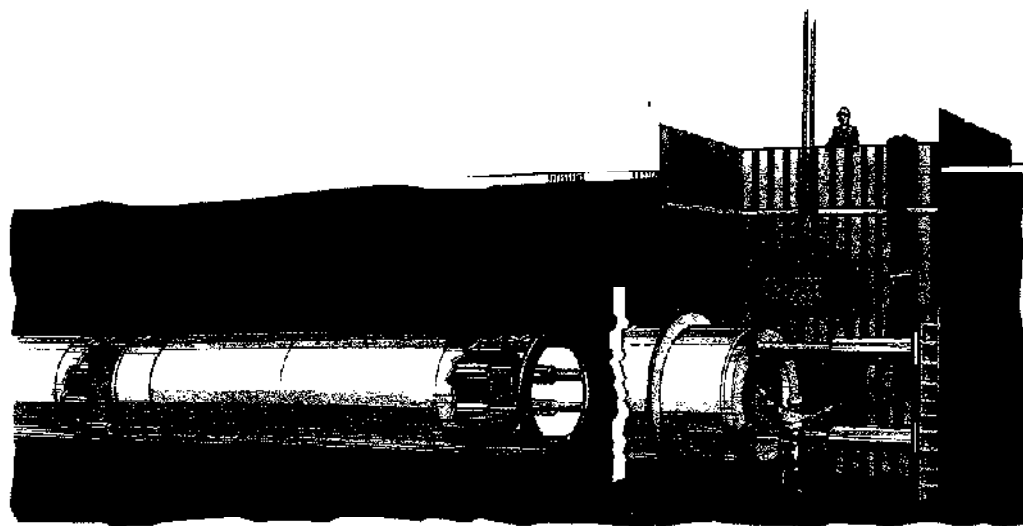


**Figure 1.4 Intermediate jacking stations (courtesy the PJA).**

## **1.2 THE RESEARCH PROGRAMME**

The research programme into pipe jacking at Oxford University has now been in progress since 1986. It was prompted by the Pipe Jacking Association (PJA) and the Construction Industry Research and Information Association (CIRIA) with a review of procedures published as 'Pipe Jacking, a State of the Art Review', Craig (1983). The overall objectives of the research follow the recommendations listed in the report by Craig (loc cit):

- i) prediction of frictional resistance in different ground conditions,
- ii) load/deflection characteristics of different joint packing materials,
- iii) the effect of cyclic loading on pipes at intermediate jacking stations;
- iv) the effect of lubrication in reducing frictional resistance,
- v) the development of a site investigation test to better predict frictional forces.

The measurement and prediction of ground movements associated with pipe jacking has been added to the list of objectives

Stage 1 of the research project, from 1986 to 1989, was laboratory based and involved the testing of model concrete pipes with different joint packing materials,

Ripley (1989) The main findings from Stage 1 were that steel-banded butt joints are superior to in-wall spigot and socket joints for transmitting jacking loads, and that medium density fibreboard was the most suitable joint packing material. Stage 2, from 1989 to 1992, involved the monitoring of actual pipe jacks in different ground conditions by incorporating a specially-instrumented pipe in the pipe string on five schemes, (Norris 1992b) – results from this second stage of work are summarised by Milligan and Norris (1994).

This thesis reports the third stage, which also involved the monitoring of full-scale pipe jacks but with a different emphasis to the previous phase. The structural performance of pipes and pipe joints during jacking is now, as a result of Stage 2 research, reasonably well understood. However, after Stage 2 there remained considerable uncertainties regarding pipe-soil interface stresses in some ground conditions and the effects of pipeline misalignments on these stresses. The special instrumented pipe in this reported stage contained a greater number of instruments so that more information could be gathered on the distribution of interface stresses along and around the pipe. Measurements were also made of the ground response, movements and stresses, in the different ground conditions of Stage 3 schemes. The two fieldwork phases have been supported by the PJA, the Engineering and Physical Sciences Research Council<sup>1</sup> (EPSRC), and five U.K. water utility companies (North West Water, Northumbrian Water, Severn Trent Water, Thames Water and Yorkshire Water).

Running concurrently with this reported phase was Stage 4, a numerical modelling based exercise, supported by EPSRC, to model variations in concrete pipe joint design. The most promising modifications were constructed in model concrete pipes and tested in a simplified form in the laboratory, Zhou (1998).

### **1.3 STAGE 3 RESEARCH**

In site selection for Stage 3 research, differing ground conditions were required with particular emphasis being placed on a scheme in London clay, as only limited data were obtained from such conditions in Stage 2, and in soft clay, as no such scheme had yet been monitored. The monitoring of five schemes was planned,

---

<sup>1</sup> Previously named the Science and Engineering Research Council or SERC

but construction of the proposed final scheme was delayed and as a consequence could not be included within the fieldwork programme. The five sites monitored during Stage 2 will throughout this thesis be referred to as Schemes 1 to 5 and for consistency and for clarity, Stage 3 schemes will follow the sequential numbering as Schemes 6 to 9

The progress of Stage 3 research is presented in Figure 1.5. The design of modifications to instrumentation and the data acquisition system, instrument manufacture and calibration procedures took up the first year. The next year and three months saw the fieldwork on four schemes carried out. Progress of the pipe jack on Scheme 8 was slow due to unavoidable tunnelling delays and the planned monitoring period of one month took about seventeen weeks. The three-year project period was extended by six months to try and monitor a proposed Scheme 10, but the start date was set back even beyond the extended period. The author was unable to complete analysis and writing up within the forty-two month contract period. During the fieldwork a two-second logging rate produced an enormous amount of data – approximately three million data points. This created many problems in handling data, computing, data processing and detailed analysis and has been a contributory factor in the protracted writing of this thesis. With hindsight, a slower sampling rate should have been adopted to restrict data to an amount that could have been reasonably handled by one person.

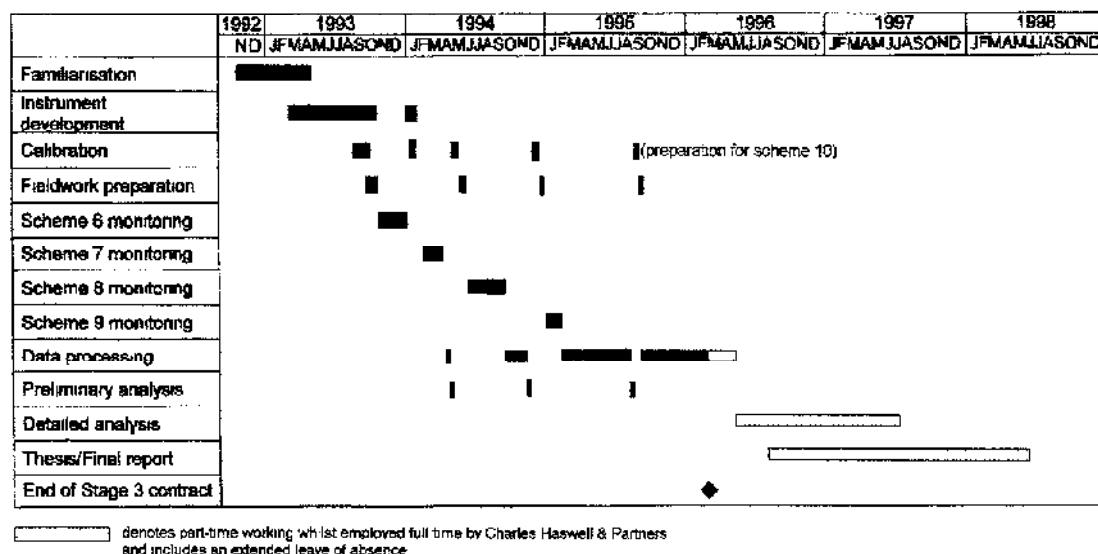


Figure 1.5 Stage 3 research programme.



The total budget for Stage 3 research was approximately £300,000, provided by the EPSRC, the PJA and the five sponsoring water utility companies. Additional fieldwork costs amounting to about £15,000 per scheme (for the manufacture of a special pipe for incorporation of instruments, a liner to protect the instrumentation, any loss of production due to the research and instrument retrieval) were carried mainly by the water companies. Work was completed within the allowed budget despite the special conditions associated with site-based research. The work was overseen and guided by a management group, the membership of which is given in Table 1.1. The research team met and reported to this group four times a year. Research funds were managed through a special account with the PJA, except the EPSRC contribution that was managed directly through the University to support the author.

<b>Institution</b>	<b>Representative</b>
Pipe Jacking Association	A. Moss J Marshall* / P Jacques (A. Marshall)
North West Water	P Moore* / B Cox
Northumbrian Water	T. Thomson* / E Styan
Severn Trent Water	R. Farley* / G Bateman
Thames Water	P. Homersham
Yorkshire Water	P. Freckleton
Oxford University	G Milligan

\* denotes replacement during contract period.

**Table 1.1 Composition of the management group.**

This thesis for Stage 3 research contains seven further chapters. Aspects of the pipe jacking technique are discussed in Chapter 2. A comprehensive review of results from Stages 1, 2 and 4 is presented before summarising other recent site-based research in the United States, Europe and Japan.

Chapter 3 provides a description of all instrumentation, comprising pipe jacking and geotechnical instruments, and also includes some modifications and an instrument that could not be fulfilled for use in the field. Chapter 4 describes the site

selection procedures and provides scheme details for the fieldwork element of the research.

The main results of Stage 3 work are presented in Chapters 5 to 7 – Chapters 5 and 6 also include some data from Stage 2 schemes (after Norris 1992b). Only a fraction of the many data collected during Stage 3 monitoring can be included in the thesis and the author has endeavoured to present representative samples. Chapter 5 is concerned with jacking loads and the influence of stoppages, bentonite lubrication and pipeline misalignment are considered in relation to the ground conditions. Local pipe-soil interface stress measurements are included as Chapter 6, which also considers the affects of the above construction-related factors.

The resulting ground response due to pipe jacking operations at the reported four schemes is the subject of Chapter 7 and includes stress changes and ground movements. Measured surface settlements are presented and compared to predicted settlement profiles. Subsurface displacements close to the tunnels are evaluated and detailed measurements from a series of electro-levels show the development of a subsurface longitudinal settlement profile just above a tunnel in stiff glacial clay.

Conclusions drawn from the fieldwork are included in Chapter 8 together with recommendations for future research.

## chapter two

---

### literature review

#### 2.1 INTRODUCTION

The pipe jacking technique for installing monolithic tubes as a tunnel lining had its earliest recorded use in the United States at the turn of the century, Loving (1938). Its early use was predominantly for rail crossings that would otherwise have been completed by more traditional methods of open-cut trench or tunnel by heading. Thompson (1993) provides a general historical perspective on the use and technological development of the technique to the present day.

Pipe jacking is now used for many small diameter tunnels, typically 900mm to 3000mm internal diameters, in soft ground and rock. Some authors, particularly in the United States, prefer to distinguish between pipe jacking and microtunnelling according to the excavation technique, where pipe jacking involves manual or mechanical excavation by operators at the face and microtunnelling is remotely controlled from the surface (Chapman, 1996).

Pipe jacking applications include short crossings, multiple sewer lengths and primary linings that can be economically adapted to smaller diameters (by re-inverting) or used for the accommodation of public utility pipes and cables. Many, including the American Concrete Pipe Association (1960), Clarkson and Thompson (1983), the Pipe Jacking Association (1995a), and Thompson (loc cit) describe the principles of the technique. The U.K. Pipe Jacking Association (PJA) provide notes on the benefits of pipe jacking, its applications, design examples (Pipe Jacking Association, loc cit and 1995b), and also summarise results and recommendations from the Oxford research Stages 1 and 2 (Milligan and Norris, 1994).

Published books on pipe jacking and microtunnelling include Stein et al (1989) and Thompson (loc cit). The former presents a comprehensive source of technical information on many aspects of microtunnelling, also applicable to pipe jacking, whilst the latter provides a review of the technique and its applications and summarises results from some of the previous research.

## 2.2 SUMMARY OF RELATED WORK

### 2.2.1 Oxford Research

#### 2.2.1.1 Stage 1

Pipe jacking research, prior to the work reported here, includes Stages 1 and 2 at Oxford University. The laboratory research of Stage 1, Ripley (1989) and Milligan and Ripley (1989), investigated concrete pipe behaviour during installation and the use of packing materials in pipe joints. Microconcrete model pipes were used to primarily study the distribution of stress concentrations between misaligned pipes and the ability of different wood based packing materials to reduce these concentrations. The main results from this work suggested that:

- Thick packing materials are most beneficial.
- Misalignment angles greater than  $0.2^\circ$  combined with high axial loads are to be avoided.
- Wet packing materials improve load transfer capabilities by up to three times
- Cyclic loading conditions need to be considered due to permanent compression of packing material.
- Of the materials tested, 18mm thick medium density fibreboard gives the greatest capacity for transmitting jacking loads and for distributing concentrations of stress.

Ripley's work improved the understanding of concrete jacking pipe behaviour by identifying the main pipe failure modes; it also confirmed the superiority of butt to in-wall joints for jacking pipes. The work was not however able to progress the understanding of the interaction between pipes and ground.

#### 2.2.1.2 Stage 2

The first phase of monitoring the performance of full-scale pipe jacks has been termed Stage 2 and is described in detail by Norris (1992b). The total budget of about £220,000 was divided between the SERC, the PJA and the five water companies listed earlier in Section 1.2. Work was completed within budget and within the programmed three and a half years. Details of the five schemes monitored are presented in Table 2.1 and the instrumentation is illustrated in Figure 2.1. On completion of the fieldwork most instruments were in working order and were to be used, some in a modified

form, during Stage 3 research. Design of the instrumentation and data acquisition systems are described in Norris and Milligan (1991) and Norris (1992a).

Scheme No	1	2	3	4	5
Location	Bolton, Lancs.	Gateshead, Tyneside	Honor Oak, SE London	Chorley, Lancs	Cheltenham, Glos
Date	August 1990	January 1991	March 1991	July 1991	December 1991
Ground Type	Stiff glacial clay	Weathered mudstone	London clay	Dense silty sand	Sand and gravel
Pipe size (I/D mm)	1200	1350	1800	1500	1200
Depth (m)	1.3 – 1.5	7 – 11	11 – 21	7 – 10	4 – 7
Length (m)	60	110*	78	158	384
Excavation	Hand	Hand	Hand	Hand	Slurry TBM
Client	North West Water	Northumbria Water	Thames Water	North West Water	Severn Trent Water
Contractor	Laserbore	DCT	Barhale	Barhale	Lilley
Pipe Supplier	Buchan	ARC	Buchan	Spun Conc	Spun Conc

\* denotes monitoring for only part of drive

**Table 2.1 Details of Stage 2 schemes.**

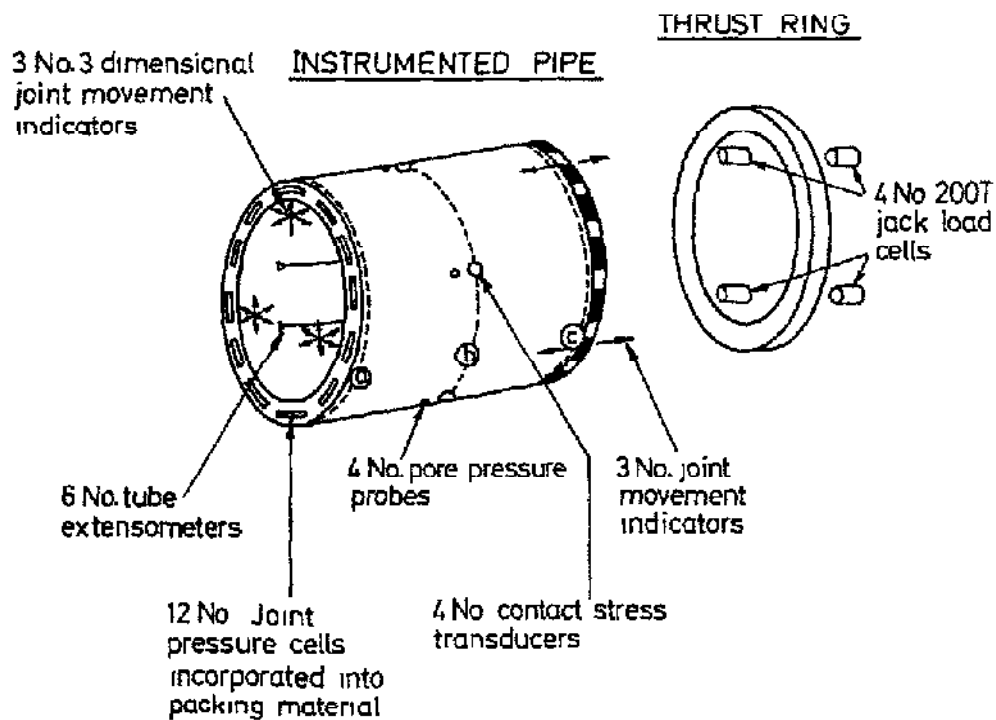


**Figure 2.1 Schematic of Stage 2 instrumentation (after Norris, 1992a).**

At the five monitored schemes, pipe internal diameters ranged from 1200 to 1800mm with cover depths from 1.5 to 21m. Ground conditions included a wide range from highly plastic London clay to sand and gravel. The first four schemes were relatively short hand-excavated drives; Schemes 1 to 3 were unlubricated while at Scheme 4 lubrication was used only during the later stages. The final scheme was a longer slurry machine drive that was lubricated throughout. The instrumented pipe allowed measurement of contact stresses between pipe and ground, pipe joint stresses and pipe and joint compressions. Jacking loads and movement of the pipe string were also measured and all the results were correlated against a detailed log of all site activities and tunnel alignment records.

Measurements of angular deviation at the pipe ends coupled with pipe barrel strains (measured by tube extensometers) and joint pressure cell measurements allowed load-paths through the instrumented pipe to be determined, Norris (1992b) and Norris and Milligan (1992a). Load-paths varied from acting along one edge of the pipe (edge loading) to acting diagonally from top to bottom or side to side (diagonal loading) over the pipe length. On all five schemes the pipe strains were always within the elastic range for the concrete and no cracking was observed in the pipes. It was concluded therefore that the pipe barrels could be designed as stocky columns for the full range of possible loads.

Pressure cells in the pipe joint measured high stress concentrations for joint misalignment angles as small as  $0.3^\circ$ . The Australian Concrete Pipe Association's design approach (Appendix A) was found to give reasonable predictions of the measured stress concentrations, provided an appropriate value was used for the packing material stiffness. Using this approach Norris (1992b) produced design curves giving allowable jacking loads on pipes for increasing joint misalignment angles with different packing material types, widths and thicknesses. The work has shown that, even if relatively high local stresses are allowed in the concrete pipes, allowable jacking loads are severely curtailed at a joint angle of  $0.5^\circ$ , and that considerable benefits are obtained by using thicker and softer packers.

The state-of-the-art work completed by Norris (*loc cit*) considerably advanced the understanding of the behaviour of concrete jacking pipes and their joints under loading in actual pipe jack conditions. Other advances from his work included:

developments in field instrumentation and a demonstration that major monitoring exercises can be carried out during pipe jacking with little disruption to construction operations. The elaborate arrangement of instrumentation allowed the simultaneous measurement of jacking loads and interface stresses to be related to time, distance and misalignment. With regard to the measurement of pipe-soil interface stresses however, the use of instruments separately recording pore pressures and radial stresses created difficulties, due to the rapid variation of stresses during pushing, in interpreting effective stresses. Further research required instrument modifications to merge these two cell types.

Elements of the Stage 2 research that required further investigation were identified as the effects on total jacking loads and interface stresses of stoppages, lubrication and misaligned bores. A greater number of contact stress cells, modified to include pore pressure measurement, was needed to examine the variation in contact stresses along and around jacking pipes.

#### 2.2.1.3 Stage 4

The fourth stage of the research programme ran concurrently with Stage 3 and involved the use of finite element modelling to analyse jacking pipe joints incorporating compressible packing material, Zhou (1998). Initial analyses investigated stress concentrations in pipe joints and demonstrated the importance of using packing material with low Poisson's ratio. The numerical modelling was then extended to investigate stress distributions in misaligned pipes, first in air then in soil, under edge and diagonal loading conditions. Results from the numerical model compared sufficiently well with data from earlier model tests and field measurements (from Stage 2) to give confidence that it could be used to study deformations and detailed stress distributions in concrete jacking pipes.

The analytical work and earlier experimental work in Stage 1 had suggested that minor changes to the pipe joints may allow increased jacking loads while reducing the likelihood of damage. Small-scale model pipes with modified pipe joints were tested under uniform and non-uniform end loading conditions, Zhou (loc cit). The results from these experiments were sufficiently promising that a further one-year

project was carried out investigating new ideas to improve the structural performance of pipe joints, Holt et al (1997)

### **2.2.2 Pipe Jacking and Microtunnelling in Europe**

In the U.K. a laboratory based study concerned with ground behaviour associated with trenchless operations, including pipe jacking and microtunnelling, has been carried out at Loughborough University, Chapman (1993). In a project at City University, the response of the ground to the installation of a full-scale pipe jack was monitored in the field and is reported by De Moor and Taylor (1989). Some results from these projects are discussed in Section 2.5.

Ground movements, jacking loads and tunnel alignments have been measured, generally by contractor or client, on several pipe jacks and microtunnels in the UK. Case histories include Rogers et al (1989) and Atkin (1993)

Research into microtunnelling in Germany has been summarised in the English language by Stein et al (loc cit). In France, seven full-scale microtunnels were monitored at five different sites as part of the national French 'Microtunnels' project to provide data on jacking forces and pipe friction (Kastner et al, 1996).

Any results from the European research that are relevant to this thesis are discussed below.

### **2.2.3 Microtunnelling in the United States**

In the United States there is a microtunnelling test programme underway at the U.S. Army Waterways Experiment Station (WES). Microtunnelling tests were performed during September and October 1992 (Bennett and Taylor, 1993). The research involved microtunnelling through a specially constructed test bed, 4m deep, comprising six different types of soil. The 'man-made' ground profile includes compacted layers of silty clay, dry sand, highly plastic clay, wet sand, clay gravel and silt. The test facility was heavily instrumented with inclinometer tubes (vertical and horizontal), settlements plates and surface survey points to evaluate ground movements. Jacking loads, cutterhead torque and jacking pipe strains were also measured. Some problems were encountered during the tests and few data have been published to date.



One element of the project, for which some results have been published, was a 600mm diameter microtunnel test using a slurry machine, Bennett et al (1994) Ground movement results are reported as being less than 6mm at all levels but the authors do not indicate how these measurements compare to predictions. After a 3 day shutdown during the test, jacking loads increased by over 70% and the pipe string could not be moved. An investigation trench revealed clay being in intimate contact with the pipes. lubricant had not been used during the test. To allow the test to proceed, portions of the test bed were excavated to reduce soil resistance loads. In all, following the shutdown, eight failure incidents are reported to have occurred including damage to thirteen jacking pipes. Evaluation of the many data collected and of the failure incidents continued but conclusions have not yet been published.

Coller et al (1996) present jacking loads measured on seven full-scale pipe jacks installed at various locations in the United States. The factors affecting jacking forces are identified and explored and lead the authors to draw conclusions and make general recommendations on lubrication, the overbreak and misalignment.

#### **2.2.4 Research in Japan**

The first instance of pipe jacking/microtunnelling in Japan was in 1948 when a 600mm diameter cast iron pipe was installed to carry a gas pipeline under a railway. Strict restrictions imposed on occupying road space have resulted in the technique becoming very popular there. Technological advances have been considerable but publications in the English language are few. Kanari et al (1996) report recent research in developing 'stress absorbers', packing material in pipe joints, to prevent concentration of stresses when jacking around large radius curves.

#### **2.2.5 Pipe Barrel and Pipe Joint Behaviour**

A discussion on pipe barrel and pipe joint behaviour has been deliberately omitted from this thesis since they are not major issues in Stage 3 research. These topics are discussed in detail by authors including Ripley (1989), Norris (1992b) and Zhou (1998).

## 2.3 JACKING LOADS

The total jacking load is the force required to overcome frictional resistance of the pipe string and face resistance at the shield. Accurate prediction is important to the design of the jacking pit and thrust wall; selection of jacking equipment (jacking frame and main rams) and jacking pipe wall thickness; the need for and placement of intermediate jacking stations; and lubrication requirements.

### 2.3.1 Penetration Resistance

Penetration or face resistance opposes the advance of the shield and varies according to its shape and boring action. For open face operations (hand excavation and auger or cutter heads) the resisting force is primarily related to the diameter of the cutting edge of the shield. Cutting edge resistance has been extensively researched in Germany and is summarised by Stein et al (loc cit) who also provide various methods for calculating the resistance. In slurry tunnelling operations, the penetration resistance mainly comprises boring head contact pressure and the supporting hydraulic pressure. To avoid settlement or heave of the ground the boring head contact pressure should be equal to the lateral earth pressure at rest; hydraulic pressure should be set to match the hydrostatic pressure of the groundwater. Stein et al (loc cit) also provides methods for determining the face resistance in slurry pressure balance operations.

The penetration resistance component of total jacking loads has not yet been explicitly measured as part of the Oxford fieldwork monitoring. On jacking records, as measured by load cells on the main jack rams, the intercept at zero length is assumed to represent a constant face resistance whereas in practice the resistance would probably vary throughout the drive. Using this assumption the face loads from Stage 2 pipe jacks were found to vary between 100 and 1200kN. The larger face resistances were recorded for the slurry machine and when the shield was used to trim the excavation in strong cohesive soil. The smaller values occurred in stable cohesive soils where the face was excavated by hand to the full diameter of the shield.

Norris (1992b), during Stage 2 fieldwork, only managed to monitor one mechanised pipe jack at Scheme 5. As hand-excavated pipe jacks are becoming few, further fieldwork monitoring of mechanised drives was required.

### 2.3.2 Frictional Resistance

Frictional resistance results from the integration of skin friction acting on areas of the external surface of pipe string and shield. This thesis is concerned only with friction on concrete pipes and the factors influencing that resistance. In the U.K., the mean interface shear stresses assembled by Craig (1983), Table 2.2, have typically been used to predict jacking forces, the experience of German practice (Stein et al, loc cit) is also reproduced in the table. The authors fail to provide any detail on how the interface shear stresses have been arrived at. Craig (loc cit) only states that the information was obtained from representatives from all sides of the industry. It is suggested that the quoted values are based on stabilised jacking loads read from crude instrumentation on jacking rigs the accuracy of which may have been questionable.

The values contained in Table 2.2 are of too broad a range to be of practical use and should not be used with any degree of confidence for design purposes. Also, frictional resistance should be quoted in terms of force per metre because mean shear stress implies uniform contact around the pipeline and contact stress data from Stage 2 research generally show non-uniform contact around the instrumented pipe.

Ground Type	Mean interface shear stress (kPa)			
	U.K. (Craig, 1983)	Germany (Stein et al, 1989)	France (Craig, 1983)	Australia (Craig, 1983)
Rock	2 – 3			1
Boulder clay	5 – 18	3 – 18		
Firm clay	5 – 20	5 – 9	8 – 10	5 – 8
Wet sand	10 – 15	2 – 16		13
Silt	5 – 20	5 – 9	17	
Dry dense sand		1 – 7		
Dry loose sand	25 – 45		20 – 30	
Fill	up to 45			
Dense gravel		2 – 6	50	

**Table 2.2 Typical values of mean interface shear stresses.**

The principal parameters identified as affecting frictional resistance may be categorised as site-related and construction-related.

Forces determined by site conditions include:

- Surcharge load and transient live loading
- Type of ground and variation along the pipeline
- Primary load from the ground
- Position of the water table
- Stability of the soil

Construction-related factors include:

- Amount of overbreak during excavation
- Use of lubricant in the overbreak void
- Use of intermediate jacking stations
- Pipeline misalignment
- Frequency and duration of stoppages

More field-based research was required to further investigate all of the above parameters.

### 2.3.3 Factors Influencing Jacking Loads

#### 2.3.3.1 Soil stability

The ability of the soil to support itself is an important factor in frictional resistance. If a soil collapses onto the pipe string, friction loads will increase and could result in failure of the pipe jack. For tunnels in cohesionless soils without surcharge loading, the required support pressure is given by

$$\sigma_T = \gamma D T_\gamma \quad (2.1)$$

(Davies et al, 1980 and Atkinson and Mair, 1981) where  $T_\gamma$  is the stability number given in Figure 2.2 and is only a function of the angle of friction for the soil,  $\phi'$ . If the tunnel is at shallow depth and a large surcharge  $\sigma_s$  acts on the surface, the weight of soil may be neglected and

$$\sigma_T = \sigma_s T_s \quad (2.2)$$

where the stability number  $T_s$  is given in Figure 2.3. Both solutions apply to dry soil, if water pressure is present it is added to  $\sigma_T$  and the buoyant weight,  $(\gamma - \gamma_w)$ , should be used in Equation 2.1 for soil below the water table

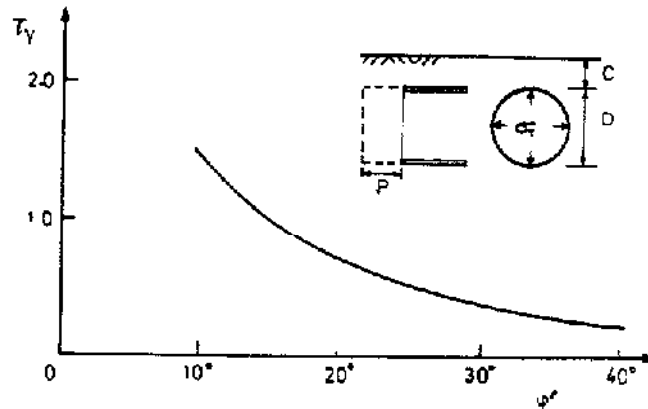


**Figure 2.2 Relationship between tunnel stability number  $T_\gamma$  and drained angle of internal friction  $\phi'$  – without surcharge (after Atkinson and Mair, 1981).**

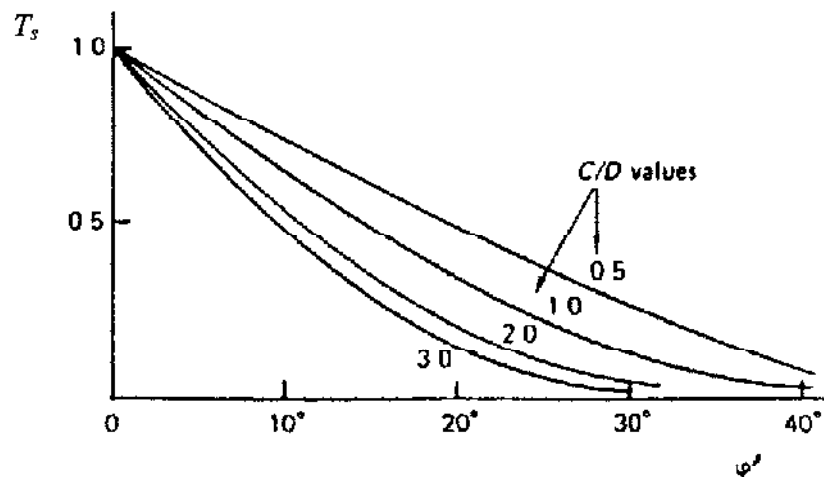


**Figure 2.3 Relationship between tunnel stability number  $T_s$  and drained angle of internal friction  $\phi'$  – shallow depth with surcharge**

In cohesive soils, the support pressure required to maintain stability of the tunnel face is given by

$$\sigma_T > \gamma(C + D/2) - T_c s_u \quad (2.3)$$

where the stability ratio  $T_c$  is given in Figure 2.4 (Atkinson and Mair, loc cit). In pipe jacking the unsupported length  $P$  is usually small or zero, and  $P/D = 0$ .

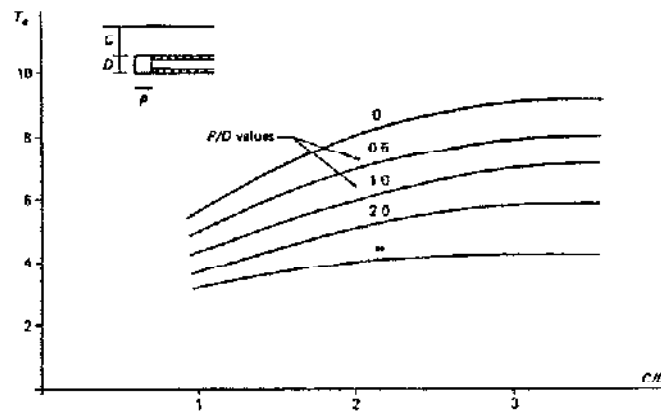


**Figure 2.4** Face stability ratio in cohesive soils (after Atkinson and Mair, 1981).

For stability of an excavated bore behind the shield in cohesive soil, the conditions correspond to the case in Figure 2.4 of  $P/D \rightarrow \infty$  and by re-arranging Equation 2.3, the support pressure to prevent collapse is given by

$$\frac{\sigma_T}{s_u} = \frac{\gamma D}{s_u} (C/D + 0.5) - T_c \quad (2.4)$$

### 2.3.3.2 Overbreak

The overbreak is the annular gap between excavated tunnel bore and the outer pipe wall and is typically 10-15mm on radius. The overbreak ratio is given by

$$R = \frac{D_e - D_p}{D_p} \quad (2.5)$$

where  $D_e$  is the excavated bore diameter and  $D_p$  is the pipe diameter

In experimental pipe jacks in sand at Loughborough University, Chapman (loc cit) reports significant draw-along of soil at the pipe-soil interface. Rogers and Yonan (1992) suggest a minimum overbreak of 10mm to minimise friction caused by the draw along effect in granular soils. The tests at Loughborough used 200mm diameter

pipes installed in dry sands with overbreak ratios varying between 0 and 0.14. The optimum overbreak ratio was found to be 0.04, which equates to a relatively large 20mm overbreak (on radius) on a 1.0m diameter pipe. Forces were reported as remaining low as the ratio was increased, but increased significantly as the ratio reduced to zero.

### 2.3 3.3 Lubrication

The use of bentonite suspensions as lubricants in pipe jacking is now common practice. Lubrication can only work effectively if a discrete layer of the lubricant is maintained between the sliding surfaces of the pipe and the excavated soil surface. If the ground collapses onto the pipe, the effect of lubrication will be greatly reduced. The first and most important function of bentonite suspensions or other lubricant is therefore to provide sufficient internal pressure to stabilise the tunnel bore. The slurry must be designed to form a filter cake in the surrounding soil without excessive bleeding of material and be pressurised to the necessary level to overcome ground water pressures and stabilise the tunnel bore; it must fill the complete overbreak void before this can be achieved. Filling the overbreak to maintain the bore is also assumed to minimise settlement in the short-term and possibly in the long-term also.

Bentonite – natural clay minerals – and water are mixed in colloidal type grout mixers at the jacking pit area and ideally are left to swell for several hours before use. The ready suspension is then pumped into the overbreak void through a temporary pipe system connected to injection sockets cast into the pipes. The arrangement and distribution of injection sockets has often been a matter of experience but should be designed to ensure an even distribution of suspension around the pipe string. If a continuous layer of lubricant suspension can be formed, the pipes could theoretically become buoyant. Some authors including Haslem (1986) and Stein et al (1989) have indicated that pipes may become buoyant in ideal conditions, but have been unable to substantiate the suggestion. Norris (1992b) was probably the first to demonstrate pipe buoyancy occurring in practice from the field measurements of Scheme 5.

Bentonite suspensions have thixotropic properties – temporarily liquid when agitated but of a gel consistency when at rest. In cohesionless soils excess fluid

pressures are expected to form in the suspension and the dissipation will be restricted by the thixotropy of the material (Thompson, 1993).

Stein et al (loc cit) lists the factors influencing the effectiveness of bentonite suspensions as:

- i) the quality and grade of bentonite;
- ii) the consistency of the suspension, and
- iii) control of injection pressures and volumes pumped.

High grade bentonite swells readily and provides lubricant of the required viscosity. Pre-treating the mixing water for hardness and acidity may also help maximise yield. The consistency of the suspension and injection pressure is reported as greatly influencing lubricant efficiency a stiff suspension is said to yield better results than one of a thin consistency. A lower injection pressure is thought to allow a steady flow of suspension and a more uniform distribution whereas high pressures may force the volume of pumped material only into certain areas.

Rogers et al (1989) measured jacking loads during the installation of a 1.8m diameter pipe jack on which 'Friction Cut', a bentonite-based lubricant, was used part way into the drive. After the lubricant was pumped into the overbreak void an approximately linear increase in jacking load was halted and forces for the remainder of the drive deviated around a lower and relatively uniform jacking resistance.

Variation in jacking load reduction due to bentonite lubricant is significant because the process is site and procedure specific. Kastner et al (1996) reports a 25% reduction in clayey-sand and a 73% reduction in fine sand. Ishibashi (1988) reports load reductions of 30-50% in clays and 20% in sands. Coller et al (1996) report up to a 56% reduction in black volcanic sand and that the volume of lubricant influenced the magnitude in reduction. In Stage 2, Norris (1992b) measured reductions of 59% and 90% (in sands and gravels) at Schemes 4 and 5 respectively.

At the time of writing the benefits of bentonite lubricants in maintaining tunnel bores and reducing frictional resistance have been recognised but there is still little attempt to standardise their use. Many of the above authors, by examination of total jacking loads only, have demonstrated that lubrication is beneficial and can reduce frictional resistance. To better understand the function of lubrication further work was required to investigate their effects on pipe-soil interaction. Improving the knowledge



of the lubricity mechanism at the pipe-soil interface will ensure that lubricants are properly and effectively used in the future.

### 2.3 3 4 Pipeline misalignment

Inevitably, the excavation of a pipe jacked tunnel will deviate from the intended line and level by some degree. Steering jacks within pipe jacking shields are used to make corrections and with good control line and level can be maintained within typical specified tolerances of 50 or 75mm. Resulting 'wobble' of the pipeline is usually a series of shallow oscillations about the true line (Milligan and Norris, 1998) A misaligned pipeline will result in increases in total jacking load by introducing a series of radial forces acting on the pipes, Figure 2.5.

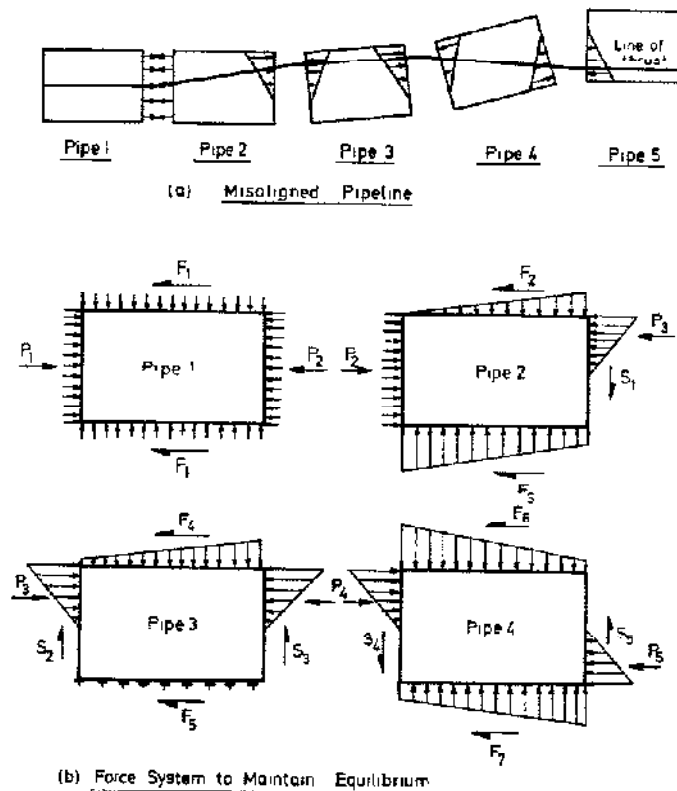


**Figure 2.5 Misalignment forces assuming elastic deformations (after Norris 1992b).**

Previous authors (Haslem, 1983 and O'Reilly and Rogers, 1987) have tried to relate the increase in axial jacking load to an increase in radial stresses on the outside surface of a curve, assuming that the pipeline acts as a continuous structural unit. Stevens (1989) and Ripley (1989), by maintaining model pipes in misaligned positions

and applying axial loads, found larger radial forces acting on the lateral supports representing the *inside* of a curve. The observations also confirmed that smaller angular deviations result in less interaction between pipe and supports. The field measurements of Norris (1992b) in a pipe jack with large horizontal but small vertical deviations, found that pipe-soil contact was also made on the inside of the curves.

Only Norris (1992b) has previously been able to relate changes in alignment to increased contact stresses on actual pipe jacks. Further research was required to widen this database so that future theoretical, or numerical, models for misaligned pipelines could be developed, validated and modified.

#### 2.3.3.5 Stoppages

It has been widely reported that stoppages in cohesive soils will create restart jacking loads greater than those needed to maintain steady motion. Interruptions in pipe jacking, such as the introduction of a new pipe, may be accompanied by considerable increases in axial load that must be considered when calculating jacking loads. Few authors have published data quantifying the stoppage phenomenon because records from many schemes plot only jacking forces that have stabilised.

Restart jacking loads on a 1.8m tunnel in alluvium, Rogers et al (1989), were typically 50% greater than the average jacking resistance after relatively short stoppages. After longer weekend breaks, restart forces were as much as 150% higher. The peaks usually associated with large restart loads are not evident in the jacking record for this drive. Norris (1992b) measured considerable increases in force even after very short stoppages, in the highly plastic London clay of Scheme 3. There is a marked time dependent response in the jacking record (presented and discussed further in Chapter 5) illustrating an increase in resistance at the start of every push followed by an abrupt decrease to the average jacking resistance line. A substantial part of the stoppage effect in London clay was found to occur within very short periods of time.

Further research was required to determine the mechanisms causing increases in restart loads after stoppages. In particular, more pore pressure and radial stress measurements during delays between pushes were required in different clays.

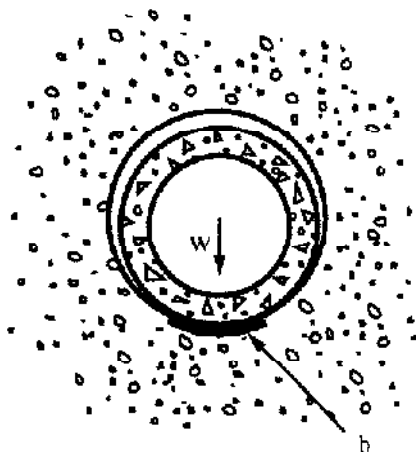
Understanding the mechanisms will be of direct benefit to industry in that recommendations can be made on how to minimise or prevent the stoppage effects

### 2.3.4 Theoretical models

For pipes sliding along the base of a stable bore, two alternative models may be considered (Milligan and Norris, 1998) The first assumes that the average resistance is frictional and should be related simply to the weight of the jacking pipes so that the frictional resistance  $F$  is given by

$$F = W \tan \delta$$

where  $W$  is the weight of the pipe and  $\delta$  the angle of interface friction between pipe and soil The second model is that of Haslem (1986) shown in Figure 2.6, in which the undrained adhesion between pipe and soil is multiplied by a contact width determined from elastic theory (Roark and Young, 1976).



$$F = \alpha_s s_u b$$

Where  $\alpha_s s_u$  is the 'adhesion' between pipe and clay  
 $b$  is the contact width between pipe and ground

**Figure 2.6 Model for pipe-soil interaction in cohesive soil with a stable bore (after Haslem, 1986).**

Cohesionless soil will collapse onto the pipes and Auld (1986) has suggested that contact stresses may be obtained from Terzaghi's (1943) analysis for soil settling in a trench, Figure 2.7



## 2.4 CONTACT STRESSES

Contact stresses at the pipe-soil interface had not been measured during pipe jacking until Oxford research Stage 2. Contact stress cells in the instrumented pipe provided information on the extent to which pipe and ground are in contact and a measure of pipe-soil interface friction. Frictional resistances cited by other authors (Craig, 1983 and Stein et al, 1989) generally assume that measured jacking loads act over the full pipe area. Norris (1992b) has shown that contact stresses are highly localised and the very approximate average resistances traditionally adopted in pipe jack design grossly simplify the extremely complicated mechanism of pipe-soil interaction.

In his measurement of contact stresses, Norris (*loc cit*) found that for stiff soils at low cover depths, the overbreak remained open and pipes were sliding along the base of an open bore, contact was only recorded along the bottom of the pipe. This occurred through most of Schemes 1 and 2. In the London clay at greater depth in Scheme 3, very high contact stresses at the sides of the pipe were registered early in the drive and were large enough to damage most of the stress cells. The very high horizontal stresses appeared to be caused by local plastic yielding around the tunnel sufficient to close the overbreak and allow some contact between pipe and clay. This 'squeezing' effect was probably exacerbated by horizontal deviations in the pipeline. At Scheme 4, observations showed some collapse of the silty sand on to the top of the pipe and stresses on the side walls varied from zero to relatively large values, dependent on the direction and magnitude of pipeline misalignments. Scheme 5, in cohesionless soil below the water table, yielded contact stress measurements showing high frictional resistance when slurry support and lubrication was not effective, but low resistance when effective.

Examination of individual pushes highlighted apparently frictional behaviour, in terms of total stress, in cohesive soils. In Scheme 3, London clay, pipe-soil interface behaviour was frictional at lower stress levels but there was an indication of a limiting shear stress at about 150kPa. Frictional behaviour with no upper limit was observed in the stiff glacial clay and weathered mudstone of Schemes 1 and 2. More cohesive

behaviour occurred in softened glacial clay at the end of Scheme 1, Milligan and Norris (1998)

The change in contact stresses before and after stoppages on Scheme 3, where stoppage effects were marked, indicated that excess pore pressures generated during the jacking process dissipate during the delay and lead to increases in effective radial stresses. However, the data studied were limited and further research was required to try to determine the exact mechanism.

## 2.5 GROUND MOVEMENTS

Ground movements above tunnels in soft ground are now generally well understood. Many authors have published data on movements caused by conventional tunnelling but there have been few documented observations on movements due to the pipe jacking technique. A database of both surface and subsurface movements is required to check the appropriateness of existing, and widely accepted, design solutions (Peck 1969, O'Reilly and New 1982, Attewell and Woodman 1982, Lake et al 1992, Mair et al 1993, etc) to displacements induced by pipe jacking.

Rogers et al (1989) describe the ground movements induced by a 1.2m diameter pipe jacked tunnel installed at a depth of 5-6m in very soft alluvium. There were some anomalies in the measurements but a maximum surface settlement of 3-4mm through a road pavement is reported. Dyer et al (1996) monitored movements above a 1.2m diameter pipe jack in loose glacial sand. Surface settlements were measured on an array of survey pins across the tunnel centre line in a road pavement. Small settlements, about 1mm, were detected with the tunnel shield about one pipe length from the pins. The approach and passing of the shield caused settlements of 13mm, equivalent to approximately 6% surface volume loss. As pipe jacking continued the total measured volume loss increased to 20% corresponding to a considerable maximum settlement of 43mm. The authors suggest shearing of the loose glacial sands by the unlubricated pipes caused the continued volume loss. Cowan (1993) describes the surface settlements caused by a 1.0m diameter hand excavated drive 4m below a runway at Birmingham International Airport in stiff to very stiff silty clay and weak mudstone. A bentonite suspension was used as a lubricant during the drive and the overbreak void was grouted on completion. The observations

showed maximum surface settlements of about 3mm on the runway pavement and 6mm on grassed areas. The author predicted a maximum settlement over the tunnel centre line of 7mm.

Chapman (1996) carried out field measurements during the microtunnelling installation of a 600mm external diameter sewer, at an average depth of 5m, using a slurry machine in soft to medium firm clay. As the machine approached the monitoring points, noticeable heave (about 10mm) was observed, indicating over-pressurisation of the slurry face support. The heave movements subsequently reduced relatively quickly after the machine passed. Three months after completion, dissipation of excess pore pressures and possible collapse into the overbreak resulted in settlements of about 4mm. The author applied O'Reilly and New's (1982) model to the measurements and found it to seemingly fit the heave profile and the short-term settlement trough quite well; the longer-term settlement trough however was not as accurate a fit. De Moor and Taylor (1989) applied the error function curve to monitored ground displacements due to a 2.1m diameter sewer tunnel constructed at a depth of approximately 10m in soft clay at Tilbury. Comparison between their observations and predicted profiles was good for short-term movements but less good for the longer-term settlements.

Few of the above authors have related their measured ground movements to full or partial overbreak closure, which should be an important aspect in pipe jacking/microtunnelling induced settlements. Further research was required to compare predicted profiles (calculated assuming that only closure of the overbreak contributes to volume loss) to field measurements.

No research had been carried out on subsurface longitudinal settlements above pipe jacks. The measurement of longitudinal ground movement profiles close to the crown of a pipe-jacked tunnel were required to provide valuable information on how longitudinal profiles develop and compare to predicted cumulative probability curves. The information was also needed to determine any face loss ahead of the tunnel, movements above and behind the shield, and settlements due to consolidation.

More work on subsurface deformation due to pipe jacking through soft clays was needed to further investigate the effects of face pressures in such ground. This

work would require the measurement of ground pressures close to the tunnel to attempt to correlate ground movements to any change in measured soil stresses.

## **2.6 INSTRUMENTATION AND FIELDWORK**

### **2.6.1 Pipe Jacking Instrumentation**

The instrumentation programme for the pipe jacking fieldwork was established and used successfully by Norris (1992b) for Stage 2 fieldwork. The robust design of instruments led to few failures and the satisfactory monitoring of five schemes established their suitability for further use. Only the ground convergence indicator – designed to measure closure of the overbreak – performed poorly during the pilot test of Scheme 1 and was not used further. A phase difference between pore pressure probe readings and measurements from the adjacent contact stress cells led to difficulties in interpreting effective radial stresses. Norris (*loc cit*) recommended that for future work the contact stress cells – based on Bond and Jardine's (1989) surface contact transducers in model piles – should be modified to incorporate pore pressure measurement. All other pipe jacking instruments including, pipe joint pressure cells, tube extensometers, one-dimensional joint movement indicators, jack load cells and linear displacement units, were to be used as originally designed by Norris.

The data acquisition system, also developed by Norris (*loc cit*), performed extremely well and required little work for further use. Only additions, for an increased number of instruments, and minor electronic adjustments were required.

### **2.6.2 Measurement of Ground Movements**

#### **2.6.2.1 Surface settlements**

To measure ground surface movements by precise levelling, Dunnicliff (1988) recommends seating the measuring point below the soil surface. Taylor (1994) suggests an arrangement similar to that illustrated in Figure 2.9. This type of levelling station is ideal for 'greenfield' sites but may be difficult to install over pipe jacks in urban environments. A less ideal but nevertheless acceptable method is to monitor settlement troughs within a road pavement or similar structure into which measuring points should be securely installed and have domed heads on which to seat the levelling staff.



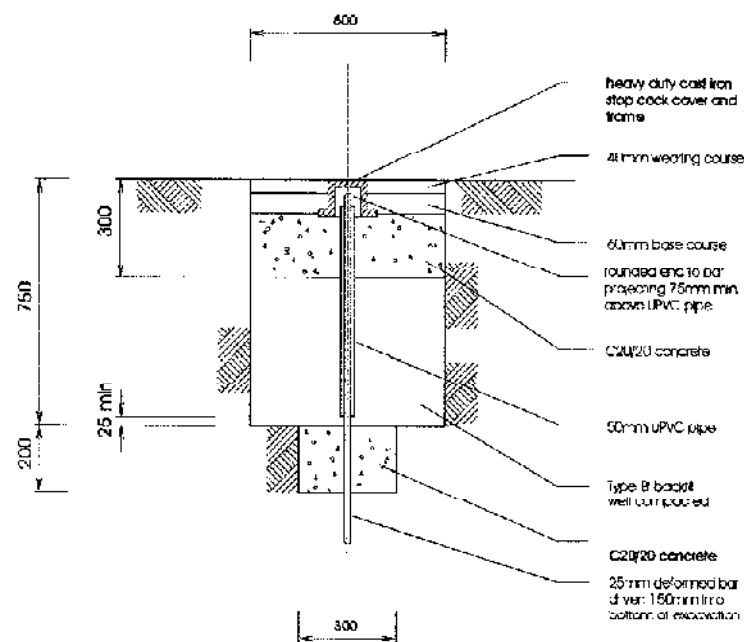


**Figure 2.9 Surface settlement levelling station.**

### 2.6.2.2 Subsurface movements

#### *Inclinometer and Magnetic Probe Extensometer*

Many authors including Dunnycliff (loc cit) and Hannah (1985) provide the principles of inclinometer operation – shown in Figure 2.10. Inclinometer access tubes (termed ‘guide casing’ in Figure 2.10) can be installed above or alongside tunnels to monitor the extent and rate of any horizontal ground movements. One end of the tube should be fixed from translation or the translation should be measurable by separate means. Deformation of the access tubes is measured by means of an inclinometer probe raised incrementally from bottom to top of the tubes. The difference between a set of initial datum readings and subsequent sets define any tube deformation.

A probe extensometer is a device for monitoring the change in distance between a datum point and magnetic measuring plates, Dunnycliff (loc cit). Ring or ‘spider’ magnets can be sleeved around access tubes to measure vertical movement of the surrounding ground. A tape suspended probe, incorporating a reed switch, travels within the access tube and senses the relative position of the magnets. A limitation of the tape suspended probe is a reading accuracy of  $\pm 2\text{-}5\text{mm}$ . It is often conveniently combined with inclinometer installation.

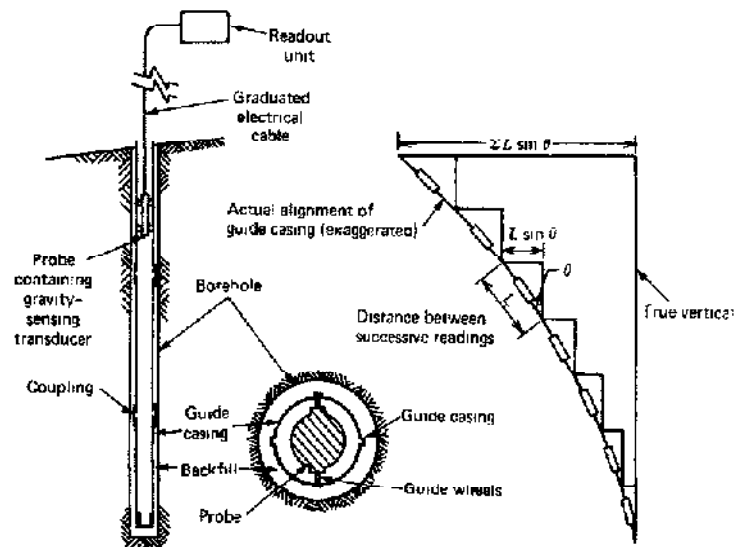


**Figure 2.10 Principles of inclinometer operation (after Dunnicliff, 1988).**

### *Electro-levels*

The Building Research Establishment (BRE) first used electro-levels on a series of pile tests in the 1970s (Cooke and Price, 1973). Their early use was in monitoring bending strains in piles but they were later further developed to measure ground and structural movements. Price et al (1996) report the use of electro-levels to measure ground displacements around major tunnelling works on the Docklands Light Railway and 104 Trial Jubilee Line Extension contracts.

Electro-levels had not been used to measure ground movements due to pipe jacked tunnelling prior to the research reported here.

### **2.6.3 Execution of the Fieldwork**

Norris (1992b) lists the key elements for executing a successful field instrumentation programme as:

#### **Planning Phase**

- Maximise the lead in time and try to be involved with the design
- Have clear and realistic objectives
- Understand the roles and motivations of the parties involved
- Work with the designers for proper provisions in contract documents

- Explain the aims of the research to the Contractor and encourage his interest
- Use the expertise of experienced groups such as BRE

### **Fieldwork Phase**

- Try to install instruments when the site is not busy
- Make research team part of the Resident Engineer's staff
- Arrange for a member of the Contractor's staff to be personally responsible
- Communicate clearly and beware of unbriefed subcontractors
- Be prepared for delays and disruptions
- Process data promptly and feedback to site staff

---

## chapter three instrumentation

### 3.1 INTRODUCTION

This chapter describes the two categories of instruments used in Stage 3 research: pipe jacking and ground response. The former category includes instrument clusters in the jacking pit and pipe string. Ground response instrumentation includes geotechnical instruments used to measure soil properties and ground displacement. Appendix B gives an inventory of the instrumentation.

### 3.2 PIPE JACKING INSTRUMENTS

All pipe jacking instrumentation was developed by Norris (1992a) for Stage 2 fieldwork. These instruments were refurbished, modified and increased in number where necessary for use in the fieldwork reported here. A typical arrangement of Stage 3 instrumentation is illustrated in Figure 3.1. In the jacking pit the total jacking loads were recorded by load cells where possible and hydraulic oil pressure transducers on the main jack rams where jacking rig configurations did not allow the fitting of load cells. A linear displacement unit measured the forward progress of the pipe in the jacking pit. The instrumented pipe contained the following instruments:

- i) Twelve contact stress cells measuring total radial stress, shear stress and pore pressures. The cells were glued into the pipe wall (using a fast acting structural glue) and had an active measuring face flush with the pipe surface.
- ii) Six joint movement indicators, three at each end, measuring the variation in joint gaps.
- iii) Flat pressure cells in the joint at the pipe rear. These cells could only be installed on pipes with steel collar joints and a minimum wall thickness of 150mm.
- iv) Data acquisition boxes.

A detailed site diary was kept of all construction activities likely to affect readings. In addition to the diary, line and level surveys were regularly carried out as the pipe jacks progressed to measure pipe wriggle.

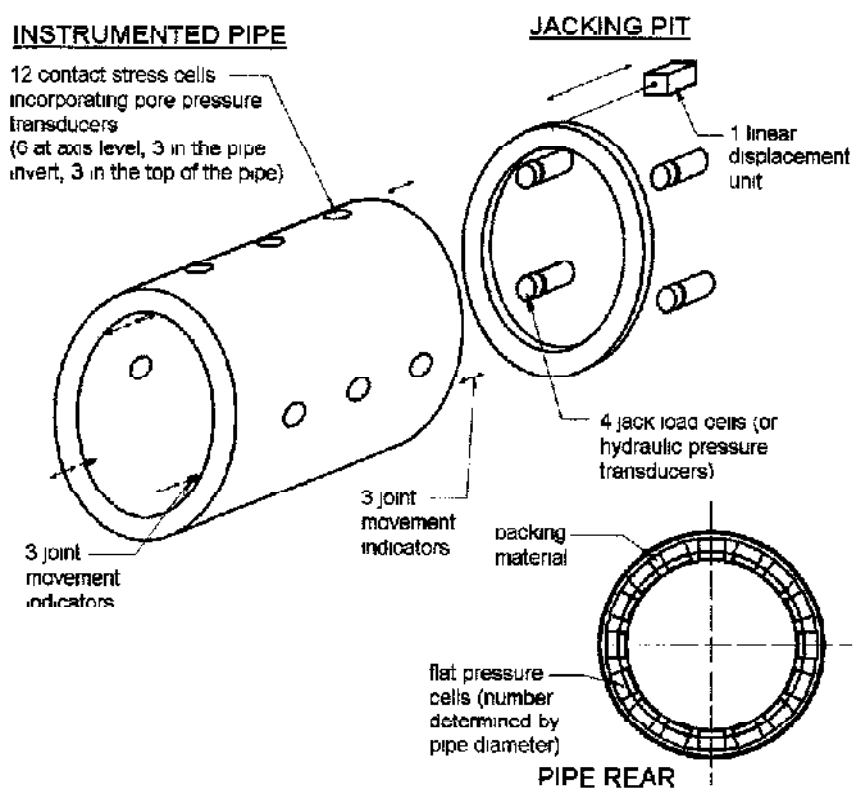


**Figure 3.1 Schematic of pipe jacking instrumentation.**

### 3.2.1 Contact Stress Cells

Contact stress cells to measure total radial stresses and shear stresses acting on the concrete jacking pipe were developed by Norris (1992a) who provides a detailed description of design and manufacture. The cells comprise a three-part housing with a Cambridge earth pressure transducer – Figure 3.2 – at their centre. The loading platen or active face was designed to have a similar frictional resistance to jacking pipe concrete. In a series of shear box tests Norris (1992a) found ground polymer modified mortar the material best for the active face.

#### 3.2.1.1 Cell modification

Only five cells were manufactured for use in Stage 2 fieldwork; an additional seven were required to complete the required complement of twelve cells for Stage 3. From experience gained in the fieldwork Norris (1992b) recommended cells for future research be modified to measure pore pressures. To keep the very expensive manufacturing costs to a minimum, the stainless steel housing design was

standardised so the five existing housings could be re-used, only the loading platen design was modified to accommodate pore pressure measurement devices. A modified contact stress cell is illustrated in Figure 3.3. The existing Cambridge earth pressure transducers required some minor modifications as the pore pressure transducers were to share the same cable for excitation voltage and signal.

The pore pressure cells comprise miniature transducers glued into titanium housings placed in acetyl copolymer thrust blocks. Between the thrust block and underside of the loading platen, a large rubber O-ring prevents moisture ingress. The porous stone and small void, between stone and miniature transducer, is saturated by affixing a temporary pot containing Glycerol oil over the stone, Plate 3.1. The system is de-aired by attaching the affixed saturation pot to a vacuum for a minimum period of twenty-four hours or until no more air bubbles are visible. The de-airing procedure consisted of several cycles of vacuum and positive pressure to atmospheric. Saturation pots are removed from the cell just before the instrumented pipe is lowered for insertion in the pipe jack.

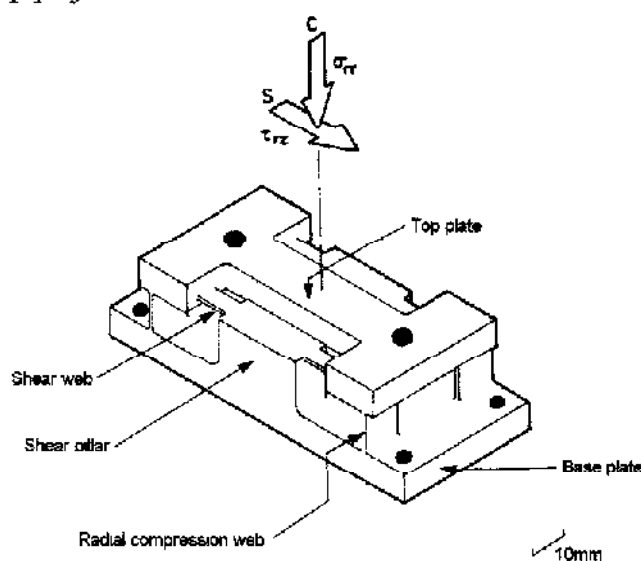


**Figure 3.2 Cambridge earth pressure transducer (after Bond and Jardine, 1989).**

Transducers retrieved from the pore pressure probes of Stage 2, were the well proven, but expensive, Druck PDCR81. A less expensive alternative to the Druck transducer, the Keller piezoresistive 2Mi, was tested in laboratory conditions but from a batch of six, only two gave meaningful output. All the faulty transducers were returned to Keller and eventually replaced with the Druck PDCR81. Unfortunately the

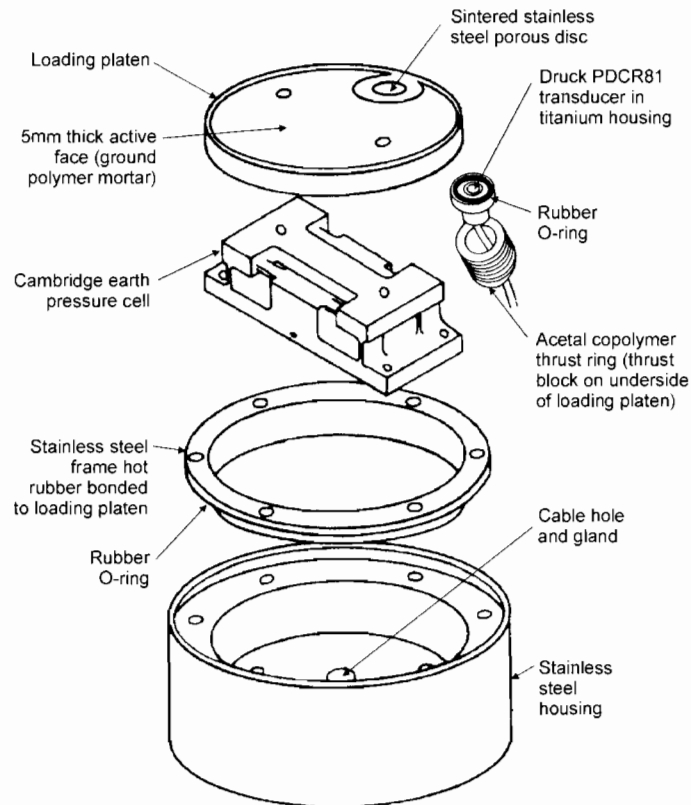


**Figure 3.3 Modified contact stress cell (part of figure after Norris 1992a).**

delay in testing and replacing some of the pore pressure transducers resulted in only six of the twelve modified contact stress cells having pore pressure measurement capabilities for Scheme 6.

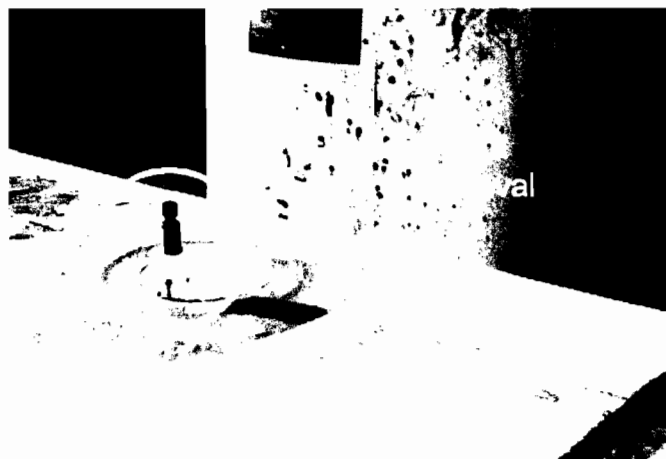


**Plate 3.1 Modified contact stress cell with pore pressure saturation pot.**

### 3.2.1.2 Calibration

Calibration procedures formed an integral part of the fieldwork. It was essential that all instruments were calibrated prior to Scheme 6, the first site in Stage 3 research, and ideally re-calibrated before all ensuing schemes. The contact stress cells were calibrated using a special calibration rig developed by Norris (1992a) that enabled simultaneous application of radial and shear forces to the active face. Metal weights (checked on an independently calibrated set of scales) were used for load application in the first calibration and the procedure (steps 1 to 12 in Table 3.1) took about seventy-two hours per cell. Prior to Scheme 6, calibration of all twelve cells was completed in thirty-six days. The calibration rig was subsequently modified to use hydraulic jacks fitted with transducers for applying the loads and automatically logging forces and the cell response, Plate 3.2. After Scheme 6, calibrations were carried out on the modified rig in less than half the time taken with the weights. Changes in calibration coefficients of the cells are negligible (about 1%) as indicated in Table 3.2.

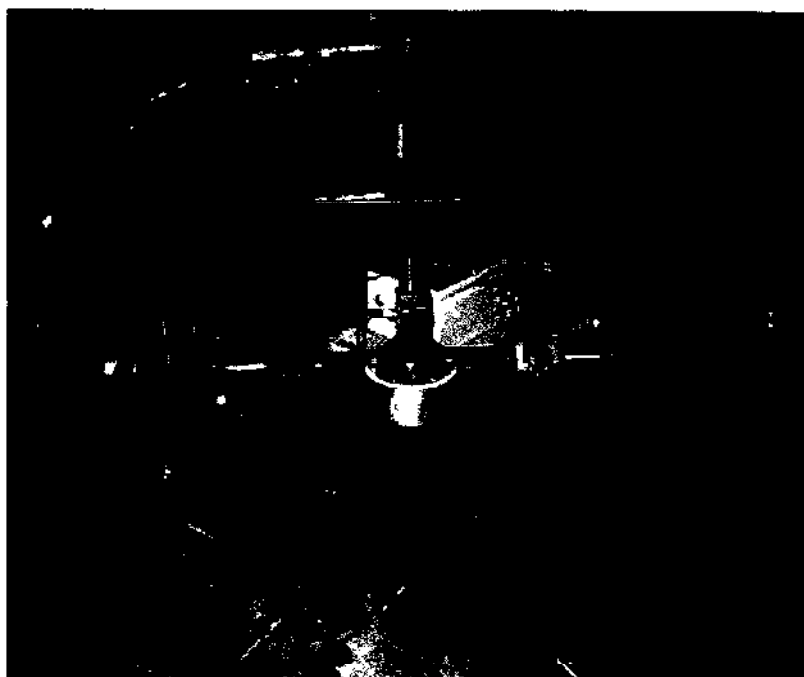


**Plate 3.2 Contact stress cell calibration.**

The calibration procedure for the pore pressure cell component (steps 13 to 18 in Table 3.1) could only be carried out after completing radial and shear calibration.



Step	Stage	Calibration	Radial kPa	Shear kPa
1	Cell assembly	-	-	-
2	Exercise	Sustained loads	450 450	-202 +202
3	Exercise	Rapid cycling Rapid cycling	450 450	0 to -202 0 to +202
4	Shear stress calibration	Radial stress constant, shear stress varied	450	±202
5			348	±202
6			243	±202
7	Radial stress calibration	Shear stress constant, radial stress varied	0-450	0
8			0-450	25
9	Eccentric loading	Radial load at +10mm Radial load at -10mm	0-450	0
10			0-450	0
11	Creep testing	Sustained loads	450	+202
12			450	-202
13	Assemble saturation pot	-	-	-
14	De-airing	-	-	-
15	Pore pressure exercise	Rapid cycling	0	0
			243	±202
16	Pore pressure calibration	Apply incremental pressure up to 500kPa	0	0
17	Pore pressure calibration	Release incremental pressure down to atmospheric	0	0
18	Pore pressure calibration	Repeat 16 and 17	0	0

**Table 3.1 Calibration procedure for modified contact stress cells.**

Figure 3.4 illustrates the pore pressure cell calibration. After saturating/de-airing the pore pressure transducer, pressures of up to 500kPa were applied and released incrementally through a nitrogen/glycerine interface and a Druck Digital Pressure Indicator (DPI)

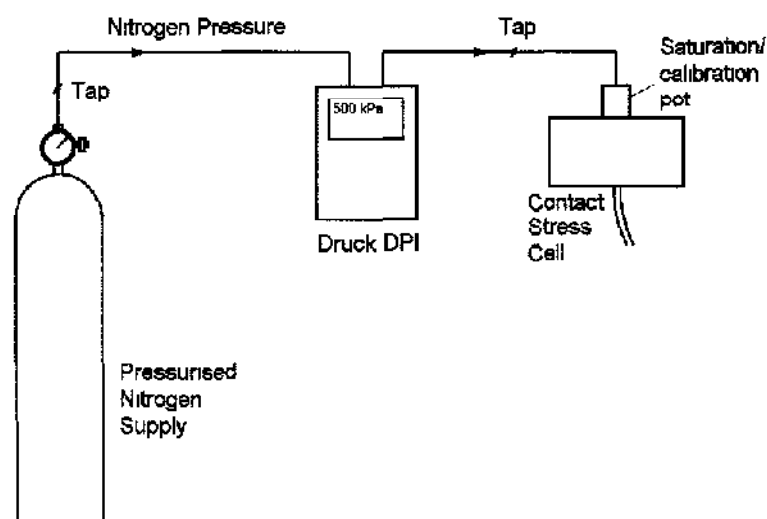


**Figure 3.4 Schematic of pore pressure cell calibration.**

Contact stress cell		Combined non-linearity & hysteresis (%FS)	Long term zero drift (%FS)	Long term change in calibration coefficients (%)
1	Radial	±0.3	1.0	0.9
	Shear	±0.5	1.1	1.1
	Pore pressure	±1.0	0.4	0.5
2	Radial	±0.3	0.8	1.2
	Shear	±0.3	0.9	1.0
	Pore pressure	±1.1	0.3	0.6
3	Radial	±0.4	1.0	1.4
	Shear	±0.6	0.7	1.1
	Pore pressure*	±2.8	2.2	4.0
4	Radial	±0.4	0.8	1.1
	Shear	±0.6	1.0	1.1
	Pore pressure	±0.9	0.3	0.7
5	Radial	±0.7	0.6	1.3
	Shear	±0.6	0.9	0.9
	Pore pressure	±0.9	0.2	0.9
6	Radial	±0.6	1.0	1.0
	Shear	±0.4	0.8	1.2
	Pore pressure	±1.1	0.5	0.4
7	Radial	±0.2	1.1	0.9
	Shear	±0.7	0.8	1.5
	Pore pressure	±0.8	0.4	1.0
8	Radial	±0.5	0.9	0.8
	Shear	±0.7	1.0	1.2
	Pore pressure*	±2.4	2.7	4.7
9	Radial	±0.4	1.1	1.1
	Shear	±0.5	1.0	1.1
	Pore pressure	±0.7	0.7	0.5
10	Radial	±0.8	0.9	1.3
	Shear	±0.6	1.2	0.9
	Pore pressure	±0.6	0.5	1.0
11	Radial	±0.9	0.5	1.0
	Shear	±0.6	1.1	1.3
	Pore pressure	±1.0	0.2	0.5
12	Radial	±0.4	1.0	1.3
	Shear	±0.7	1.0	0.8
	Pore pressure	±0.8	0.3	0.8

\* denotes pore pressure cells with Keller 2Mi transducer.

**Table 3.2 Modified contact stress cell calibration performance.**

### 3.2.1.3 Installation and retrieval

A further recommendation of Norris (1992b) was a need to improve the method of installation and retrieval of the in-wall contact stress cells and it was intended to revise installation/retrieval for Stage 3 fieldwork. The principal design requirements for such an arrangement were:

- i) ease of fixity,
- ii) easy removal of the instrument, and

iii) height adjustment for different wall thicknesses

Two Cambridge earth pressure transducers were crushed during Stage 2 fieldwork, so a proposed additional design feature was a fail-safe mechanism to prevent crushing damage. To reduce the risk of crushing, installation cradles were designed to move into the pipe wall if stresses became large enough to damage radial compression webs on the transducers. Crushing forces were determined empirically by the controlled loading to failure of all good webs on two damaged/corroded transducers recovered from old stress cells.

Several cradle systems were considered including the friction grip system illustrated in Figure 3.5 (unreliable, not sufficiently repeatable and not easily set accurately) and a compressed air bag with release valve (too complicated) but the preferred option was a simple spring system, illustrated in Figure 3.6. The arrangement comprised four bolts each carrying a pack of disc springs, commonly known as Belville washers. It was proposed that the springs would secure the cell housing against a flange with a force that could be accurately set by measuring the height of the spring pack. Steel tube and flange would be cast into the special pipe<sup>2</sup> during its manufacture and left in as part of the permanent works. This would also give the option of making the pipe good for the permanent lining by bolting in a specially designed plug.

Jacking pipe manufacturers were shown the spring design for comments on: the permanent lining, the hole size and method of fixing to the pipe wall. Already concerned over the twelve holes required for the contact stress cells in a special pipe, they were anxious about an increase in hole size and a weakening of overall pipe strength. An additional concern of the author was that spring displacements in the system can never be truly equal and any displacement of the cell would cause a redistribution of stresses that would be difficult to interpret. Displacements could have been monitored by installing linear variable differential transformers (LVDTs) below the cell housing but the disadvantages were: an increase in cell installation time, additional expenditure in purchasing LVDTs and an extra demand on the data acquisition system. The decision was therefore taken to glue the stress cells into bored or cast holes of a high tolerance so that the instruments formed an integral part of the

---

<sup>2</sup> Refers to the specially prepared pipe before the installation of or after the removal of instrumentation.

instrumented pipe. Retrieval was again to be by over-coring carried out by specialist diamond drillers.

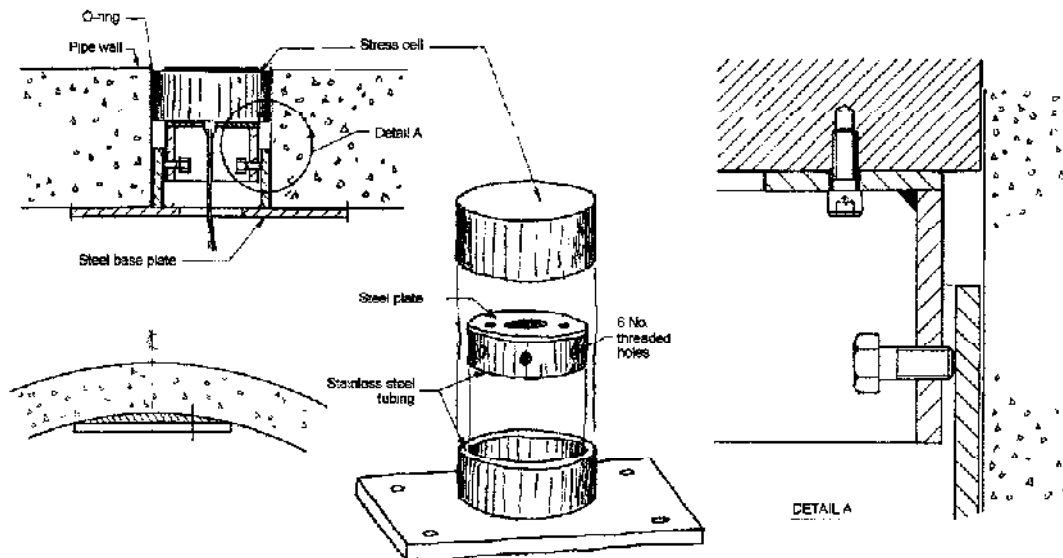


**Figure 3.5 Proposed contact stress cell installation/retrieval friction grip cradle.**

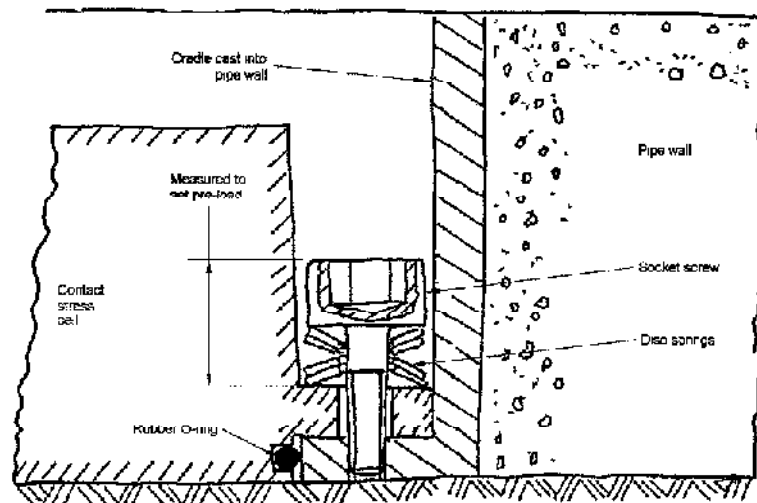


**Figure 3.6 Proposed contact stress cell installation/retrieval disc spring cradle.**

### 3.2.2 Jacking Forces

Heavy-duty load cells (Figure 3.7 and Plate 3.3) fixed to the end of jacking rams were used to measure the jacking loads. The load cells are a commercially available 200 tonne compression type, with modified cables and connectors for operation under possible submerged conditions. Figure 3.8 illustrates the method of

fixing the load cells to jacking rams. They were used on only Schemes 6 and 9: Schemes 7 and 8 had jacking rigs with integral thrust rings making it impracticable to fit these cells. At Schemes 7 and 8 pressure transducers were fitted to the hydraulic circuit – at the feed point in the rams – to monitor oil pressures. By calibrating oil pressures against the jack load cells, it was possible to convert these pressures to jacking forces.

Two pressure transducers were used in the hydraulic feed circuit on the Scheme 7 rig. Calibration was performed in the factory by placing two of the jack load cells between thrust ring and a reaction wall and carrying out several load/unload cycles – output from load cells and pressure transducers was automatically logged through the data acquisition system. Laboratory determined load cell calibration coefficients were applied to the output to calculate the calibration coefficients for the pressure transducers.

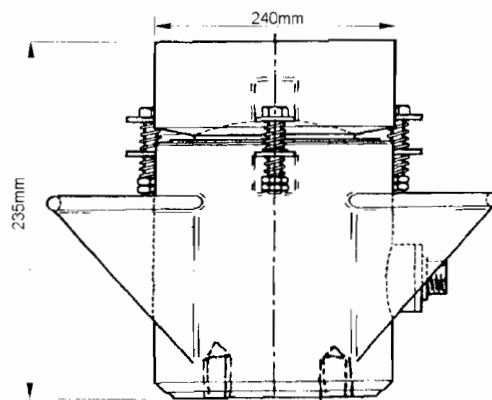


**Figure 3.7 Jack ram load cell.**

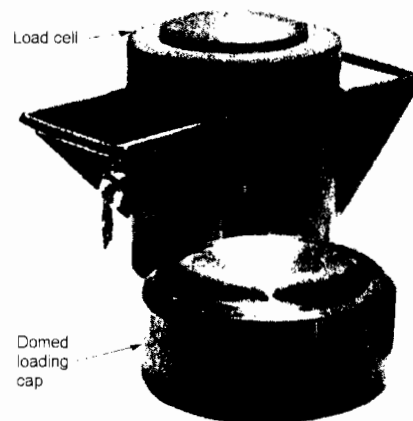


**Plate 3.3 Jack ram load cell.**

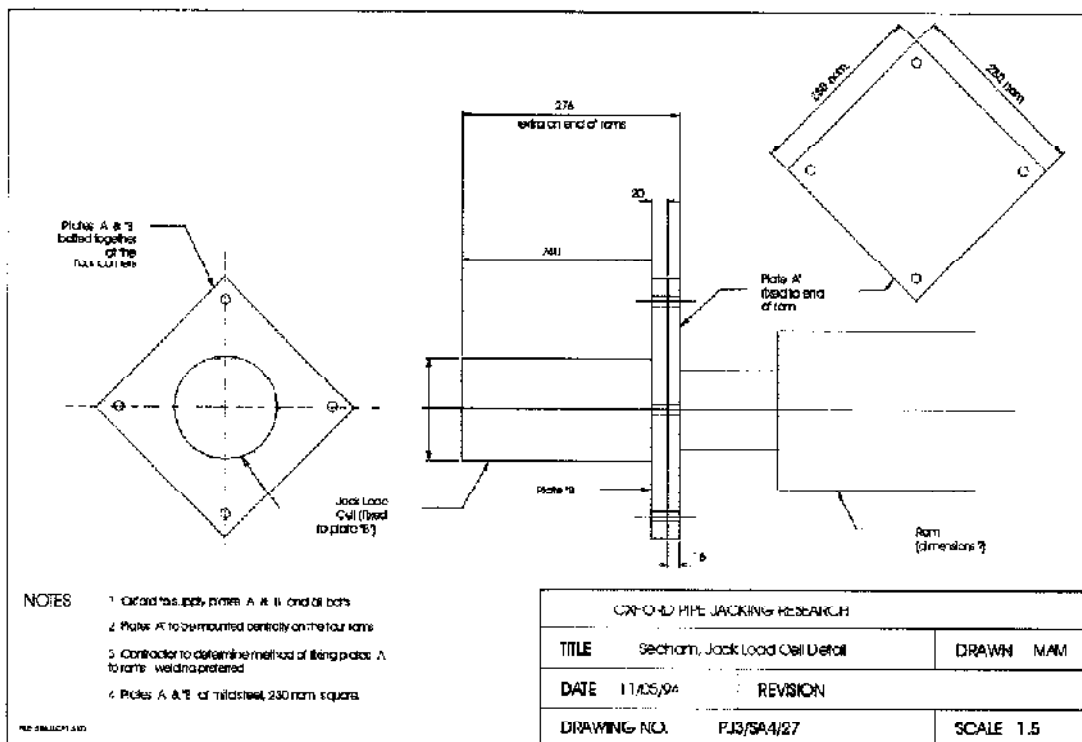


**Figure 3.8 Proposed fixing of jack load cells at Scheme 8 for oil pressure calibration.**

At Scheme 8 one transducer was fitted at the feed point of each ram on the jacking rig. It was possible to carry out the calibration in-situ by temporarily removing the thrust ring and fixing the load cells to the ram ends. Two calibrations were performed: the first before pipe jacking operations began in earnest while launching the tunnelling machine; and secondly, following completion of the drive while closing up the inter-jacks, when greater jacking forces and oil pressures were generated

Calibration of the jack load cells was performed on a Denison loading machine that is independently calibrated twice yearly

### 3.2.3 Instrumented Pipe Movement

#### 3.2.3.1 Electromagnetic distance measurement

To monitor forward progress of the instrumented pipe, the use of electromagnetic distance measurement (EDM) techniques was investigated. An EDM system works by setting the instrument over one end of the line to be measured and a reflector (usually a corner cube prism) at the target end such that the line of sight is

unobstructed. The instrument transmits an electromagnetic wave towards the reflector where part of it is returned. By comparing the phase difference between transmitted and reflected signals, the EDM computes the distance which can then be displayed or automatically saved to a data storage unit. The proposed use in the fieldwork was to have an EDM instrument positioned at some protected location in the jacking pit, with a clear line of sight through to the instrumented pipe, Figure 3.9.

It was thought that pipe roll and/or inevitable deviation from line and level would cause a single prismatic target to almost certainly move from the line of sight. An EDM capable of detecting a wave bounced off a larger strip of reflective material was found. Relatively large areas of this strip – a material similar to that found on reflective road signs – were to be positioned around the trailing end of the instrumented pipe so that within acceptable line and level tolerance, the fixed line of sight would always hit a target sheet. Another advantage to using the reflective sheeting was its low cost. Buying or hiring an array of target prisms to mount on the instrumented pipe would have been beyond the project budget, whereas the reflective strip was relatively inexpensive and could be considered as a disposable item.

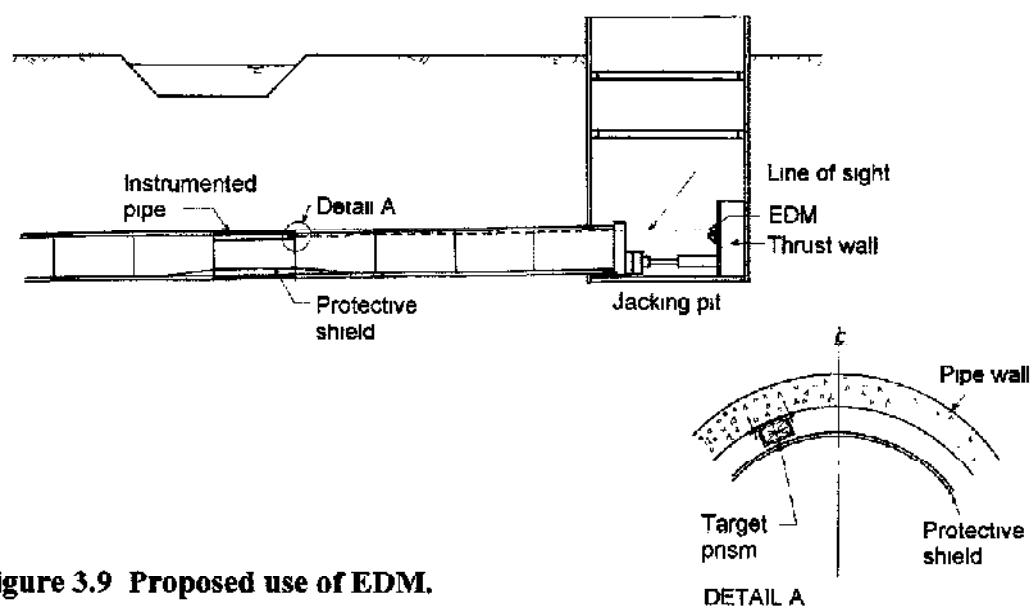


**Figure 3.9 Proposed use of EDM.**

A reconditioned Geodimeter 210 EDM was loaned to the project by Geotronics Ltd. on a one month approval basis. Controlled laboratory tests were carried out to ensure that the instrument gave accurate distances when using the

reflective strip as a target. Once satisfied that accuracy and repeatability were within acceptable tolerances,  $\pm 10\text{mm}$ , work commenced on a power supply and serial interface between EDM and the data acquisition system.

Fieldwork at Scheme 6 commenced before the serial interface was complete. The method used to monitor pipe progress during Stage 2 - a linear displacement unit with stainless steel cable attached to the pipe in the jacking pit - was again used. The EDM, with serial interface, was finally ready for field trials part way through Scheme 6 monitoring. The intention was to compare output from the EDM to that from the displacement unit. In the event however, the EDM did not produce a signal that could be interpreted by the data acquisition system, and as it could not be used as a stand-alone unit - all fieldwork data required a consistent time stamp - the EDM field trial was abandoned. Back in the laboratory, it became evident that substantial work would be required to make EDM and data acquisition system compatible. At that time it was decided to pursue the use of EDM no further.

### 3.2.3.2 Linear displacement units

The type of linear displacement unit used during the fieldwork is illustrated in Figure 3.10. A Celesco unit (purchased during Stage 2) was used on Schemes 6 and 7. It is a commercially available instrument producing an electrical signal proportional to the extension of a pre-tensioned cable on the drum of a rotary potentiometer. It was found to be easily susceptible to damage in the harsh environment of the jacking pits and required some repair work on both schemes.

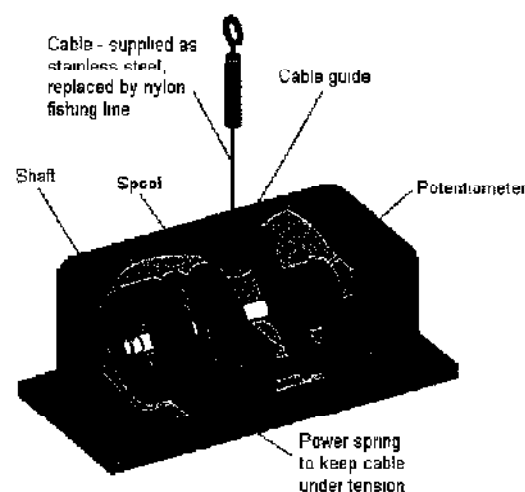


**Figure 3.10 Linear displacement unit.**



The Celesco unit was subsequently replaced by a similar instrument manufactured by IBS. This unit operates on the same principle as the Celesco but is of a more robust design and came with a stroke of four metres. The required length of stroke was a jacking pipe (2.5m) plus about one metre to the location of the instrument on the back wall of the jacking pit. The unit was calibrated in the laboratory against one-metre rules laid end to end.

The stainless steel cables supplied with these types of transducer were found to be prone to 'kinking' causing the cable to catch at the opening, lose tension, and produce false readings. The stainless steel cable in the IBS unit was subsequently replaced by heavy duty nylon fishing line.

#### 3.2.4 Misalignment Angle

One-dimensional joint movement indicators developed by Norris (1992a) were fixed at three equidistant locations around each end of the instrumented pipe. The instrument simply comprised an LVDT securely held in an aluminium housing, Plate 3.4. The LVDTs were calibrated against a micrometer bench screw.

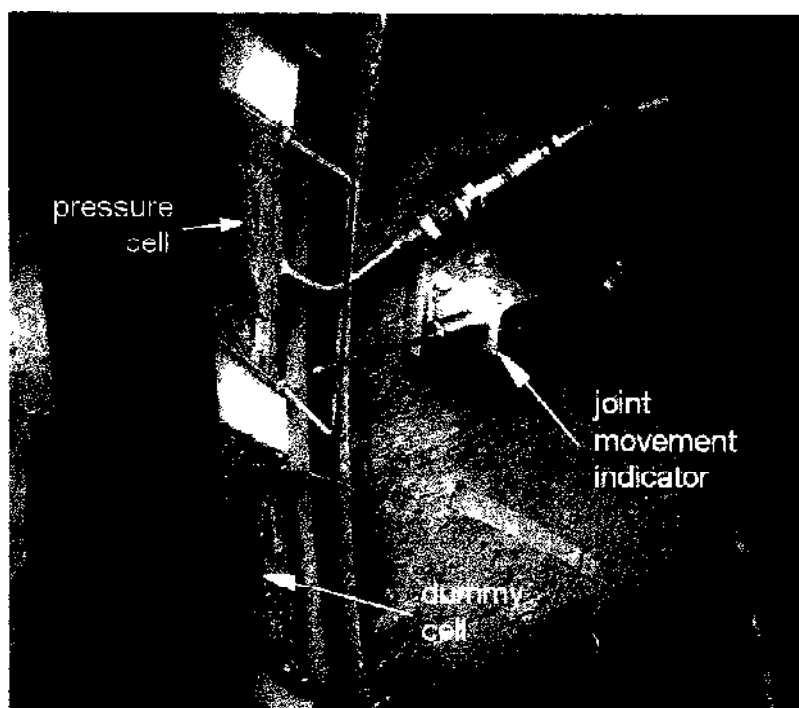


Plate 3.4 Instrumentation at the pipe joint (Scheme 8 instrumented pipe).

### 3.2.5 Joint Pressures

Pressures in the joint between instrumented pipe and adjacent pipe were monitored using the commercially available flat pressure cell described by Norris (1992a), Plate 3.4. The cells were calibrated in a Denison loading machine.

### 3.2.6 Line and Level

Surveying techniques were used to monitor line and level of the tunnel as it progressed. Typically four or five surveys would be carried out – at suitable breaks in mining – during the monitoring period. Techniques adopted were:

- i) Taking offsets from the Contractor's laser - both for line and level – at the end of every pipe using spirit level, plumb line and tape.
- ii) If the internal diameter was sufficiently large to set up level and tripod, levels were taken at every pipe joint

### 3.2.7 Data Acquisition

The data acquisition system was purpose built for the pipe jacking research programme - a full description is presented in Norris (1992a). The system comprised commercially available "Datascan" control and analogue input modules (housed in protective steel boxes) mounted in the instrumented pipe (Plate 3.5) and jacking pit. It was capable of reading a variety of transducer types and could be powered from either a mains supply point or a 20kVa portable generator supply. The network of input modules used in Stage 2 research required some modification and additions to accommodate the increased number of contact stress cells, each of the modified cells requiring four data channels. Figure 3.11 shows a schematic diagram of the system used at Schemes 6 to 9. An on-line uninterruptable power supply unit was used to eliminate spikes from power surges and also provide up to thirty minutes of battery back-up during a power loss.

A sophisticated software package for logging purposes was purchased that allowed multiple real-time graphical traces to be displayed on the logging computer. This had many advantages including the logging operator being able to immediately see any problems occurring with the readings. The software – Labtech Notebook/XE – also had switching options letting the user set trigger events to start or end logging.

or change the sampling rates. Push events were set to trigger a 2 second sampling rate; non-push events (during breaks, introducing new pipes etc.) triggered a 30 second rate.

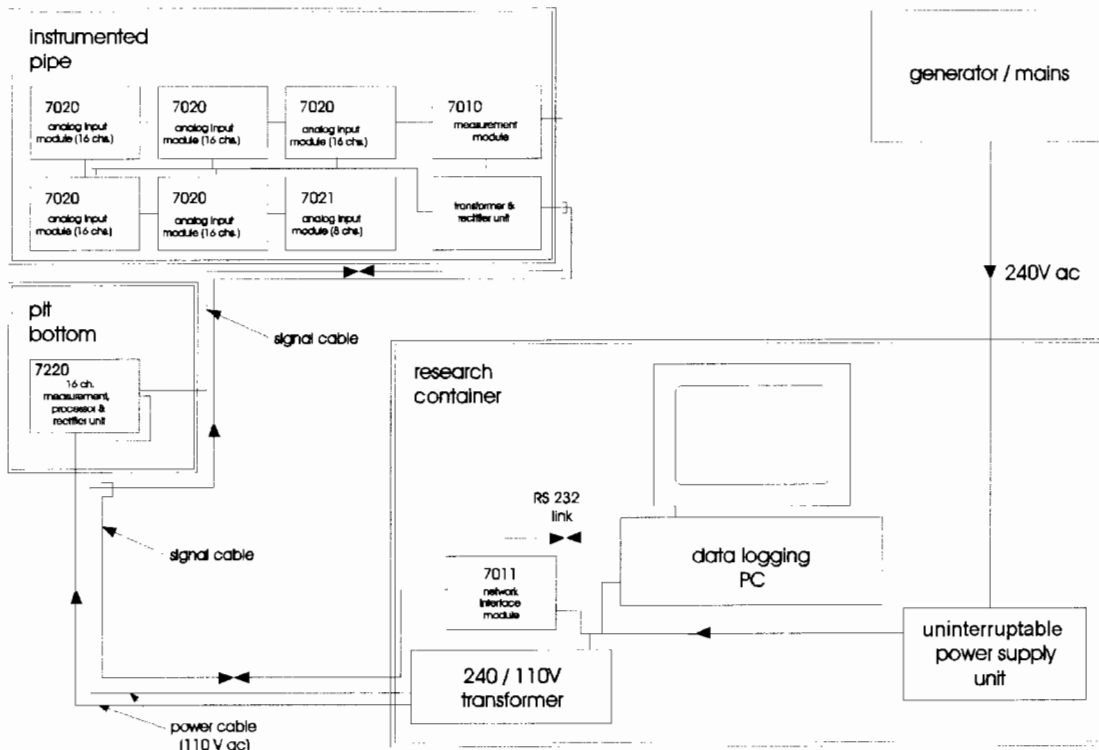


Figure 3.11 Schematic of data acquisition system.



Plate 3.5 Data acquisition boxes in the instrumented pipe of Scheme 9.

### 3.3 GROUND INSTRUMENTATION

Instrumentation to measure ground movements and horizontal stress response was newly purchased for use on Schemes 6 to 9. The equipment includes an inclinometer with logger (Plate 3.6), reed switch probe, electro-levels and push-in spade cells. Pressuremeter testing was carried out at Scheme 6 by a specialist contractor to augment site investigation data provided by the Client.

#### 3.3.1 Inclinometer

A uni-axial inclinometer was used to monitor subsurface ground displacements parallel and normal to the direction of drive. Access tubes were installed over the centre line, close to the crown, and at offsets close to the tunnel axis. It was assumed that tube fixity was at the top as the tubes were grouted to the road base (or concrete slab at Scheme 9). Surveying methods were used to monitor transverse and vertical movement of the top of the casings.

The procedures followed in taking field readings were:

1. Torpedo lowered to bottom of the casing in grooves parallel to the drive.
2. Temperature stability allowed for a minimum of 10 minutes.
3. Readings taken at 0.5m intervals and saved to the automatic readout unit.
4. Torpedo removed (guide wheels cleaned), rotated through 180 degrees and lowered to the same point.
5. Pause for temperature stability.
6. Repeated readings taken, inspecting the automatic readout unit for check-sum errors (Dunnicliff, 1988).
7. 1 to 6 repeated using casing grooves normal to the drive direction.
8. Reed switch probe (with spacer for inclinometer tubing) lowered to record the depth of magnetic settlement plates.
9. Level and lateral position of casing tops taken as soon as was practicable.
10. Data from the readout unit down loaded and saved to floppy diskette.

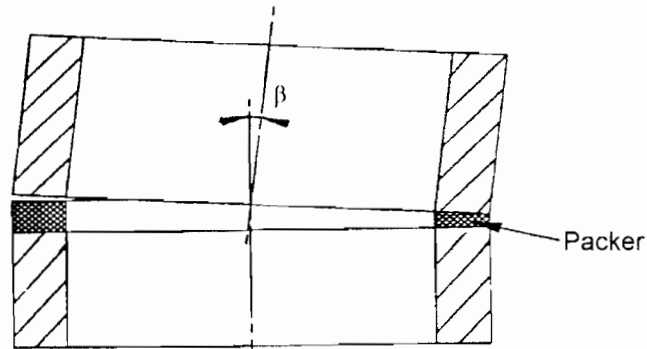


**Figure 5.14** Misalignment angle,  $\beta$ .

The normal practice has been to specify allowable limits for errors in line and level at any point along the tunnel, typically 50 or 75mm. While these limits may be necessary to maintain adequate clearance from obstructions or other services, or to provide correct hydraulic flow conditions, Ripley (1989) and Norris (1992b) demonstrate that they are insufficient as a means of controlling angular deviations between successive pipes to within acceptable limits for transmission of large axial forces. The measurement of actual angular deviations achieved in practice will therefore allow reasonable specifications in terms of misalignment angles and line and level tolerances.

The effect of misalignment on jacking loads is very difficult to assess. A direct comparison of jacking forces for misaligned and perfectly straight pipe jacks, in similar conditions, is not possible due to the limited database. The effect of misalignment will therefore be assessed by considering the increase in radial and shear stresses on misaligned pipes – discussed in Chapter 6.

### 5.3.2.2 Alignments achieved in practice

#### *Measuring misalignment*

To investigate the effect of misalignment, some angular deviation on the instrumented pipe jacks was desirable. However, the author did not influence in any way the miners or machine operators in steering control; measured alignments therefore are typical of those normally achieved in practice. Line and level surveys were carried out to measure horizontal and vertical deviations respectively and

electrodes changes, altering the electrical resistance between them, and thus gives a change in angle. Figure 3.12 shows simple details of the electro-level and a schematic diagram of the reading circuit. Change in angle is converted into a movement by assigning a gauge length to the electro-level over which the angular movement applies giving.

$$\text{movement (mm)} = \text{angular movement (radians)} \times \text{gauge length (mm)}$$

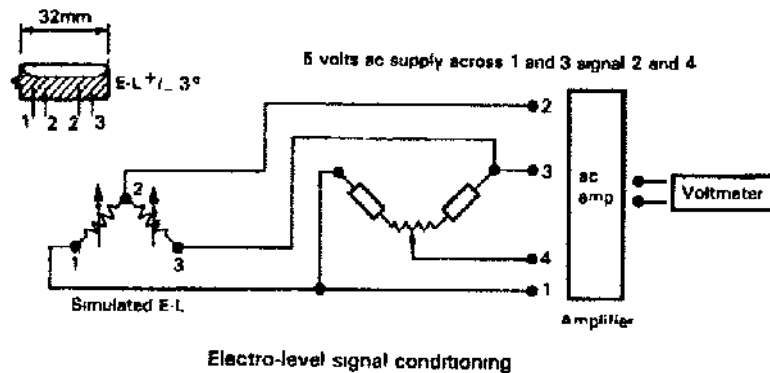
For inclinometer tube installation the gauge length should be taken as an arbitrary distance either side of the sensor and the electro-level is assumed to monitor average change in angle over this distance. The instruments are usually mounted at fixed spacing in the tubing and the gauge length is then taken as equal to the spacing.

Ten BRE  $\pm 3$ -degree electro-levels were purchased for intended use on Schemes 8 and 9. They were pre-fitted in inclinometer tube carriages (illustrated in Figure 3.13) and came with a purpose-built logging system. The  $\pm 3$ -degree sensor has sufficient range to be relatively easy to set up and can monitor angular changes to a second of arc. Its cross sensitivity (change in reading due to change in angle in an orthogonal plane) is also relatively low, less than 3%. Using a gauge length of 1m at a resolution of 1 arc seconds gives a movement of 1000/206000, i.e. 0.005mm.

The electro-level logging system developed by BRE has a controller module and multiplexing modules. Controllers comprise the signal conditioning, a 16-bit analogue to digital convertor, storage capacity (16,000 readings), microprocessor (programmed to run a user defined logging program), alarm facilities, and date/time functions. Multiplexers allow 16 instruments to be linked to the controller – up to 16 multiplexers can be connected to one controller. Fast and slow read systems exist. The fast system energises and reads at 10 channels/second, whereas the slow system powers and reads each channel individually at 1 channel every 3 seconds thereby increasing the life and stability of the system.

The electro-level logging system was not compatible with the Datascan data acquisition system and required a separate and dedicated logging computer. The system is illustrated in Figure 3.14.

Calibration of the electro-levels was a very specialised operation and could only be performed by BRE who supplied zero values and calibration coefficients.



Electro-level signal conditioning

Figure 3.12 Schematic representation of the BRE electro-level system (after Price and Wardle 1983).

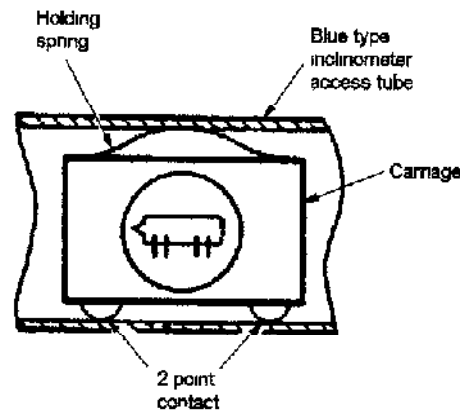


Figure 3.13 BRE electro-level installed in horizontal inclinometer tubing

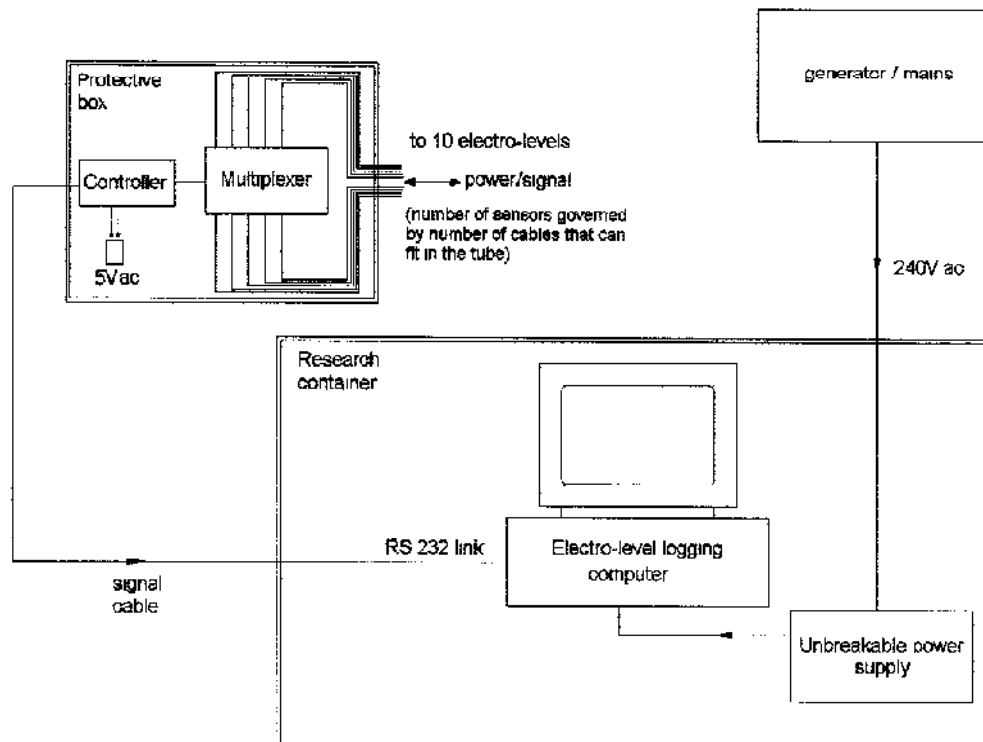


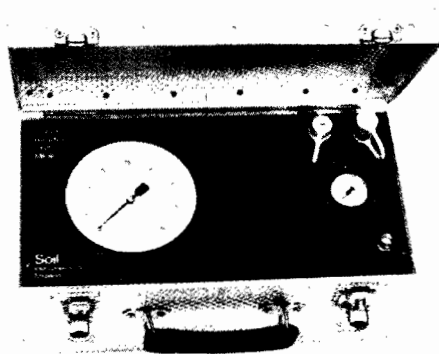
Figure 3.14 Electro-level logging system.

### 3.3.4 Push-in Pressure Cells

Push-in pressure cells, comprising pneumatic type transducers and piezometers, were installed at Schemes 6 and 9 to record in-situ stresses close to the tunnel during construction. Soil Instruments Limited supplied and installed the cells, Plates 3.7(a). Readings were taken manually using a portable read-out unit, Plate 3.7(b). The supplier who provided zero values and calibration coefficients carried out instrument calibrations.



a) pressure cell



b) read-out unit

**Plate 3.7 Push-in spade cell.**

### 3.3.5 Self-boring Pressuremeter

Cambridge Insitu carried out a series of self-bored pressuremeter tests at Scheme 6. The instrument used was a Cambridge Self Boring Pressuremeter (SBPM) Mk VII, similar to that illustrated in Figure 3.15. A purpose built, trailer mounted drilling system was used to drive the SBPM to the required depths. All calibrations, testing, analyses and interpretation of results were carried out Cambridge Insitu. A factual report and copies of the raw data were supplied.



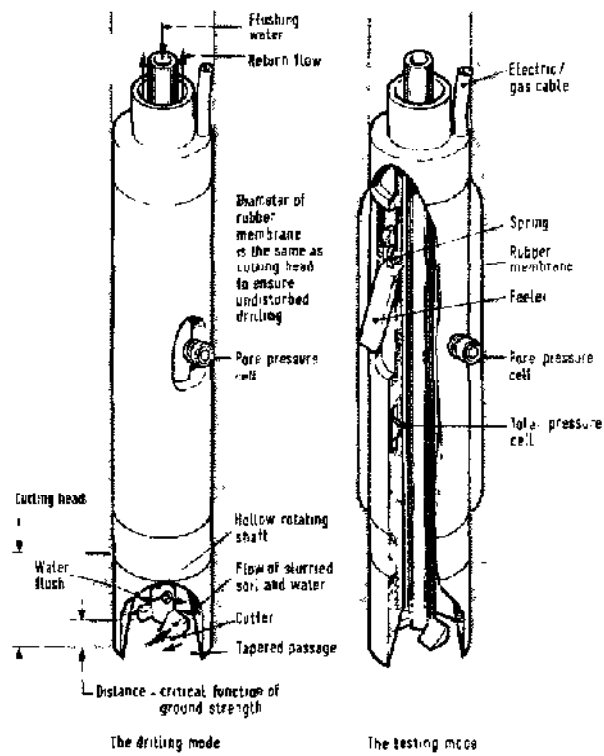


**Figure 3.15 Self-boring pressuremeter (after Windle and Wroth, 1977).**

---

## **chapter four**

### **fieldwork**

#### **4.1 INTRODUCTION**

This chapter discusses the fieldwork element of Stage 3 research. Site selection procedures, ideal requirements and sites chosen are described. Details of each scheme, including ground conditions and monitoring work are presented. Installation, performance and retrieval of instrumentation are discussed.

#### **4.2 SITE SELECTION**

The intention for Stage 3 research was to monitor pipe jacks on five different sites. Ideally, each sponsoring water company would provide a suitable scheme within their area with enough lead time to include items and specifications relating to the research work in the contract documents.

##### **4.2.1 Ideal Sites**

On the basis of fieldwork by Norris (1992b) it was recognised that the actual process of selecting pipe jack schemes would be very different to the ideal selection procedure. In order to carry out a search for suitable pipe jack schemes it was necessary to list the main factors affecting the choice of sites for the fieldwork. These were:

- Ground material
- Pipe size
- Lubrication
- Overburden loading
- Cover depth
- Length of drive
- Position of instrumented pipe and its retrieval
- Method of excavation

The most important factors affecting the choice of pipe jacks for monitoring were type of ground material, a minimum pipe size of 1200mm internal diameter and the proposed period of works.

Pipe jacks in a variety of ground conditions were again sought to compare data with that collected during Stage 2 and take analysis further but with a different emphasis, and to also measure ground movements. Since the Scheme 3 drive in London clay had produced some inexplicable contact stress data (discussed in chapter 2), another drive in similar ground was required to gain a better understanding of the shear mechanism. A soil type not encountered during Stage 2, but considered important for this reported research stage, was soft clay. A pipe jack within such material was required to assess the contact between pipe and a soil expected to collapse quickly onto the pipe string.

The proposed period for fieldwork was from September 1993 to April 1995. Ideally a period of about twelve weeks between sites was required to re-calibrate instrumentation and process data. Pipe jacks commencing during the above period with enough lead time between them were therefore sought. It was anticipated that the fieldwork on each site would take about six weeks. As the length of potential pipe jacks directly affects the monitoring period, long drives with mechanical excavation were preferred to short hand excavated drives. Results from Scheme 5, where a tunnelling machine was used, had shown that electrical noise within the tunnel does not corrupt signals from the instrumented pipe.

Pipe jacks with an internal diameter greater than 1200mm were ideally sought. The fitting of instrumentation and a protective liner to the instrumented pipe reduces the diameter by about 300mm and 900mm was at the time the minimum diameter for man-entry. A further factor was the use of lubrication; pipe jacks were preferred where a lubricant could be introduced part way into the drive to assess its effectiveness on reducing jacking loads. Uniform and simple overburden conditions, i.e. uniform cover with little or no live loading, were required to simplify data interpretation. Packing material was specified as medium density fibreboard or chipboard because joint pressure cells were calibrated on these materials.

Considering the above factors, the ideal requirements were summarised – Table 4.1 – for circulation to Clients and pipe jacking contractors. The sequence of schemes was not important but was subject to site availability.

Scheme	6	7	8	9	10
Ground	Stiff glacial clay	London Clay	Sand/gravel	Soft clay	Soft clay or cohesionless
Pipe size (I/D mm)	1200 mm	1200 mm	1200 mm	1200 mm	1200 mm
Depth	< 10m	< 10m	< 10m	< 10m	< 10m
Length	> 100m	> 100m	> 100m	> 100m	> 100m
Lubrication	No/yes	No/yes	No/yes	No/yes	No/yes
Packer	Medium density fibreboard or chipboard				
Excavation	Hand/TBM	Hand	TBM	Hand/TBM	Hand/TBM
Monitoring period	Short term				

**Table 4.1** Ideal site requirements.

#### 4.2.2 Available sites

The search for available sites was initiated by sending copies of Table 4.1 to the five sponsoring Water companies and members of the Pipe Jacking Association. Unfortunately, the choice of schemes was led not by ideal requirements, but by any sites available within the Water companies' areas and as it ensued, also within the remit of a non-sponsoring water company – Anglian Water. The available sites offered throughout the research period are listed by water company in Table 4.2.

Some of the schemes offered were, due to programming or ground conditions, unsuitable for the research and could easily be discounted – sites of interest that were pursued are highlighted within the table. The search for a drive in soft clay led to an interest in a major scheme in Bangkok, Thailand, which included many pipe jacks.

One of the sponsoring Water companies has an involvement in the design, build, and operate contract of the Bangkok scheme and initial enquiries were promising. However, due to the logistics involved with taking the fieldwork overseas, extra costs, programming, and initial difficulties on the scheme itself, it was reluctantly discounted.

It became apparent during the search for suitable sites that it would again not be possible to monitor a pipe jack in each of the five sponsoring Water companies' areas. Three Water companies, namely North West, Northumbrian and

Water Company	Location	Agent / Consultant	Contractor	Pipe I D (mm)	Ground Conditions	Excavation	Proposed start date	Proposed end date
North West Water	Southport	Sefton Borough Council	Muller-Markham	1000	Alluvial Sand	TBM	February 1994	March 1994
North West Water	Fylde Coast (Contract III)			1800	Glacial clay / Alluvial sands	TBM	April 1994	May 1995
Northumbrian Water	Roker / Whitburn			2100	Rock / Boulder clay		July 1993	May 1994
Northumbrian Water	Seaham	Entec	Donclon	1800	Glacial clay	TBM	November 1993	November 1994
Severn Trent Water	Birmingham	Haswell		1200	Sandstone	Hand / TBM	1994	
Severn Trent Water	Walsall	Haswell		1200	Clay / Coal	TBM	1993 / 1994	
Severn Trent Water	Newark	Haswell		Various	Glacial clay		1994	
Thames Water	Leytonstone		Clancy	1500	London clay	Hand	November 1993	December 1993
Thames Water	East Barnet	L.B. Barnet		1200 / 2400	London clay		September 1993	September 1995
Thames Water	Cray Valley		Murphy	1600	Mixed face (Chalk and gravels)	TBM	January 1996	
Yorkshire Water	Bradford	Bradford City Council						
North West Water Consortium	Bangkok		Laserbore	Various	Very soft clay	TBM	1995	1997
Anglian Water	Thurrock		AMEC Tunneling	1500	Soft clay	TBM	January 1995	February 1995

Note Bold text indicates schemes in which an interest was shown

Table 4.2 Available schemes

Thames, had suitable pipe jacks within their respective areas Yorkshire Water had few pipe jacks so instead funded the fieldwork at Thurrock, an Anglian Water scheme. Although there were several pipe jacks within Severn Trent Water's area, none proved suitable. The company were however willing to fund the extra costs associated with the fieldwork to monitor a drive on a Thames Water scheme in the Cray Valley Unfortunately, the programme for this scheme was revised such that the drive of interest started outside the research contract period and could not therefore be monitored. As a consequence only four of the intended five pipe jacks were instrumented. The four schemes are discussed in detail below

### 4.3 SCHEME DETAILS

The geographical location of the four monitored pipe jacks are illustrated in Figure 4.1. Details of the drives are summarised in Table 4.3 and discussed in detail below. Except where indicated, a fully instrumented pipe as described in chapter 3 was used on each scheme.



Figure 4.1 Location of Stage 3 schemes.

Scheme No	6	7	8	9
Location	Leytonstone, East London	Southport, Lancashire	Seaham, Co Durham	Thurrock
Dates (start to finish of drive)	17/11/93 - 9/1/93	24/2/94 - 8/3/94	12/7/94 - 5/9/94	04/01/95 - 20/01/95
Ground type	London clay	Dense silty sand	Glacial till (clay)	Soft peaty clay
Pipe size (I/D mm)	1500	1000	1800	1500
Depth to axis (m)	8.5	5.6	6.95	6.2
Drive length (m)	75	160	310	250
Excavation method	Hand	Slurry TBM	TBM	Slurry TBM
Client	Thames Water	North West Water	Northumbrian Water	Anglian Water
Contractor	M J Clancy	Miller- Markham	J F Donelon & Co	Amec Tunnelling
Pipe supplier	ARC (spun)	Spun Concrete (spun)	C V Buchan (cast)	C V Buchan (cast)

**Table 4.3 Scheme details.**

### 4.3.1 Scheme 6 – Fillebrook Surface Water Sewer Relief Scheme

#### 4.3.1.1 Background

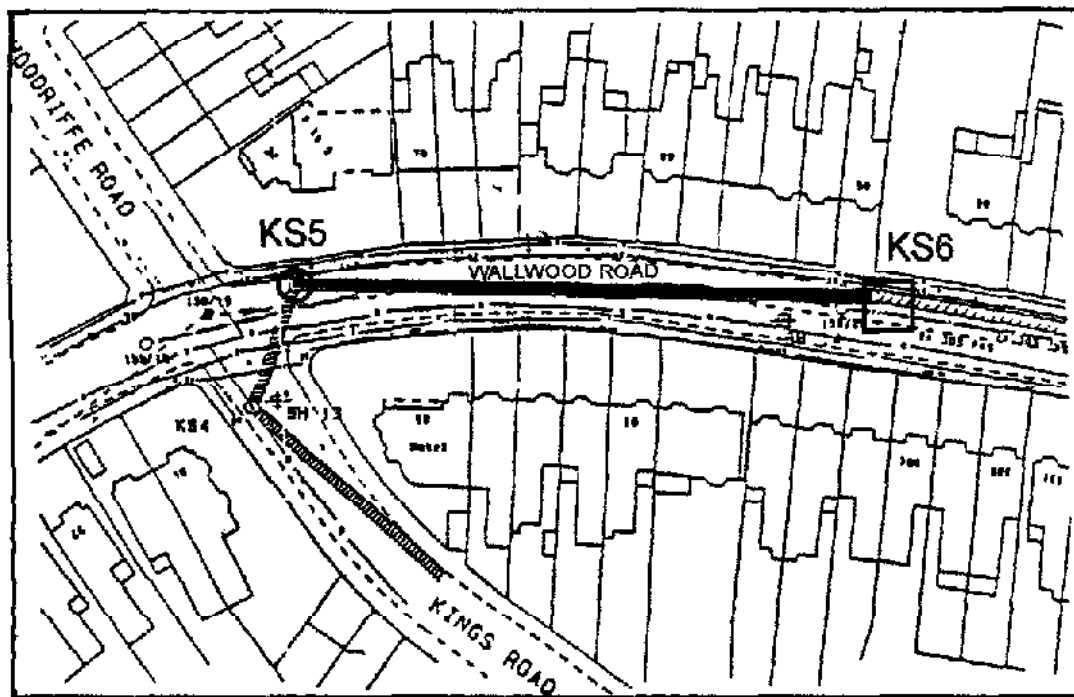
Scheme 6 was in Leytonstone, East London and formed part of the Fillebrook Surface Water Sewer Relief Scheme during November and December 1993. The Client was Thames Water, Contractor for tunnelling work was M. J Clancy and the pipe supplier was ARC.

The monitored drive was along Wallwood Road, Leytonstone – Figure 4.2. A 75m long drive wholly within London clay, the depth to axis was approximately 8.5m and pipe size was 1.5m internal diameter, 1.8m outer diameter. Excavation was carried out by hand using pneumatic tools within a simple steerable shield.

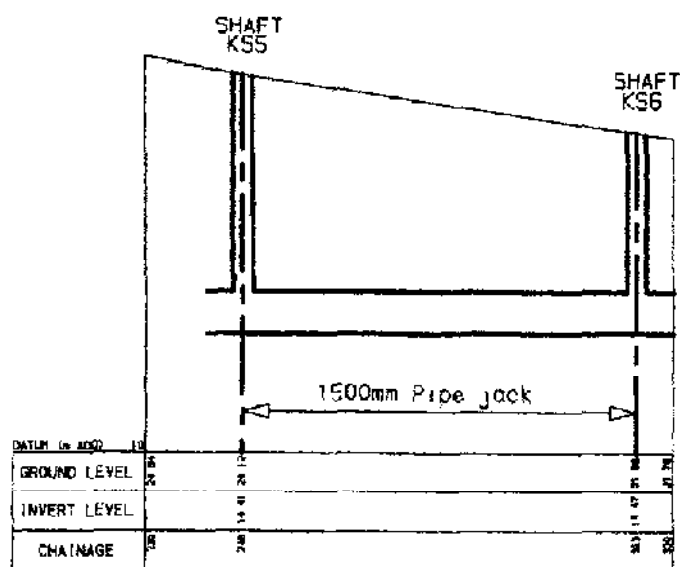
#### 4.3.1.2 Ground conditions

A site investigation was carried out around the area for the Client in November 1992. This comprised five boreholes to depths of 5.0 to 12.0m along the centre line of proposed tunnels. Representative disturbed and undisturbed samples were taken at regular intervals or at changes of stratum. Relatively unweathered highly plastic London clay composed of stiff grey fissured silty clay with sandy

laminations was encountered at depth. The material was classified as essentially firm to stiff, becoming stiff at depth (see Table 4.4).



(a) Site plan.



(b) Simplified long section.

Figure 4.2 Details of Scheme 6.



Depth (m)	Description	Triaxial Compression			
		Cell Pressure kPa	Bulk Density Mg/m <sup>3</sup>	Moisture Content %	Shear Strength kPa
1.50	Stiff orange-brown slightly sandy silty CLAY				
2.50	Firm to stiff orange-brown silty CLAY with pockets of sandy silt and traces of medium gravel	50	2.17	19.0	64
3.50	Water				
4.55	Stiff brown blue-grey veined fissured silty CLAY with pockets of sandy silt and rootlets	90	1.98	27.2	80
6.00	Stiff brown blue-grey veined fissured silty CLAY with occasional pockets of sandy silt	120	1.93	27.1	84
7.55	Stiff grey fissured silty CLAY with occasional pockets of silty fine sand	150	2.04	24.7	102

**Table 4.4 Results of Unconsolidated Undrained Triaxial Compression Tests – Scheme 6.**

In addition to the Client's site investigation, Cambridge Insitu were commissioned by the research project to carry out a series of self-boring pressuremeter tests before tunnelling work commenced. Eight undrained expansion tests were carried out in two boreholes close to the proposed tunnel axis to a maximum depth of 11m. Results from the pressuremeter tests are summarised in Table 4.5. The undrained shear strengths determined from the tests, together with those from the Client's investigation, are also shown in Figure 4.3. At tunnel axis level – about 8.5m – the total horizontal stress measured was about 330 kPa and the initial shear modulus<sup>3</sup>,  $G_i$ , averaged about 50 MPa.

A more reliable method for obtaining an estimate of the shear modulus is to take the slope of the chord of the unload/reload loops. Average values from the

<sup>3</sup> Value of the shear modulus obtained from the initial slope of the pressure versus cavity strain relation prior to material yield. This initial value can be strongly affected by disturbance caused by insertion of the pressuremeter.

unloading/reloading tests are  $G_{ur1} = 23\text{MPa}$  at an amplitude of 0.38% cavity strain, and  $G_{ur2} = 20\text{MPa}$  with an amplitude of 0.46% cavity strain

Test	Depth m	$P_0$ kPa	$s_u$ kPa	$G_r$ Mpa	$G_{ur1}$ Mpa	$G_{ur2}$ Mpa	$P_l$ kPa
B1T1	6.4	287	94	90	18	14	997
B1T2	7.4	327	92	55	27	20	1001
B1T3	10.1	329	97	56	26	22	1012
B1T4	11.1	349	141	50	28	24	1121
B2T2	6.8	328	112	35	20	18	1050
B2T3	8.0	369	89	45	17	18	1011
B2T3	9.0	289	159	14	25	20	1134
B2T5	10.0	292	150	95	24	24	1169

**Table 4.5 Results of pressuremeter tests – Scheme 6**

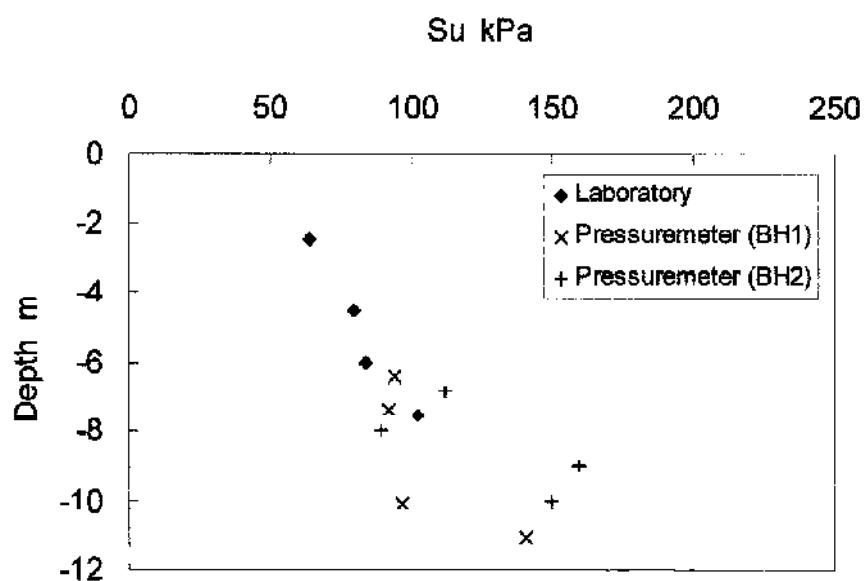


**Figure 4.3 Undrained shear strength – Scheme 6.**

#### 4.3.1.3 Monitoring Work

Jacking forces were recorded from the start of the drive by fixing jack load cells to the end of the rams on the jacking rig – shown in Plate 4.1. The rams had a short stroke and required the use of spacers to fully push home 2.5m pipes. The jacking rig consisted of four hydraulic rams, but due to a faulty hydraulic seal on one of the cylinders, only two of the four rams were used. Lubricant slurry was little used

during the drive but most pipes were inserted wet due to water falling onto them from a ruptured drain in the top of the jacking pit.



**Plate 4.1** Scheme 6 jacking pit.

The joint pressure cells described in chapter 3 could not be used because the jacking pipes used on this site were of the in-wall type – Figure 4.4. The instrumented pipe was inserted at Pipe 11, 27.5m behind the shield. Modification to all twelve contact stress cells was not complete before the start of the monitoring work; only five cells of the twelve had pore pressure transducers.

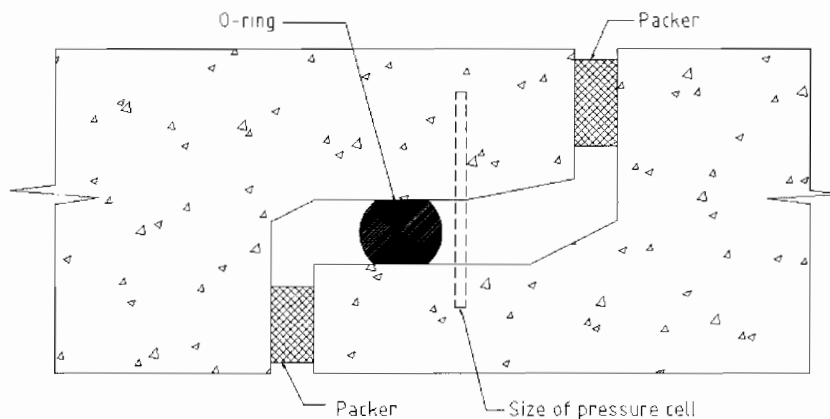


**Figure 4.4** In-wall pipe joint.

Excavation was carried out by hand using pneumatic "clay spades" to break up the face – see Plate 4.2. Spoil was shovelled into a wheeled skip to be then pushed by the miner's assistant through the pipeline into the jacking pit for extraction by crane. Plate 4.3 shows excavated material in a skip on the surface. Instruments in the pipe were protected from the skips by a steel liner.

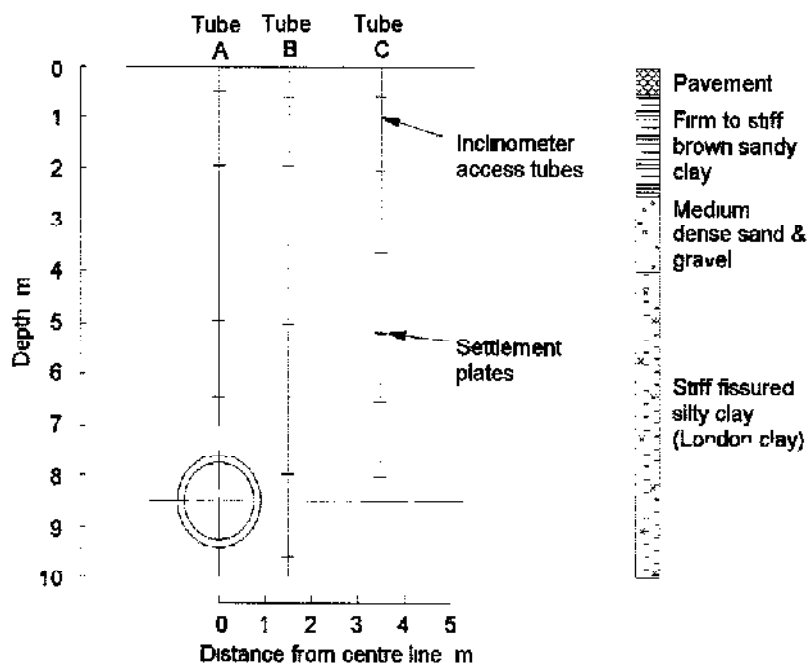
Scheme 6 ground instrumentation is illustrated in Figure 4.5. Ground movement instrumentation comprised three inclinometer access tubes with settlement magnets and an array of road nails. Push-in pressure cells were installed close to the line of the tunnel to record changes in ground stresses close to the tunnel. The thin blades of the spade cells were positioned to record in-situ total stresses and pore water pressures perpendicular to the line of the tunnel as the pipe jack approached and passed. A miscalculation in installation depth of the pressure cell over the tunnel centre line resulted in it being uncovered at the face of the excavation.



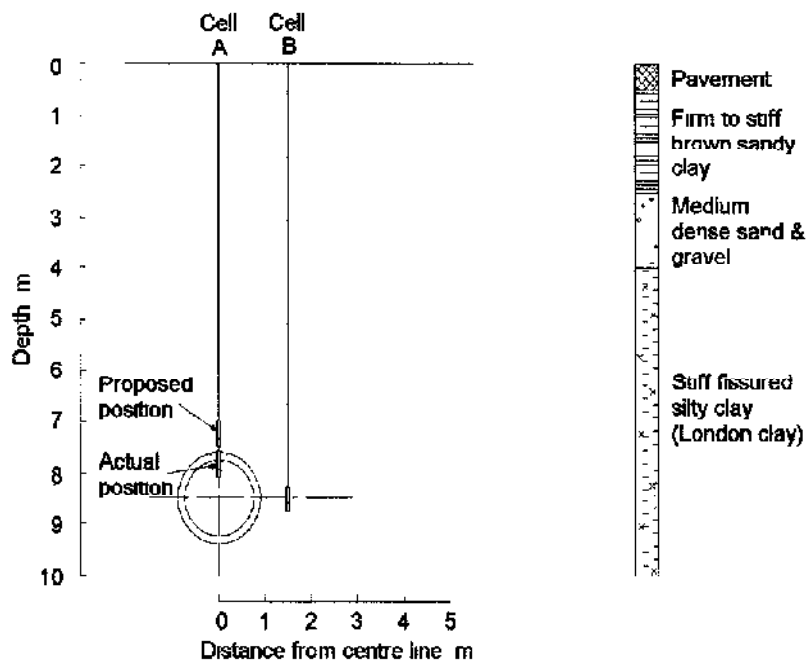
**Plate 4.2** Scheme 6 face.



**Plate 4.3** Excavated material – Scheme 6.



(a) Array A –inclinometer access tubes.



(b) Array B –push-in pressure cells.

Figure 4.5 Scheme 6 ground instrumentation.

### 4.3.2 Scheme 7 – Southport Coastal Waters Interceptor Tunnel, Nevill Street Microtunnel

#### 4.3.2.1 Background

The second monitoring exercise for Stage 3 research took place in Southport. The overall scheme was for the construction of 5.3km of interceptor sewer, using segmental tunnelling, for North West Water. It involved intercepting three existing outfalls and also the construction of two new spurs using microtunnelling techniques. The Sub-Contractor employed to carry out the microtunnelling was Miller-Markham, an association between Miller Civil Engineering and Markham (tunnelling machinery manufacturer). The steel banded jacking pipes were supplied by Spun Concrete. One of the microtunnels, in Nevill Street (see Figure 4.6), was identified as a drive of interest to this Research Project and the monitoring work commenced in February 1994.

The microtunnelling was carried out using a full-face slurry tunnel boring machine named the Miller-Markham "Super Mighty" – Plate 4.4. The fully lubricated drive, below the water table, was 160m long in dense silty sand. Average depth to axis was about 7.4m and the pipe size was 1.0m internal diameter, 1.2m outer diameter.

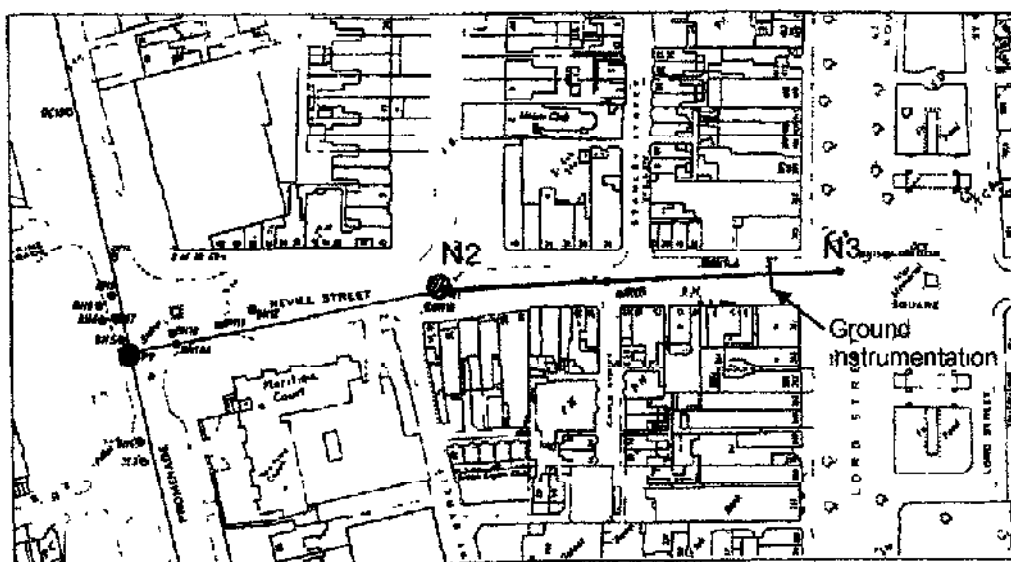
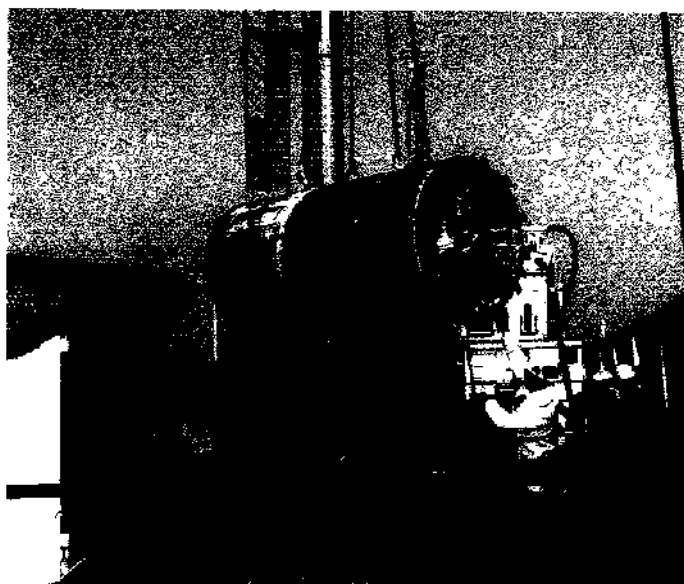


Figure 4.6 Scheme 7 site plan.



**Plate 4.4 'Super Mighty' slurry machine.**

#### 4.3.2.2 Ground conditions

The stratum below the road pavement to a depth of about 3.5m was aeolian sand, comprising medium dense silty fine sand. The tunnel passes through the stratum underlying the aeolian sand. This material is alluvium, consisting principally of medium dense grey fine sand. Bedrock, Mercia mudstone, typically lies at about 24m below ground level.

As part of the Client's site investigation, a borehole was sunk close to the centre line of the proposed microtunnel. Information from the borehole is summarised in Table 4.6. Results from Standard Penetration Tests (SPTs) are shown in Figure 4.7. The average N value in the alluvium is 16.

Depth (m)	Description
0.40	Road pavement - tarmac over concrete
1.80	WATER
3.60	Medium dense fine to medium SAND with occasional angular shell fragments up to fine gravel size. Rare angular fine to medium gravel to 1.50m
12.00 (end of borehole)	Medium dense silty fine SAND with occasional angular shell fragments up to 3mm. Becoming less silty with depth, medium sand content increasing. Organic in parts. Average permeability $2 \times 10^{-3}$ m/s. Shear strength parameters: $c' = 0 \text{ kN/m}^2$ , $\phi' = 43^\circ$

**Table 4.6 Borehole details – Scheme 7.**

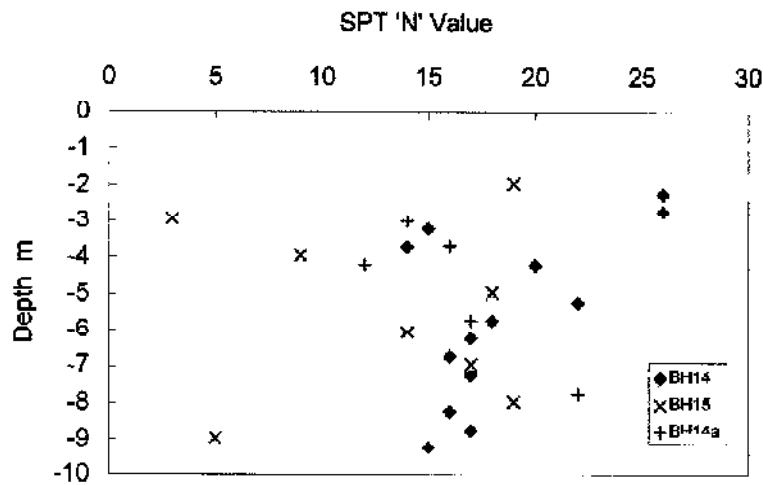


**Figure 4.7 SPT N values.**

Groundwater in Nevill Street was about 2.5m below ground level. During the site investigations variation in groundwater levels in any one observation well was minimal, typically less than 0.2m. Since readings were taken at roughly the same time each day, it was concluded that there is no significant tidal variation in groundwater levels.

#### 4.3.2.3 Monitoring Work

The "Super Mighty" variable speed thrust jack unit – shown in Plate 4.5 – was fitted with two hydraulic rams mounted either side of the jacking pipe. Two strokes of the thrust rams were required to complete the jacking of one pipe, achieved by inserting large pins into the assembly to move the reaction point from the front flange of the ram to the rear. The jacking unit was of a design that prevents the fixing of the jack load cells. To monitor jacking forces, pressure transducers were fitted to the hydraulic feed circuit to record change in output due to oil pressure variation – see Section 3.2.2. Output from the transducers was later converted to jacking forces by calibrating in controlled conditions the hydraulic pressures against load cells.

With ten pipes buried, the Celesco linear displacement unit developed a fault and could not be repaired. The main functions of this transducer – placed on the jacking rig – were to record any pushing event and the length of stroke against time. Having recorded the constant stroke lengths during the pushing of ten pipes, only the



start of, end of, and delays during pushes were recorded by hand subsequent to the failure. Since the change in hydraulic oil pressure during pushing is logged against real time, the oil pressure records confirm the noted push times.

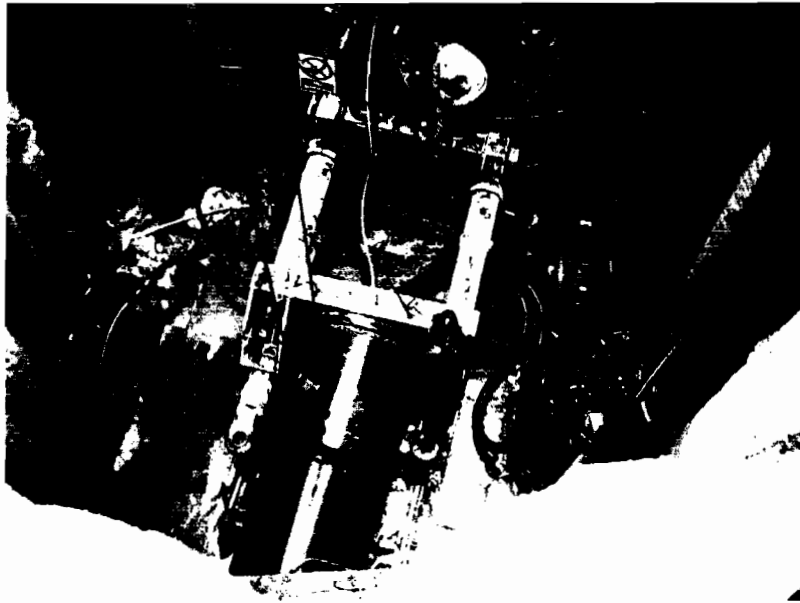


**Plate 4.5 'Super Mighty' jacking unit.**

The pipes were brushed with "Clay cap" – a lubricant – before lowering to the jacking pit. Also, a slurry lubricant was pumped from the start of the drive, but due to a pump failure, there was a significant break in pumping the slurry. The effectiveness of the pumped lubricant is discussed in detail in chapters 6 and 7.

The jacking pipes used on the microtunnel were thin-walled, at 100mm thick, which again prevented the use of joint pressure cells. The instrumented pipe was positioned 2.5m behind the machine at Pipe 2. A protective liner was not required in this instance since man-entry was required only occasionally and spoil was removed through slurry pipes.

All twelve of the contact stress cells had been modified since the fieldwork of Scheme 6 to include pore pressure measurement. Fear of glue line failure around the cells with the possible catastrophic result of ground water inundating the pipeline and machine, led to an additional safeguard within the instrumented pipe of bolting steel straps behind each cell – illustrated in Figure 4.8.

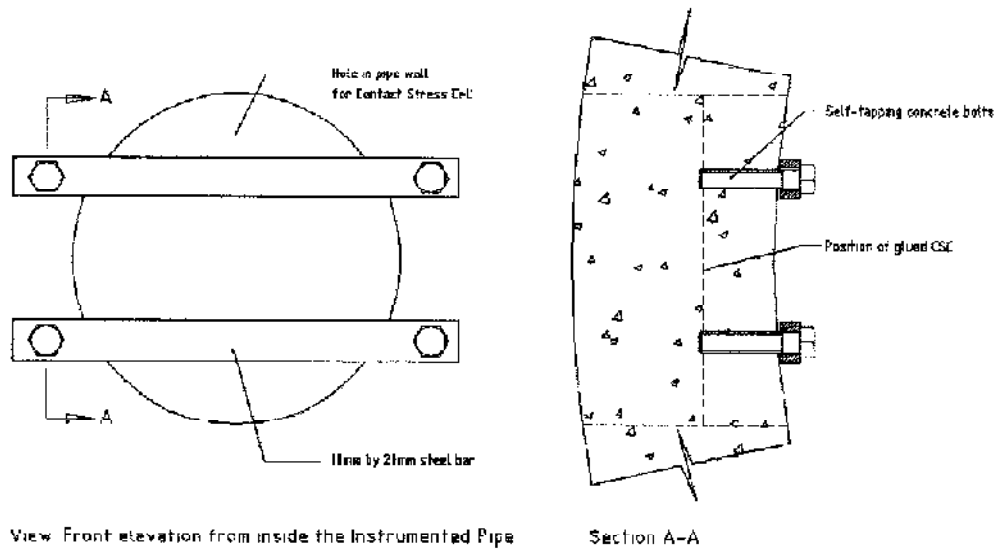


**Figure 4.8 Steel straps behind contact stress cells.**

Ground instrumentation comprised two vertical inclinometer access tubes with settlement magnets – illustrated in Figure 4.9 – and to monitor surface settlement, a series of studs driven into the road pavement

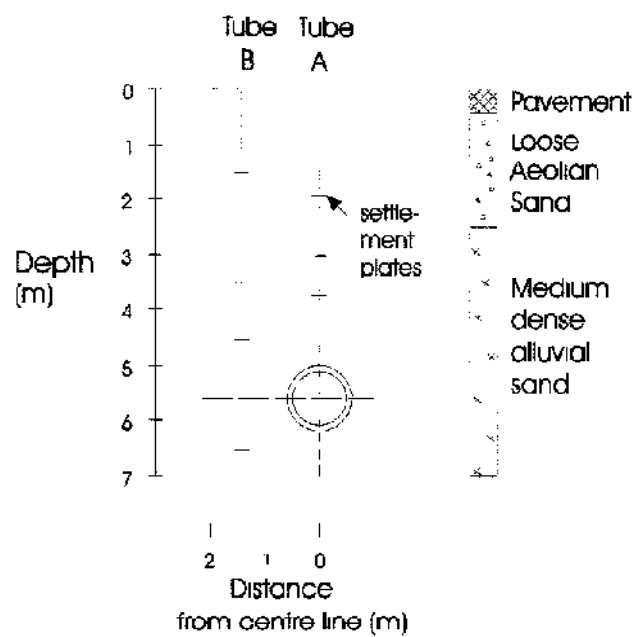


**Figure 4.9 Scheme 7 ground instrumentation.**

### 4.3.3 Scheme 8 – Seaham Bathing Water Scheme

#### 4.3.3.1 Background

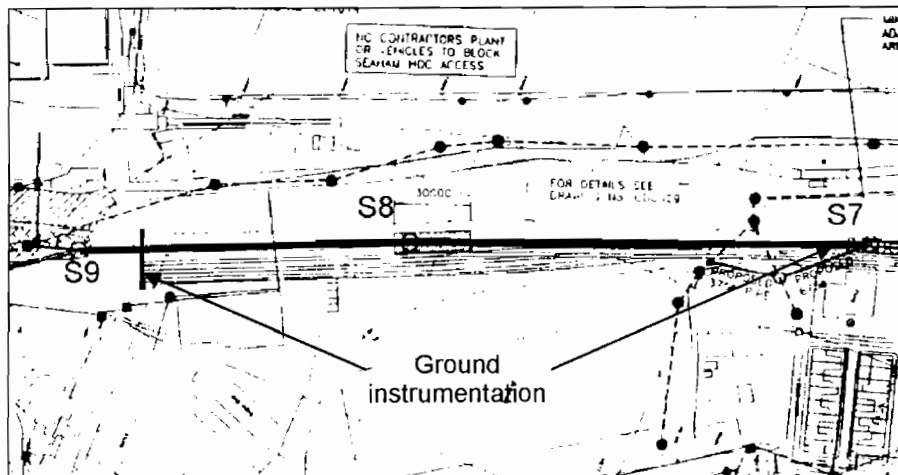
A North-South interceptor sewer, sewage treatment works and marine outfall at Seaham, County Durham together comprise the Seaham Bathing Water Scheme. The site is centred on the Seaham Harbour area and the site of the former Dawdon Colliery, located to the south of Seaham. The Client was Northumbrian Water and J F. Donelon was the Contractor employed to construct the sewer. As part of the works, several pipe jacks were required and one particular drive, S9 to S7 – see Figure 4.10 – had been identified at an early stage in the research for monitoring. Entec Engineering, Consulting Engineers to Northumbrian Water, were able to include research items in the Contract Documents before going to Tender. Tendering Contractors were therefore aware of the research fieldwork and could price for it accordingly. On all other Stage 3 schemes, due to shorter lead-in times, the research work was carried out contractually as variations to the Contract.

The monitored drive was a 1.8m internal diameter pipe jack (using C V Buchan steel-banded pipes) in stiff glacial clay with a depth to axis of about 7m. It was 310m long from jacking pit, S9, to reception shaft, S7, and was driven through an intermediate shaft, S8. Excavation was undertaken with a Lovat open-face tunnelling machine – Plate 4.6.

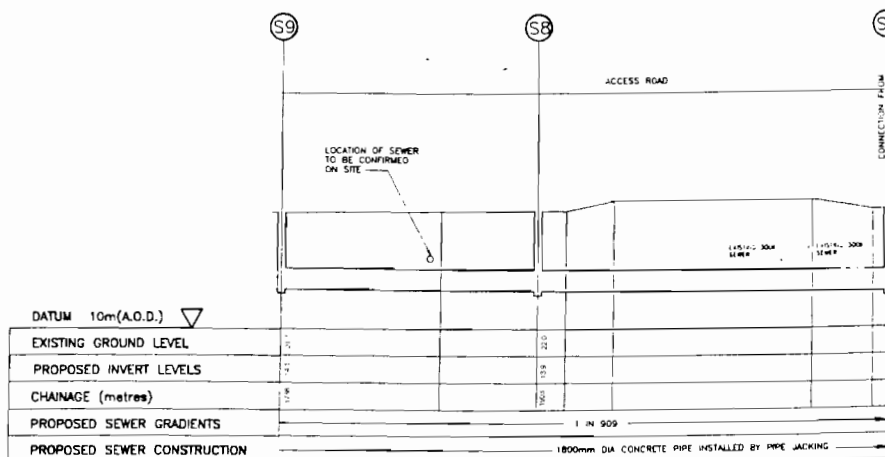
The Lovat machine advanced when excavating by pushing off the pipe string using six hydraulic rams at the rear of the machine. When the machine's rams were fully extended and in neutral, the jacking pipes were pushed up using the main jack rams in the drive shaft.

#### 4.3.3.2 Ground conditions

In the area of the monitored pipe jack below the road pavement the Client's Site Investigation indicated approximately 3m of made ground, comprising mainly colliery waste, overlying boulder clay to depth. Several boreholes were put down along the proposed centre line of the monitored drive of which details from one, including results from the laboratory testing, are summarised in Table 4.7 and Figure 4.11. Groundwater was encountered approximately 12m below ground level.



(a) Site plan.



(b) Longitudinal section.

Figure 4.10 Scheme 8 details.

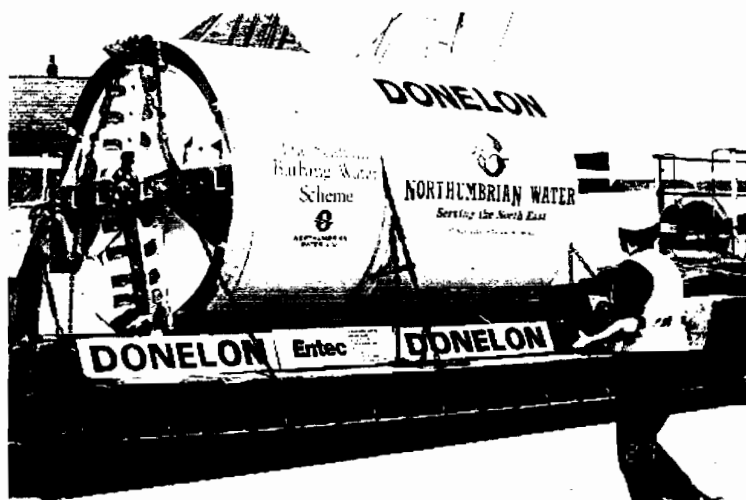
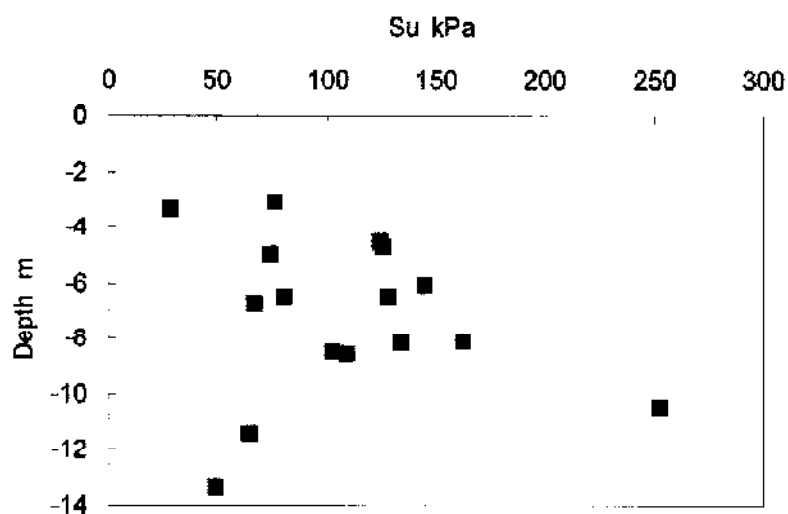


Plate 4.6 Lovat tunnelling machine.

Depth (m)	Description	Triaxial Compression			
		Cell Pressure kPa	Bulk Density Mg/m <sup>3</sup>	Moisture Content %	Shear Strength kPa
3 10	MADE GROUND includes tarmac road pavement				
4 25	Grey brown sandy CLAY with a little fine to medium gravel	85	2 23	17	124
5 80	Stiff becoming very stiff dark grey brown sandy CLAY, with much fine to coarse gravel	120	2 25	16	144
8 20	ditto becoming very stiff with occasional cobbles	164	2 39	12	102
11 10	ditto	222	2 09	14	64
11 85	WATER				

**Table 4.7 Results of Unconsolidated Undrained Triaxial Compression Tests – Scheme 8.**



**Figure 4.11 Undrained shear strength – Scheme 8.**

#### 4 3 3 3 Monitoring Work

As with the microtunnel on Scheme 7, the jacking rig – Plate 4.7 – had an integral thrust ring fixed to the rams and it was not therefore possible to use the load cells to directly monitor jacking forces. Hydraulic oil pressures were measured and later converted to jacking loads using calibration coefficients determined against the

load cells – see Section 3.2.2. An IBS linear displacement unit to monitor forward movement of the jack rams replaced the previously damaged Celesco unit.

Lubrication was not used during the pushing of the first ten pipes, but after that a bentonite-based lubricant slurry was pumped regularly. Times of lubricant pumping were noted in the author's site diary.

For the first time during Stage 3 fieldwork, the pressure cells were used in the joint of the instrumented pipe. A steel liner was again employed within the pipe to protect instrumentation against mechanical damage. To ease instrument retrieval on completion of the drive, it was inserted at Pipe 74 – approximately 185m behind the machine – so that its final position would be in the intermediate shaft, S8.

There were several delays during the drive due to the machine encountering large boulders. By retracting the machine head, access was possible to enable boulders to be broken into smaller manageable fragments manually using pneumatic tools. The smaller pieces were then manhandled or passed along the conveyor belt for removal.

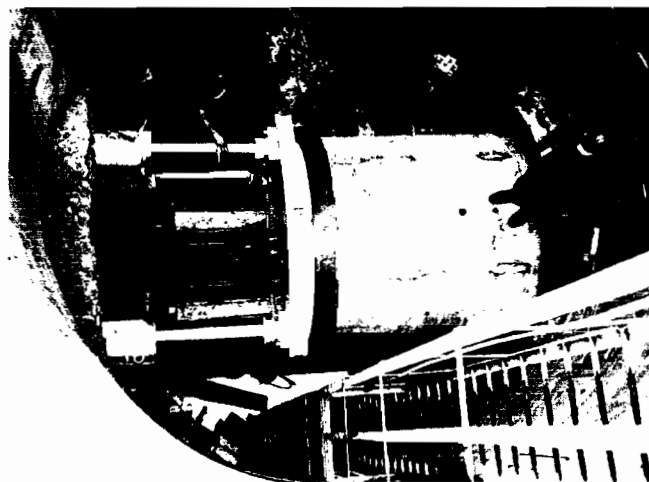


**Plate 4.7 Scheme 8 jacking rig.**

In addition to the inclinometer access tubes, settlement magnets and surface settlement points, shown in Figure 4.12, an array of electro-levels was also used to monitor ground movements. Ten electro-levels were installed in a near-horizontal tube from the reception shaft – illustrated in Figure 4.13. The tube was installed close to the tunnel crown to record vertical ground deformation as the machine and pipe

string passed below To log the distance from the face to the tube, the author spent three days in the tunnelling machine recording the rate of advance of the machine relative to the pipe string – the machine can advance by about 1.7m ahead of the lead pipe. Using this information with that of the distance travelled by the pipe in the jacking pit using linear displacement data – and knowing the number of pipes in the pipe string, the distance from the face to the instrumented tube was accurately calculated

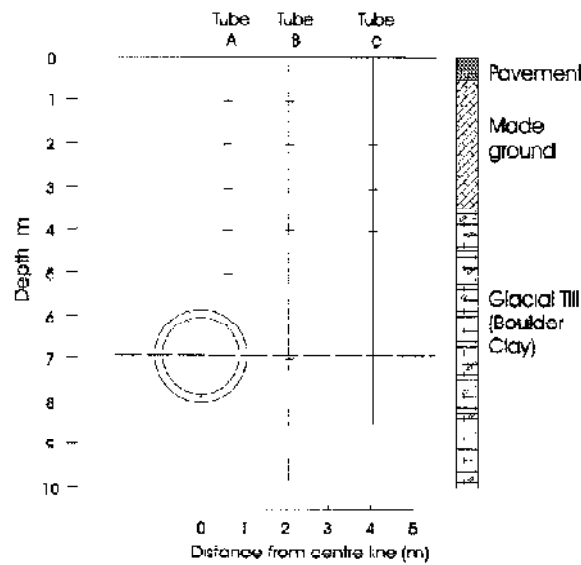


Figure 4.12 Scheme 8 ground instrumentation.

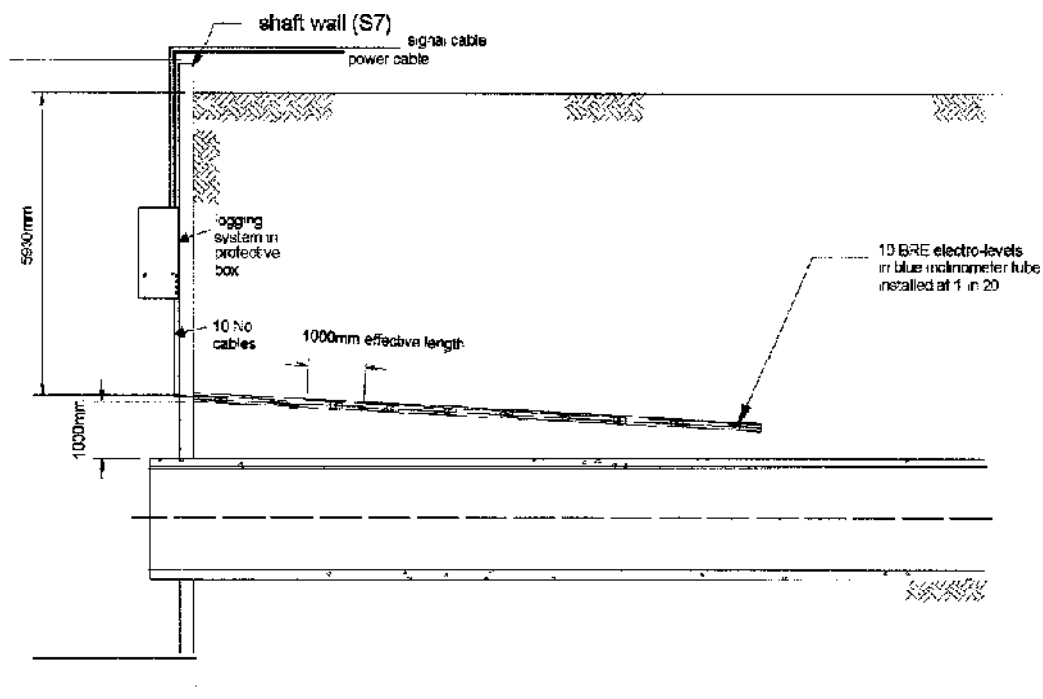
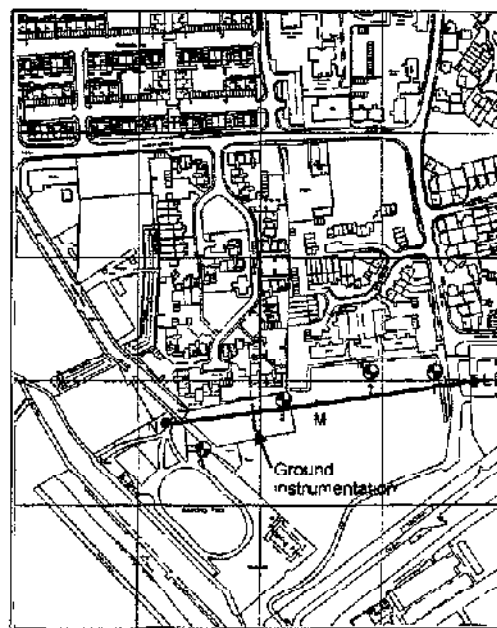


Figure 4.13 Scheme 8 electro-level arrangement.

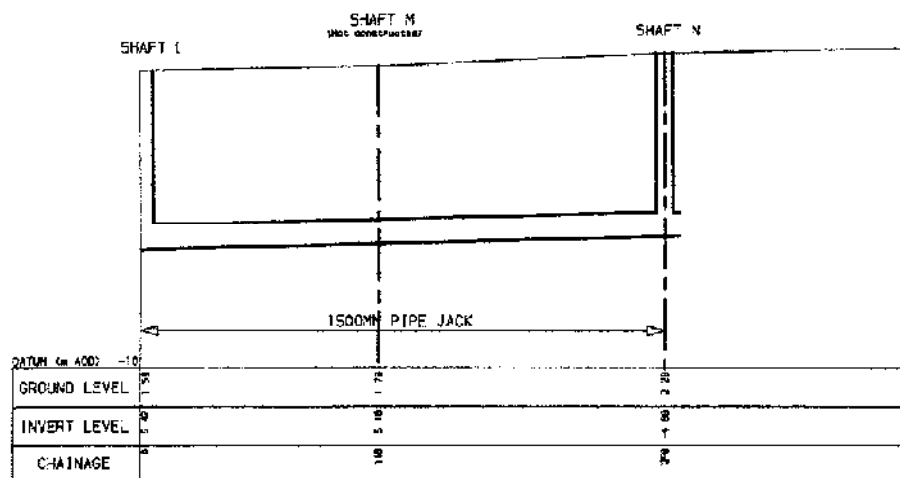
### 4.3.4 Scheme 9 – Thurrock Southern Trunk Sewer

#### 4.3.4.1 Background

Few details are known about this scheme as the Client, Anglian Water, are a non-sponsoring water company. The Contractor awarded the phase of works in which the monitored pipe jack was included, was AMEC Tunnelling. The pipe jack from Shaft L to N – Figure 4.14 – was a 260m long slurry machine drive in soft clay. The size of pipe was 1.5m internal diameter and cover depth varied between 5.5m and 6m. The steel banded jacking pipes were again supplied by C V Buchan.



(a) Site plan.



(b) Longitudinal section.

Figure 4.14 Scheme 9 details.



#### 4.3.4.2 Ground conditions

The ground type through which the pipe jack was driven was soft peaty clay. Table 4.8 describes the soils types – extracted from the client’s site investigation. Results from laboratory tests pertaining to boreholes 1 to 4 are shown in Figure 4.15.

Depth (m)	Description
1.80	WATER (G.W.L. close to 0.00m A.O.D.)
2.20	Soft to firm grey and brown silty CLAY
4.20	Soft to very soft silty CLAY with occasional green brown rotting fibres with strong organic odour
5.10	Soft to firm clayey PEAT
7.10	Very soft grey silty CLAY with some green brown rotting fibres and a strong organic odour
9.60	Dense fine to coarse GRAVEL and grey sand
15.20	Dense medium to coarse grey SAND and coarse gravel
18.50 (end of borehole)	Weak CHALK with some firm to coarse flint gravel

**Table 4.8 Borehole details – Scheme 9.**

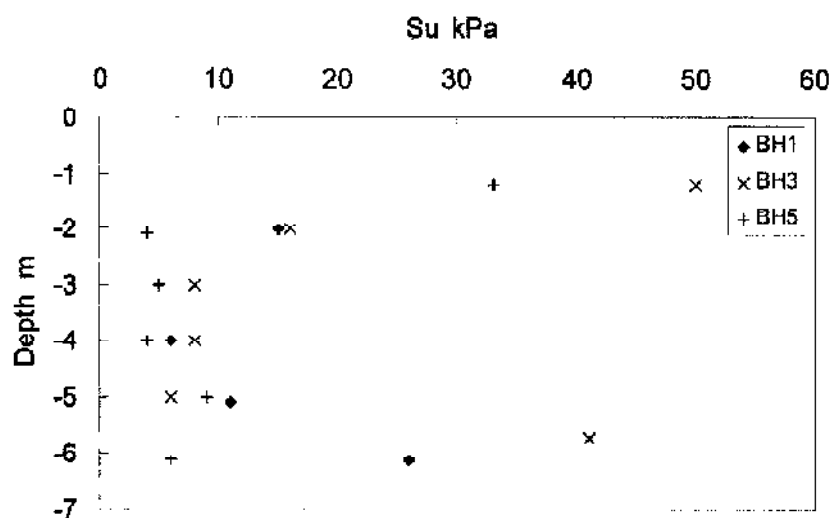


**Figure 4.15 Undrained shear strength – Scheme 9.**

#### 4.3.4.3 Monitoring Work

Some of the pipe jacking team, including the machine operator and the pit bottom men, were familiar with the research operation as they were previously employed by Lilley – subsequently taken over by AMEC Tunnelling – on the

monitored drive of Scheme 5, Cheltenham. This made for a smooth running fieldwork exercise. The Contractor operated double shifts so monitoring work was shared between the Research Assistant and an Oxford University technician.

Jacking forces were monitored by fixing load cells to the four rams of the jacking rig. The drive was unlubricated for 130m but lubricant slurry (bentonite-based) was introduced following a weekend break and was pumped for the remainder of the drive. The instrumented pipe was inserted at Pipe 19, 47.5m behind the machine, immediately in front of an interjack station. Pressure cells were placed in the joint between the instrumented pipe and the lead interjack pipe. Since man-entry was infrequent and the slurry spoil was removed through a pipe, a protective steel liner was not required.

The slurry machine experienced severe roll during the drive resulting in pipes as far back as Pipe 25 rolling also. Operators of this type of machine generally counteract roll by reversing the direction of the cutterhead while excavating. The clay being excavated however, was too soft for the cutterhead to "bite into" and the machine roll could not easily be corrected. As that particular machine has three steering rams at its articulation joint, the machine roll also made it difficult for the operators to steer to line and level.

Ground instrumentation comprising three inclinometer access tubes and two push-in pressure cells are illustrated in Figure 4.16. An array of settlement points was again installed on the surface to measure settlements perpendicular to the drive direction. A planned second use of the electro-levels did not occur due to the Contractor misunderstanding the specialist nature of installing a near horizontal inclinometer tube for the sensitive instruments.

## **4.4 INSTRUMENTATION**

### **4.4.1 Installation**

The instrumented pipes were manufactured to the author's specification – Figure 4.17 – with enough lead-in time for the pipe to gain 28 days strength. Holes for contact stress cells were either cast or drilled at the works, depending on the manufacturing process, to a high tolerance (+1.0mm, -0.0mm of the instrument diameter). As the fit of these instruments in the pipe wall was crucial to the research, a

specially built dummy cell was provided for the manufacturer to check the tolerance of the holes before shipping the pipe to site. The pipe suppliers generally waived any additional costs for the manufacture of the special pipes.

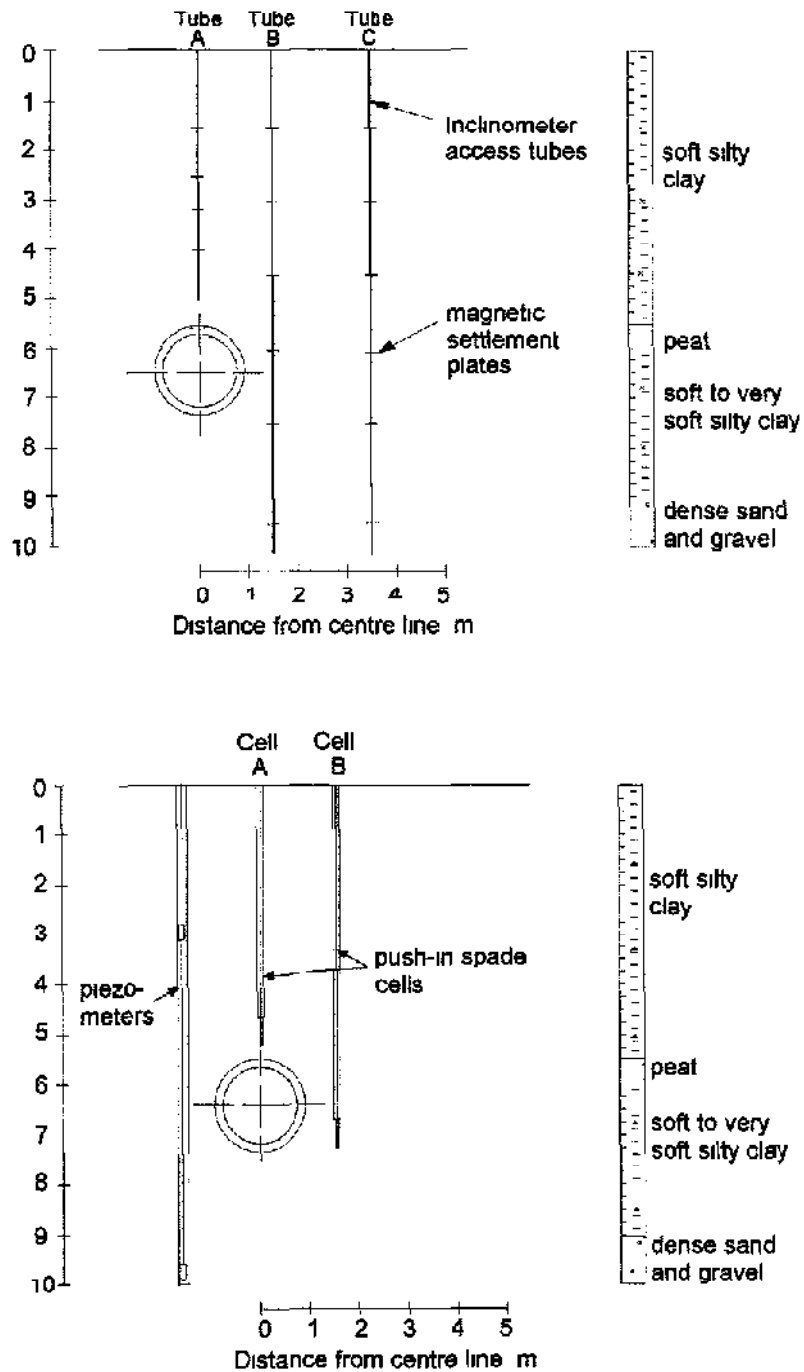
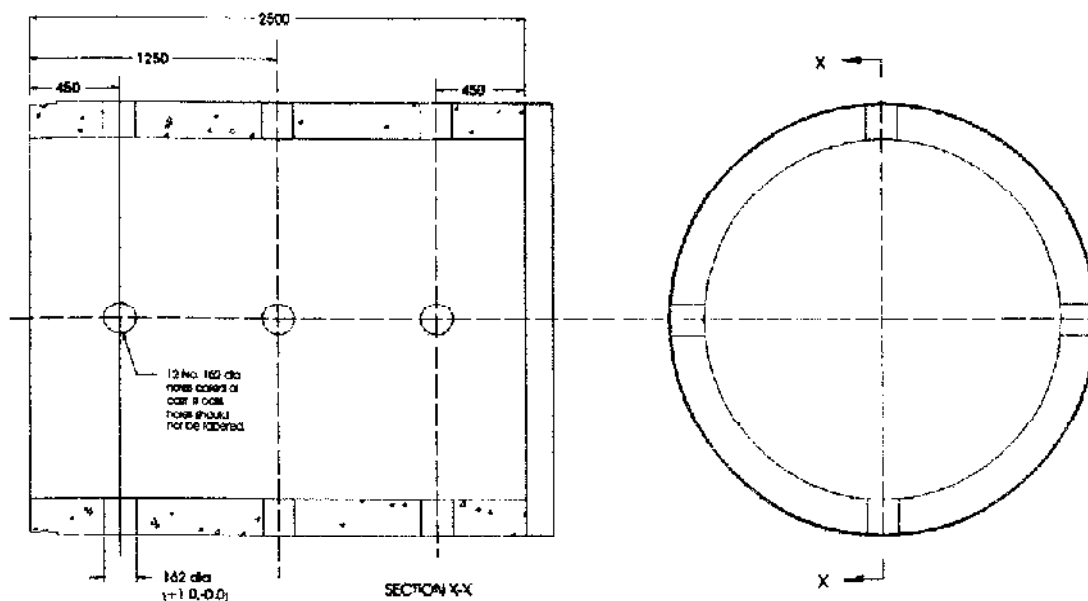


Figure 4.16 Scheme 9 ground instrumentation.



**Figure 4.17 Special pipe.**

Instrumentation was fitted into the special pipe on site by the author and an aide. Fitting out the instrumented pipe and testing the instrumentation would typically take about five days. Firstly the CSCs were glued into the pipe wall with a two-part structural adhesive. The active face of the instruments were held flush to the outer surface of the pipe by a specially built hand-held frame. On the glue "going-off", any gaps between CSC and outer surface of the pipe were filled with a cement grout. Tube extensometers would next be fixed to the inside of the pipe by drilling and screwing into the concrete followed by the fixing of the data acquisition boxes. Finally, if used, the flat pressure cells were glued to the packing material at the rear of the pipe.

Instrumentation in the pit bottom was installed by the author under the supervision of the Contractor's Engineer in a position away from potential damage from the lowering of jacking pipes. Jack Load Cells were fitted only to the jacking rigs of Schemes 6 and 9. They were fixed to the end of the hydraulic jacks by welding a mating plate to the ram ends. On Schemes 7 and 8, where due to the design of the jacking rigs, the load cells could not be fitted during jacking operations, pressure transducers on 'T-piece' fittings were installed on the hydraulic circuit close to the feed on the rams, Plate 4.8.

therefore required. The liners were based on the design shown in Figure 4.18 comprising two halves resting on a timber cradle with ramps in the leading and trailing pipes. It was designed to allow the two halves of the liner to slide by 10mm relative to each other and avoid a significant stiffening response of the concrete pipe. When installed in the pipe, the liner caused a constriction by reducing the internal diameter by about 300mm. The final design therefore was agreed with the Contractor to optimise the constriction.

On Scheme 6 a circular liner, based on the Norris (1992b) design, was used. The large skips used on Scheme 8 however, required the use of a non-circular liner, Figure 4.19. A major disadvantage with the non-circular design became evident when pipe roll occurred as shown in Plate 4.10. The locomotive drivers took considerable care when taking skips through the instrumented pipe but some contact between liner and skips was inevitable.

### **4.4.3 Performance**

#### **4.4.3.1 Jacking Pit**

The Celesco linear displacement unit proved to be less than robust in the adverse conditions of the jacking pits. It failed during the monitoring on Scheme 6 and was repaired by the author. On Scheme 7 another failure resulted in it being discarded. On this particular scheme, the Contractor's instrumentation on the jacking rig included a similar unit – but of a far more robust design – to monitor length of stroke. Enquiries by the author led to the purchase of the same type of unit for use on Schemes 8 and 9 where it was employed with few problems.

The jack load cells were of a robust design and performed very well throughout the fieldwork producing consistent data. Mistreatment by some of the Contractors' employees on decommissioning, resulted in shearing some of the bolts fixing the domed head to the main body of the instrument. These were easily repairable in the laboratory between schemes.

The continued breaking of cable connectors at the introduction of new pipes resulted in an accumulation of dirt on the pins that caused a loss of signal. The author regularly maintained and cleaned the cable connectors in the pit bottom and the pipeline to avoid signal loss where possible.

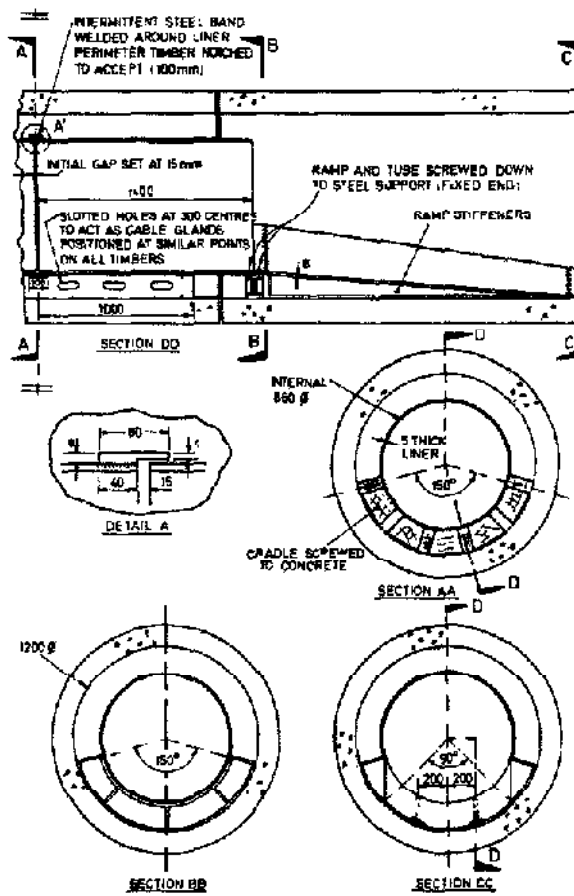


Figure 4.18 Circular liner (after Norris, 1992b).

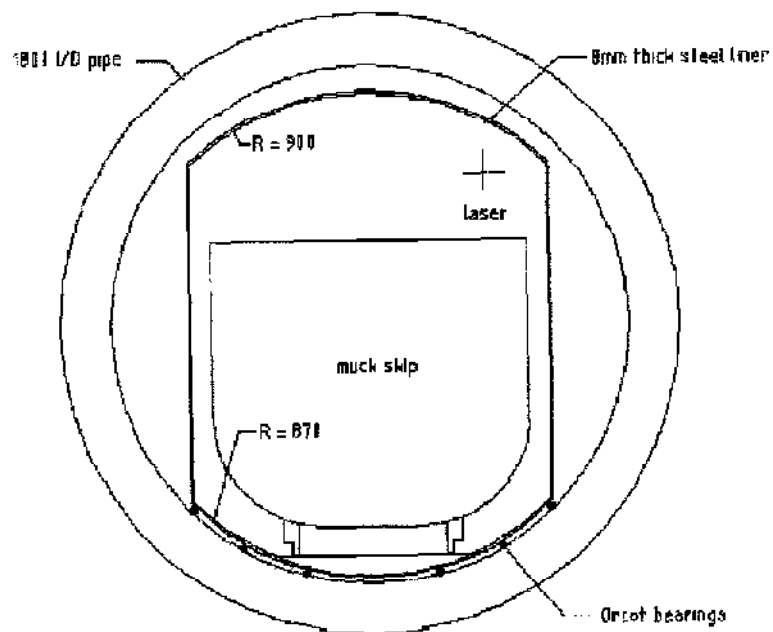
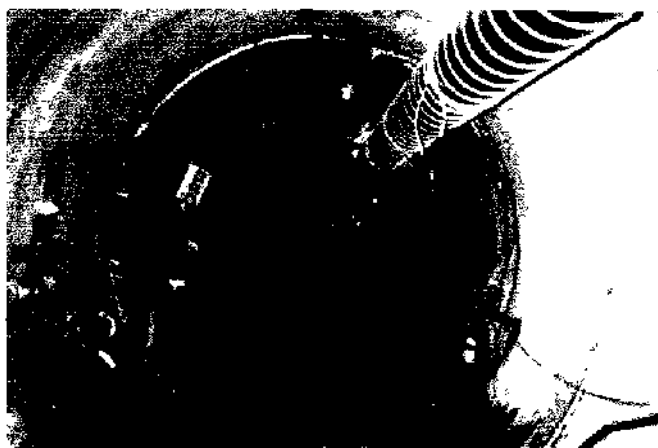


Figure 4.19 Non-circular liner used in Scheme 8.



**Plate 4.10 Scheme 8 liner in position.**

#### 4 4 3.2 Instrumented Pipe

All instruments in the instrumented pipe performed well in the adverse environment of an active pipe jack. Temperature within the instrumented pipe was found to be constant and there was therefore no temperature effect on instrumentation. Only on Scheme 9 were there glue line failures around the contact stress cells. The pipe supplier had not been able to test the contact stress cell holes with the dummy cell and two holes were slightly oversized resulting in both having glue line failures part way into the drive.

The data acquisition units, notwithstanding problems with dirt in the cable connectors, were reliable and performed very well. On Scheme 6 however, as a result of a general systems failure it was necessary to delay the Contractor by three hours to remove the protective liner for access to the boxes. The failure was traced to a faulty power cable connector and not the electronics.

#### 4 4 3 3 Ground instrumentation

The push-in pressure cells provided useful data on the relative change of horizontal soil pressures and with the exception of the built-in piezometers, the performance was satisfactory. In the stiff clay of Scheme 6, it has been suggested (Tedd et al 1984) that the cells may over-read by about half the undrained strength.

The reed switch probe used to measure depth to the magnetic settlement plates was not sufficiently accurate to monitor the small sub-surface movements of the magnetic settlement plates.

During heavy rain on Scheme 9, the inclinometer logger failed when taking a set of readings. Several useful data were lost at a critical time as the failure occurred as the machine approached the array of inclinometer access tubes. The logger was returned to Soil Instruments Ltd for repair the following day where it was discovered that such loggers should not be used unprotected during heavy rain. This came as a surprise as the loggers are invariably used outside and should be robust enough to operate in conditions of wet weather.

The use of electro-levels to measure subsurface ground movements was a resounding success, the only disappointment being that they were not used on more than one scheme. The accuracy of the resulting data was an order of magnitude greater than that from the inclinometer and settlement plates.

#### 4.4.4 Retrieval

On Schemes 6, 8 and 9, the special pipe was left in-situ. Instruments fixed to the pipe wall, and the data acquisition boxes were easily retrieved following removal of the protective liner when used. Once the pipe was stripped of on-wall instruments, the contact stress cells were recovered by specialist drilling contractors who over-cored concrete plugs containing the instruments – Plate 4.11. The resulting holes were made good by the Contractor. Pressure cells in the pipe joints were removed by pushing apart the joint using the interjacks on Scheme 9 and breaking up the pipe on Scheme 8 (the final position of the instrumented pipe being in an intermediate shaft).



Plate 4.11 Over-coring contact stress cells (Scheme 6).



For Scheme 7 the instrumented pipe was pushed through into the reception shaft, lifted out and taken to the Contractor's compound. On this relatively small pipe (1000mm internal diameter), retrieval of instruments was made much easier. Contact stress cells were removed from the pipe wall by over-coring from outside – the drill bit and drilling rig were together too long to core from the inside.

#### 4.5 DATA HANDLING

Signals from the 120 channels of the pipe jacking instruments were sampled at 2 second intervals throughout the monitoring periods. This resulted in large amounts of raw data, in ASCII format, being generated – typically 15Mb to 20Mb per shift. A laptop computer was used to download data from the inclinometer logger and also for logging electro-level data on Scheme 8. All data collected during a shift were copied onto floppy diskettes as illustrated in Figure 4.20, with two copies made to keep in separate locations. A suite of programs was specially written to reduce raw data to manageable amounts and convert them to engineering units for analysis.

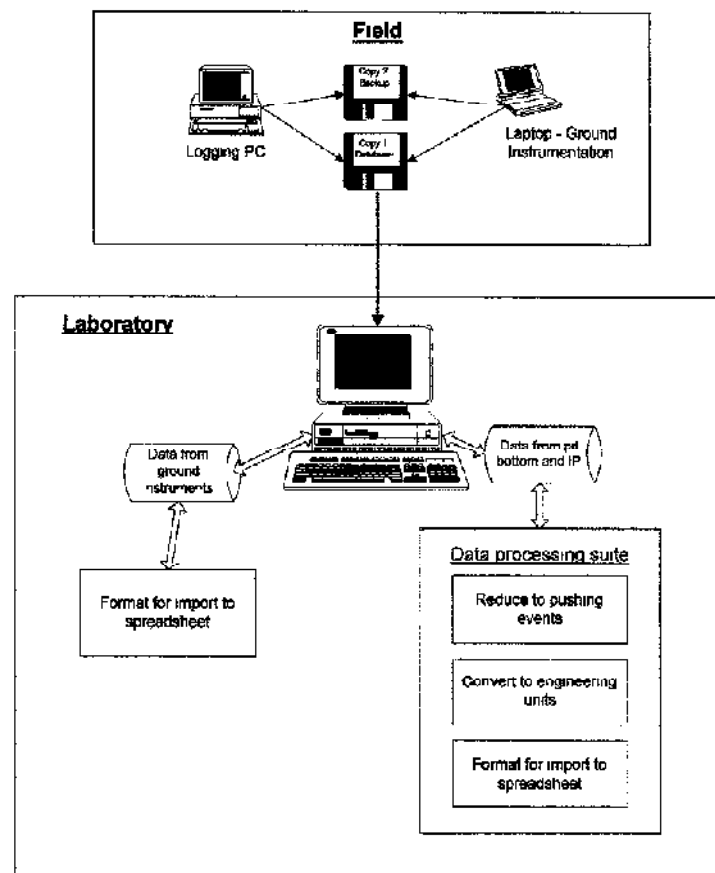


Figure 4.20 Schematic representation of data handling.

---

## chapter five

### jacking loads

## 5.1 INTRODUCTION

### 5.1.1 General Information

The jacking load is a combination of penetration resistance of the shield and frictional resistance to the pipes. Frictional resistance along the pipe string results from integration of skin friction over the contact area on the jacking pipe surface. Penetration resistance is the force required to push the shield into the excavation.

The accurate prediction of jacking loads is fundamental to the successful operation of pipe jacks. The predicted forces enable correct selection of jacking pipes, choice of excavation method, design of jacking pit and thrust wall, and the need for lubrication and intermediate jacking stations.

### 5.1.2 Penetration Resistance

Penetration resistance, commonly referred to as face resistance or face load, opposes the advance of the shield or boring head and varies according to the method of excavation. In open-face operations, including hand excavation and cutting head machines, penetration resistance is the force required to overcome the cutting edge resistance. In pressure balance operations, it is a combination of the contact pressure of the cutting face and hydraulic pressure supporting the face.

It is not the intention of this reported research programme to cover in detail penetration resistance. It has been researched in Germany and a review can be found in Stein et al (1989). An indication of the penetration resistance during the instrumented pipe jacks has been obtained from the jacking records at the intercept of the average increase in jacking resistance with the zero axis.

### 5.1.3 Frictional Resistance

Frictional resistance, also known as line friction, is influenced by many factors and is difficult to calculate. In this thesis frictional resistance is defined as the jacking force divided by the pipeline length and will be expressed in terms of force per unit linear metre. It is governed by ground related parameters – soil type, cover depth etc.

-- and construction-related factors including lubrication, misalignment and stoppages. Estimates of frictional resistance in the UK have until recently been based on the range of mean interface shear stress for different ground types given by Craig (1983). Recent publications based on results from the Oxford pipe jacking research – Pipe Jacking Association, (1996) and Milligan & Norris (1996) – provide calculation models to estimate frictional resistance in different ground conditions.

This chapter considers the frictional resistance for each of the Stage 3 schemes. A detailed examination into pipe-soil interaction follows in Chapter 6. Construction-related factors including the use of bentonite-based lubricants, pipeline misalignment and the effect of stoppages will each be investigated and where applicable compared to the data from the schemes of Stage 2 research.

## **5.2 JACKING RECORDS**

The measured jacking loads together with progress records for Schemes 6, 7, 8 and 9 are illustrated in Figures 5.1 to 5.4. Average frictional resistance (calculated using linear regression analysis) has been added to each graph.

### **5.2.1 Scheme 6**

The hand drive of Scheme 6 resulted in the jacking record shown in Figure 5.1. The miner excavated approximately 0.5m ahead of the shield throughout the drive and did not use the shield to trim the excavation, resulting in a face resistance of zero. Average progress throughout the drive was 4.3m per shift. The pattern of jacking load build up shows a peaky time dependent response where the magnitude of oscillation increases with drive length. Average frictional resistance is 12.7kN/m and an upper bound increase due to the restart forces is 19.6kN/m. A lower bound, or 'baseline' resistance to which the jacking load returns after stoppages is 8.5kN/m. The maximum increase in jacking load due to stoppage effects is 69% and occurred after the weekend break of 4th and 5th December. Shorter delays typically result in increases of between 20 – 30%. Stoppages are considered in greater detail later in the chapter.

There is no noticeable effect due to lubrication on the jacking loads. Lubricant injection sockets were not provided in the pipes, only within the shield. Bentonite

slurry was pumped on three occasions, and it is assumed that the volume was insufficient to fill the large and erratic overbreak

### 5.2.2 Scheme 7

The jacking records for Scheme 7 are presented in Figure 5.2. The penetration resistance, measured from the vertical axis using the average frictional resistance over the initial 25m, was 592kN. A prominent feature of the jacking record is the change in average jacking resistance ranging from 2.6kN/m to 41.6kN/m. Misalignment was negligible and ground conditions were relatively uniform from the available borehole logs. The change in jacking resistance therefore is assumed to be solely due to lubrication effects. In accordance with the Client's specification, each pipe was coated with a clay-cap polymer prior to insertion. In addition to this slip coating, bentonite-based lubricant slurry was pumped into the pipe string from the start of the drive. After jacking a distance of 25m however, the Contractor began to experience problems with the lubricant pump. At a distance of 70m jacked, the pump failed completely. A further 40m of pipeline was jacked during a two day period with no lubricant pumped and the average jacking resistance increased from 9.0kN/m to 41.6kN/m. On recommencing lubrication – with a replacement pump – the average resistance decreased to 3.1kN/m. The average progress per shift of 16.2m was not impeded by the enforced break in pumping lubricant.

The effect of lubrication is discussed in more detail later in the chapter.

### 5.2.3 Scheme 8

Lubrication and stoppage effects are evident in the 54 days of jacking records for Scheme 8 – Figure 5.3. Generally progress of 7.9m per shift was achieved on this long drive. The first 25m were driven unlubricated with an average frictional resistance of 48kN/m. On introducing the bentonite-based lubricant – pumped frequently for the remainder of the drive – the average resistance decreased to 15kN/m. Although marked by several time dependent peaks, the average jacking resistance over the final 75m of the drive fell even further to 2kN/m. This further reduction in the latter stages of the drive is probably due to slurry filling the overbreak throughout the full length of pipeline. Face resistance measured from the vertical axis

using two average jacking resistance's of 15kN/m (lubricated) and 48kN/m (unlubricated) are 335kN and 328kN respectively

The well defined peaks in jacking load are due to restart forces following weekend stoppages. The maximum jacking force recorded is a restart force of 6393kN following an extended weekend break of the 19th, 20th and 21st August and is equivalent to a 66% increase in resistance.

#### 5.2.4 Scheme 9

The jacking records for Scheme 9 are shown in Figure 5.4. Double shift working was employed from the start and the only significant stoppage was during the weekend of 14th and 15th January. Continuous working resulted in few time-dependent peaks and relatively uniform jacking resistances. The drive was unlubricated for 130m with a uniform increase in jacking resistance of 25kN/m. On seeing the 44% increase in resistance on start-up following the stoppage, the Contractor opted to lubricate before pushing any further. The jacking resistance then decreased rapidly to a lower uniform frictional resistance line of 14kN/m – this effect is discussed later in the chapter. Face resistance from the intercept of the average frictional resistance is 680kN and 746kN for unlubricated and lubricated respectively.

The rate of advance depended upon the shift team, one team generally progressed at 18.1m per shift and the second team at an average of 10.4m per shift.

#### 5.2.5 Summary of all monitored schemes

Average frictional resistance and measured face loads for the nine monitored schemes are summarised in Table 5.1. The measured frictional resistances are also expressed as mean interface shear stresses to compare them to the limits quoted by Craig (1983). With the exception of Scheme 5, the measured interface shear stresses are lower than the Craig values.

The penetration resistance was relatively small in the stiff cohesive soils of schemes 1, 3 and 8, and negligible at scheme 6 where the miner excavated a generous overbreak slightly ahead of the shield. At scheme 2 the large face load resulted from the shield being used to trim the base of the excavation. At scheme 4 the resistance

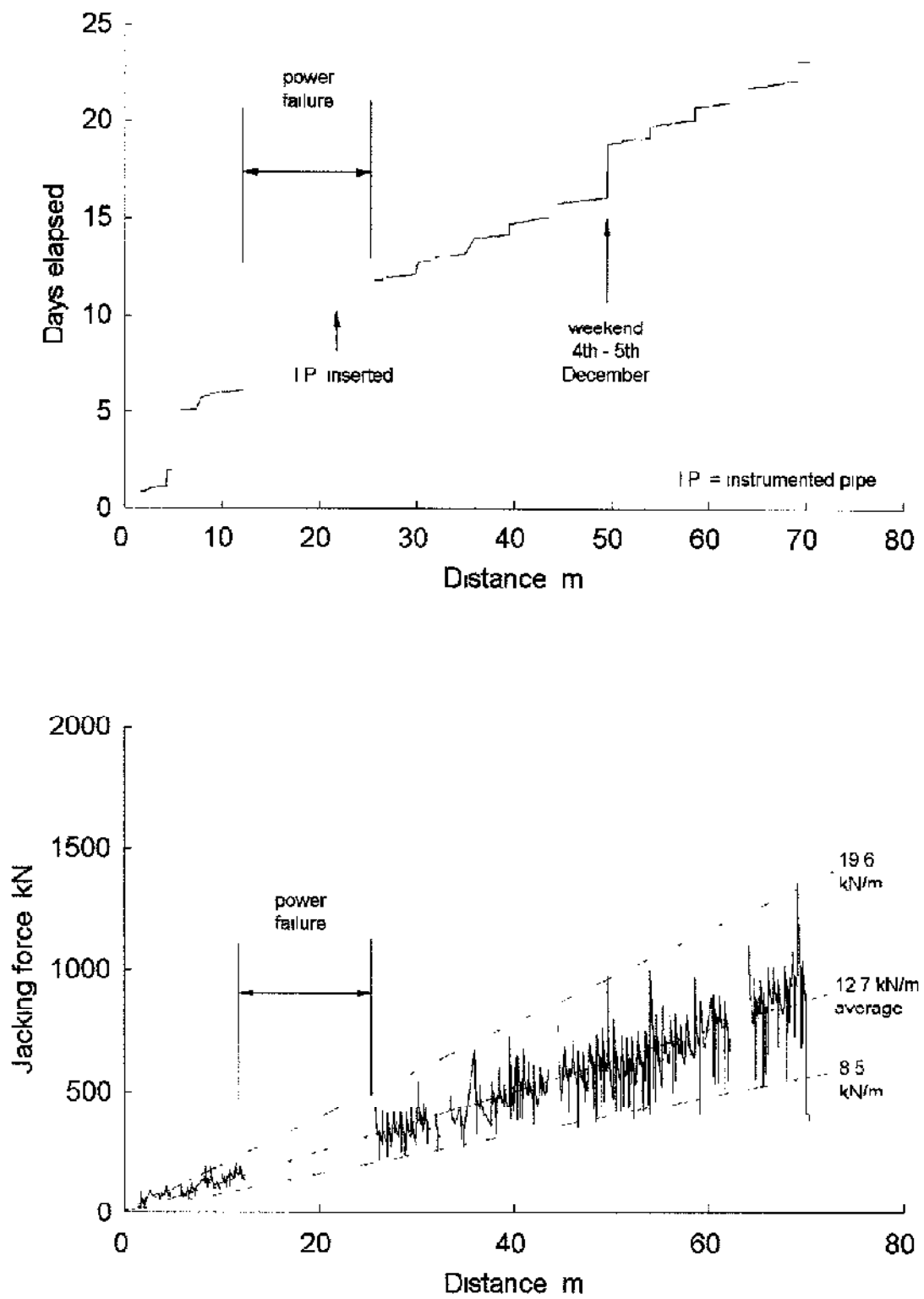


Figure 5.1 Jacking record for Scheme 6.

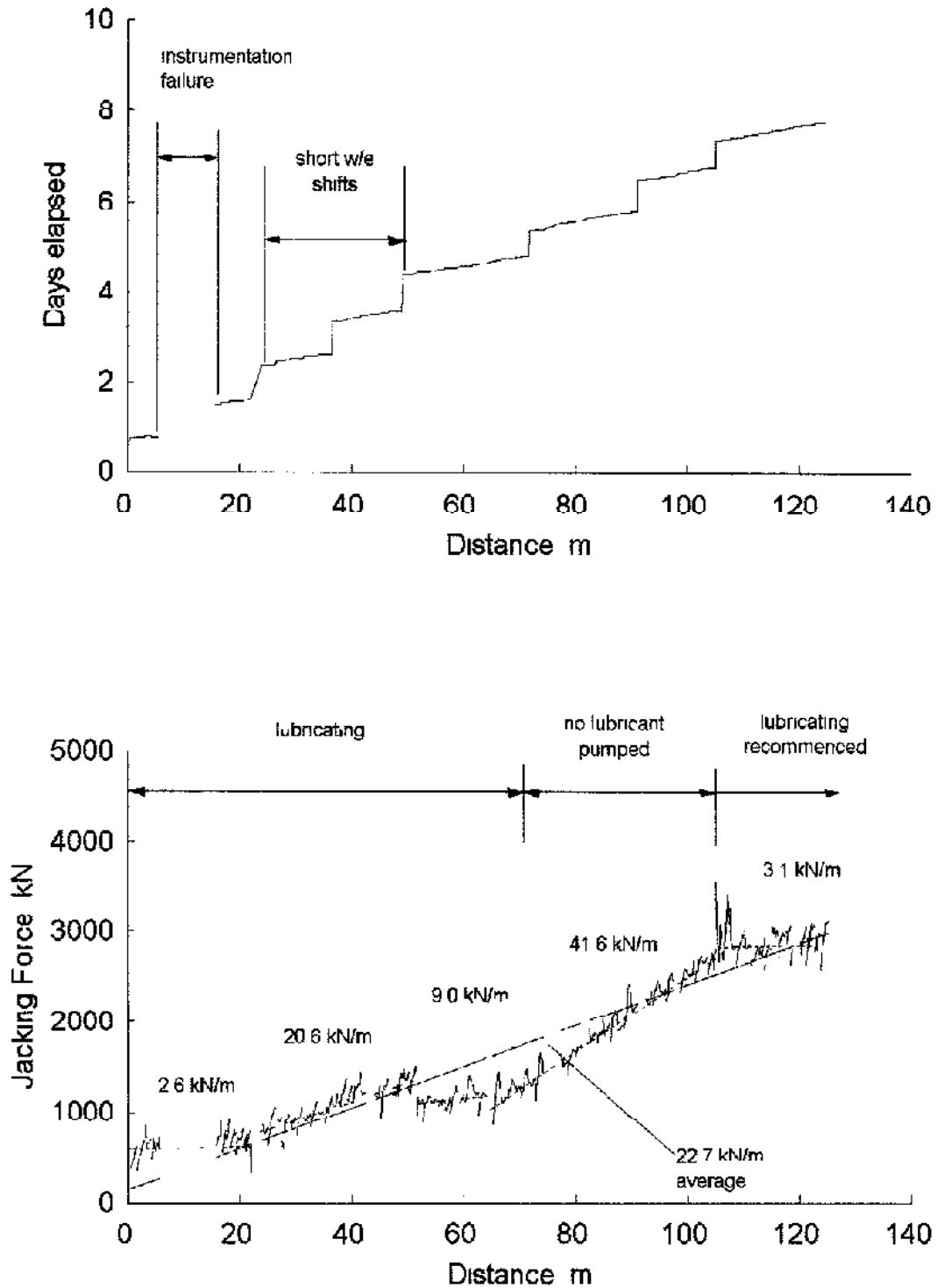


Figure 5.2 Jacking record for Scheme 7.

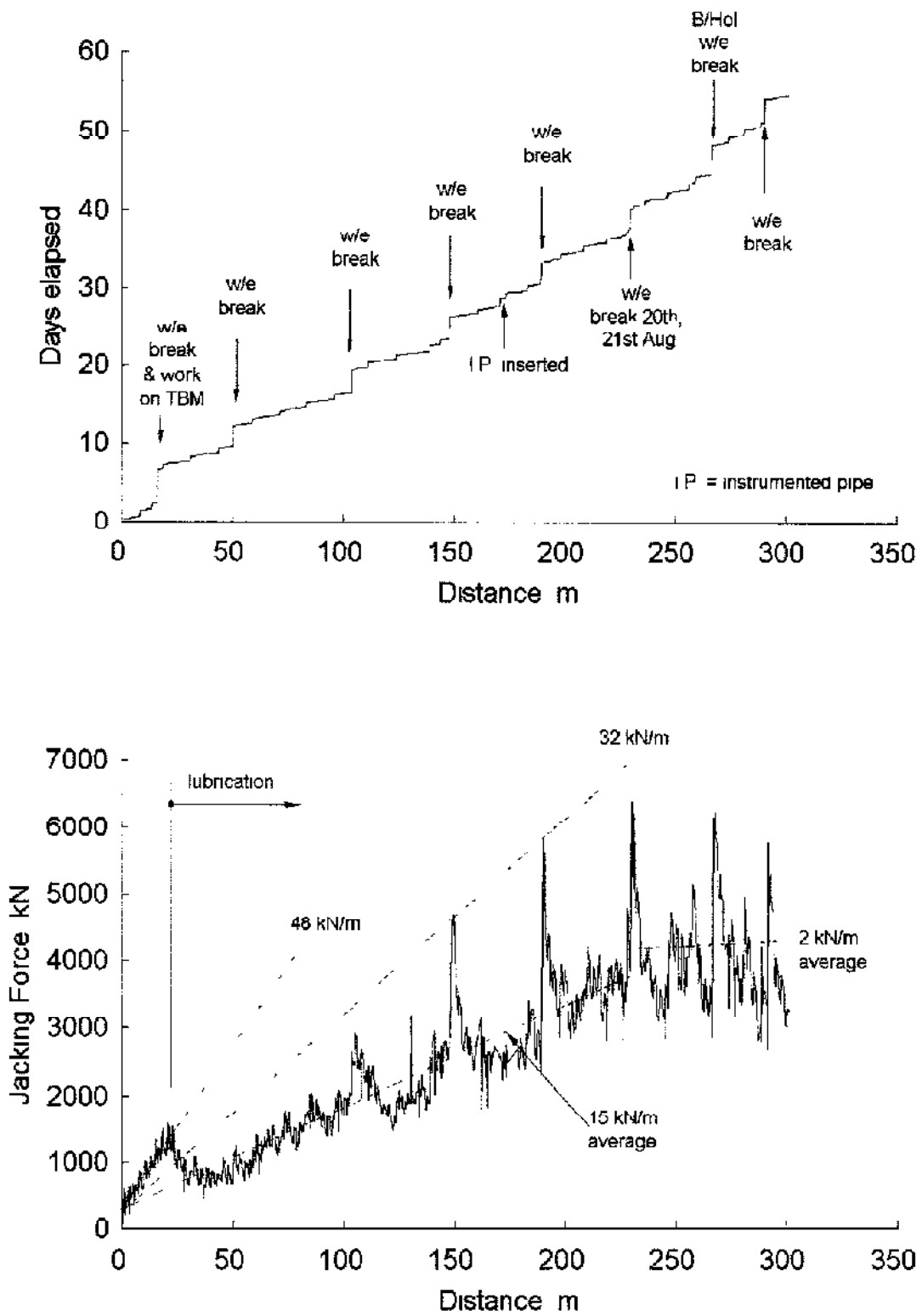


Figure 5.3 Jacking record for Scheme 8.



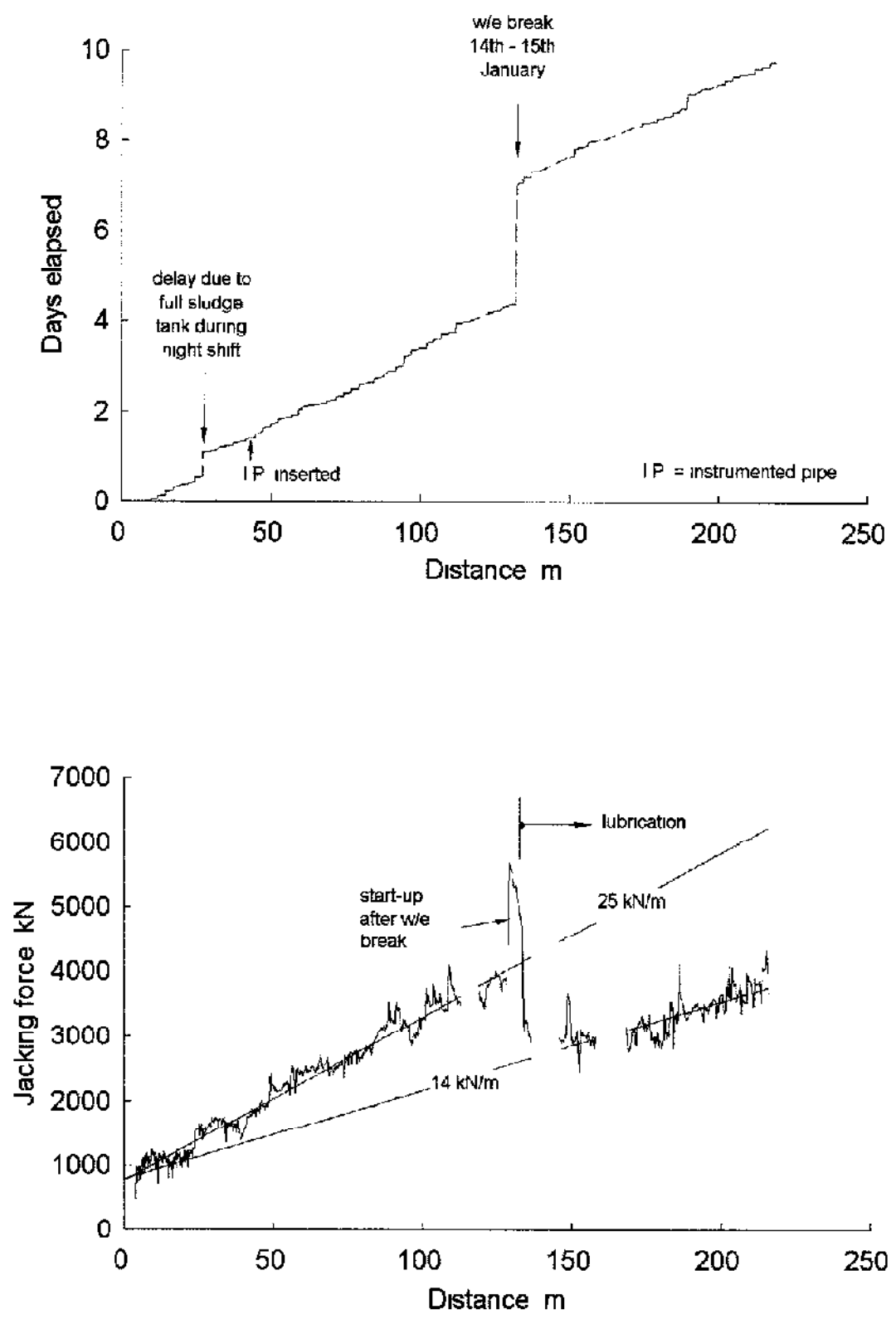


Figure 5.4 Jacking record for Scheme 9.

was related to excavation and trimming at the shield. When the miner excavated to a diameter slightly larger than the shield, resistance was very small; when the shield was used to trim the excavation, the penetration resistance increased by almost 800kN. In the slurry machine drives of schemes 5, 7 and 9 the large face loads include slurry support pressure and resistance of the shield trimming the excavation.

Scheme	Soil type	Measured penetration resistance (kN)	Notes	Measured frictional resistance (kN/m)	Mean interface shear stress (kPa)	Craig (1983) limits (kPa)
1	Stuff glacial clay	120	Dry Wet	7.2	1.5	5-18
				29.8	6.2	
2	Weathered mudstone	950	First 40m	8.0	1.5	2-3
3	London clay	300		54.4	7.6	5-20
4	Dense silty sand/ sandy silt	100-800	Unlubricated Lubricated	23.1	4.2	5-20
				9.4	1.7	
5	Sand and gravel (below water table)	1200	Unlubricated Lubricated	100	22.0	10-15
				10	2.2	
6	London clay	0		19.6 upper	3.4	5-20
				12.7 average	2.2	
				8.5 lower	1.5	
7	Dense silty sand (below water table)	592	Full lubrication Imperfect lubrication	2.6	0.7	10-15
				41.6	11.0	
8	Stuff glacial clay	335 328*	Unlubricated Lubricated	48	7.1	5-18
				2.0-15	0.3-2.2	
9	Very soft clay and peat	680 746*	Unlubricated Lubricated	25	4.4	
				14	2.4	

\* Values based on lower resistance line intercept with vertical axis

**Table 5.1 Penetration and frictional resistances for Schemes 1 to 9.**

Jacking records from the nine schemes have been simplified and separated into cohesive and granular soil types in Figures 5.5 and 5.6. These plots reduce the complex field data to face loads (measured on the vertical axis) and average frictional resistances. The notable points are: the increase in resistance in Scheme 1 following heavy rainfall; the marked increase in Scheme 2 occurring as the pipeline progressed from mudstone into boulder clay; the abrupt drop in resistance in Schemes 5, 8 and 9 at positions where lubrication was introduced; and the variable change in gradient of the average resistance line due to lubrication procedures in Scheme 7.

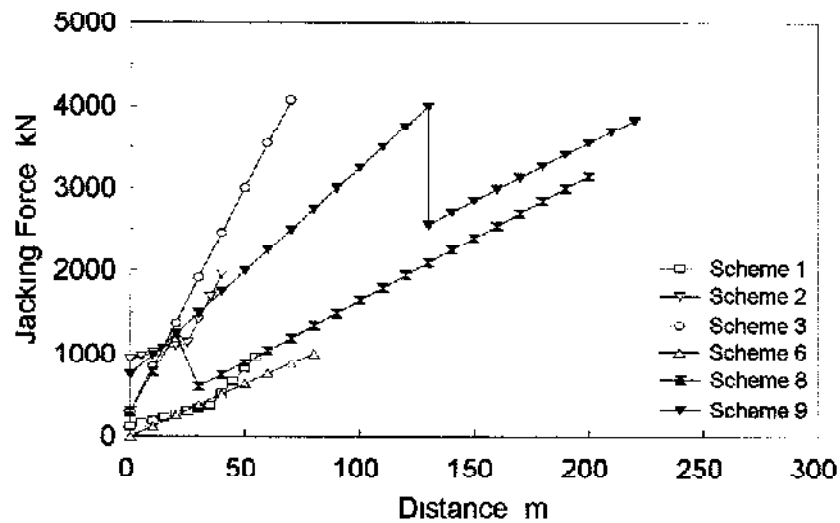


**Figure 5.5 Simplified jacking records for the schemes in cohesive soils.**

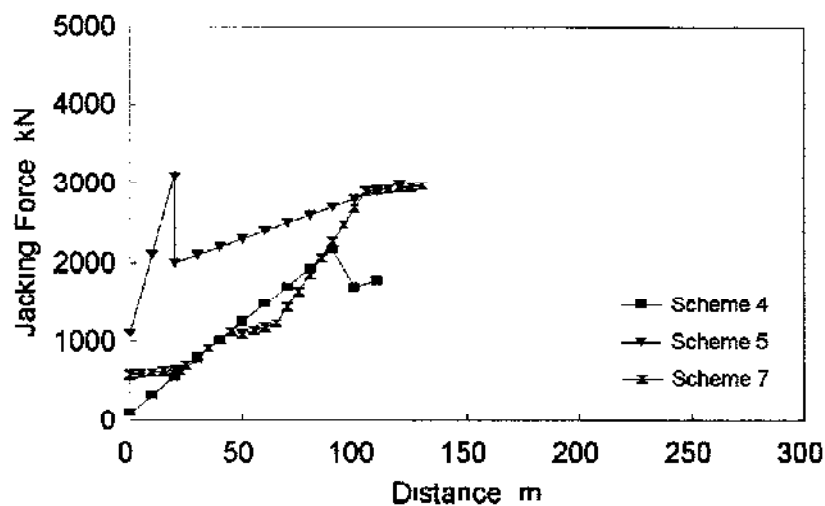


**Figure 5.6 Simplified jacking records for the schemes in granular soils.**

### 5.3 The influence of construction-related factors

#### 5.3.1 Lubrication

##### 5.3.1.1 Types of lubricant

The use of lubricants to reduce frictional resistance has long been common practice in pipe jacking. The main function of lubricant slurry is to provide sufficient internal pressure to stabilise the tunnel and prevent ground collapsing onto the pipes. The slurry must be designed to form a filter cake at the face of the tunnel bore without excessive bleeding of material and must overcome ground water pressures. Clearly it

must fill the complete overbreak space before this can be achieved. In this situation, large diameter concrete pipes are theoretically buoyant.

Lubricant slurries used in pipe jacking are usually of water-based bentonite formulations. Recent developments have seen the use of polymer formulations and foams – commonly used in the oil industry – gaining acceptance as pipe lubricants but many contractors are reluctant to use them because they are not yet cost effective in comparison to bentonite. Slip coating materials including ‘clay-cap’ (a bentonite fluid with additives) are also used but are more common in non man-entry microtunnelling where temporary pipes within the pipeline cannot be set up. Bentonite lubricants were used on Schemes 4 to 9 – a clay-cap coating was also applied to the pipes in Scheme 7.

### 5.3.1.2 Injection arrangement

Bentonite slurry is generally made from powder and water and is prepared with the aid of a colloidal or grout mixer. It is good practice to allow freshly mixed slurry suspension to swell for several hours before use. The slurry is injected into the overbreak void by a suitable pump through injection sockets connected to a temporary pipe system as illustrated in Figure 5.7. The injection sockets should be designed to ensure that slurry is uniformly distributed along and around the pipe string to form a continuous layer of lubricant.

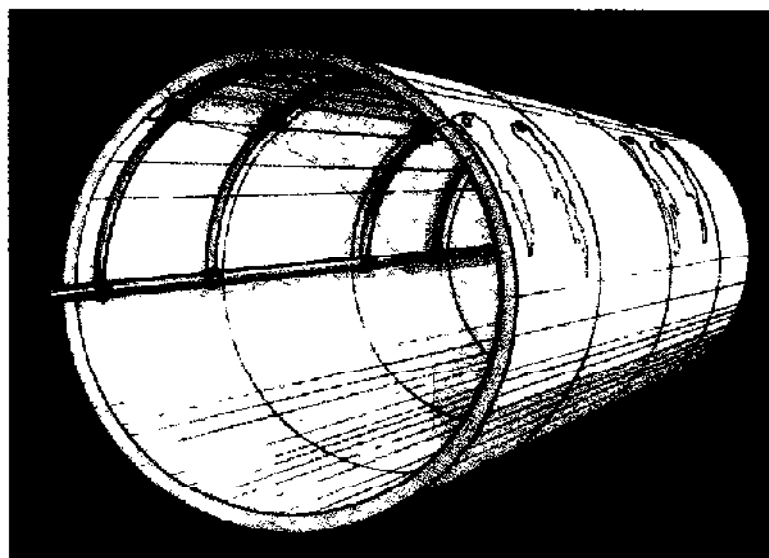


**Figure 5.7** Typical lubrication arrangement (courtesy the Pipe Jacking Association).

In Scheme 7, 'lubricant pipes' (jacking pipes with lubricant injection sockets) had single sockets and were inserted every fourth pipe but there was no apparent pattern to the attitude of the sockets. At the front of the pipe string, injection sockets were located on the right of the pipeline in the shield and pipe 4 – Figure 5.8. The next two sockets were in pipe 8 and pipe 12, on the right and in the top respectively.

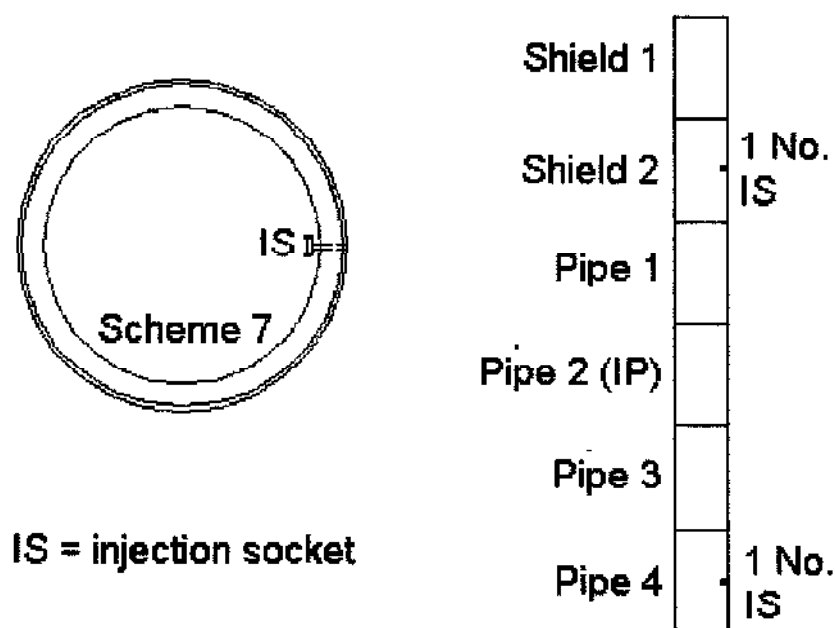


**Figure 5.8 Lubrication injection arrangement in Scheme 7.**

Shear stresses recorded around the rear of the instrumented pipe placed at pipe 2 – Figure 5.9 – are very low on the bottom and right of the pipe, consistent with the shear resistance of bentonite slurry, but significantly greater at the top and left positions

These data show that contact between ground and pipe only occurred on the top-left quadrant due to a non-uniform distribution of slurry as depicted in Figure 5.10. In contrast, lubricant pipes in Scheme 8 had three sockets – one in the top and two at axis level as illustrated in Figure 5.11 – and were inserted every third pipe

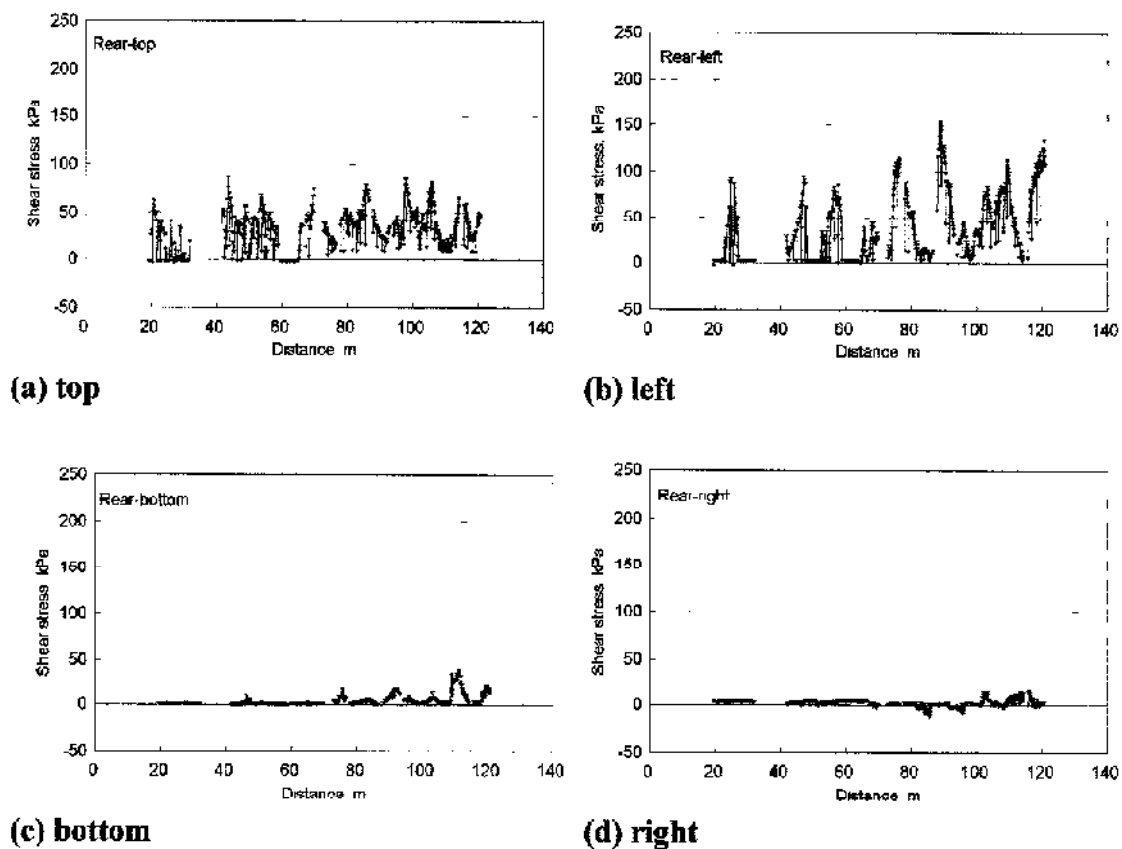


Figure 5.9 Scheme 7 shear stresses – pipe rear.

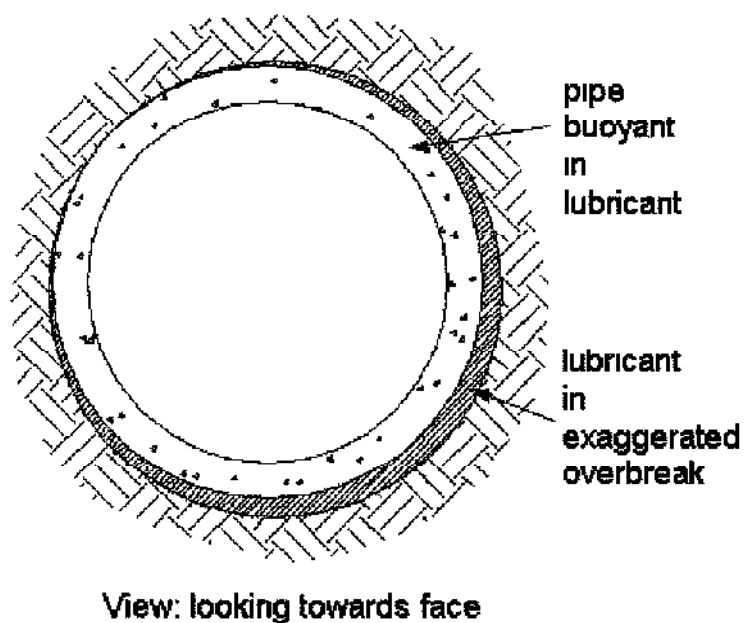
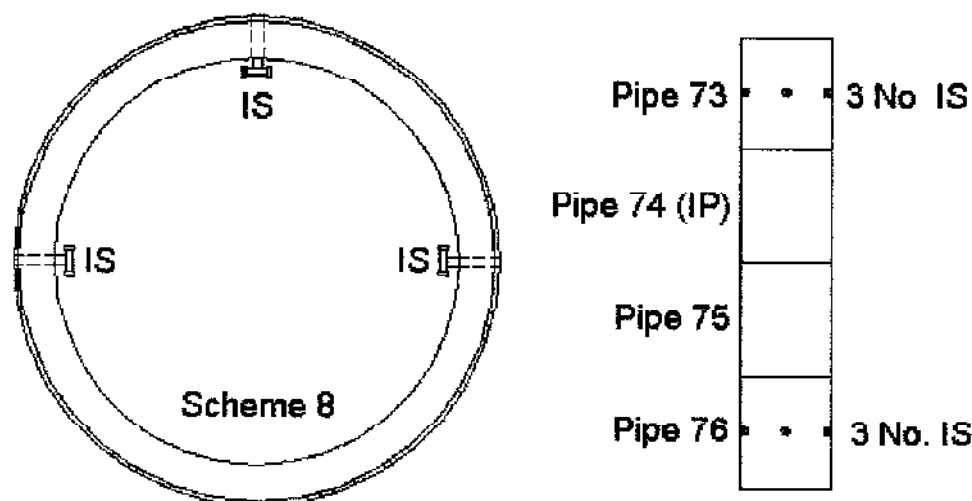


Figure 5.10 Non-uniform distribution of lubricating slurry in Scheme 7.



IS - injection socket

**Figure 5.11 Lubrication injection arrangement in Scheme 8.**

Shear stress data from the Scheme 8 instrumented pipe, inserted at pipe 74 next to a lubricant pipe, are shown in Figure 5.12. These data are consistent with the whole of the pipe sliding through a low shear zone of slurry and other than the first 10m of the tunnel bore, there appears to be little contact between pipe and ground. The regular pattern and greater number of injection sockets per lubricant pipe in Scheme 8 clearly results in a more uniformly distributed and more effective lubricant. A detailed discussion on contact stress records follows in chapter 6.

### 5.3.1.3 Lubricant effectiveness

Other factors including consistency, quality and volume have been shown to influence the effectiveness of bentonite slurries (Stein et al, 1989) but since monitoring these parameters was not included in the reported research programme, they will not be discussed.

Lubricant effectiveness is also dependent upon the type of ground. In cohesive soils where the tunnel bore – depending upon its stability – may remain open, lubricant introduced some way into the drive can work its way over the whole pipe

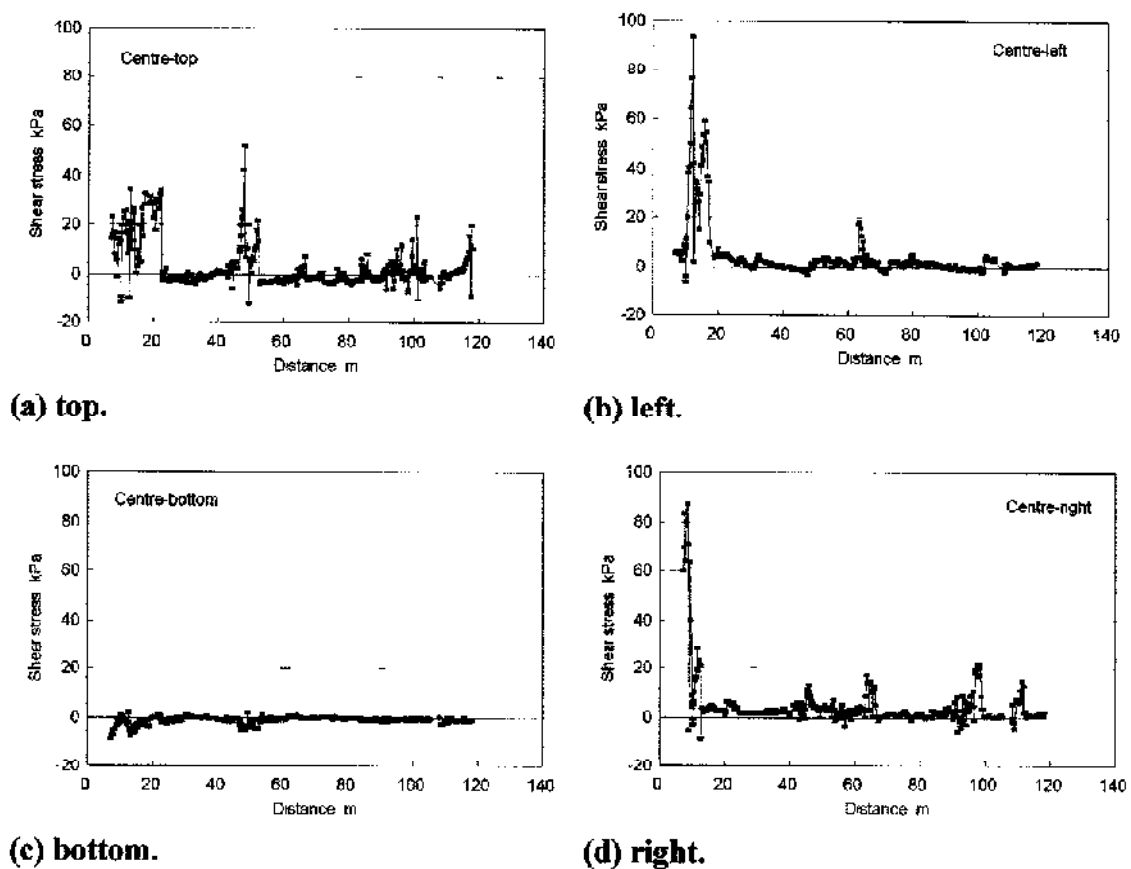


**Figure 5.12 Scheme 8 shear stresses – pipe centre.**

string resulting in reduced friction along the whole length. This situation is depicted by line I of Figure 5.13 This effect is evident in the reduction of frictional resistance in Schemes 8 and 9 – Figures 5.3 and 5.4 above – where the average frictional resistance reduces rapidly to a line of lower resistance after introducing bentonite lubrication. The lines of lower resistance are characterised by a having approximately the same intercept on the vertical axis as the unlubricated resistance. In granular ground, where soil unsupported by slurry will collapse onto the pipes, the introduction of lubricant part way into the drive may only have the effect of reducing the subsequent gradient of the average jacking resistance – depicted by line II. This is illustrated in the change in jacking resistance in Scheme 7 upon recommencement of pumping bentonite at a distance of 107m jacked – Figure 5.2 – with a reduction in gradient from 42kN/m to 3kN/m.



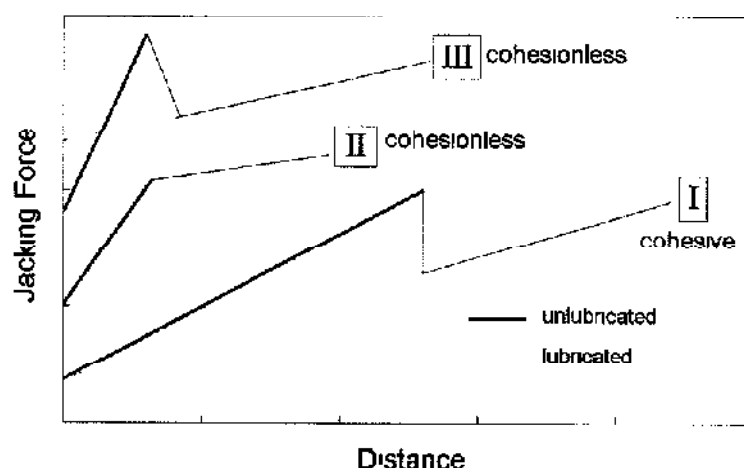


**Figure 5.13 Effect of lubrication in different soils.**

Line III of Figure 5.13 illustrates another pattern in jacking load reduction in granular soils due to lubrication. Here the reduction in friction is characterised by a rapid decay to a line of lower resistance, but unlike that in cohesive soils, with an intercept on the vertical axis of greater magnitude than the unlubricated line: in this case the lubricant has probably had some beneficial effect over the previously unlubricated length

#### 5.3.1.4 Reduction in frictional resistance

The effectiveness of bentonite-based lubricants in reducing frictional resistance on the monitored schemes is summarised in Table 5.2

Scheme No	Pipe ID (mm)	Soil type	Cover (m)	Mean frictional resistance (kN/m)		Reduction in friction (%)
				Unlubricated	Lubricated	
4	1200	Dense silty sand	7-10	23	9	59
5	1200	Sand and gravel	4-7	100	10	90
6	1500	London clay	6-8	-	13	
7	1000	Dense silty sand	5-8	-	9	
				-	42 (break)	79(increase)
				-	3	93
8	1800	Stuff glacial clay	6	48	15	69
9	1500	Very soft clay	5.5-6	25	14	44

**Table 5.2 Reduction in frictional resistance for Stages 2 and 3 schemes.**

Lubrication was not used in Schemes 1, 2 and 3. Injection sockets were provided only within the hand shield in Scheme 6 but very little lubricant was pumped

and this had no noticeable effect on the jacking loads in London clay. The lubricant pump failure in Scheme 7 resulted in a significant period where no bentonite slurry was pumped. This pause saw a 79% increase in frictional resistance to a high value of 42kN/m which on recommencement of pumping fell to 3kN/m, a 93% reduction. In the cohesive soils of Schemes 8 and 9 the introduction of bentonite resulted in reductions of 69% and 44% respectively to a similar lubricated resistance – 15kN/m.

### 5.3.1.5 Buoyancy

If the overbreak void can be filled with pressurised lubricant then the pipeline may become buoyant. Norris (1992b) reports pipeline buoyancy in Scheme 5 where tunnel surveys show the pipe level lifting by about 20mm after lubricant injection and pipe/ground contact data show larger interface stresses on the pipe top than on the bottom. The pattern of interface stresses in Scheme 7 shows pipe buoyancy occurring with most of the contact between the instrumented pipe and ground on the top as illustrated above in Figures 5.9 and 5.10. Chapter 6 includes a detailed record and description of all the contact stresses and discusses buoyancy further.

## 5.3.2 Pipeline alignment

### 5.3.2.1 Significance of pipeline alignment

The degree of misalignment between pipes within the pipe string can be of considerable significance in generating additional interface friction between pipes and soil and controlling the total jacking load that can be transmitted safely through the pipe joints. By 'misalignment' is meant the angular deviation between the central axes of successive pipes. The misalignment angle,  $\beta$ , is defined in Figure 5.14. In an ideal pipe jack, no such deviations would exist, but in practice irregularities in ground conditions, excavation methods and operator error can contribute to the front of the shield deviating from the ideal course. To maintain line and level as close as possible to that required, steering corrections are continually made, resulting in the pipe string invariably taking a zig-zag course. The most critical situation for jacking pipes usually arises from edge and diagonal loading when angular deviation – resulting from a zig-zag course – becomes relatively large.

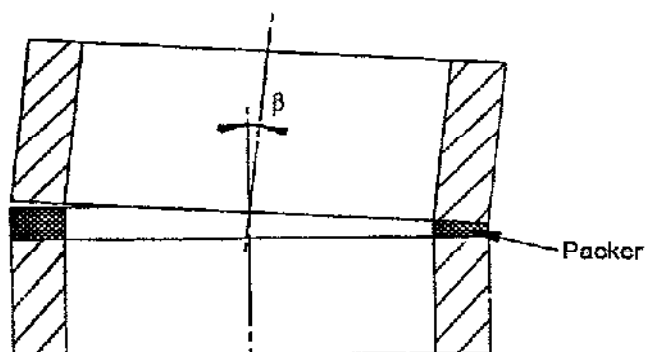


Figure 5.14 Misalignment angle,  $\beta$ .

The normal practice has been to specify allowable limits for errors in line and level at any point along the tunnel, typically 50 or 75mm. While these limits may be necessary to maintain adequate clearance from obstructions or other services, or to provide correct hydraulic flow conditions. Ripley (1989) and Norris (1992b) demonstrate that they are insufficient as a means of controlling angular deviations between successive pipes to within acceptable limits for transmission of large axial forces. The measurement of actual angular deviations achieved in practice will therefore allow reasonable specifications in terms of misalignment angles and line and level tolerances.

The effect of misalignment on jacking loads is very difficult to assess. A direct comparison of jacking forces for misaligned and perfectly straight pipe jacks, in similar conditions, is not possible due to the limited database. The effect of misalignment will therefore be assessed by considering the increase in radial and shear stresses on misaligned pipes – discussed in Chapter 6

### 5.3.2.2 Alignments achieved in practice

#### *Measuring misalignment*

To investigate the effect of misalignment, some angular deviation on the instrumented pipe jacks was desirable. However, the author did not influence in any way the miners or machine operators in steering control; measured alignments therefore are typical of those normally achieved in practice. Line and level surveys were carried out to measure horizontal and vertical deviations respectively and

misalignment angles were accurately measured at the instrumented pipe joints by pipe joint movement instruments.

*Stage 2 schemes*

Figures 5.15 to 5.18 show the plots of tunnel alignment surveys on four of the five sites of Stage 2 research. Schemes 1, 3 and 4 illustrate well controlled drives where line and level satisfy specification.

The variation in misalignment angle,  $\beta$ , in Scheme 1 is greater than for Schemes 3 and 4 because the instrumented pipe was positioned close to the shield and, in addition to variations in line and level, was influenced by steering corrections by the miners. The position of maximum misalignment angles,  $0.3^\circ$ , in Schemes 3 and 4 agree with the position of abrupt change in line and level: where steering corrections are gradual, typical misalignment angles of  $0.1^\circ$  result.

Line and level significantly exceeds specification in Scheme 5. In the section of tunnel between chainages 90m and 135m, values of  $\beta$  were as large as  $0.82^\circ$ , resulting in localised crushing damage at a number of pipe joints

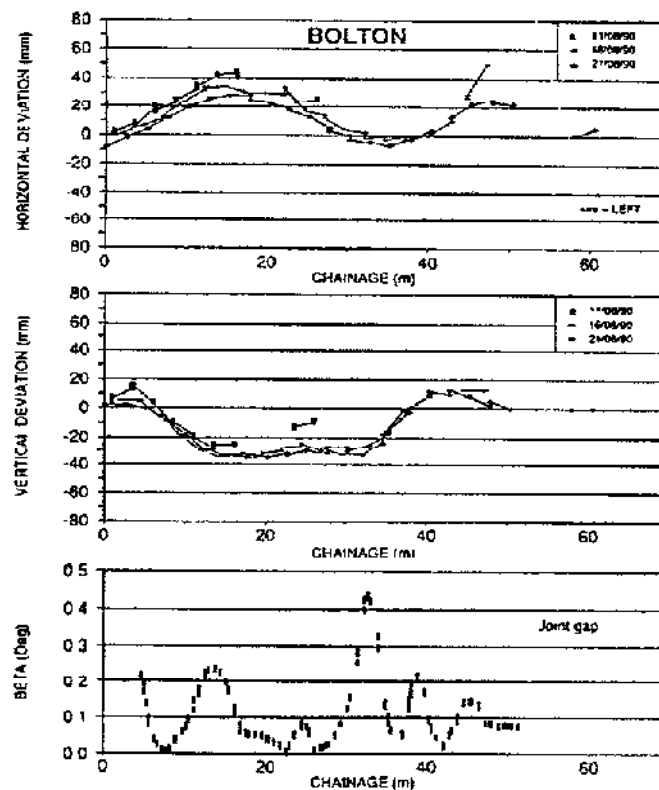


Figure 5.15 Scheme 1 tunnel alignment surveys (after Norris, 1992b).

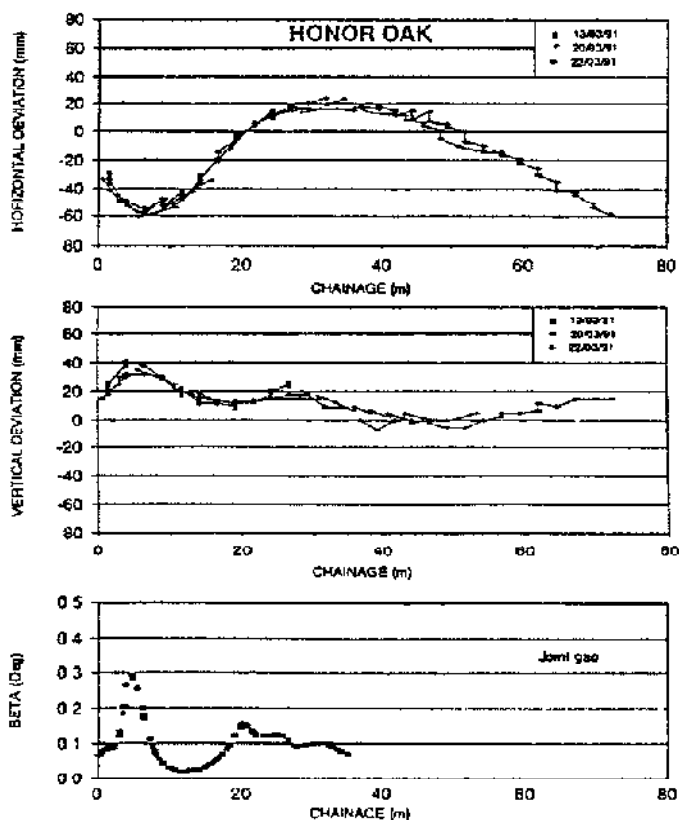


Figure 5.16 Scheme 3 tunnel alignment surveys (after Norris, 1992b).

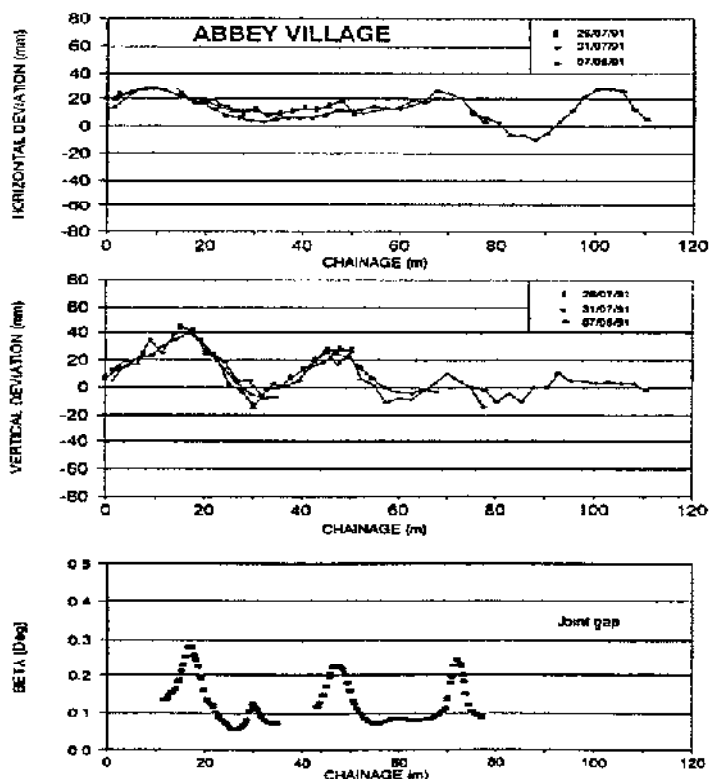


Figure 5.17 Scheme 4 tunnel alignment surveys (after Norris, 1992b).

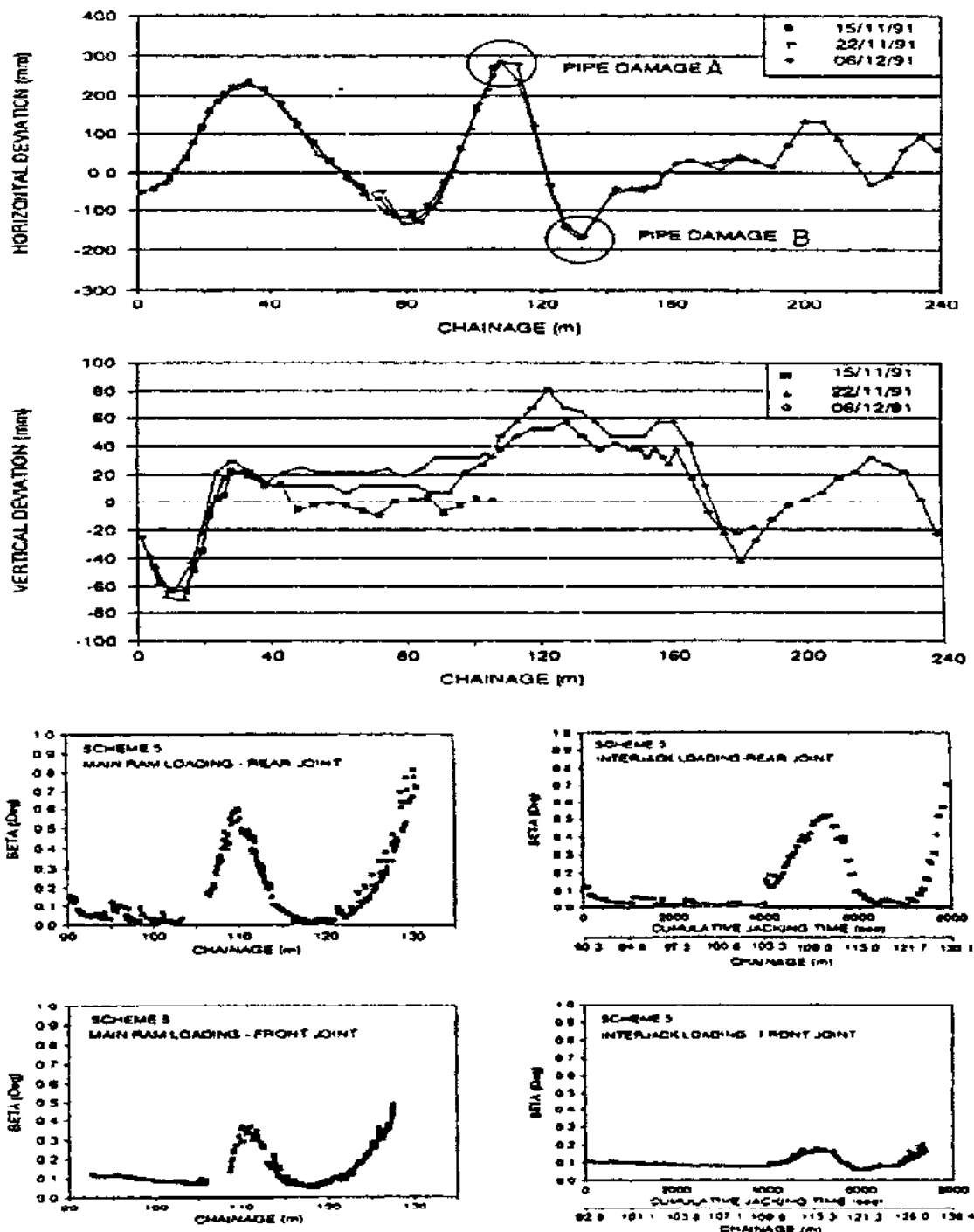


Figure 5.18 Scheme 5 tunnel alignment surveys (after Norris, 1992b).

### *Stage 3 schemes*

The tunnel alignment surveys for Schemes 6, 7, 8 and 9 are shown in Figures 5.19 to 5.22. Scheme 6 was the only hand-driven pipe jack monitored during Stage 3 research. The miner maintained very good steering control over level, but deviated considerably from line at the start of the drive. The abrupt steering corrections resulted in misalignment angles as large as  $0.8^\circ$ . A power failure to the instrumentation at chainage 10m probably means that the maximum misalignment angle was missed. Evaluation of the joint angular deflection using line and level information at this location – analysis presented in Appendix C – indicates an angle of  $0.9^\circ$ . A similar steering correction at chainage 21m gives a measured misalignment of  $0.8^\circ$ .

Only one line and level survey was carried out in the pipeline of Scheme 7 due to difficulty of surveying within a 1000mm internal diameter pipe. The results show excellent control with misalignment angles of no greater than  $0.1^\circ$ , and probably reflects the optimum performance in pipe jack alignment.

As is typical of most pipe jacks, line and level control in Scheme 8 is poorest at the start of the drive. Steering corrections to the level were very gradual and consequently had little effect on misalignment angles. The sudden changes in line at chainages 40m and 100m result in values of  $\beta$  of  $0.35^\circ$ . An interesting feature of this alignment is the apparent fluctuation in level between chainages 0-60m and 110-130m. The level of the tunnel falls by approximately 20mm between the surveys of 4 August and 16 August. This is probably due to pipe being buoyant on the 4<sup>th</sup> and sitting on the base of the tunnel bore on the 16<sup>th</sup>, slurry having lost water into the ground and consolidated under pipe weight during the weekend before.

The operators of the slurry shield used in Scheme 9 experienced steering difficulties due to the machine rolling in the soft clay. The resulting alignment deviated from axis, in both line and level, by 200mm in places. At chainage 120m, where there was an abrupt change in line, misalignment angle measurements were again missed due to an instrumentation signal failure. At about chainage 140m, where again there is a rapid change in line, there is a corresponding increase in misalignment angle to a maximum of  $0.42^\circ$ .

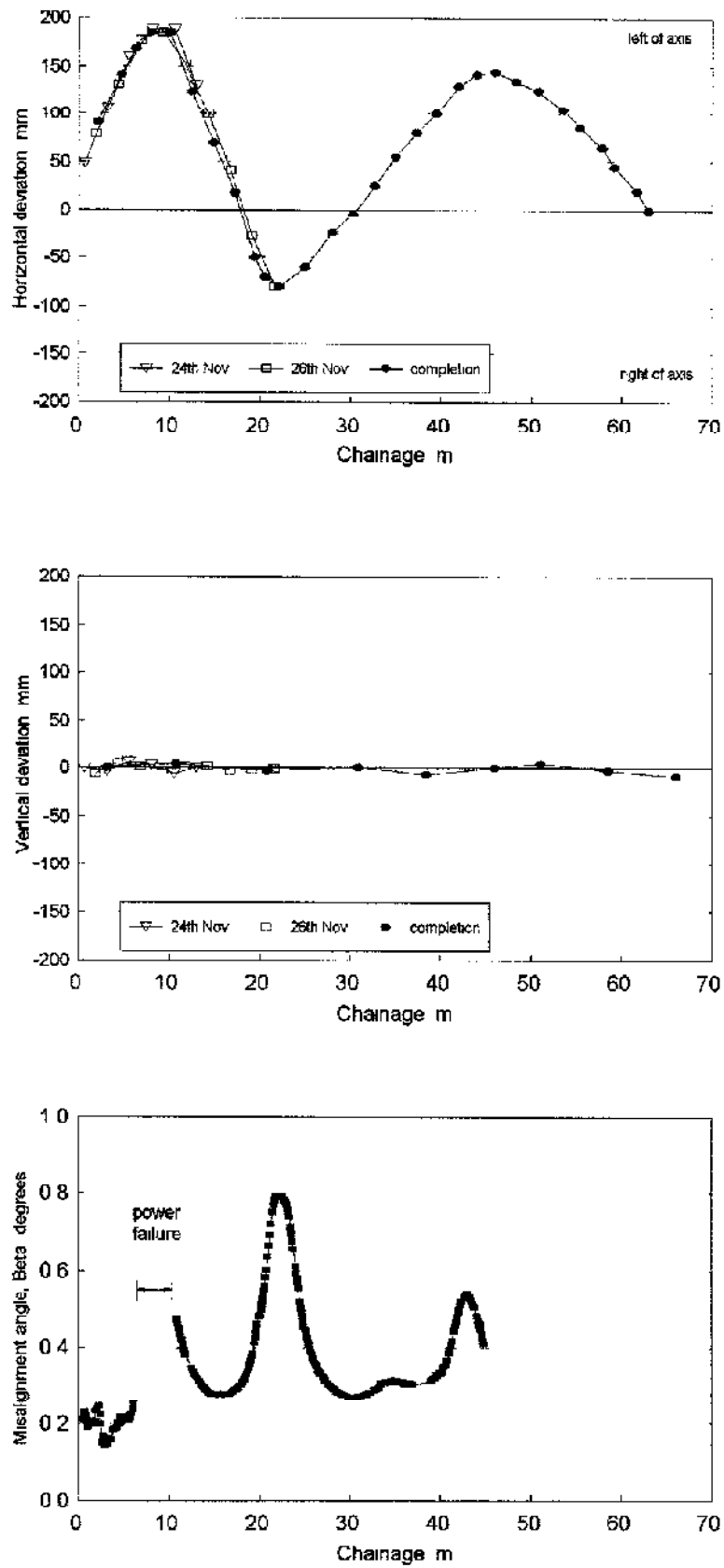


Figure 5.19 Scheme 6 tunnel alignment surveys.



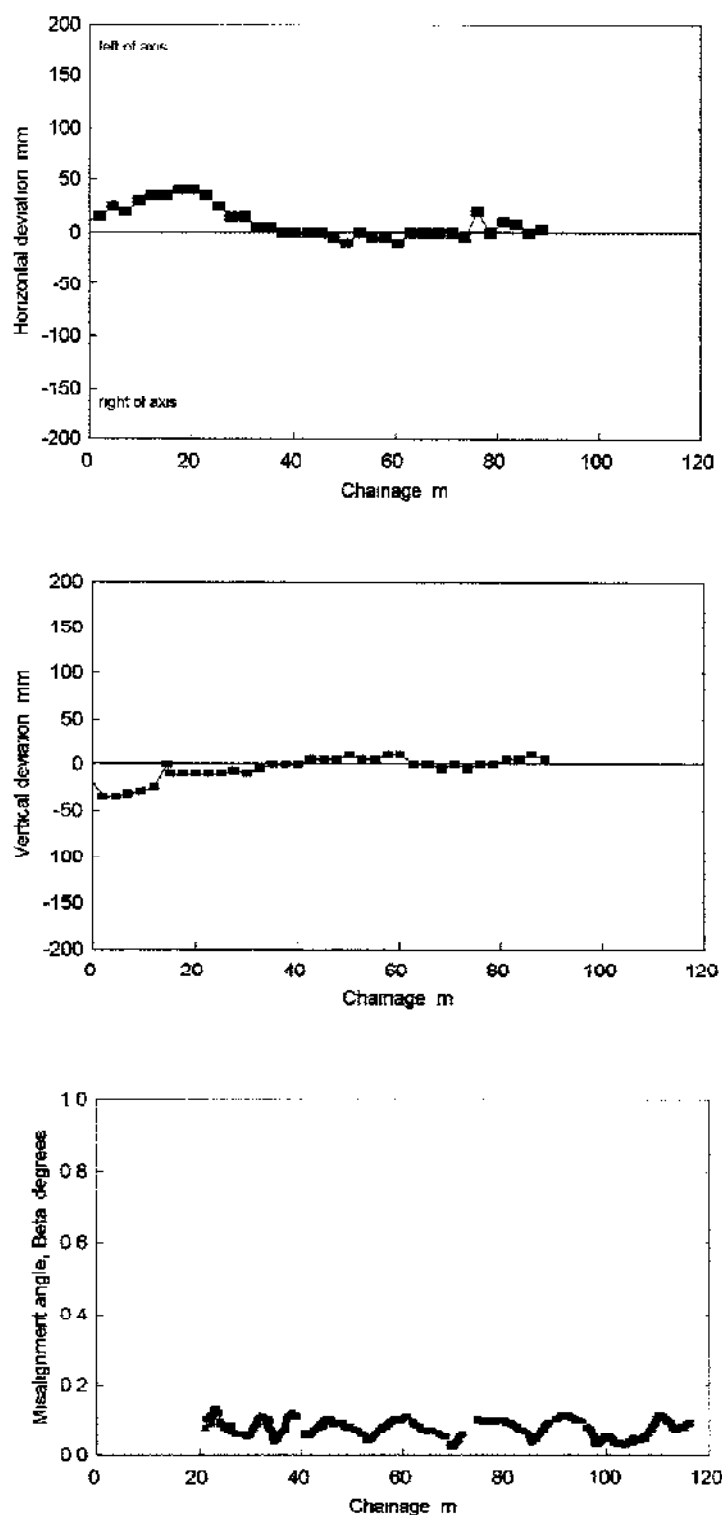


Figure 5.20 Scheme 7 tunnel alignment surveys.

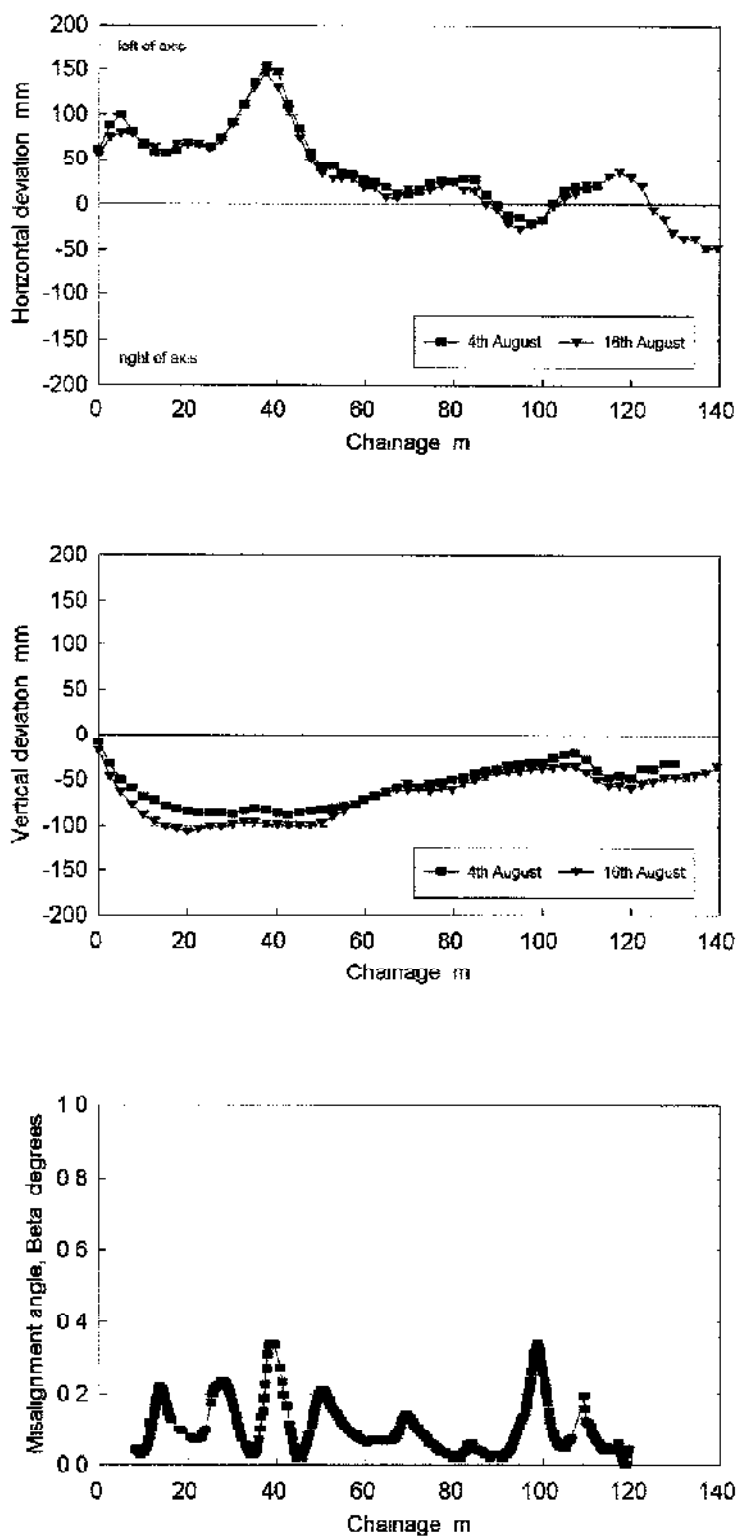


Figure 5.21 Scheme B tunnel alignment surveys.

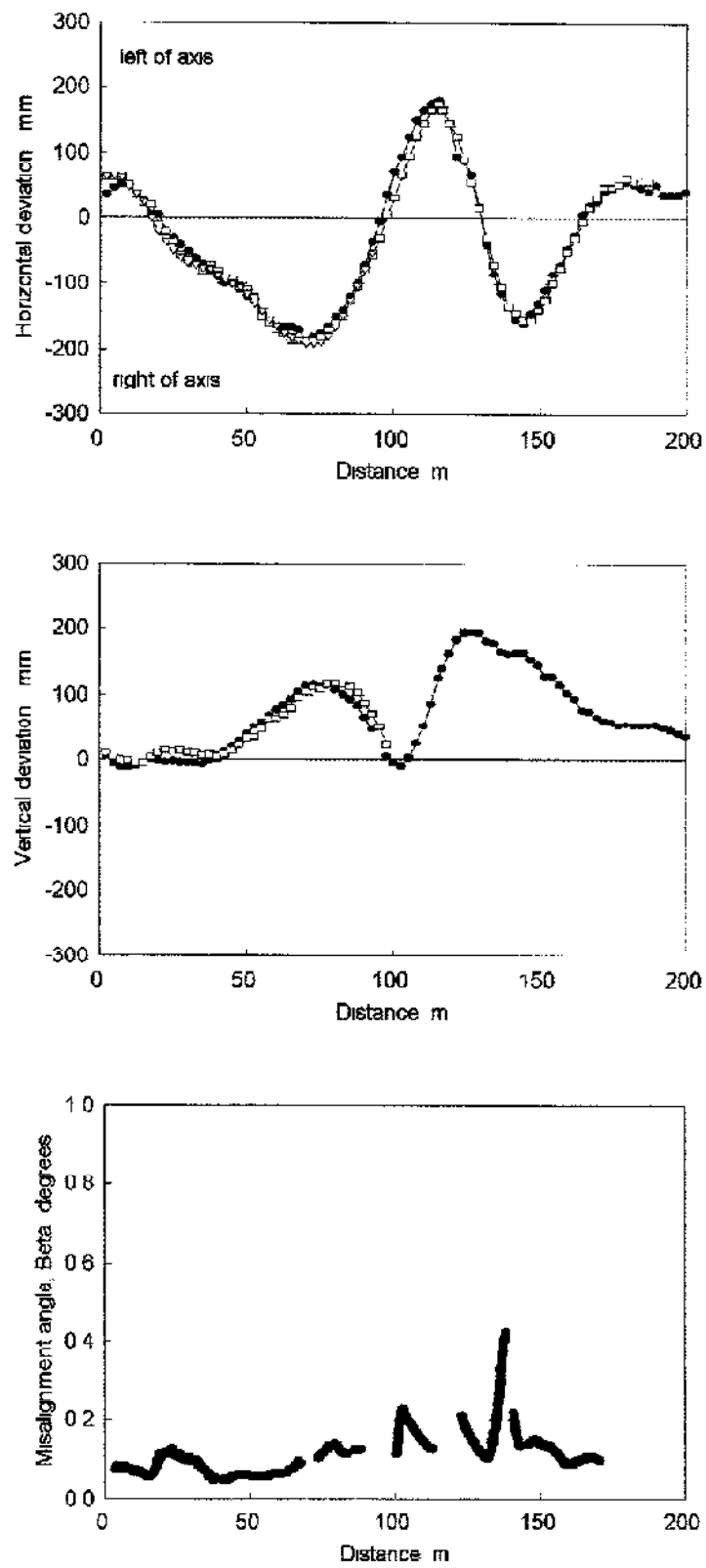


Figure 5.22 Scheme 9 tunnel alignment surveys.

### 5.3.3 Stoppages

The effect of stoppages in requiring larger jacking forces to advance the pipe string, primarily in cohesive soils, is investigated using jacking load data from Stage 2 and Stage 3 schemes

#### 5.3.3.1 London clay

The jacking loads of Schemes 3 and 6 (Figures 5.23 and 5.1 respectively), both in highly plastic London clay, show significant peaking after stoppages between pushes, between shifts, and over night or weekend breaks. A weekend stoppage in Scheme 6 resulted in a 400kN increase in jacking load while stoppages of about 2 hours typically resulted in restart forces 250kN greater than at the end of the previous push.

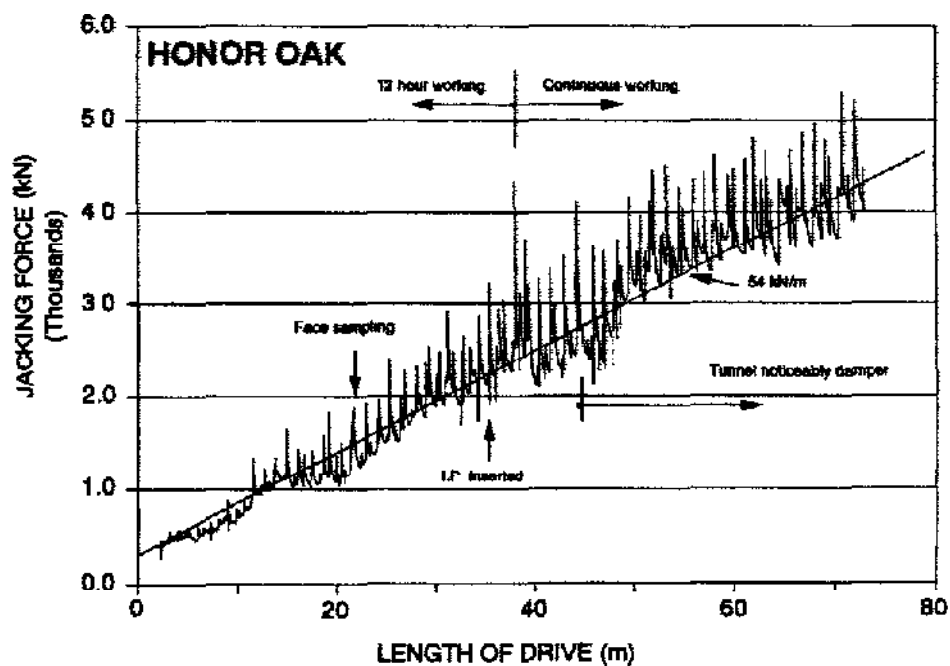
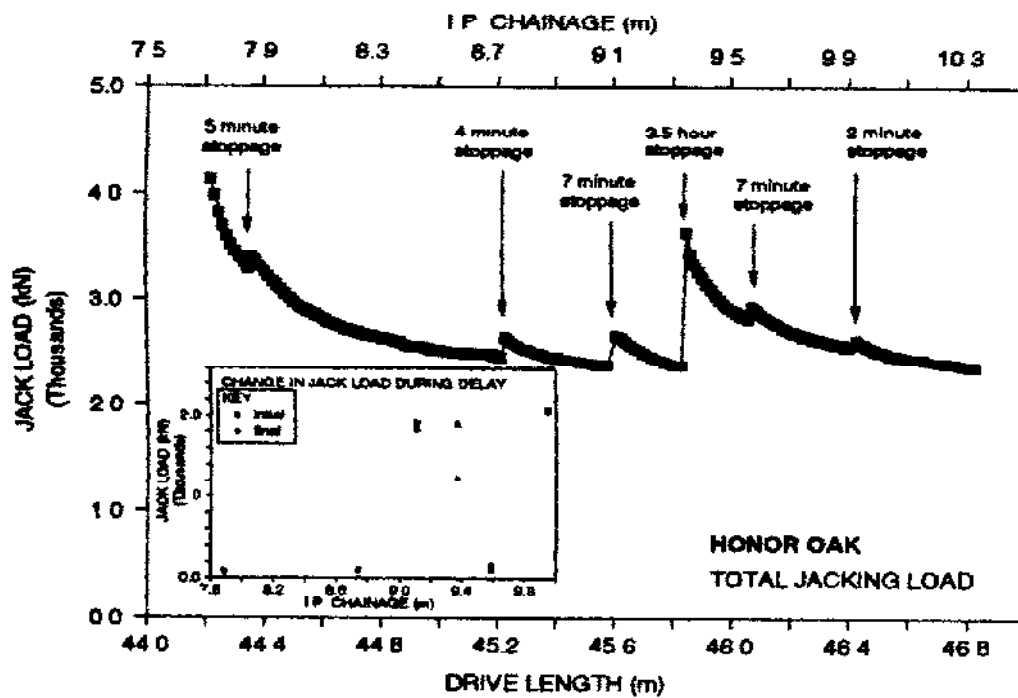
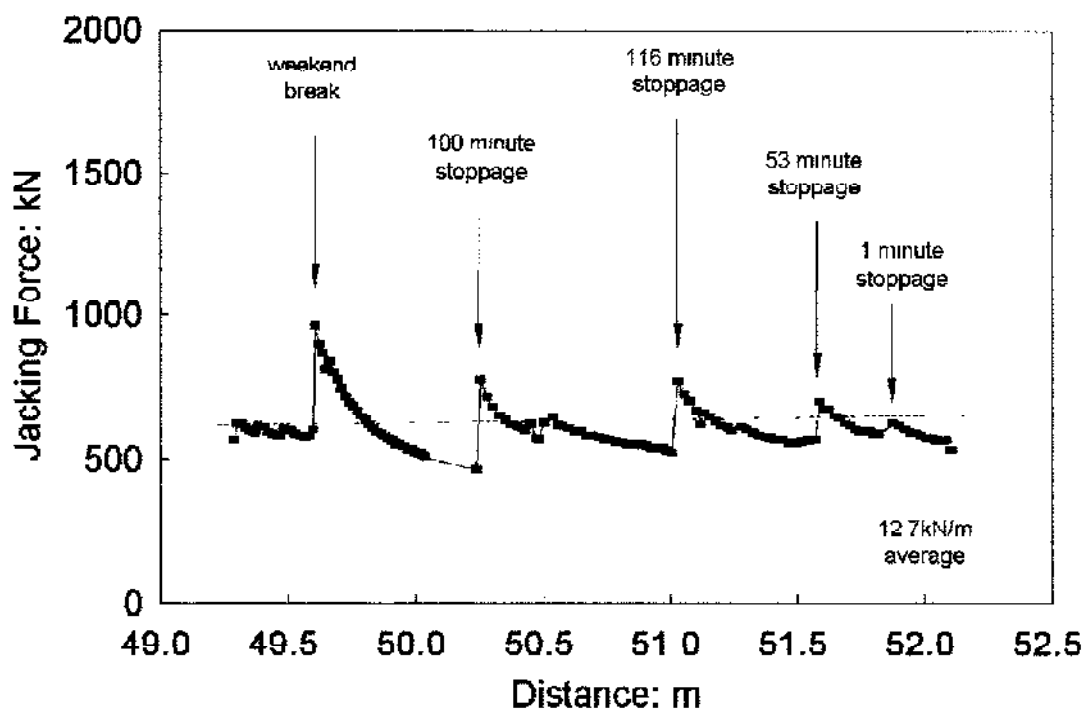


Figure 5.23 Jacking record for Scheme 3 (after Norris, 1992b).

Restart forces over short sections are presented in Figure 5.24. The repeatable pattern is one of higher restart forces required, following even very short delays, to 'break the bond' and then jacking loads decreasing to a 'base line' value. The effect of stoppages on total and effective radial stresses is discussed in chapter 6.



(a) Scheme 3 (after Norris, 1992b).



(b) Scheme 6.

Figure 5.24 Time dependent effects on jacking loads in London clay.

Increases in jacking loads have been normalised with respect to the total jacking load at the end of the previous push and plotted against the natural logarithm of stoppage time in Figure 5.25. Though marked by considerable scatter, the linear relationships obtained for both schemes – Figure 5.25(b) – are in good agreement. The linear rate of increase in jacking load can be expressed by

$$\text{Scheme 3: } \delta P/P = 0.259 + 0.058 \ln(t)$$

$$\text{Scheme 6: } \delta P/P = 0.258 + 0.039 \ln(t)$$

where  $t$  = time (hrs)

The relationship shows significant increases in load can occur within an hour or two of the pipeline becoming stationary.

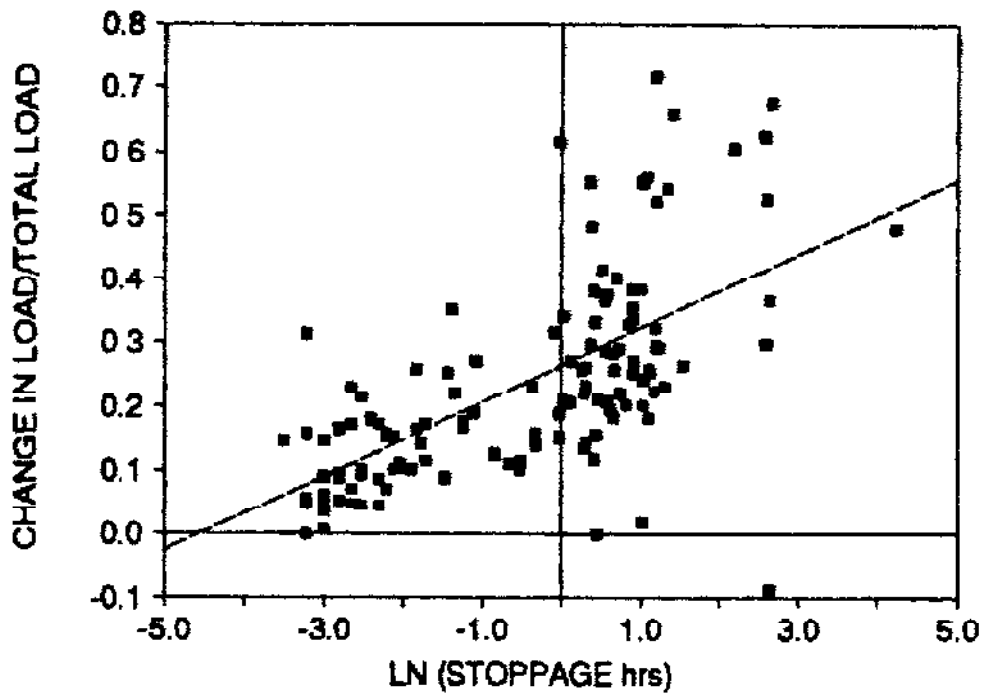
#### 5.3.3.2 Stiff glacial clay

Scheme 1, Bolton, and Scheme 8, Seaham, were in stiff low plasticity glacial clay. The time effect on Scheme 1 is not particularly marked – Figure 5.26 – but Norris (1992b) reports overnight and weekend stoppages resulting in increased restart forces of typically 200kN greater than at the end of the previous push. Normalised increase in jacking loads, Figure 5.27, show a reasonable linear relationship. The increase in moisture content during the latter stages of the drive is also shown to significantly increase the factor. The rate of increase in jacking load can be expressed as follows:

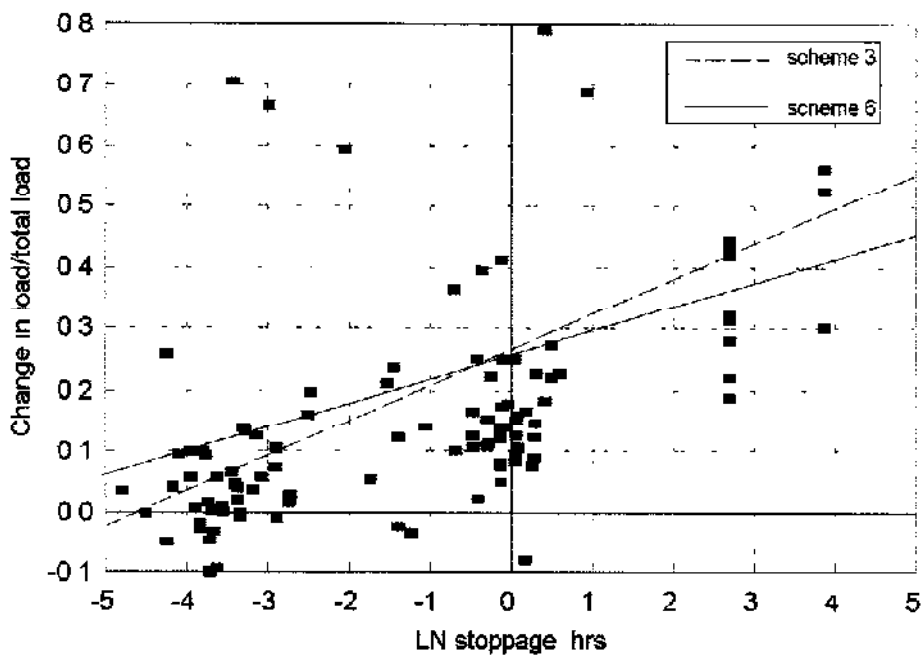
$$\text{Scheme 1 (dry): } \delta P/P = 0.113 + 0.004 \ln(t)$$

$$\text{Scheme 1 (wet): } \delta P/P = 0.042 + 0.045 \ln(t)$$

Notable features in the Scheme 8 jacking record – Figure 5.3 – are the widely spaced peaks in jacking load after weekend stoppages – details are included in Table 5.3. Following the weekend of the 6th and 7th August, the Contractor attempted to reduce the large restart forces by having the pipeline pushed a nominal 0.5m during subsequent weekends. However, reducing the time during which the pipe string was



(a) Scheme 3 (after Norris, 1992b).



(b) Scheme 6.

Figure 5.25 Stoppage factors in London clay.

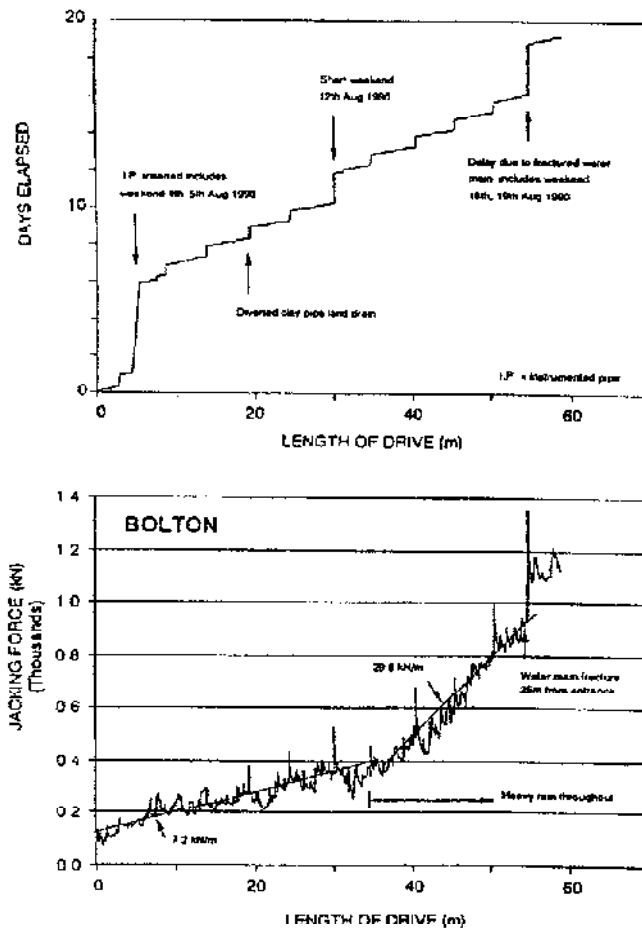


Figure 5.26 Scheme 1 jacking record (after Norris, 1992b).

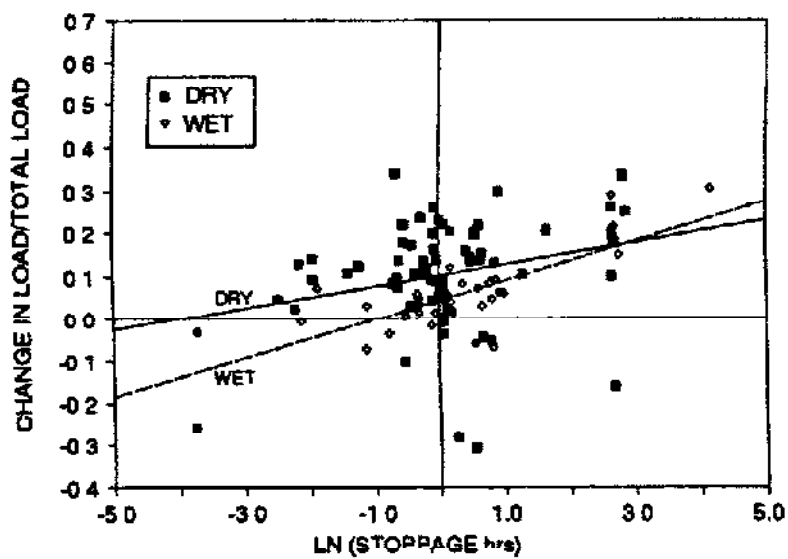


Figure 5.27 Scheme 1 stoppage factors (after Norris, 1992b).



Weekend	Distance jacked (m)	Stoppage (hrs)	Restart force (kN)	$\delta P/P$	Notes
16-17 Jul	16	102	1222	0.11	No weekend work - long stoppage due to work on TBM
23-24 Jul	51	66	1182	0.08	No weekend work
30-31 Jul	104	70	2676	0.42	No weekend work
6-7 Aug	149	70	4350	0.70	No weekend work
13-14 Aug	191	41	5834	0.83	Work half-shift on Saturday morning
20-21 Aug	230	64	6393	0.69	Line pushed 0.5m
27-29 Aug	267	90	6158	0.45	Line pushed 0.5m
3-4 Sept	291	71	5790	0.35	Line pushed 0.5m

**Table 5.3 Scheme 8 restart loads following weekend stoppage.**

stood during weekend breaks did not significantly reduce the restart loads. Jacking forces over a short section are presented in Figure 5.28. The repeatable increase in restart jacking forces, notable in London clay, is not evident in Scheme 8. The time relationship causing the large restart forces appears to be different to that observed in Schemes 3 and 6. The pronounced peaks are probably due to some of the lubricant slurry dissipating into sand layers present in the glacial till, and the pipe string settling back onto the bore invert. Moving the pipeline forward and pumping fresh lubricant brought the jacking load down to the lubricated value.

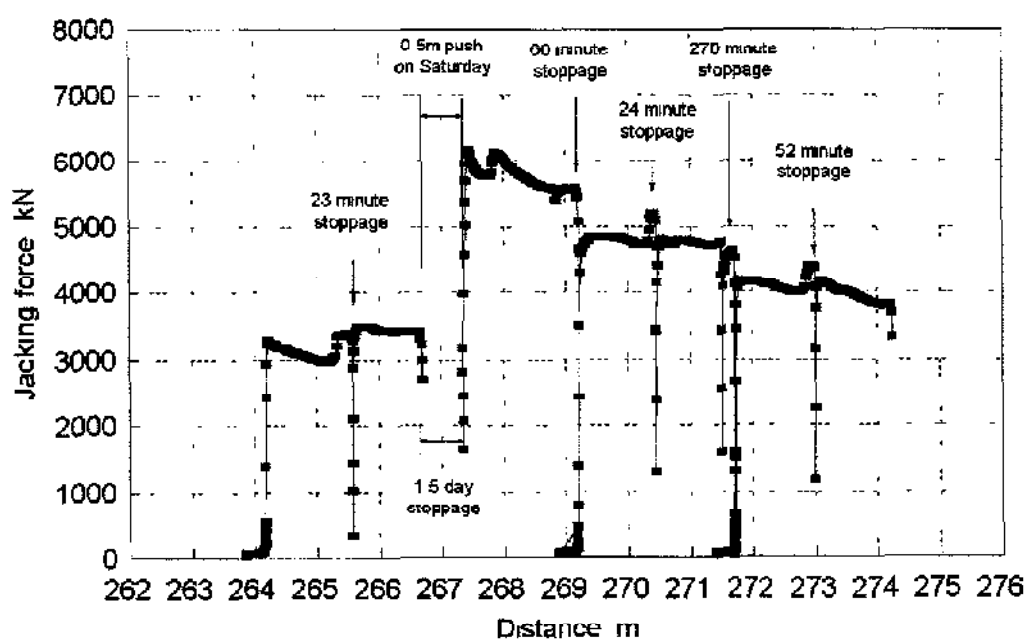


**Figure 5.28 Time dependent effects on jacking loads of Scheme 8.**

The normalised increases in jacking loads for Scheme 8 are presented in Figure 5.29. The large scatter of data and the effects of lubrication prevents a meaningful linear expression.

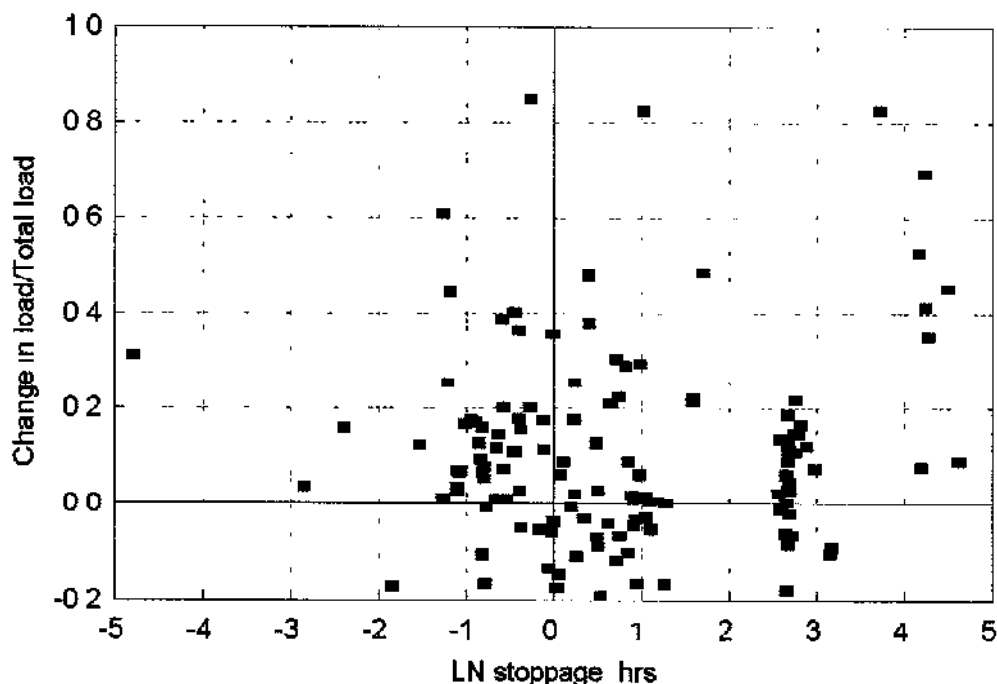


**Figure 5.29** Stoppage factors in the stiff glacial clay of Scheme 8 (including linear relationships of Scheme 1).

### 5.3.3.3 Soft clay

In the soft peaty clay of Scheme 9, continuous working gave few significant stoppages, a notable exception being the weekend of 14th and 15th January. The restart jacking load after the weekend break was 1740kN greater than the force at the end of the previous push, Figure 5.4. This increase was probably due to the ground closing onto the pipeline over a two day period. Pumping lubricant had the effect of reducing the jacking loads as pipe jacking restarted. Detailed examination of jacking forces after short stoppages show little or no increase – Figure 5.30. Data points for all stoppages have been plotted against normalised increase of jacking load in Figure 5.31. There is appreciable scatter and the lubricant appears to have little effect on subsequent restart forces. It is suggested that stoppage effects are negligible in soft clay.

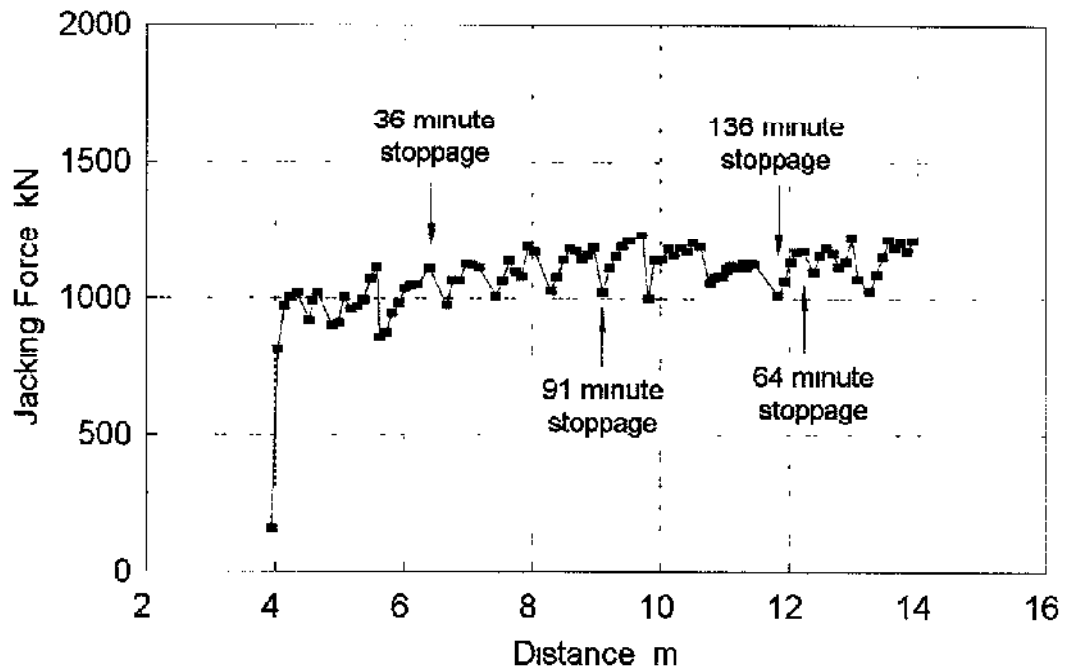


Figure 5.30 Jacking loads between 4 and 14m at Scheme 9.

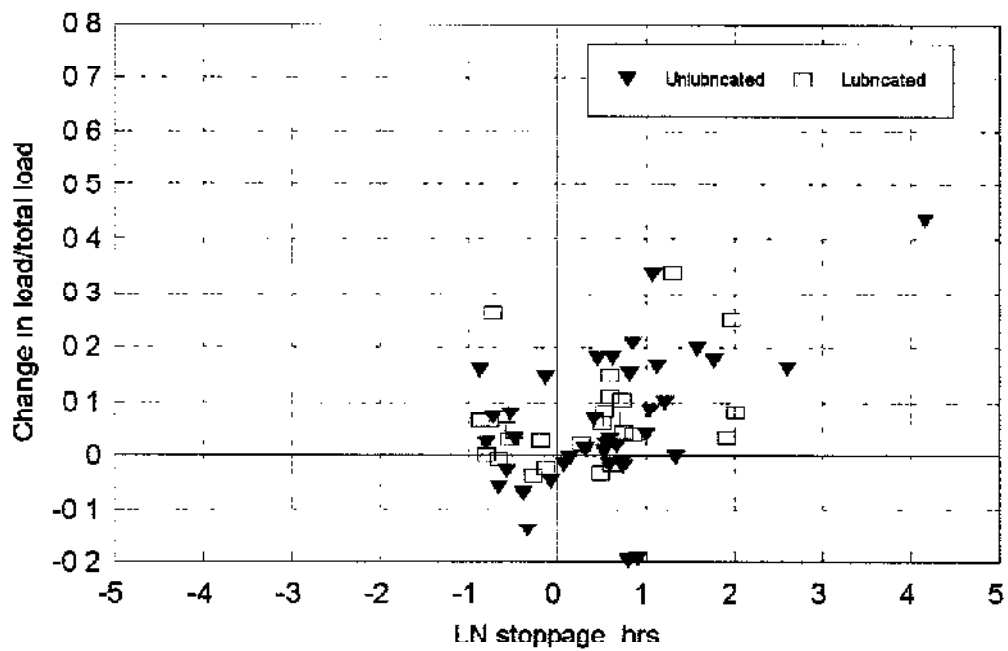


Figure 5.31 Stoppage factors at Scheme 9.

## 5.4 CONCLUSIONS

The main conclusions are:

- i Lubrication may be very effective in reducing frictional resistance if properly implemented in appropriate ground conditions.
- ii In stable bores, or bores supported by slurry pressure, pipes will become partially or wholly buoyant within a lubricating fluid.
- iii In unstable ground the lubrication operation should commence as soon as possible after the start of the drive, in very soft clay and ground where the bore is stable, lubricating need not start until the limiting jacking load is approached
- iv In high plasticity clays, delays between pushes result in significant increases in the jacking load required to advance the pipe string. This 'stoppage effect' is less significant in stiff low plasticity clays, and negligible in soft clay and cohesionless soils.

---

## chapter six

### pipe-soil interaction

#### 6.1 INTRODUCTION

The purpose of this chapter is to investigate the interaction between pipes and ground during pipe jacking. Contact stress cells built into the wall of the instrumented pipes allowed measurements to be made of pore pressures and normal and shear stresses at the pipe-soil interface. The magnitude of shear and normal (or radial) stresses indicate the extent of contact between pipe and ground and their ratio provides a measure of interface friction.

The chapter initially considers the interface stress records for each of the instrumented schemes. The four pipe jacks monitored during research Stage 3 are considered in detail, but interface stresses from Schemes 1 to 5, research Stage 2, are only summarised as full details are provided by Norris (1992b). The difference in interface behaviour in the soil types of the monitored schemes is then examined by reviewing plots of shear stress against total and effective radial stress during jacking. The influence of construction related parameters, including pipeline misalignment, stoppages and use of lubricants, on jacking loads was described in chapter five. Each of the three parameters is again covered in this chapter but with the emphasis on how interface stresses are affected.

#### 6.2 INTERFACE STRESS RECORDS

##### 6.2.1 Scheme 6

The local interface stresses in the highly plastic London clay of Scheme 6 are shown in Figures 6.1 to 6.4. Only five of the twelve contact stress cells had been fully modified to incorporate pore pressure transducers for this scheme. Two modified cells were placed in the bottom of the instrumented pipe, one in the top and one in each side. The pipe was inserted 25m behind the shield and passed through the excavation 9 days after the shield.

Peak and average values from the presented data sets (excluding effective radial stresses) are summarised in Table 6.1.

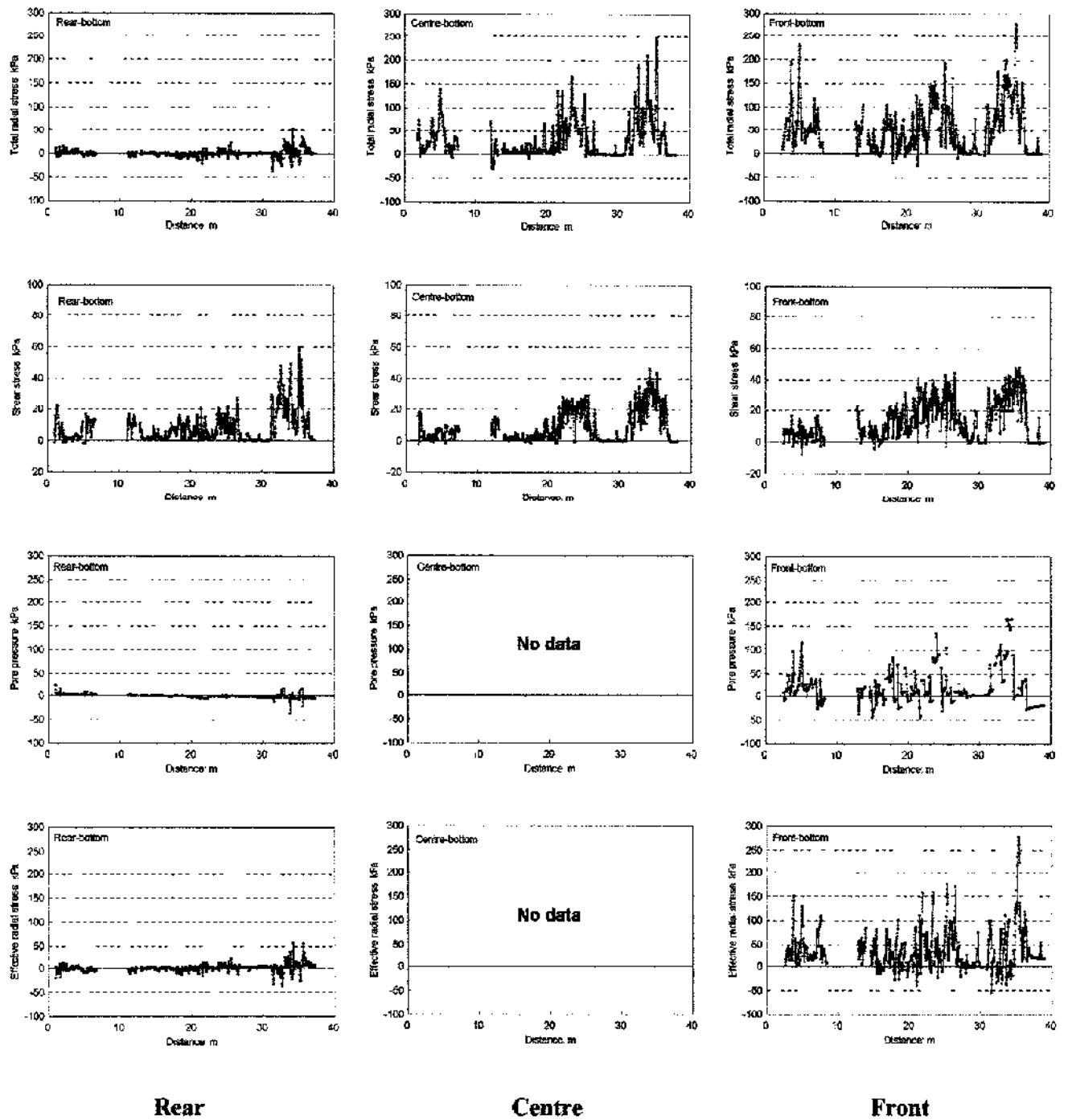


Figure 6.1 Scheme 6 interface stresses – pipe bottom.

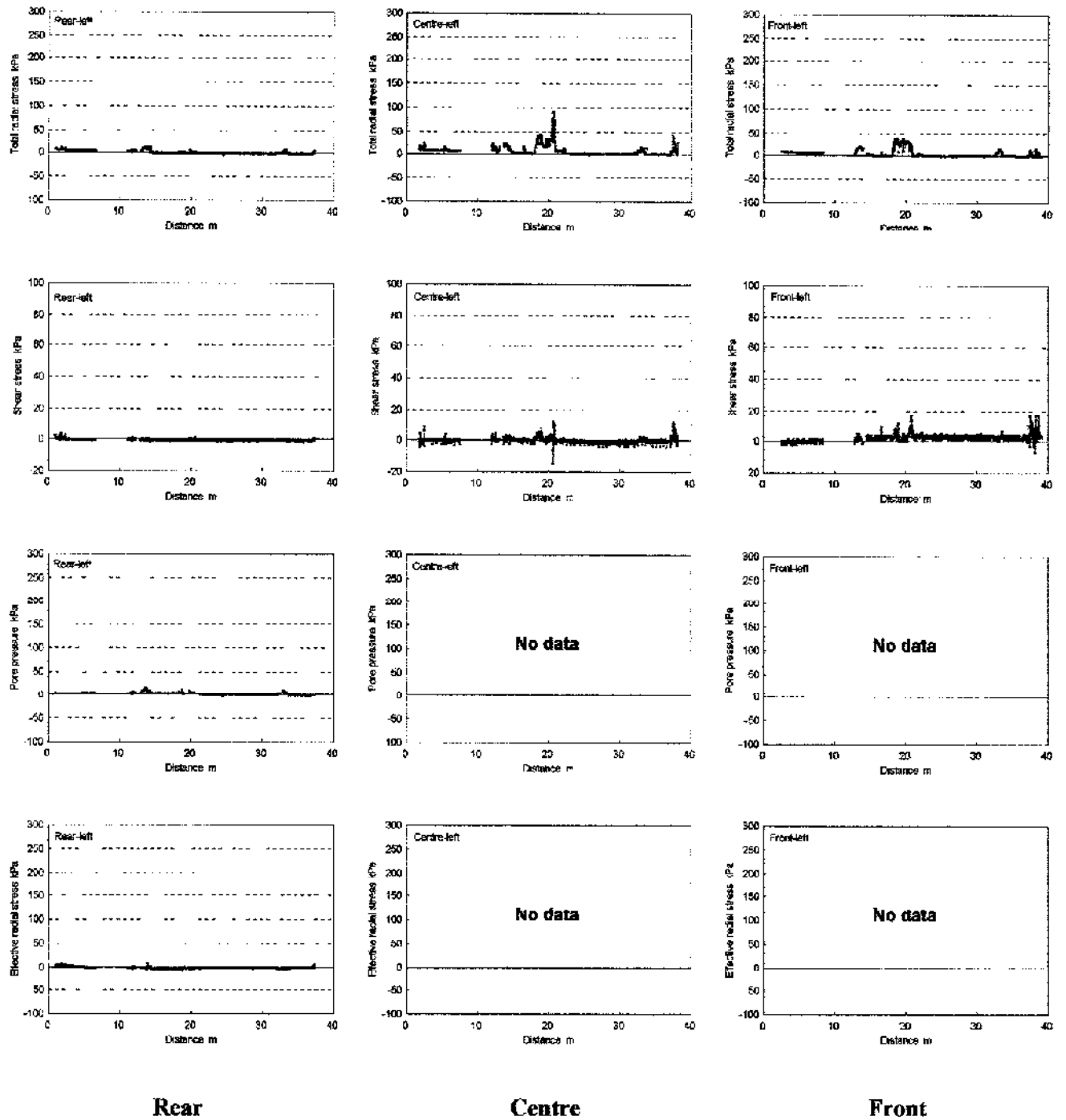


Figure 6.2 Scheme 6 interface stresses – left axis.

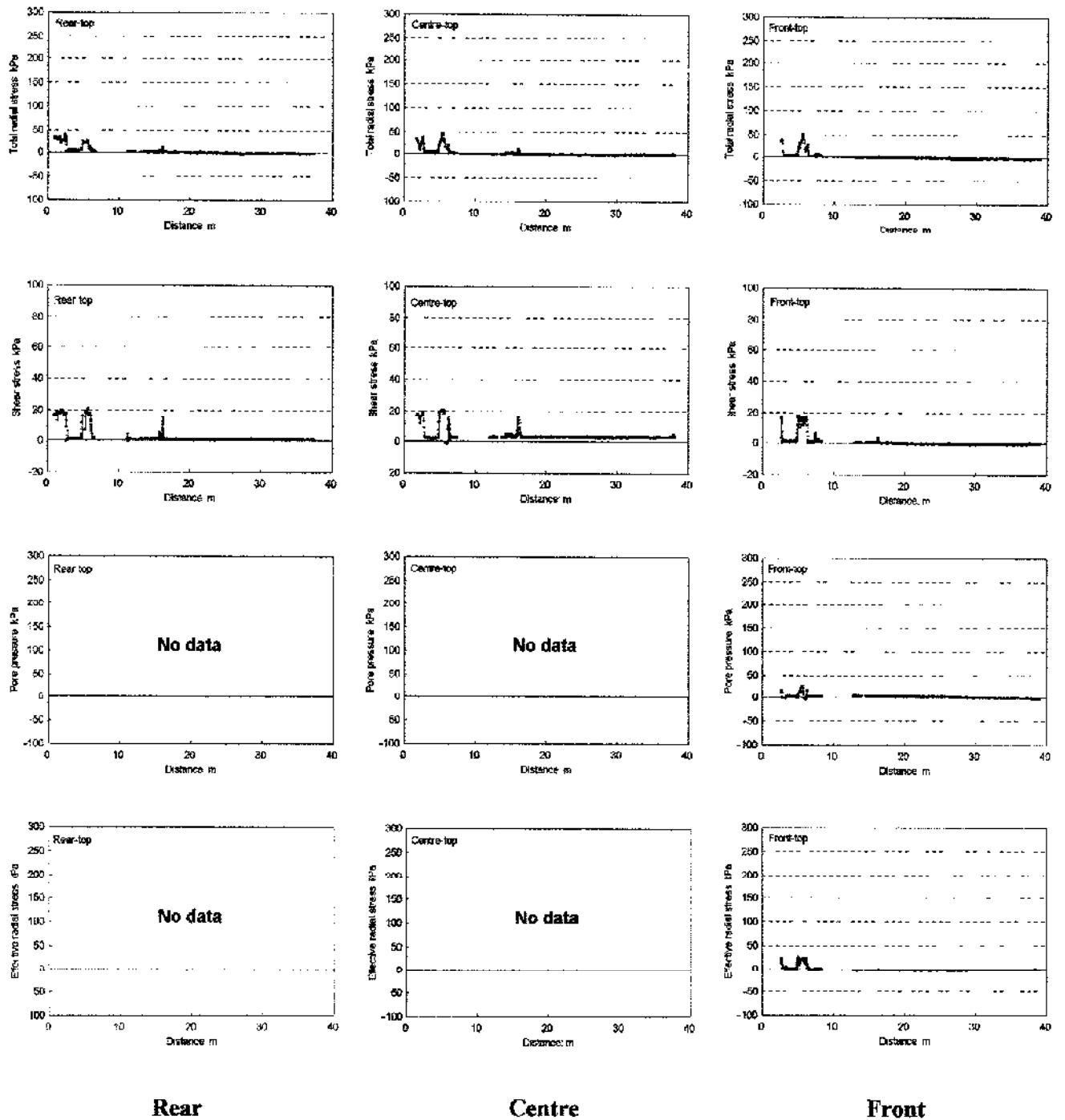


Figure 6.3 Scheme 6 interface stresses – pipe top.



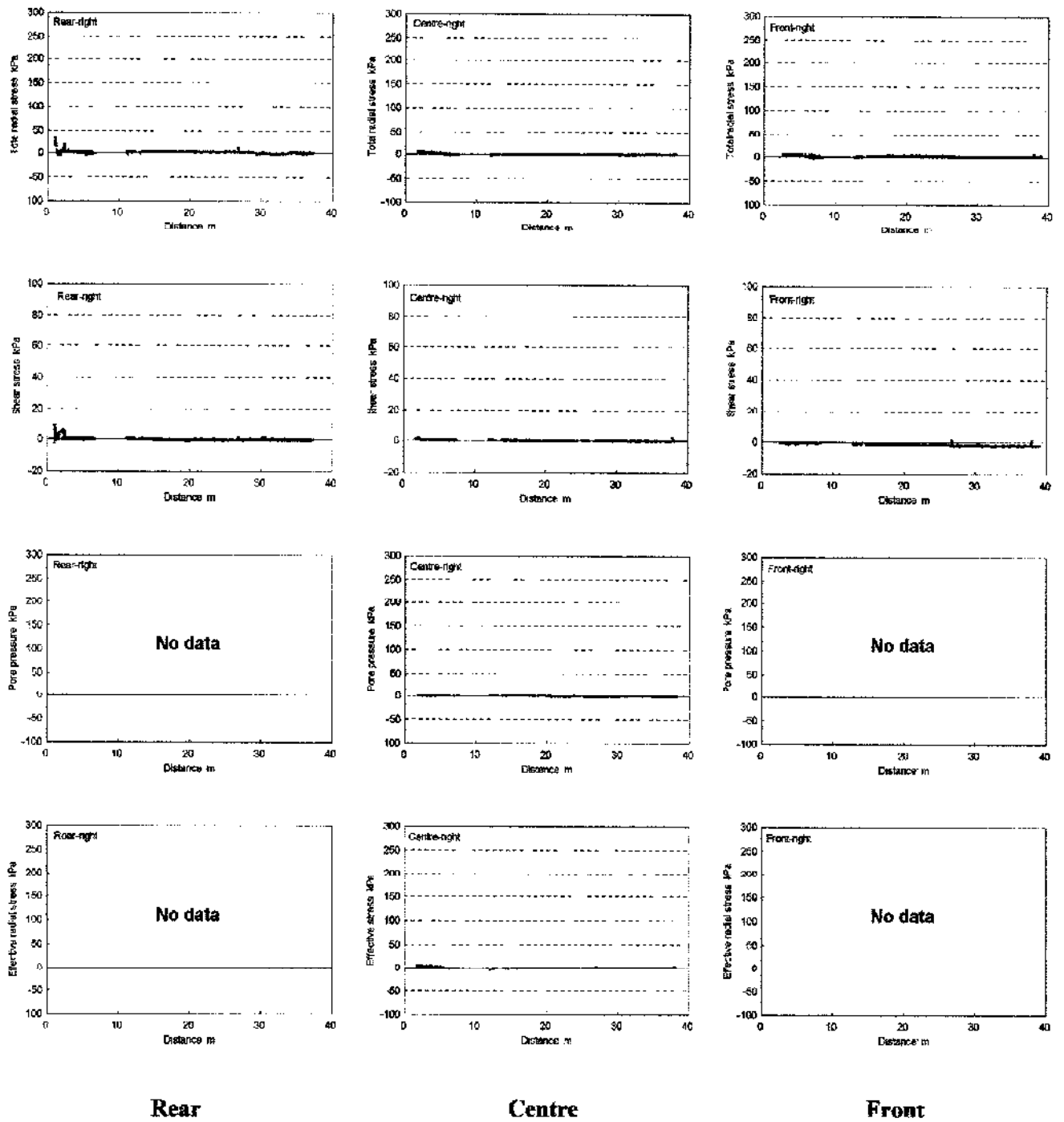


Figure 6.4 Scheme 6 interface stresses – right axis.

Position	Rear						Centre						Front					
	$\sigma$ (kPa)		$\tau$ (kPa)		$u$ (kPa)		$\sigma$ (kPa)		$\tau$ (kPa)		$u$ (kPa)		$\sigma$ (kPa)		$\tau$ (kPa)		$u$ (kPa)	
	peak	av	peak	av	peak	av	peak	av	peak	av	peak	av	peak	av	peak	av	peak	av
Bottom	-	-	60	8	20	-1	247	30	47	9	-	-	278	53	48	14	165	19
Left	12	0	3	0	17	1	93	6	12	0	-	-	39	3	17	2	-	-
Top	42	2	21	2	-	-	46	1	21	4	-	-	51	0	19	1	28	2
Right	34	1	9	0	-	-	8	0	2	0	10	0	9	2	2	-1	-	-

Note  $\sigma$  denotes total radial stress,  $\tau$  denotes shear stress,  $u$  denotes pore pressure

**Table 6.1 Scheme 6 peak and average interface stresses.**

Radial stresses at the rear-bottom position are unreliable due to an error in calibration. The pattern of pore pressure data from the two bottom cells is very different and it is not clear which, if any, response is reliable. The pore pressure transducers were checked and calibrated in the laboratory before and after the monitoring period and both had a stable and linear response. The difference in response remains inexplicable and there is therefore some doubt in the validity of the bottom pore pressures and effective radial stresses. Notwithstanding the erroneous radial stresses at the rear and questionable pore pressures, the bottom plots – Figure 6.1 – show excellent agreement between the three cells for shear stresses and good agreement for total radial stresses between the front and centre cells. Peak interface stresses were obtained over short lengths with a lower overall average for the total length. The peak values are 278kPa and 60kPa for total radial stress and shear stress respectively.

Plots representing interface stresses along the left of the pipe, Figure 6.2, are in good agreement and show the only significant contact between the pipe's left axis and ground occurring between chainages 18m to 21m. The peak radial stress of 93kPa – centre cell – corresponds with the abrupt change in pipeline alignment at about chainage 20m (Figure 5.19). Further details of misalignment effects are covered in section 6.5. Interface stresses on the top of the pipe, Figure 6.3, indicate some pipe-soil contact between chainages 2m to 3m and 5m to 6m. This is probably due to the erratic nature of hand excavation causing local irregularities in the tunnel bore. The plots of Figure 6.4 indicate no significant contact along the right of the pipe.

The overall pattern of interface stresses shows that contact between pipe and ground generally only occurs at the bottom and that the pipe is sliding along the base of an open bore

### 6.2.2 Scheme 7

The interface stresses recorded around the Scheme 7 instrumented pipe are shown in Figures 6.5 to 6.8. The pipe was inserted as the second pipe in the string, 2.5m behind the slurry shield. The contact stress cell at the front-top position was damaged prior to pipe insertion and produced no data. The damage was caused by a severe pull on the instrument cable resulting in the dislodging of wires to the Cambridge earth pressure cell. The Keller pore pressure transducer in the centre-right cell failed to produce a linear response during pre-scheme calibration and was therefore excluded from data logging during the monitoring.

All pore pressure plots show excellent agreement with calculated pressures and indicate hydrostatic pore pressures generally existed during jacking in the fine sand. Pressure increases above hydrostatic on the whole correspond with the pumping of lubricant. Pore pressure data considered together with total radial stress data provides very useful information on effective stress behaviour. Peak and average interface stresses, in terms of effective stress, are presented in Table 6.2

Position	Rear						Centre						Front					
	$\sigma'$ (kPa)		$\tau$ (kPa)		$u$ (kPa)		$\sigma'$ (kPa)		$\tau$ (kPa)		$u$ (kPa)		$\sigma'$ (kPa)		$\tau$ (kPa)		$u$ (kPa)	
	peak	av	peak	av	peak	av	peak	av	peak	av	peak	av	peak	av	peak	av	peak	av
Bottom	49	4	38	5	86	48	41	6	22	3	83	50	51	1	22	1	89	54
Left	209	49	153	40	74	41	171	45	123	29	100	46	65	7	59	10	74	43
Top	122	44	87	31	47	38	67	16	39	8	70	38	-	-	-	-	-	-
Right	26	2	14	2	80	44	46	*12	46	9	-	-	82	13	55	9	87	45

\* calculated using hydrostatic pressure

**Table 6.2 Scheme 7 peak and average interface stresses.**

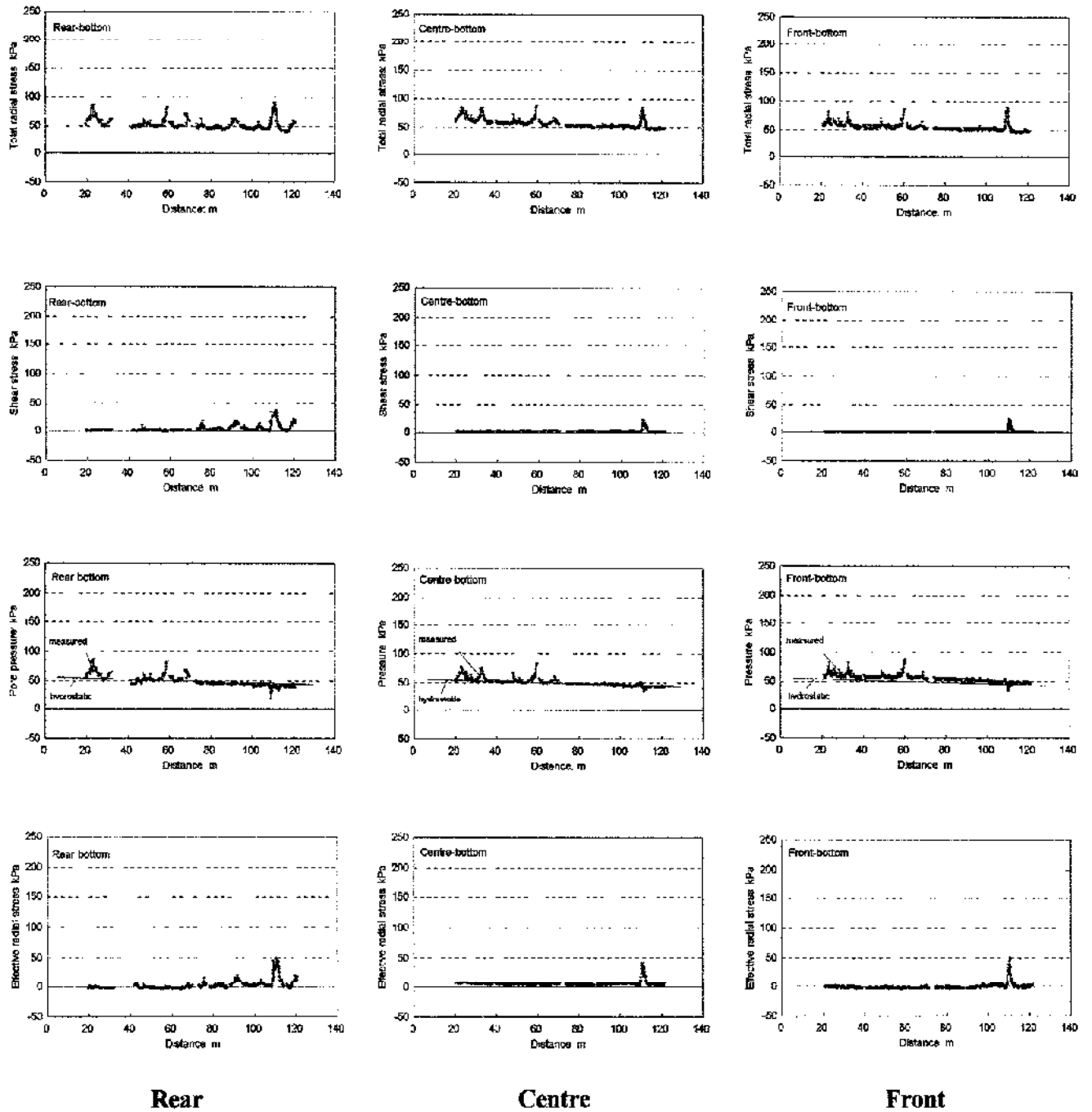


Figure 6.5 Scheme 7 interface stresses – pipe bottom.

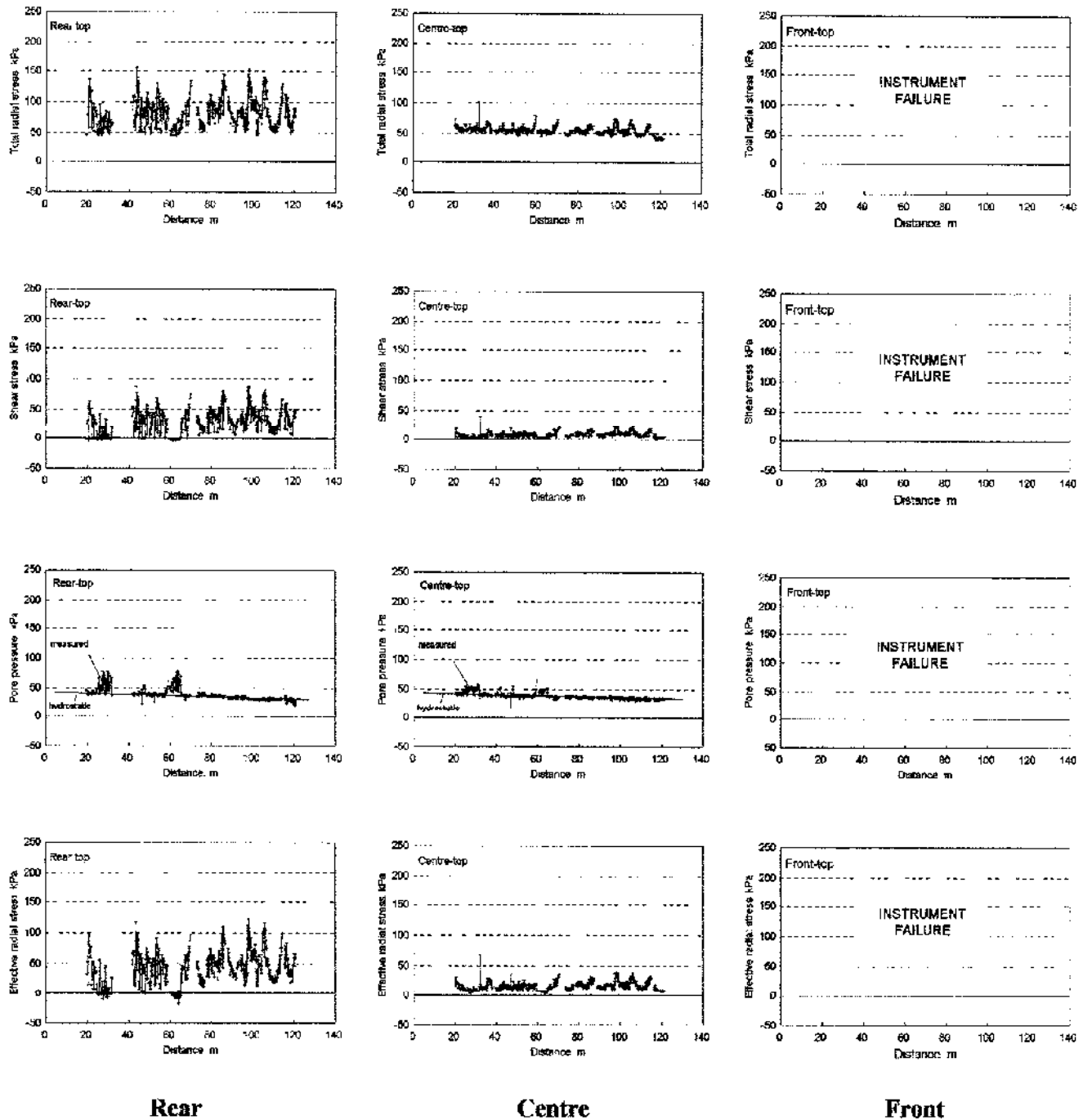


Figure 6.6 Scheme 7 interface stresses – pipe top.

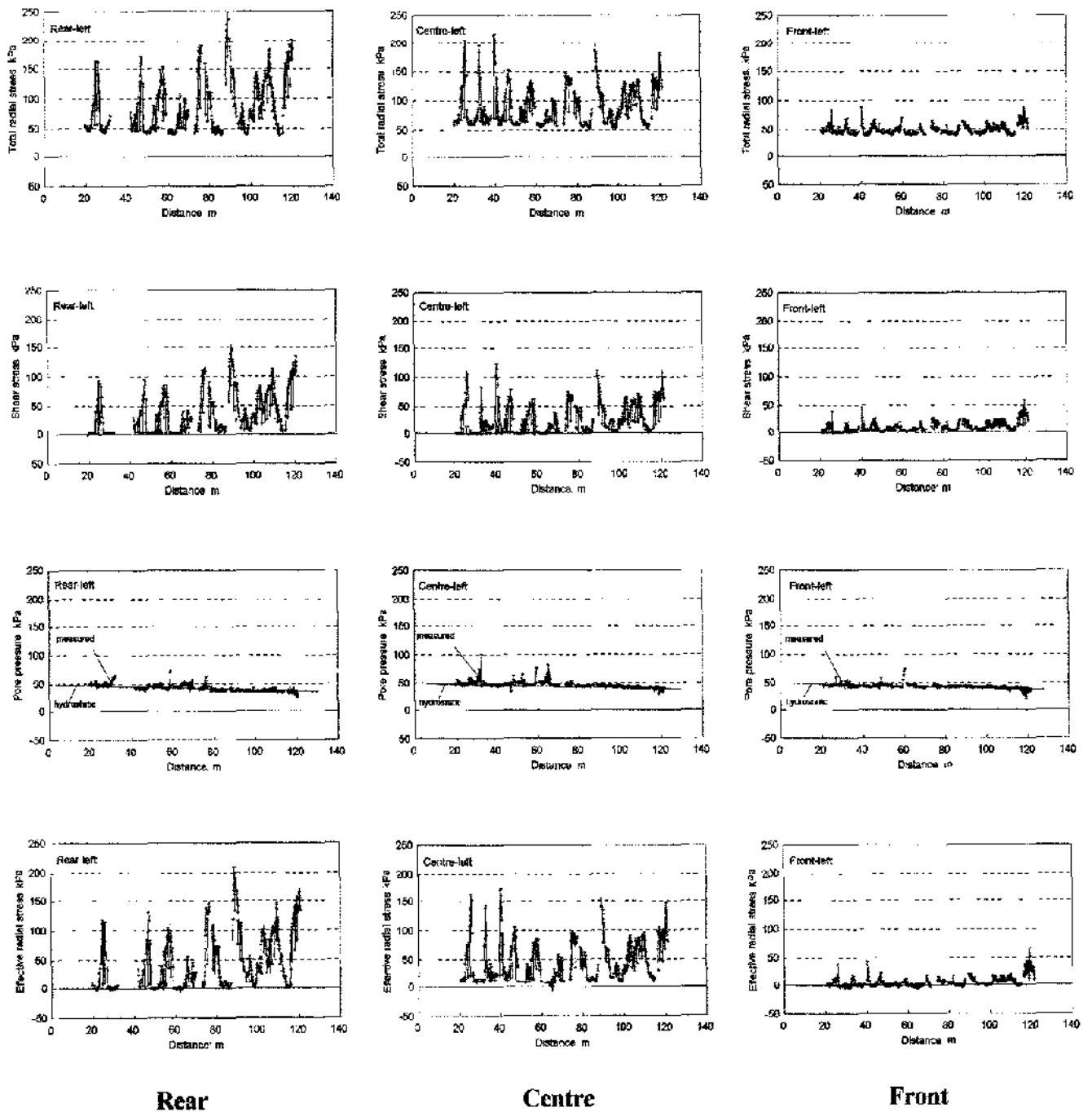


Figure 6.7 Scheme 7 interface stresses – left axis.

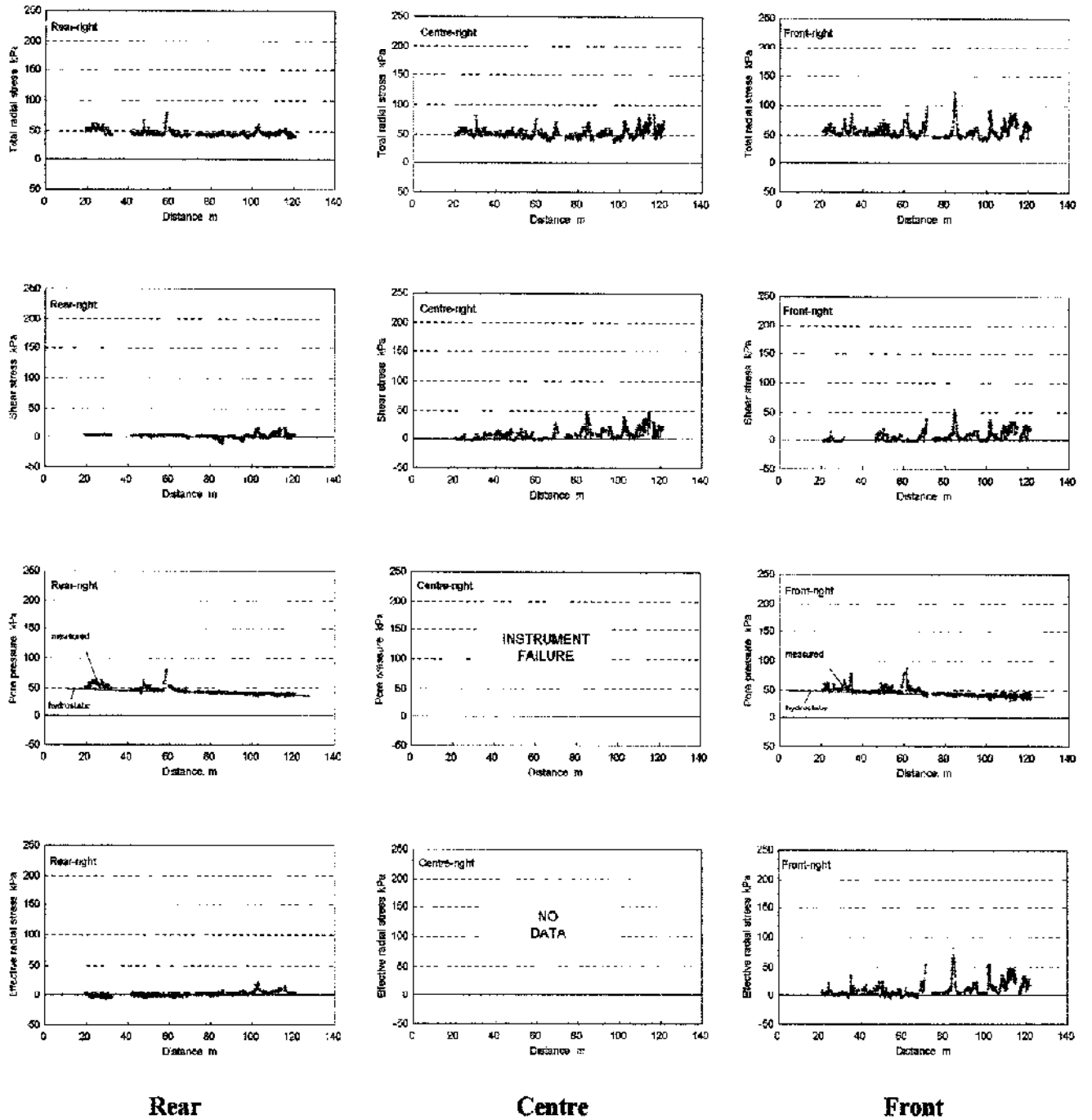
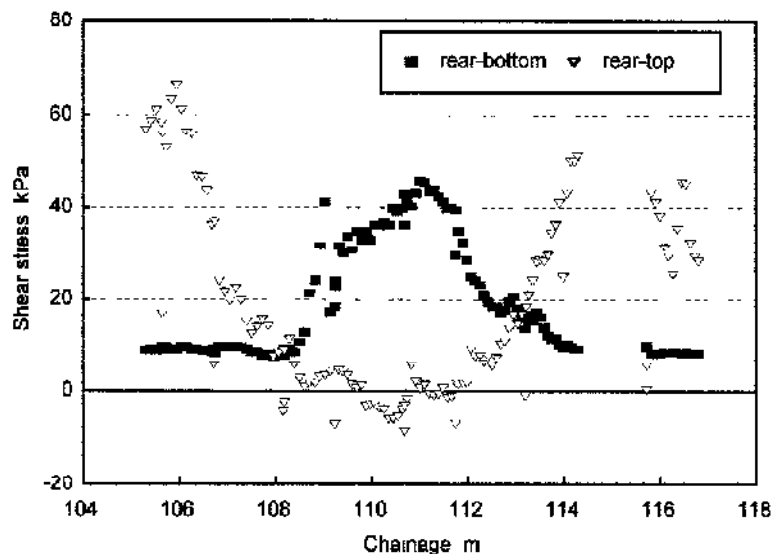


Figure 6.8 Scheme 7 interface stresses – right axis.

Bottom interface stresses – Figure 6.5 – are close to zero for most of the drive because the pipe is buoyant in groundwater and lubricant. The average shear stress, recorded at the centre position, is 3kPa and the corresponding effective radial stress is 6kPa. Peak stresses on the bottom occur at chainage 111m where there is clearly some contact between pipe and soil. Figure 6.9 shows a transfer of shear stress from the top of the pipe to the bottom at this particular location suggesting a loss of buoyancy at this position. There is no noticeable increase in jacking load at the time of this occurrence and it is assumed therefore that the effect is local. Pipe buoyancy has caused significant contact with the crown of the tunnel bore and it is interesting that the extent of the contact appears to be concentrated at the rear of the pipe (Figure 6.6). This may be due to the pipe being subject to a longitudinal rotation and/or pressurised lubricant from the front injection socket (placed in the shield) forming an effective gel around the leading half of the pipe. Buoyancy and the effect of lubrication on interface stresses are discussed further in section 6.6.



**Figure 6.9** Scheme 7 shear stresses at rear-top and rear-bottom positions between chainages 105m and 117m.

Interface stresses along the left of the pipe, Figure 6.7, clearly show pipe-soil contact occurring. The pattern, as in Scheme 6, is one of peak stresses obtained over short lengths with a lower average for the total length. As at the pipe top, the magnitude of stresses is generally greater along the trailing half of the pipe. At the pipe rear, the average shear stress is 40kPa and average effective radial stress is



49kPa. At the front of the pipe average stresses are 10kPa, shear, and 7kPa, effective radial. Conversely, interface stresses recorded along the right of the pipe, Figure 6.8, indicate very little pipe-soil contact with the ground at the rear but intermittent contact at the front, suggesting that the pipe may also have been subject to a lateral rotation. An effective layer of lubricant gel along the right of the pipe resulted in the low interface stresses, the average values at the front are 9kPa and 13kPa for shear stress and effective radial stress respectively.

In conclusion, contact between the soil and instrumented pipe only consistently occurred along its trailing half at the left axis and top. The distribution of radial interface stresses, illustrated in Figure 6.10, may be due to a combination of lubricant pressure and the heavy shield (unlikely to be buoyant) drawing pipes 1 and 2 (instrumented pipe) down towards the tunnel invert.

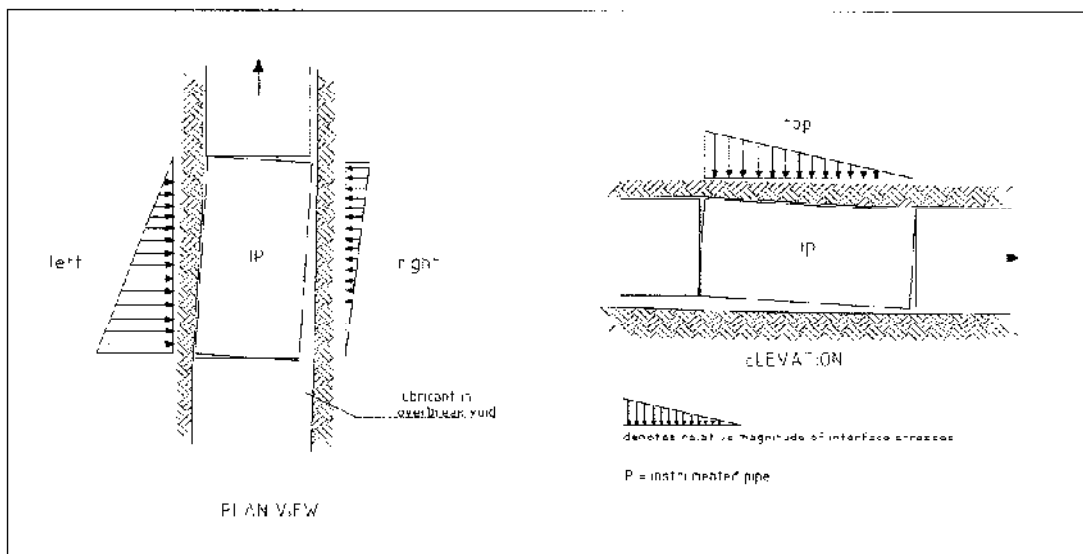


**Figure 6.10 Distribution of Scheme 7 radial interface stresses.**

Figure 5.10 shows the conjectured circumferential dispersion of lubricant around the pipe caused by buoyancy and position of lubricant injection points - discussed in the previous chapter. The data show that even in an almost perfectly straight pipeline, pipe-soil contact around and along the pipe can still vary greatly.

### 6.2.3 Scheme 8

Scheme 8 interface stresses are shown in Figures 6.11 to 6.14. The Keller pore pressure transducer in the centre-top contact stress cell failed to produce meaningful data during pre-insertion testing of instruments and has been excluded from analysis. The instrumented pipe was placed as pipe 74, about 182m behind the shield. The tunnel bore was lubricated and approximately 30 days old as the instrumented pipe was pushed through it. At chainage 58m, the cable to the front-bottom cell was nipped and damaged by an orcot bearing on the protective liner (Figure 4.19). The subsequent output became spurious and was removed from further logging.

There is excellent agreement between readings from each array of three cells, along the bottom, left, top and right of the pipe. Consistency in pore pressure and total radial stress measurements has produced very useful information on effective stress behaviour in the stiff glacial clay. The overall pattern of interface stresses shows more uniformity around and along the pipe than that observed at Schemes 6 and 7. Total radial stresses and corresponding pore pressures of almost equal value result in relatively low average effective stresses. Peak and average values of shear and effective stresses and pore pressures are included in Table 6.3.

Position	Rear						Centre						Front					
	$\sigma'$ (kPa)		$\tau$ (kPa)		$u$ (kPa)		$\sigma'$ (kPa)		$\tau$ (kPa)		$u$ (kPa)		$\sigma'$ (kPa)		$\tau$ (kPa)		$u$ (kPa)	
	peak	av	peak	av	peak	av	peak	av	peak	av	peak	av	peak	av	peak	av	peak	av
Bottom	38	1	11	2	246	78	201	15	8	1	256	80	105	20	8	2	198	62
Left	124	8	44	4	192	75	371	10	94	4	234	84	167	12	21	3	217	85
Top	192	2	43	6	354	51	-	-	12	-3	-	-	229	17	80	3	458	35
Right	198	24	74	4	255	49	205	42	88	5	368	66	208	28	122	5	344	58

**Table 6.3 Scheme 8 peak and average interface stresses.**

Bottom interface stresses, Figure 6.11, indicate the pipe sliding through a weak shear zone. The average shear stress is 2kPa and average effective stresses are, with the exception of two peaks recorded at the centre, uniformly low values ranging from 0kPa at the rear to 20kPa at the front. Examination of the plots from cells in the top of the pipe – Figure 6.12 – shows a peaky and more active response indicating sporadic

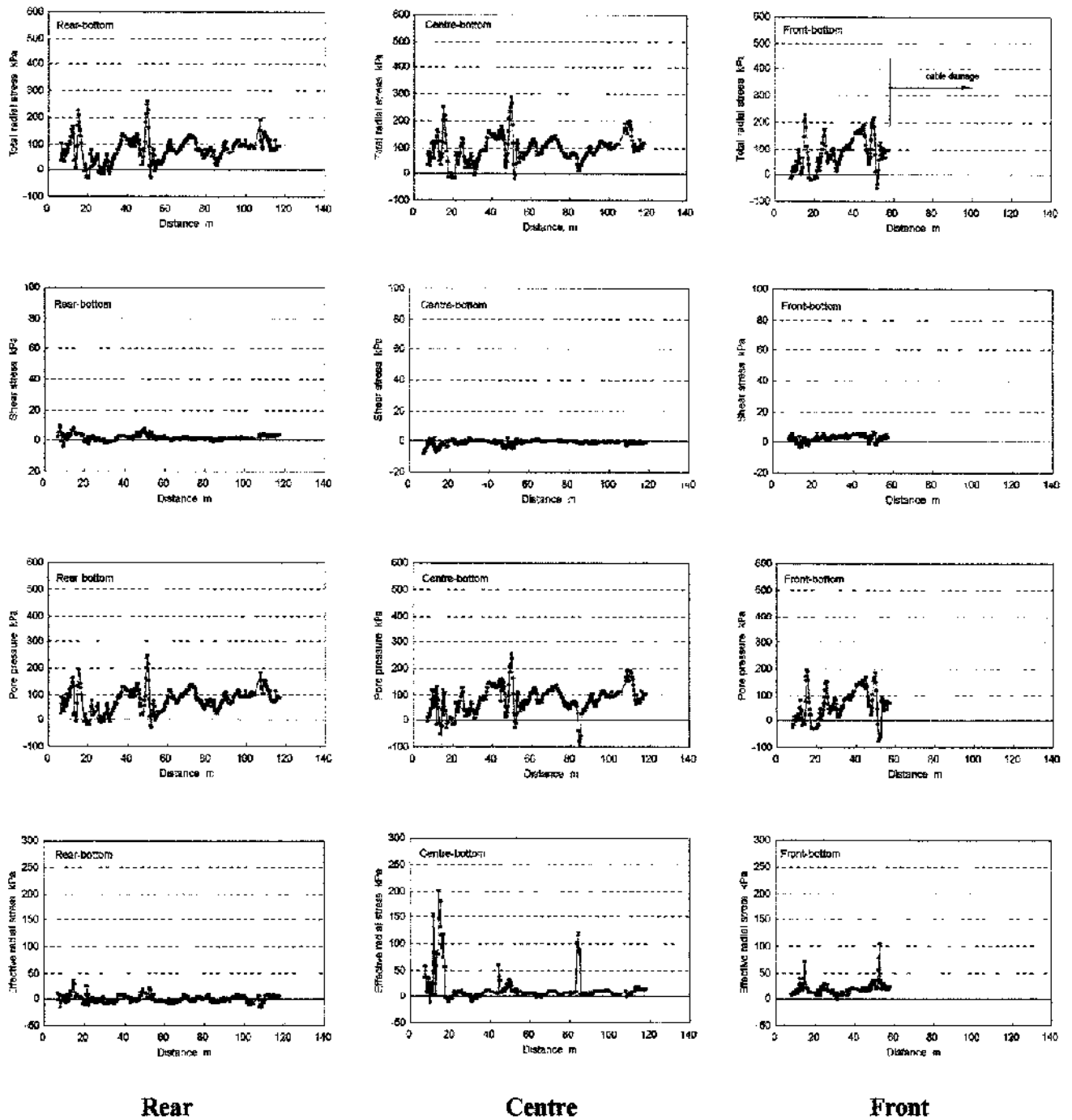


Figure 6.11 Scheme 8 interface stresses – pipe bottom.

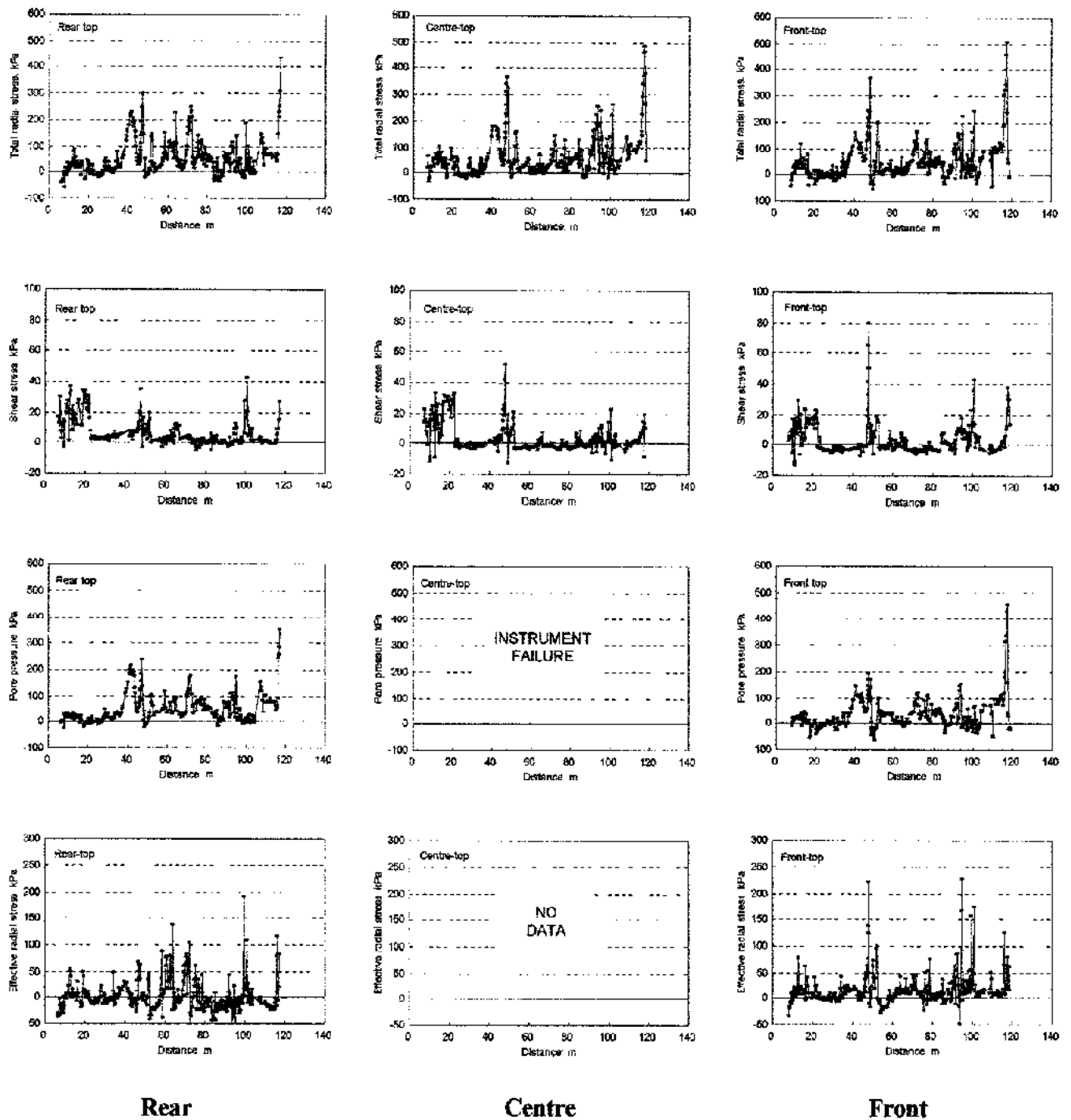


Figure 6.12 Scheme 8 interface stresses – pipe top.

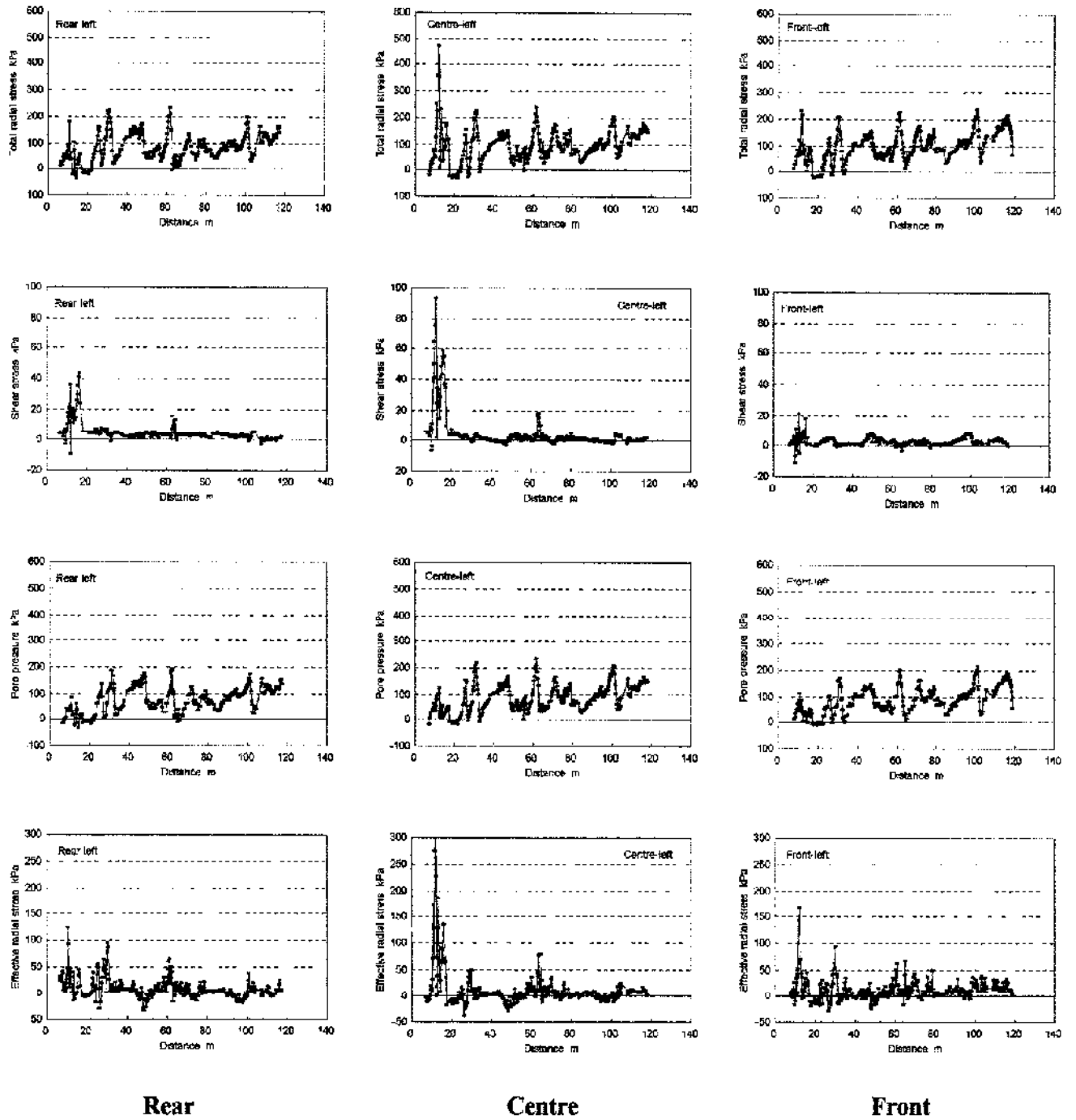


Figure 6.13 Scheme 8 interface stresses – left axis.

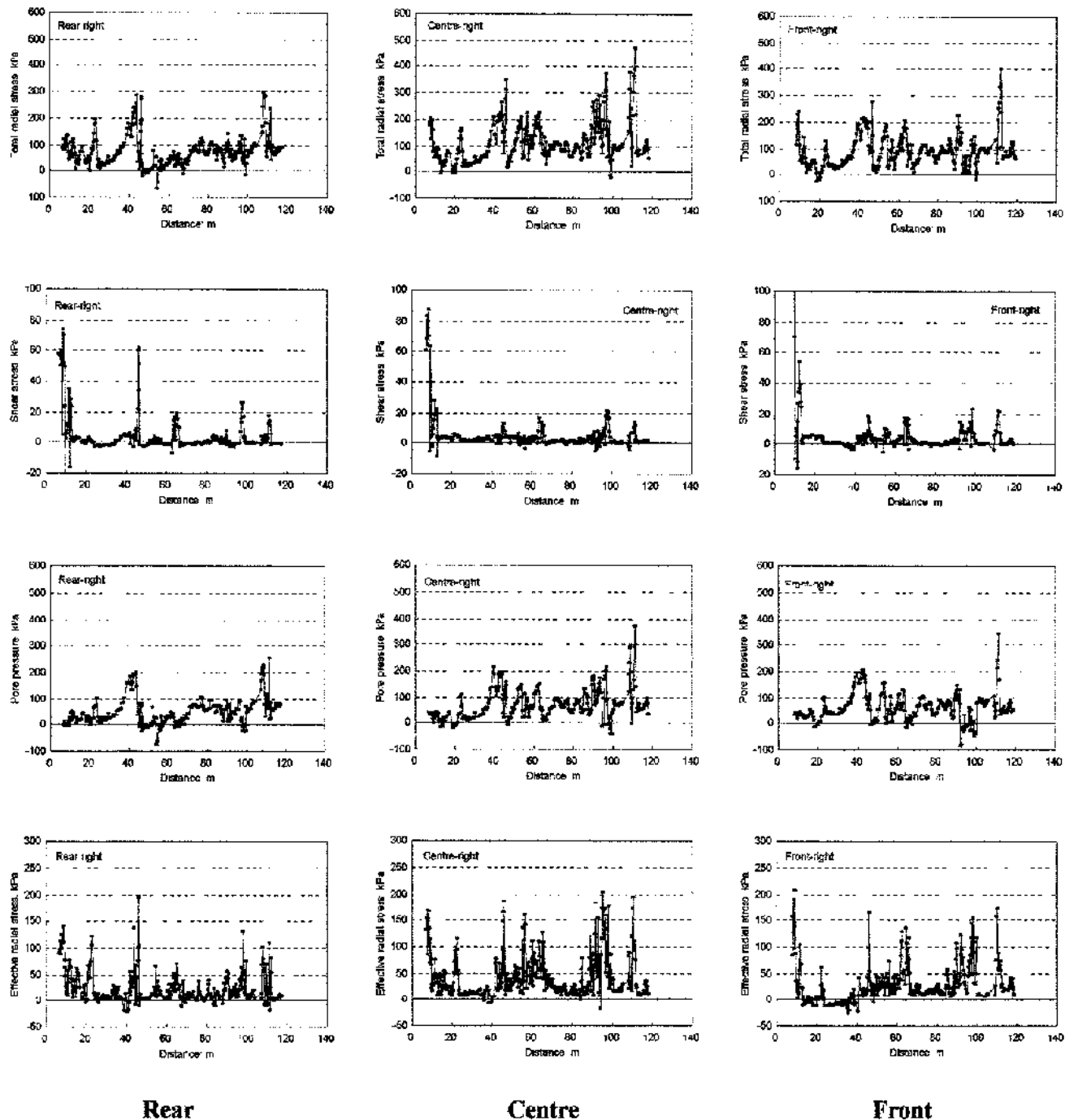


Figure 6.14 Scheme 8 interface stresses – right axis.

contact between the pipe and soil. Although average values of shear and effective stresses on the top are very similar to those at the bottom (Table 6.3), peaks are more numerous and maximum values greater along the top. Maximum shear stresses at the top range from 12kPa to 80kPa compared to a maximum value of 11kPa on the bottom. The conclusion drawn from the two data sets is the pipe is mostly buoyant in the pressurised lubricant. Shear stresses along the pipe top indicate a sustained period of pipe-soil contact in the wet clay encountered between the shaft and chainage 22m.

The pattern of interface stresses along the left of the pipe (Figures 6.13) is similar to that at the bottom where shear stresses are generally low, average 4kPa. Peak stresses, both effective and shear, occur at about chainage 15m. On the right of the pipe, low shear stresses are also evident (Figure 6.14), average 5kPa, but the effective stress response is much more peaky suggesting intermittent pipe-soil contact. The 150mm deviation from line and subsequent steering correction at chainage 39m, Figure 5.21, has not resulted in any noticeable contact between the sides of the instrumented pipe and ground.

In conclusion, the main influences on Scheme 8 interface stresses are lubrication and ground conditions. The wet clay encountered at the start of the drive has had an effect of the ground 'closing onto' the pipeline - demonstrated by the peak interface stresses recorded around the instrumented pipe as it passed through the initial 20m of tunnel bore. Pore pressures and total stress readings are very similar and both very erratic; effective radial stresses are small and shear stresses very small. The pipeline is largely buoyant in lubricant but with lubricant pressure varying rapidly, perhaps partly as a function of injection procedures, and partly by a squeezing action as the pipeline tries to straighten in the misaligned bore.

#### 6.2.4 Scheme 9

Local interface stresses in the very soft clay of Scheme 9 are shown in Figures 6.15 to 6.18. The instrumented pipe was inserted as pipe 19, about 48m behind the slurry shield. Pre-insertion testing of the instrumentation again saw the failure of one of the two Keller pore pressure transducers, the rear-top cell in this instance. This type of transducer was found to operate perfectly well in the laboratory during testing and calibration, but not in the field. Unfortunately the dummy contact stress cell, for

checking the tolerance of specially cast holes, was not made available to the special pipe manufacturer, resulting in one cell (rear-left) being installed in a slightly oversized hole the glue line failed soon after pipe insertion. The front-left cell produced a faulty response and was later found to have a crushed Cambridge earth pressure cell - damaged during the pre-scheme calibration.

Position	Rear						Centre						Front					
	$\sigma'$ (kPa)		$\tau$ (kPa)		u (kPa)		$\sigma'$ (kPa)		$\tau$ (kPa)		u (kPa)		$\sigma'$ (kPa)		$\tau$ (kPa)		u (kPa)	
	peak	av	peak	av	peak	av	peak	av	peak	av	peak	av	peak	av	peak	av	peak	av
Bottom	45	17	17	10	228	106	42	18	21	5	251	105	46	16	20	10	249	99
Left	57	19	37	21	94	29	171	30	36	12	171	78	-	-	-	-	-	-
Top	-	-	14	6	-	-	75	22	22	9	149	79	80	16	17	5	160	87
Right	56	19	24	7	182	96	85	13	37	7	181	99	68	13	26	16	163	84

Note values for rear-left location based on initial 10m of the drive

**Table 6.4 Scheme 9 peak and average interface stresses.**

Interface stress behaviour appears to be uniform around the instrumented pipe Table 6 4 contains peak and average stress values. As on Scheme 8, pore pressure and total stress readings are very similar but in the soft clay of this scheme are less erratic. Pore pressure measurements are much higher than calculated ground water pressures; along the pipe top calculated pressures range from 37kPa to 42kPa, approximately half the measured values of 79kPa, centre, and 87kPa, front

Shear stresses around the pipe are relatively consistent and results suggest an average value of 10kPa Effective stresses also exhibit some consistency with average values of about 20kPa. The introduction of lubricant (at about chainage 85m on the plots) appears to have had little effect on shear stresses (with the exception of the pipe left where there is a slight reduction) but changed pore pressure and total stress behaviour In the stress plots for the top, bottom and right of the pipe (Figures 6 15, 6.16 and 6 17 respectively) stresses become more erratic after lubricant has been introduced whereas pore pressures and radial stresses at the left of the pipe become more consistent – Figure 6 18. It is likely that there has been a non-uniform



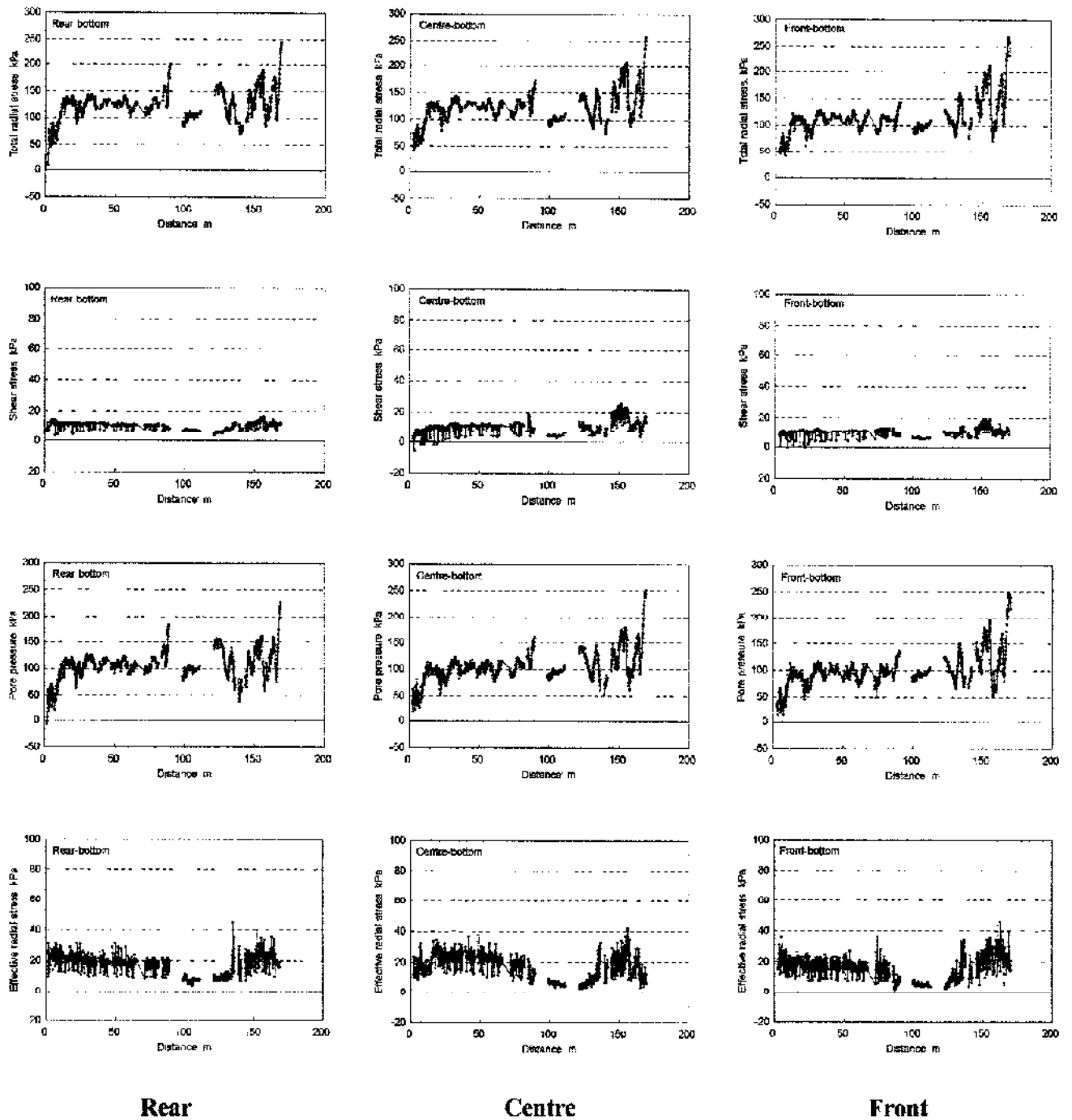


Figure 6.15 Scheme 9 interface stresses -- pipe bottom.

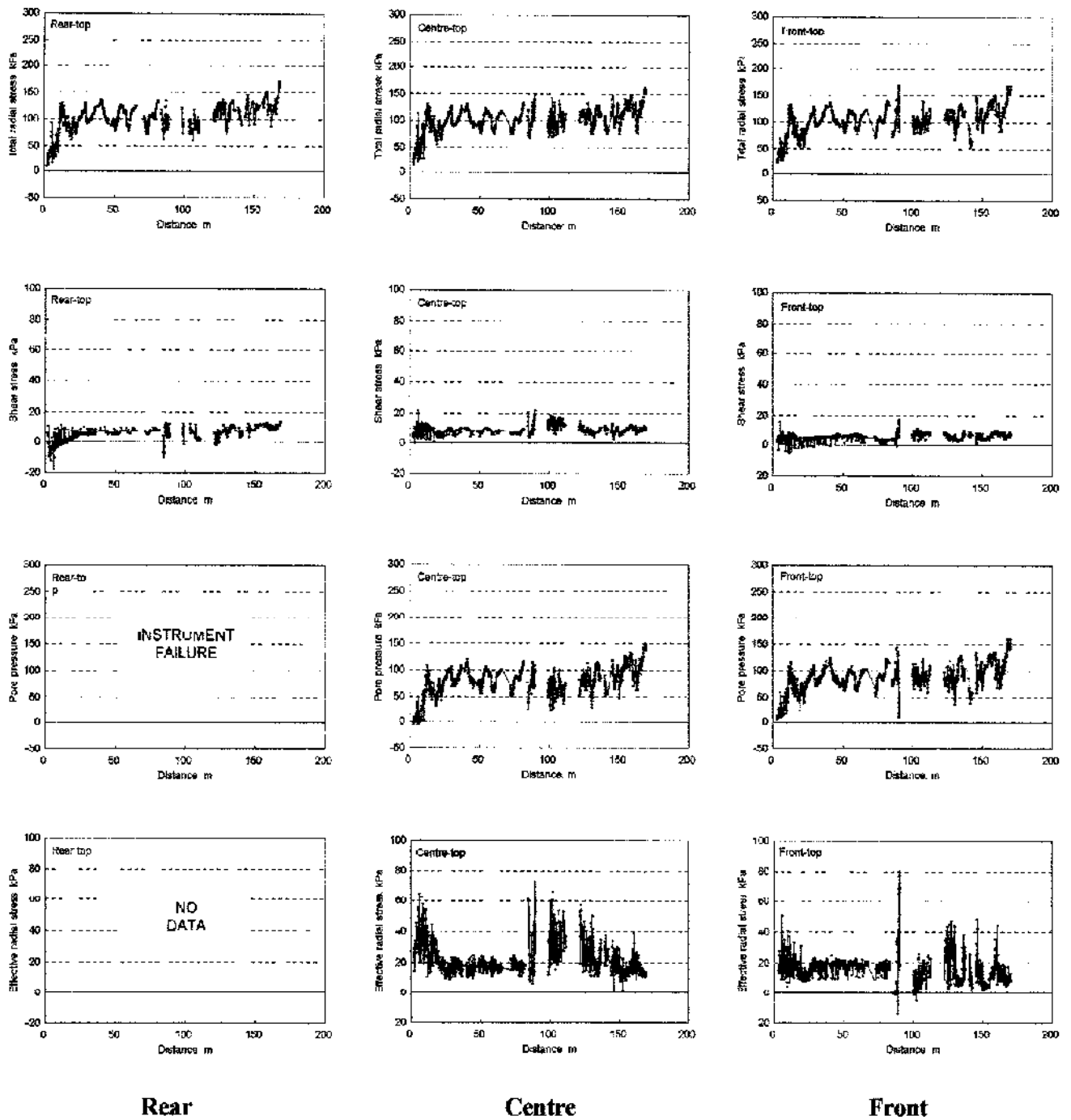


Figure 6.16 Scheme 9 interface stresses – pipe top.

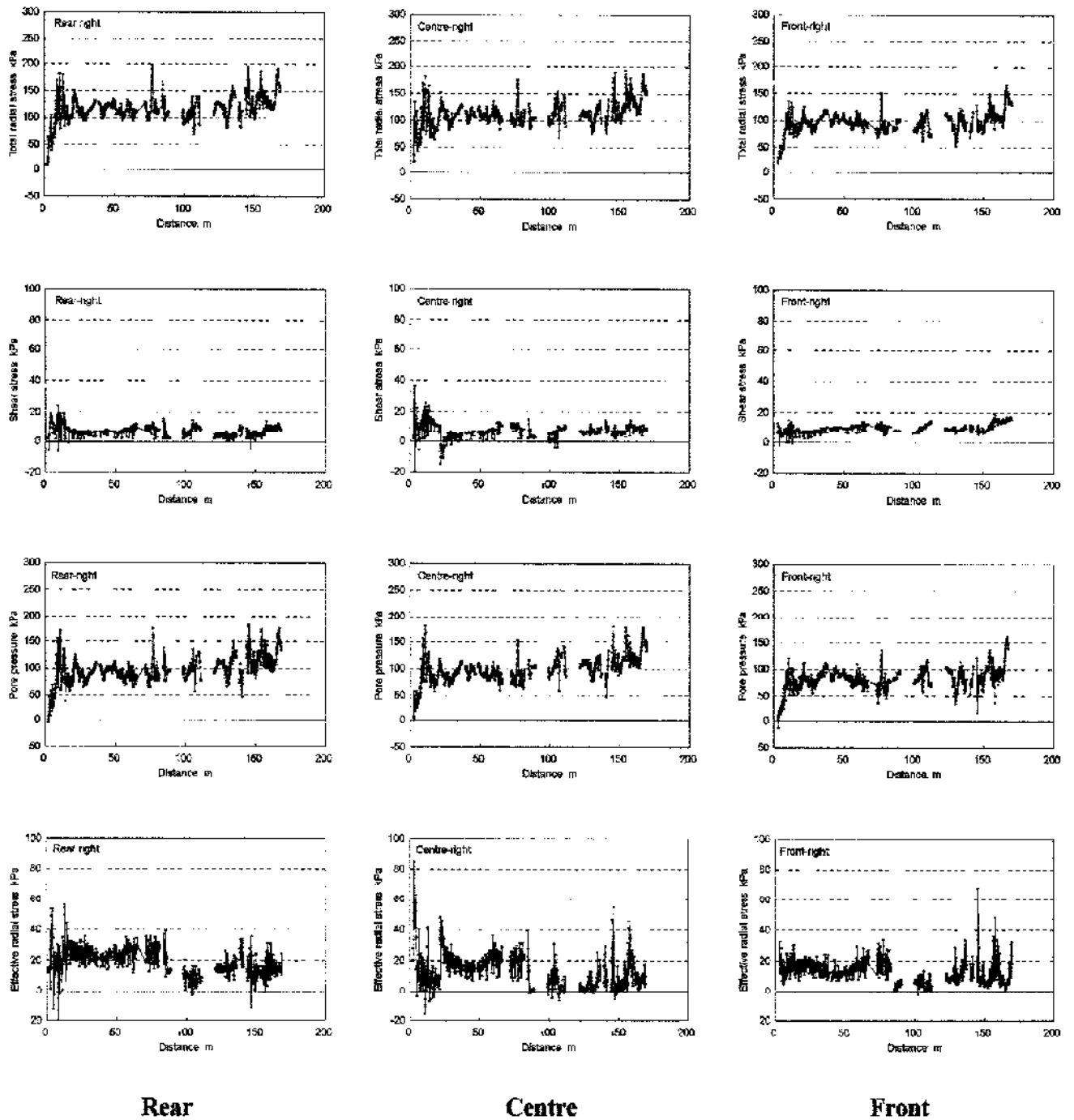


Figure 6.17 Scheme 9 interface stresses -- right axis.

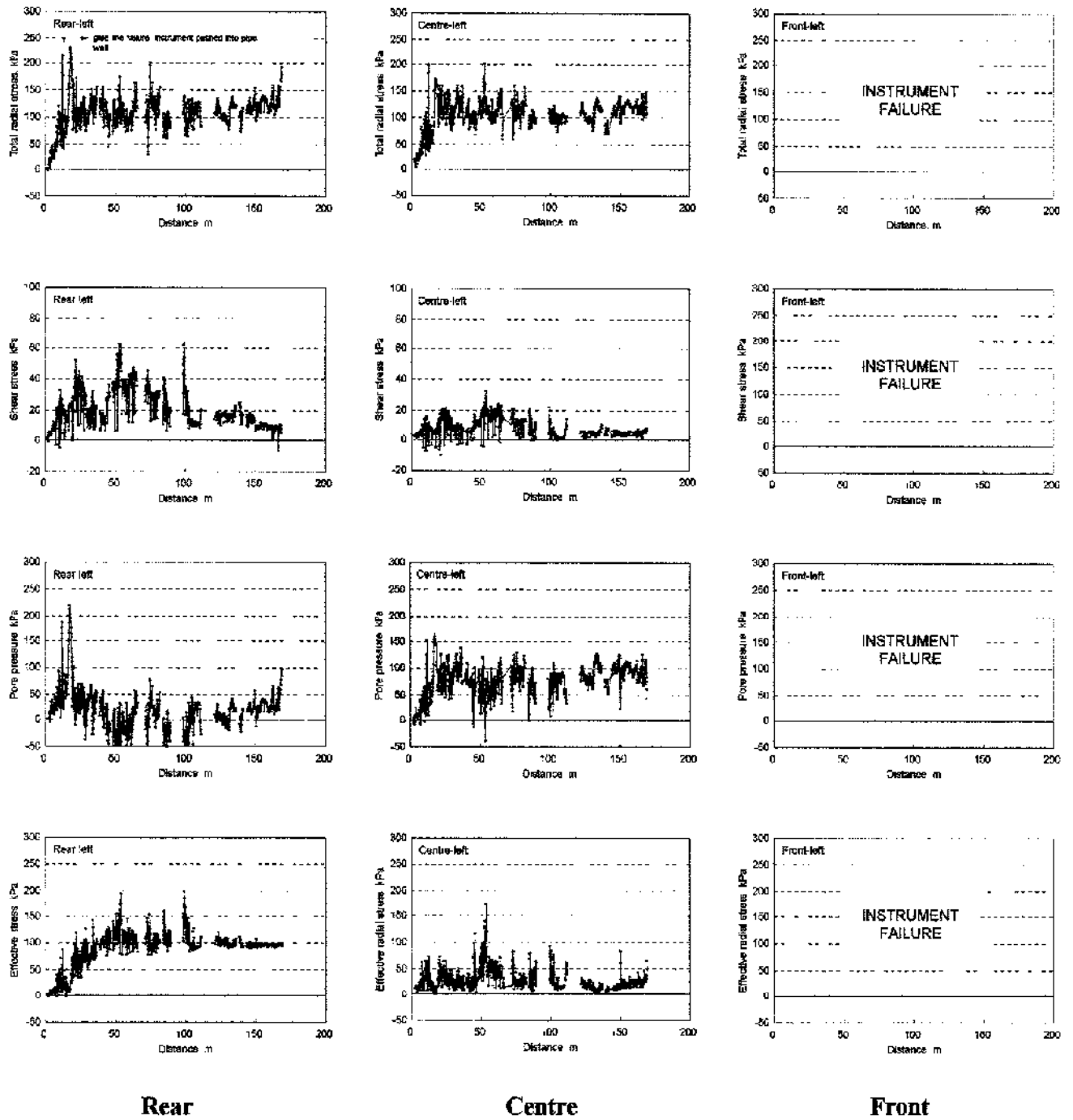


Figure 6.18 Scheme 9 interface stresses – left axis.

distribution of lubricant around the pipe, similar to that noted in Scheme 7. The overbreak annulus may have remained open before lubrication and filled with a uniform layer of natural clay slurry. Pumping in a pressurised bentonite slurry of lower shear strength resulted in the abrupt drop in jacking load, Figure 5.4, and injection procedures may have caused local changes in interface stresses.

### 6.2.5 Stage 2 schemes

Pipes sliding along the base of a stable bore was apparent in the stiff glacial clay of Scheme 1 and weathered mudstone of Scheme 2, with contact occurring only at the bottom of the instrumented pipes. In Scheme 1, the total radial stresses and shear stresses were mostly between 0-250kPa and 0-150kPa respectively. The instrumented pipe at Scheme 2 appeared also to be subject to longitudinal rotation with the front of the pipe attracting significantly larger stresses than the rear, total stresses approached 575kPa with corresponding shear stresses of 160kPa.

In the heavily overconsolidated London clay of Scheme 3, very large lateral stresses were sufficient to damage instrumentation and cause a high rate of glue line failures around the contact stress cells. Large radial stresses recorded at the sides prior to the cells being displaced, between 490kPa and 650kPa, imply that the pipe was subject to squeezing ground.

Results from the drive in dense silty sand above the water table, Scheme 4, showed contact mainly along the base of the tunnel, while on the sides and top intermittent and lower stresses indicated only sporadic contact. Peak total and shear stresses, 300kPa and 160kPa respectively, occurred over short lengths and agreed well with positions of maximum angular misalignment. The injection of lubricant into the overbreak void appeared not to have had a marked effect on the interface stresses.

Scheme 5 was in cohesionless soil below the water table, and as noted for Scheme 7, instruments generally recorded lubricating slurry pressure and very low shear stresses. Peak total radial stresses of 300-350kPa were measured at the tunnel axis but the average was about 50kPa. Pore pressures were generally similar suggesting the formation of a stabilised zone of lubricant gel around the pipe preventing the soil from developing large effective contact stresses. Pipe buoyancy was implied by larger stresses recorded at the top of the pipe than the bottom.

### 6.3 GROUND RELATED FACTORS

#### 6.3.1 Cohesionless soils

Monitored drives in cohesionless soils include Schemes 4, 5 and 7. Interface behaviour is illustrated by considering typical pushes and plots of shear stress against normal stress during jacking for Schemes 4 and 7. Unlubricated interface stress behaviour for Scheme 5, Cheltenham, has not been published

The response for the Scheme 4 drive in dense silty sand above the water table is shown in Figures 6.19 to 6.21. Data included in these figures show the pre-lubrication phase only, post-lubrication behaviour is described in section 6.7. Effective stress plots were produced only for the bottom of the pipe since the other locations were fully drained. The response is clearly frictional with a linear relationship between shear and radial stresses. There is good agreement between skin friction angles  $\delta$  of  $33.4^\circ$  and  $34.3^\circ$  at the crown and axis positions. These angles are slightly lower than the  $37.7^\circ$  recorded at the bottom probably reflecting a loosened state of collapsed material around the crown and axis (Norris 1992b). Effective stresses on the bottom show considerably more scatter than the corresponding total stresses which is most likely due to a difference in position between contact stress cell and pore pressure cell, however, the best fit line produces a similar friction angle of  $35.6^\circ$ .

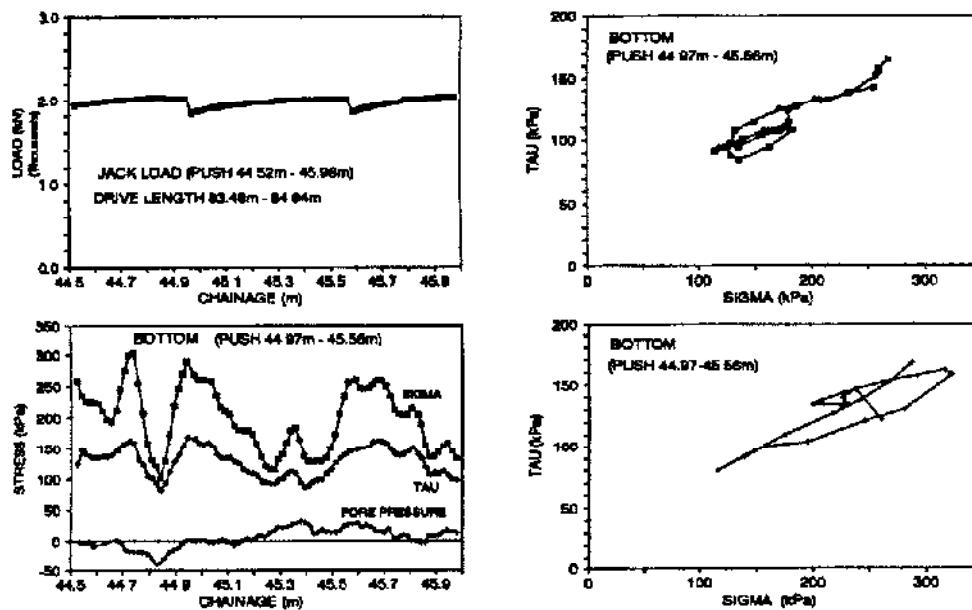


Figure 6.19 Detailed response of pushes between chainage 44.97m and 45.56m on Scheme 4 (after Norris, 1992b).

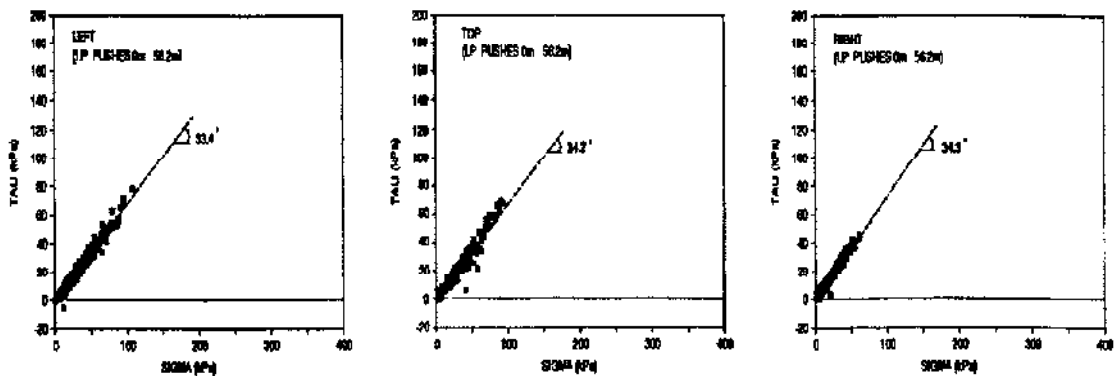


Figure 6.20 Shear stress/total radial stress relationships during Scheme 4 prior to lubrication (after Norris, 1992b).

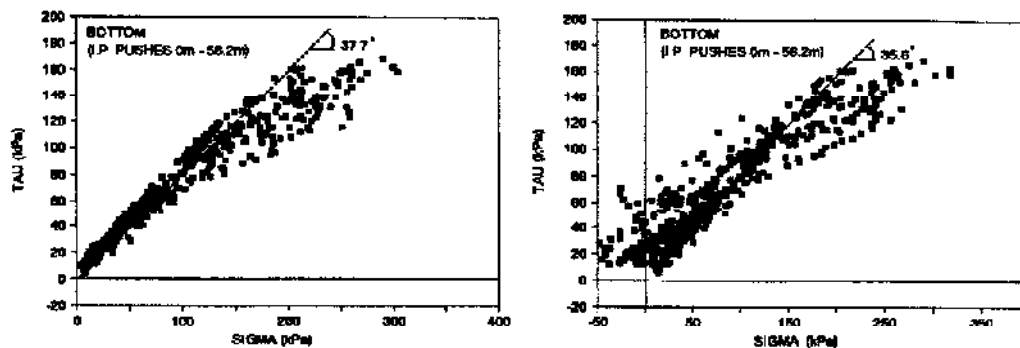


Figure 6.21 Shear stress/radial stress relationships on the pipe bottom during Scheme 4 prior to lubrication (after Norris, 1992b).

Since lubricant was used from the start of the Scheme 7 drive, it is not possible to separate interface behaviour into pre- and post-lubrication phases. Typical Scheme 7 pushes are included in Figures 6.22 and 6.23; plots are purposely taken from locations where there is some indication of contact between pipe and soil (or soil/bentonite cake).

The pore pressures, previously shown to be in close agreement with hydrostatic pressures, are constant during the illustrated pushes and the increase in total stress is therefore wholly due to pipe-soil interaction. The resulting stress paths are linear and frictional in character. Figure 6.24 comprises plots showing shear stress/effective radial stress relationships around the instrumented pipe: the plots do not include data from the centre-right and rear-right cells because lubricant prevented significant contact stresses from developing. Skin friction angles  $\delta'$  range from  $20^\circ$  to  $43^\circ$ , at stress levels over 100kPa there is excellent agreement between friction angles  $\delta'$  of  $36^\circ$  or  $37^\circ$ .

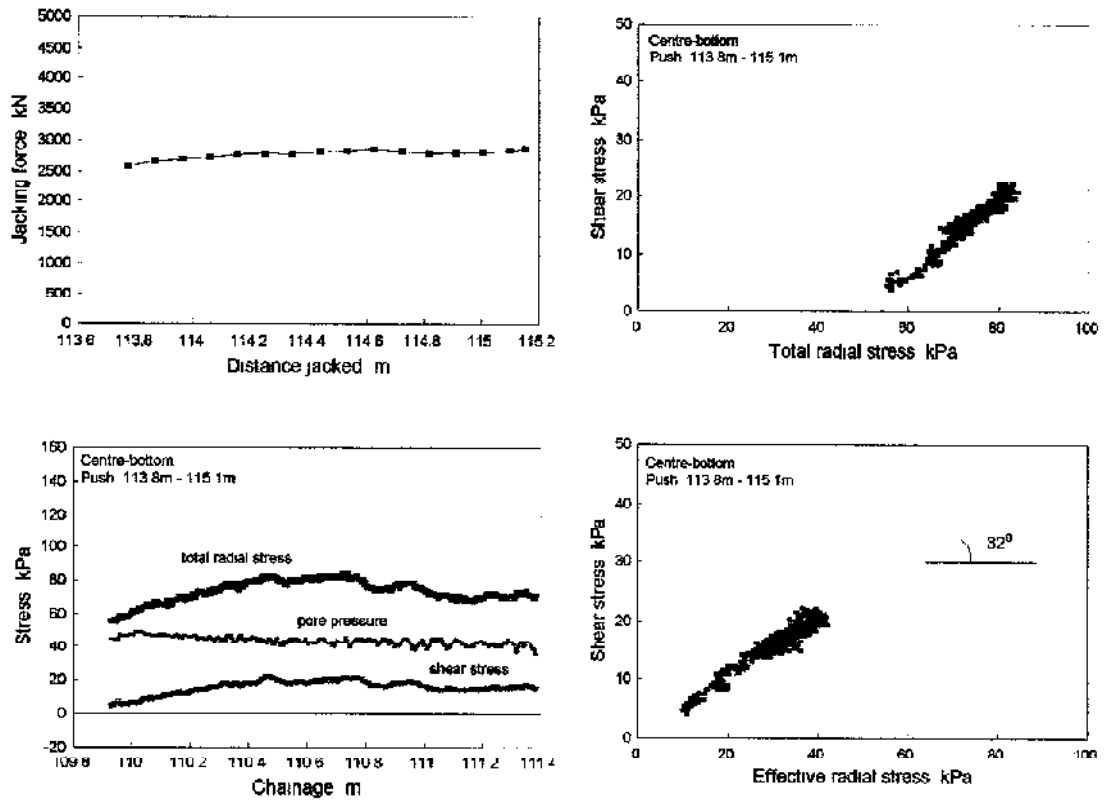


Figure 6.22 Detailed response of pushes between chainage 113.8m and 115.1m on Scheme 7.

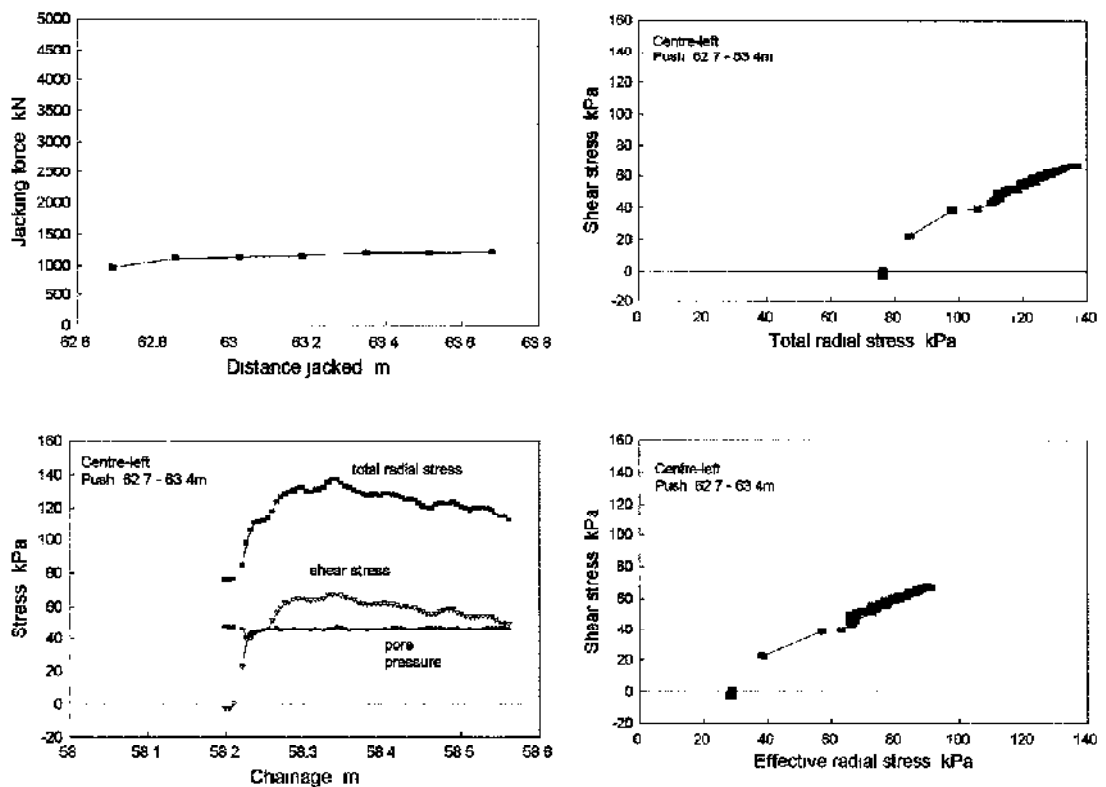


Figure 6.23 Detailed response of pushes between chainage 62.7m and 63.4m on Scheme 7.



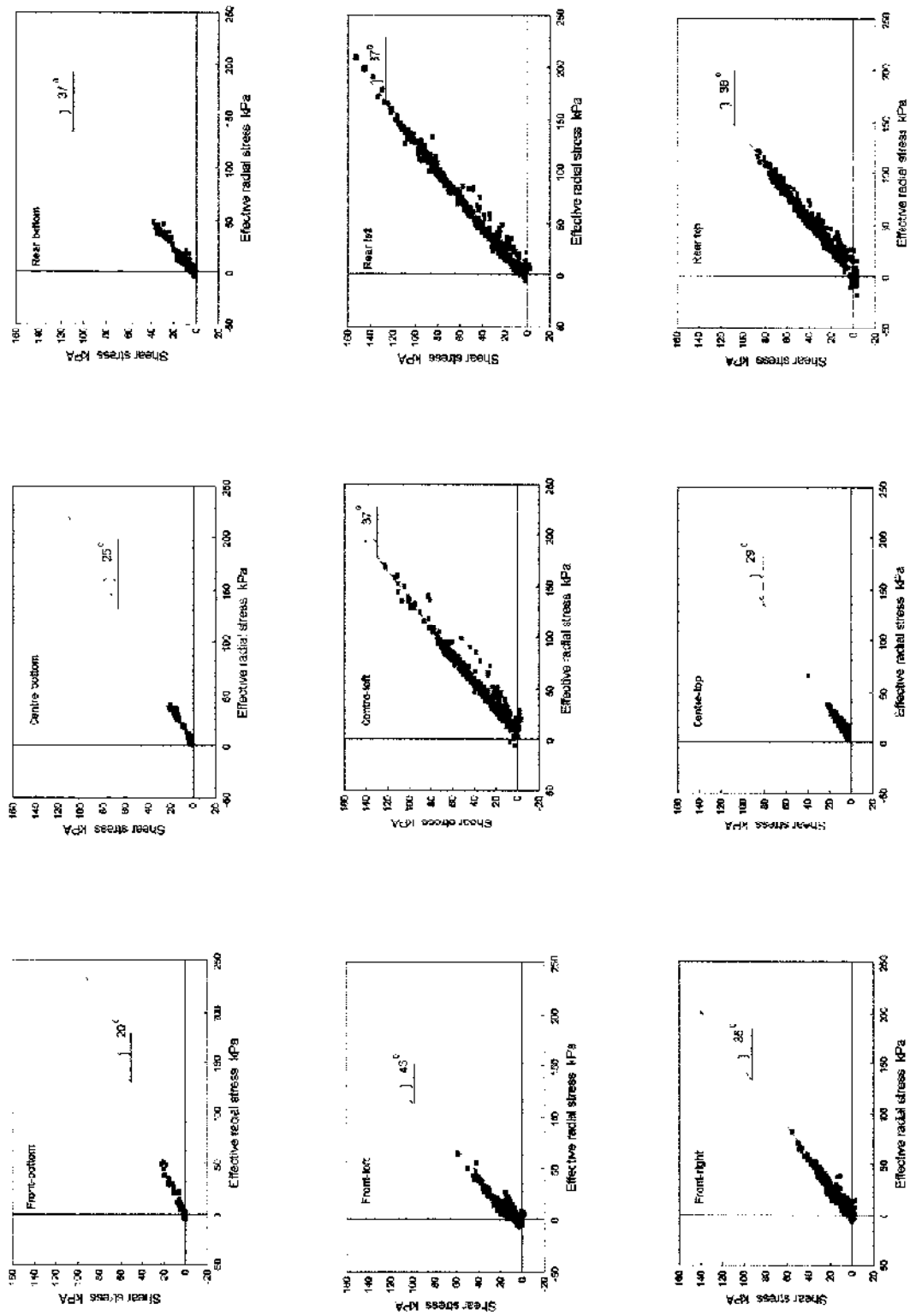


Figure 6.24 Shear stress/effective radial stress relationship during Scheme 7

In Schemes 4 and 7, the linear relationship between shear and radial stress appears to be stress level dependent at stresses in excess of 100kPa. At higher stresses there is good agreement between the two schemes, on the pipe bottom of Scheme 4,  $\delta'$  is approximately  $36^\circ$ , and in Scheme 7 at axis level  $\delta'$  is  $37^\circ$

### 6.3.2 Cohesive soils

The frictional interface stress behaviour observed in Schemes 4 and 7 is expected in sandy soils; more surprisingly, the relation between shear and total radial stresses appears to be frictional in some cohesive soils. Monitored drives in cohesive soil include those of Schemes 1, 2, 3, 6, 8 and 9.

Some results from the London clay drive of Scheme 3 are shown in Figures 6.25 and 6.26. The detailed response plots at pipe axis, Figure 6.25, indicate a frictional relationship. Shear stress/radial stress plots from the axis instruments show a reasonably linear relationship with  $\delta$  of about  $13^\circ$  and  $\delta'$  of  $11^\circ$ . At the top of the pipe there is an indication that shear stresses approach a limiting value of about 150kPa; the intact undrained shear strength,  $S_u$ , of the London clay is in the range 225kPa to 600kPa. Norris (1992b) reports the tunnel axis readings also showing indications of a limiting value around 150kPa.

Interface stress plots from typical individual pushes in Scheme 6 (also London clay) are presented in Figures 6.27 and 6.28. Maximum stresses are lower than those measured during Scheme 3, primarily due to a lesser depth of cover.

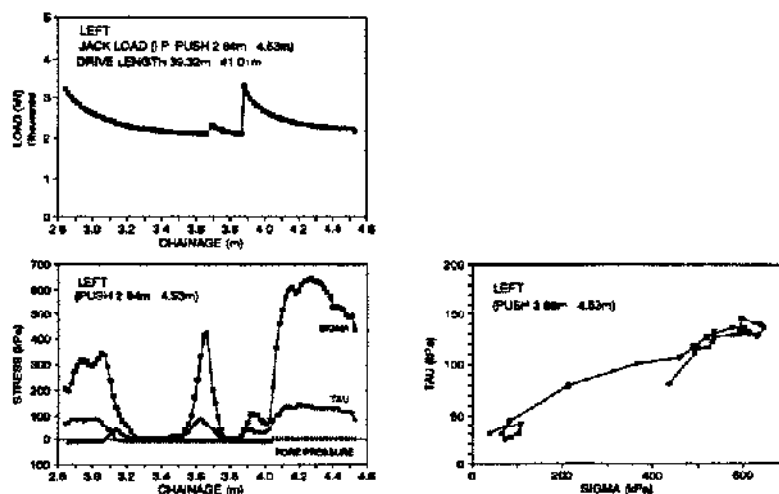
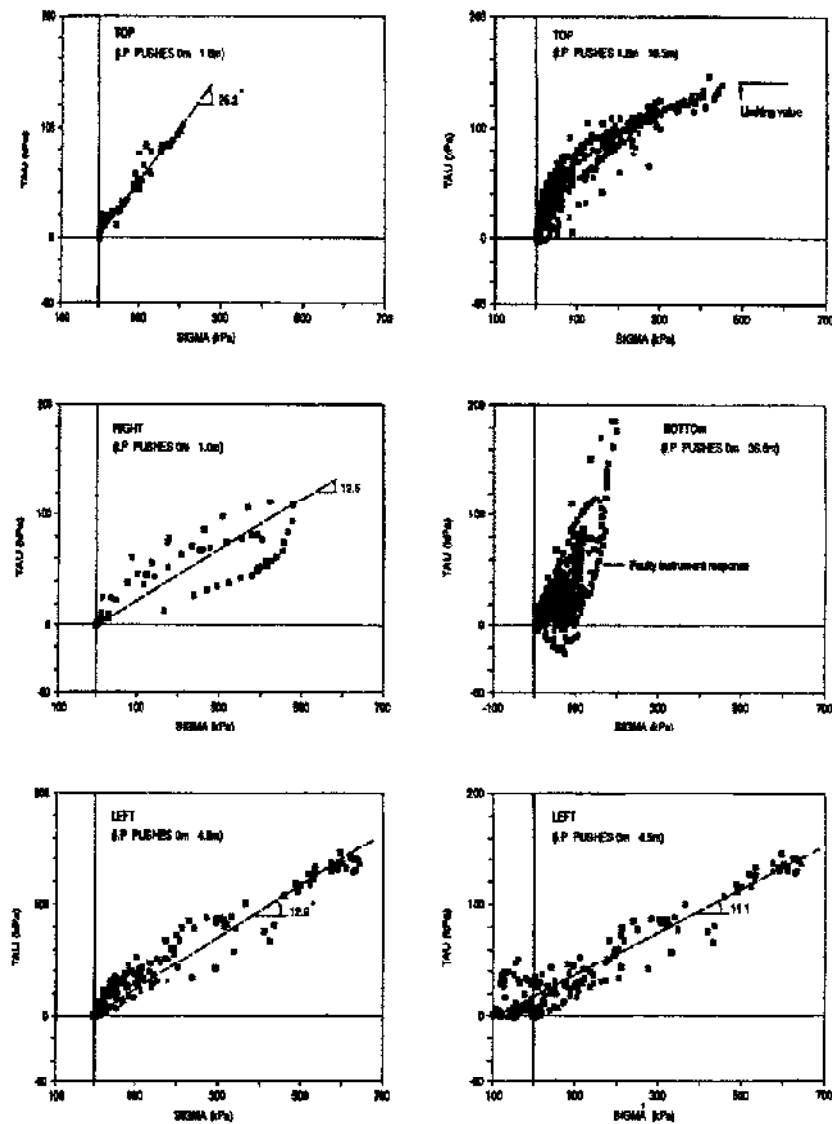
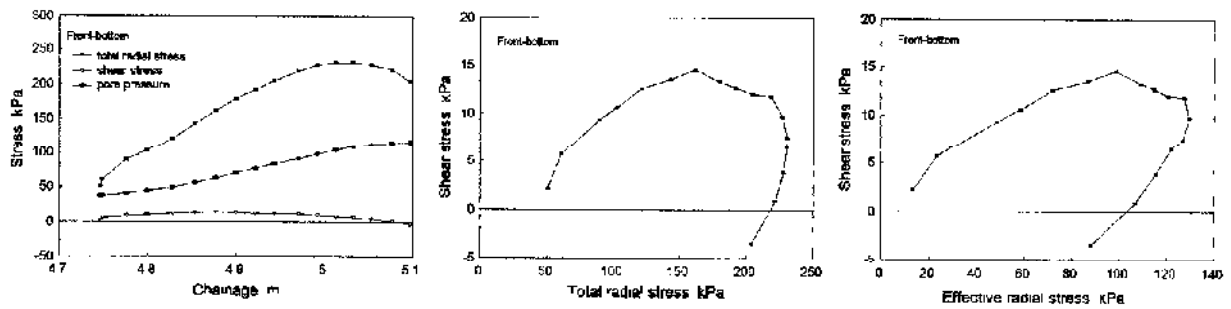


Figure 6.25 Detailed response of pushes between chainage 2.84m and 4.53m on Scheme 3 (after Norris, 1992b).

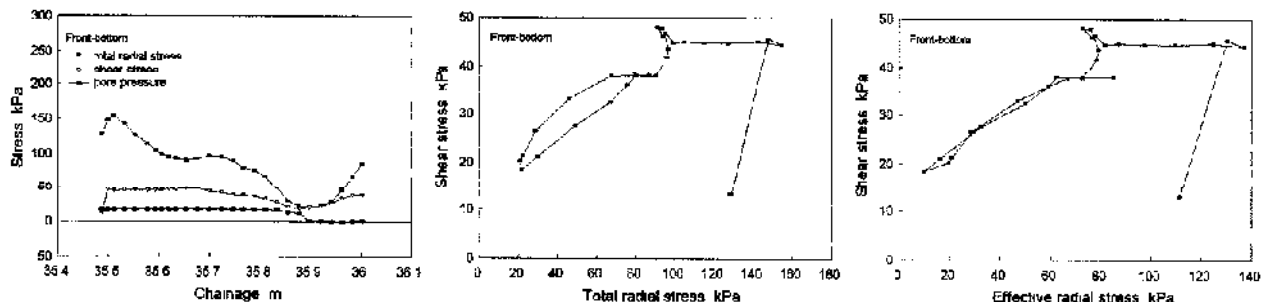


**Figure 6.26** Shear stress/radial stress relationship during Scheme 3 (after Norris, 1992b).

In Figure 6.27(a) radial and shear stresses initially increase almost linearly but the radial stress falls off and there is a corresponding decrease in shear stress. The push illustrated in Figure 6.27(b) shows an abrupt increase followed by a general decrease until the observed rise close to the end of the push. The increase/decrease, decrease/increase stress path loops appear to be common along the pipe bottom in Scheme 6 observations. At locations, other than the pipe bottom, where pipe-soil contact occurred, stress paths are markedly more erratic, Figure 6.28. A general feature of the plots (only a few of which can be presented) is that interface stresses vary rapidly over short distances, probably due to irregularities of the soil surface within the hand-excavated tunnel bore.



a) chainage 4.75m to 5.10m (front cell).



b) chainage 35.5m to 36.0m (front cell).

Figure 6.27 Detailed interface stress response on the pipe bottom during Scheme 6.

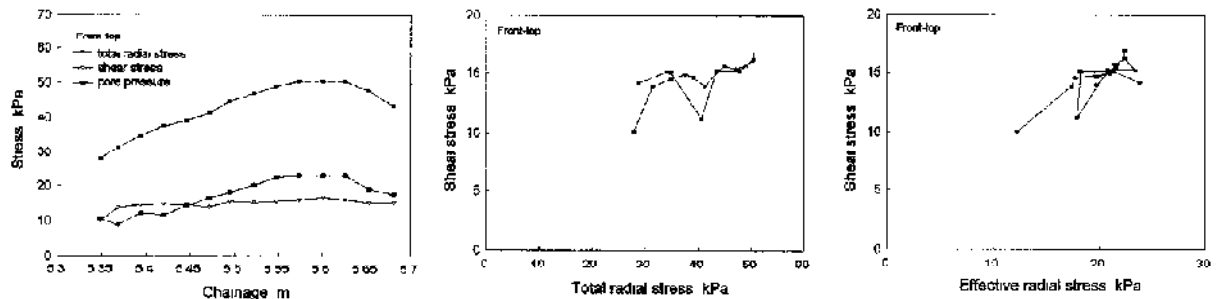
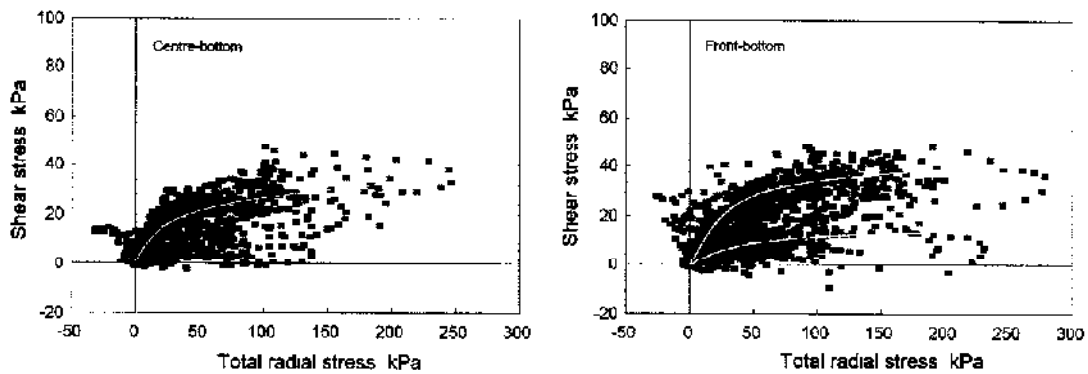


Figure 6.28 Detailed interface stress response on the pipe top during Scheme 6.

Shear stresses against radial stresses from many Scheme 6 pushes are shown in Figures 6.29 to 6.32. In plots presenting pipe bottom observations (Figures 6.29 and 6.30) there is due to the large number of data points and rapidly varying stresses, considerable scatter. Notwithstanding this, the nonlinear relationships (illustrated by best-fit white lines) are evident in terms of both total and effective radial stresses. It is notable that measurements from the front-bottom cell appear to approach two limiting values of about 40kPa and 15kPa. Plots presenting total stress data at the pipe top, Figure 6.31, confirm this relationship but for effective stresses, Figure 6.32, it is less

clear. In Scheme 3, nonlinearity was observed, but only in the pipe top - Figure 6.26. The idealized shear stress/radial stress relationship based on these observations is illustrated in Figure 6.33, showing the marked curvature before merging to limiting values. This type of nonlinear relationship is characteristic of Mohr failure envelopes of London clay (Bishop et al. 1965) and contrasts the apparent frictional behaviour largely observed in Scheme 3



**Figure 6.29** Shear stress/total radial stress relationship at pipe bottom during Scheme 6.

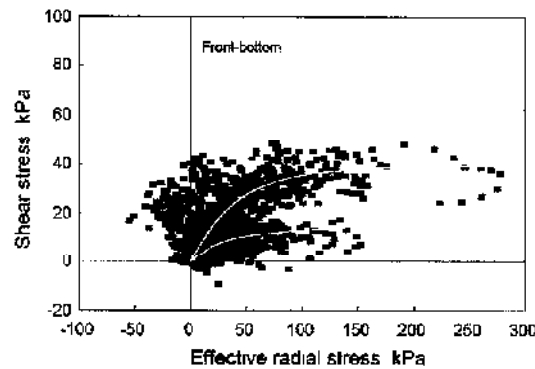


**Figure 6.30** Shear stress/effective radial stress relationship at pipe bottom during Scheme 6.

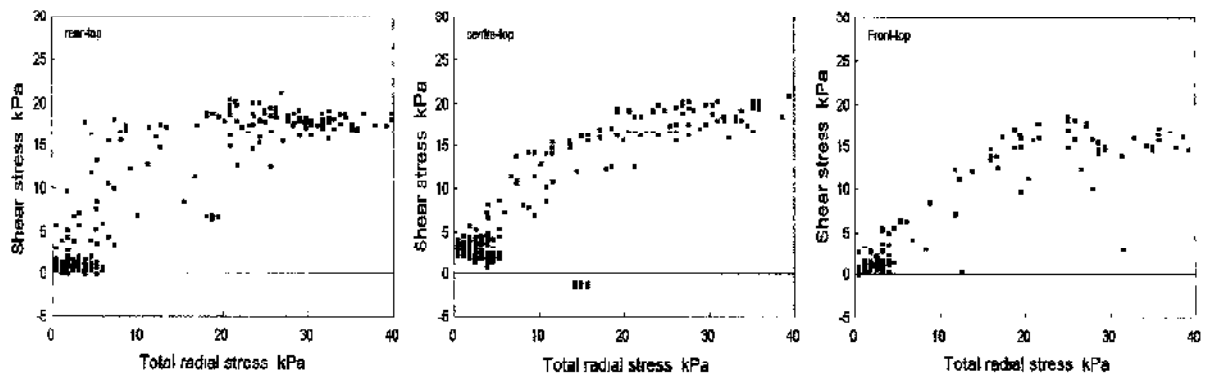


**Figure 6.31** Shear stress/total radial stress relationship at the pipe top during Scheme 6.

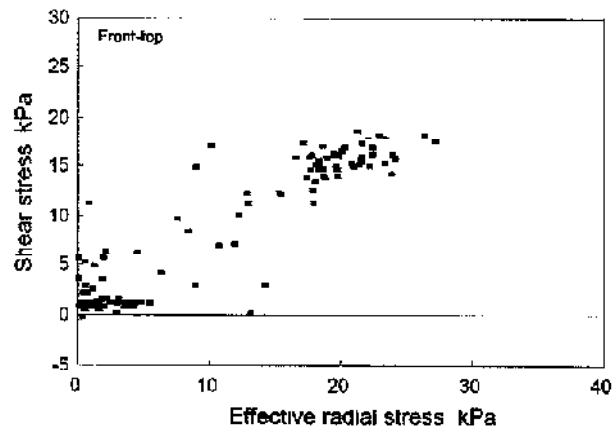


**Figure 6.32** Shear stress/effective radial stress relationship at pipe top during Scheme 6.

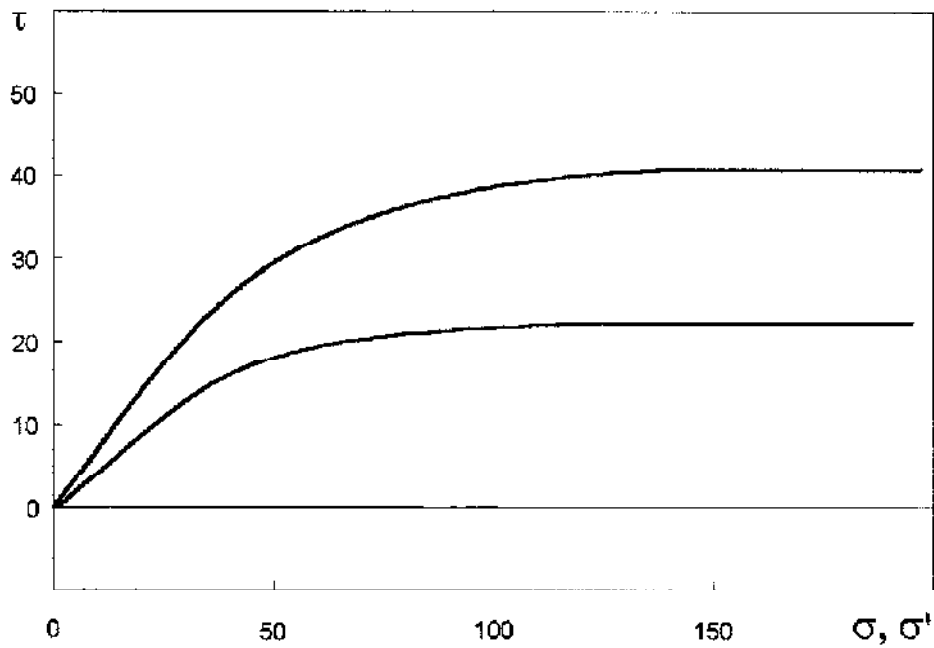


**Figure 6.33** Idealized shear stress/radial stress relationship in the London clay of Scheme 6.

Monitored pipe jacks in stiff glacial clay include Schemes 1 and 8. For Scheme 1 sliding in an open bore (unlubricated) was apparent with contact occurring primarily along the bottom of the pipe. Frictional behaviour was observed – Figure 6.34 – for most of the drive but more cohesive behaviour was found towards the end. Most interface stress measurements in Scheme 8 were affected by lubricant filling the tunnel bore. Figure 6.35 includes detailed responses from around the Scheme 8 pipe. Measurements along the bottom of the pipe indicate pipe-lubricant contact, at the pipe top and at axis level, data are purposely taken from sections where pipe-soil contact appears to have occurred and stresses vary rapidly as increase/decrease stress path loops develop.

Shear stress/radial stress scatter plots for Scheme 8 are shown in Figures 6.36 and 6.37 for total and effective stresses respectively. At the bottom and left of the pipe the use of lubricant has resulted in very low skin friction angles  $\delta$  of  $0.9^\circ$  and  $0.7^\circ$ , and  $\delta'$  of  $0.2^\circ$  and  $0.9^\circ$  respectively. Plots of the top and right stresses show considerable scatter due to sporadic contact with the ground. Regression analyses on these scattered data give  $\delta$  of  $2.1^\circ$  (top) and  $3.5^\circ$  (right) and  $\delta'$  of  $11^\circ$  (top) and  $13.3^\circ$  (right). These angles, due to lubrication, are much lower than those recorded in Scheme 1, where  $\delta$  is  $19^\circ$  and  $\delta'$  is  $20.3^\circ$ , Figure 6.34.

Detailed interface stress plots from Scheme 9, in soft peaty clay, are presented in Figure 6.38. As noted earlier in the chapter, lubricant was introduced part way into the drive and the plots, representing typical pushes at various locations, show stresses pre- and post-lubrication. With the exception of the pipe left, pore pressure measurements are similar to total stresses and resulting effective stresses and corresponding shear stresses are very low. Shear stress/radial stress plots, Figures 6.39 and 6.40, show little pattern in the relationship, scatter is substantial around apparent clusters of data points. Interface stresses are erratic and there is insufficient evidence to show clearly cohesive or frictional type behaviour in the soft clay. Section 6.6.4 includes more detailed scatter plots with the emphasis on lubricant effects.

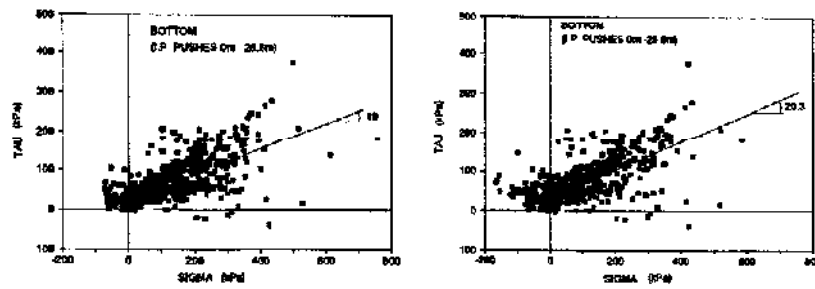
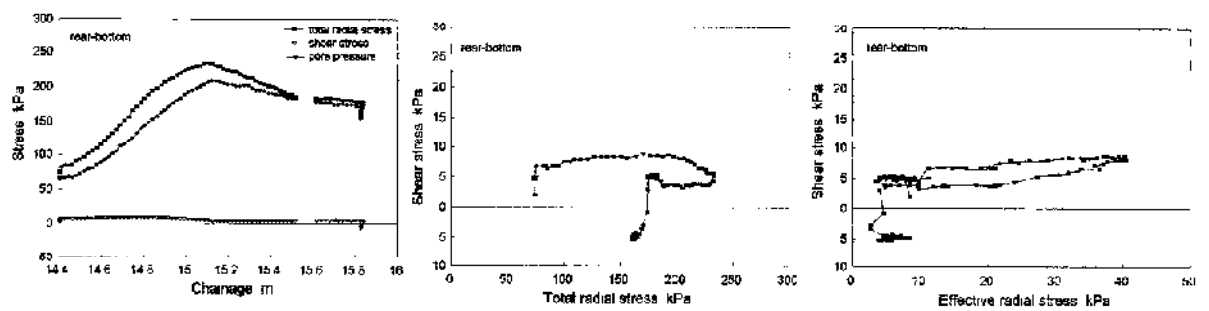
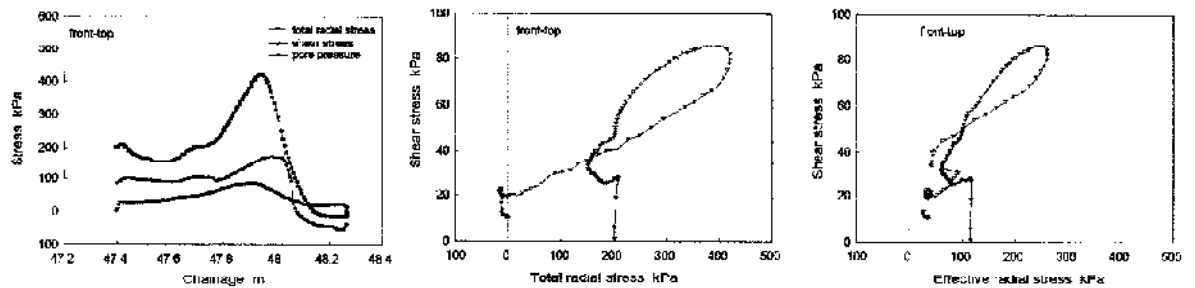


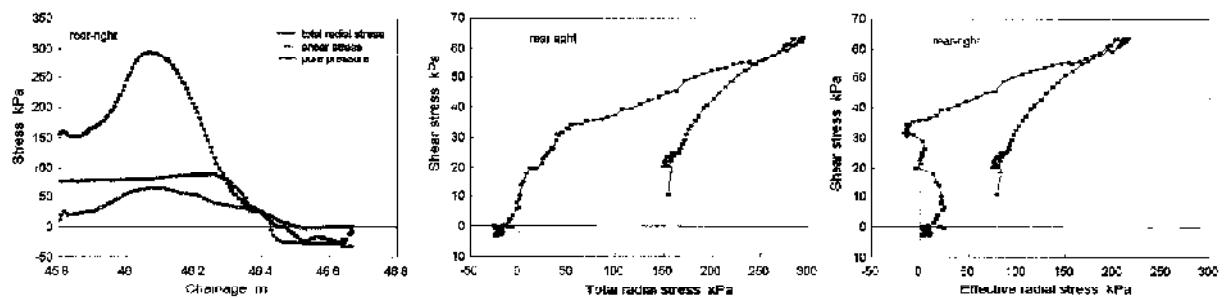
Figure 6.34 Shear stress/radial stress relationship during Scheme 1 (after Norris 1992b)



a) pipe bottom, chainage 14.4m to 15.8m.



b) pipe top, chainage 47.4m to 48.2m.



c) pipe axis (right), chainage 45.8m to 46.8m.

Figure 6.35 Detailed interface stress responses during Scheme 8.



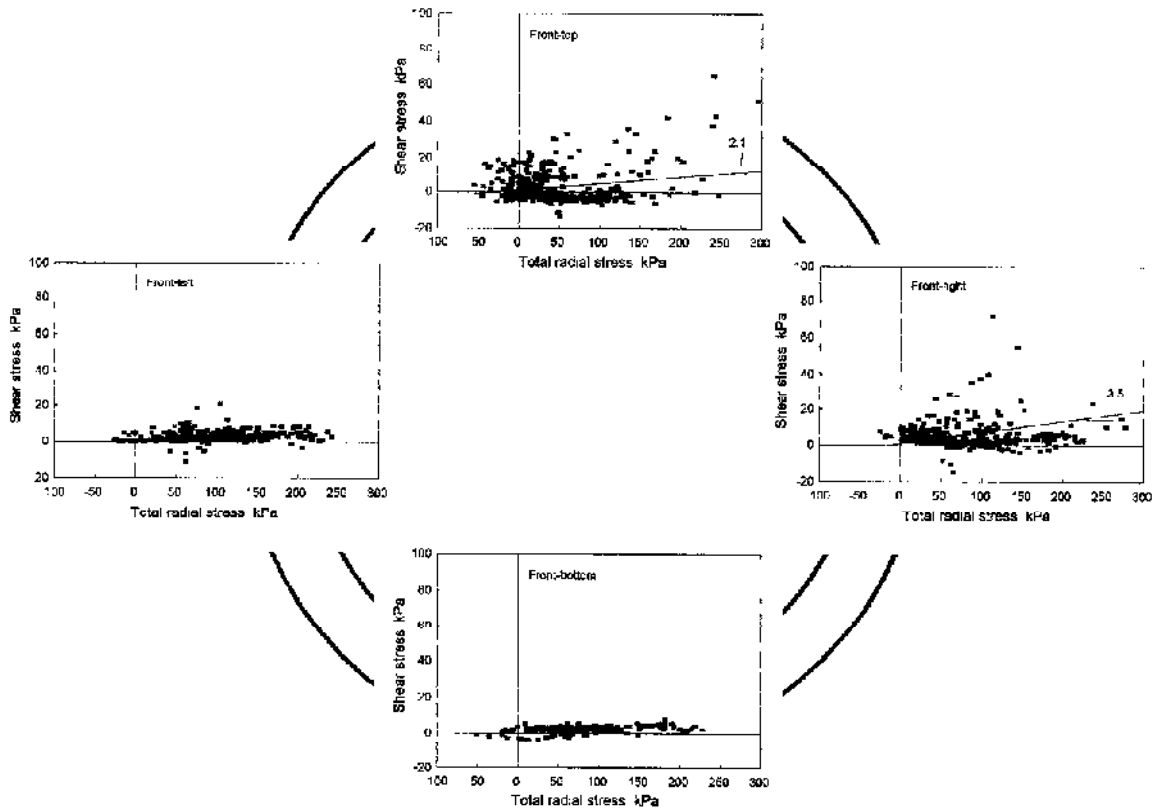


Figure 6.36 Shear stress/total radial stress relationship around the pipe in Scheme 8.

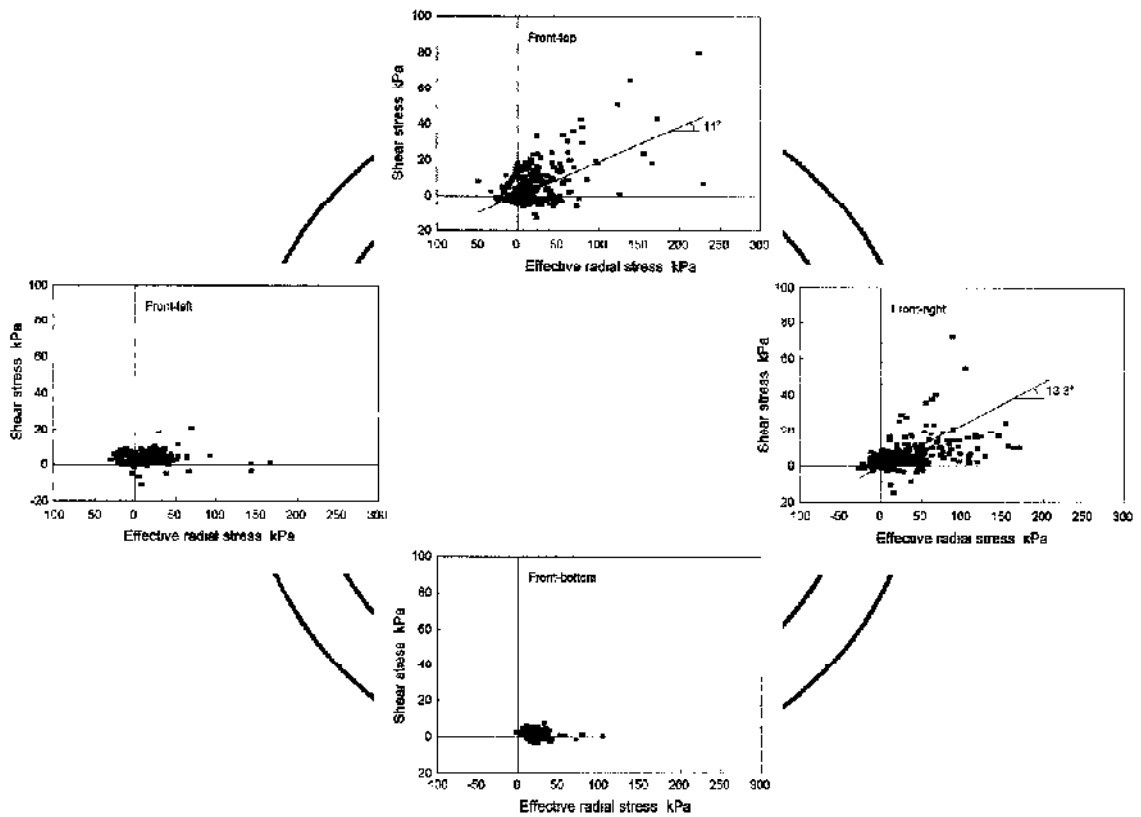
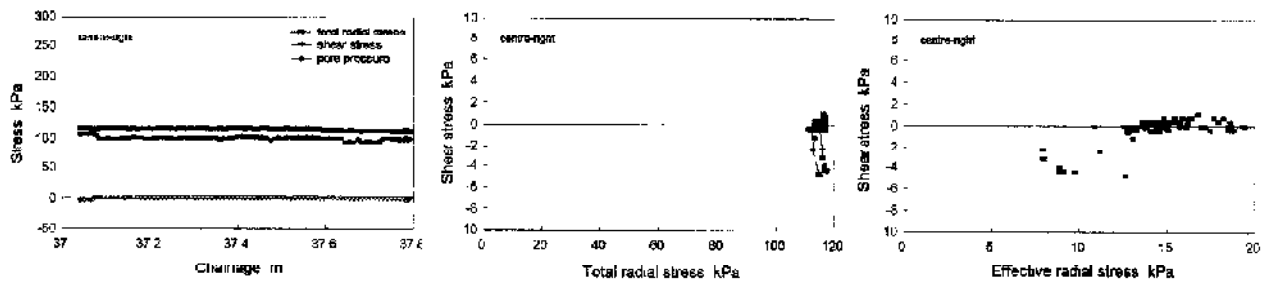
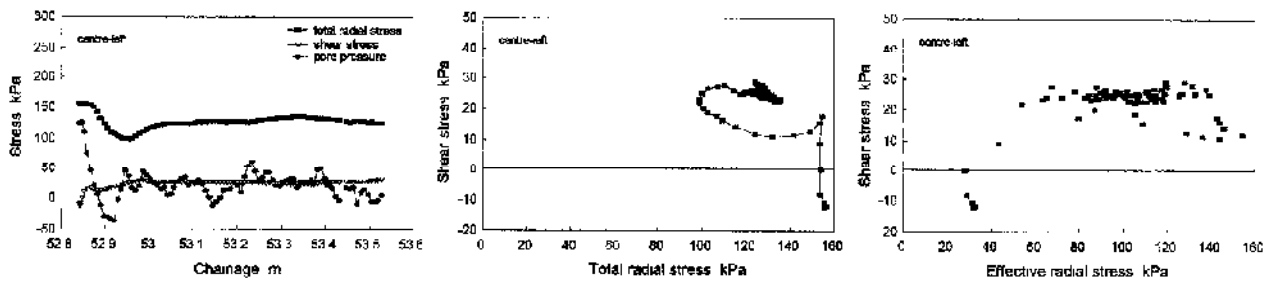


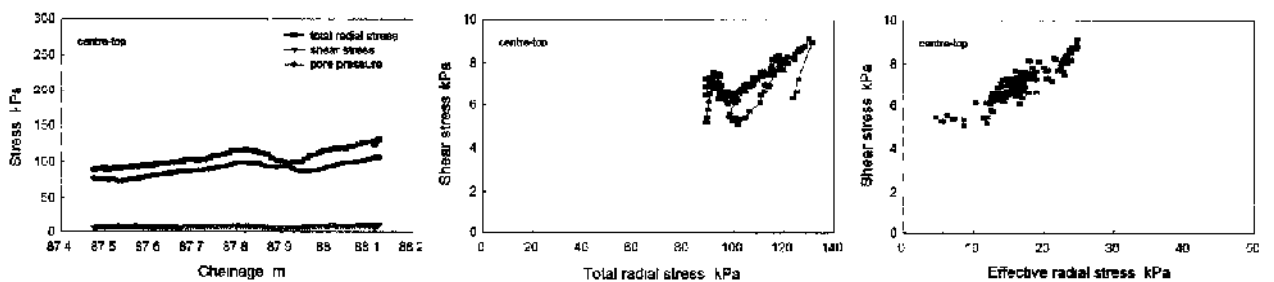
Figure 6.37 Shear stress/effective radial stress relationship around the pipe in Scheme 8.



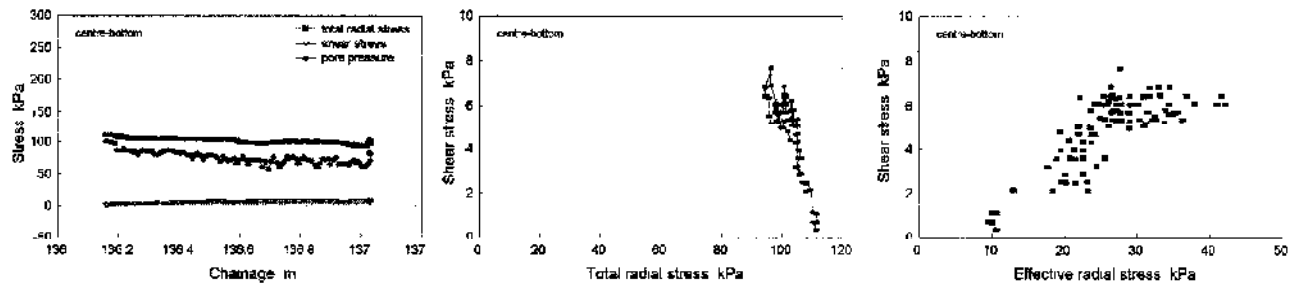
a) pipe right, chainage 37.0m to 38.0m (pre-lubrication).



b) pipe left, chainage 52.8m to 53.5m (pre-lubrication).



c) pipe top, chainage 87.5m to 88.1m (post-lubrication).



d) pipe bottom, chainage 136.2m to 137.0m (post-lubrication).

Figure 6.38 Detailed interface stress responses during Scheme 9.

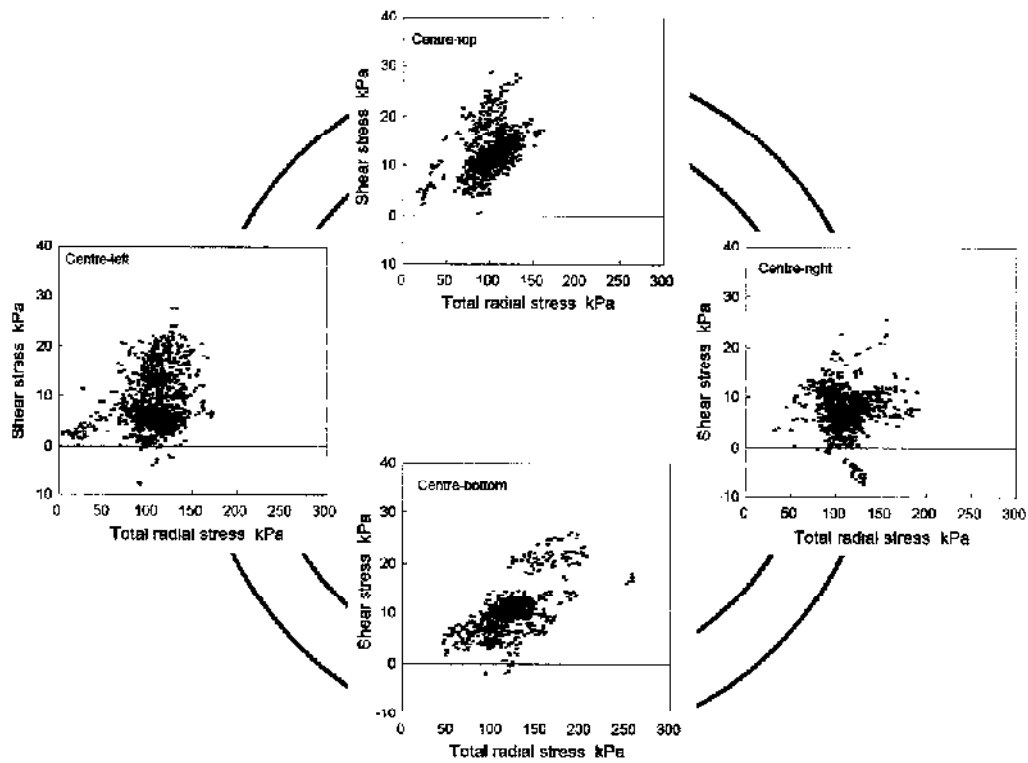


**Figure 6.39** Shear stress/total radial stress relationship around the pipe in Scheme 9.

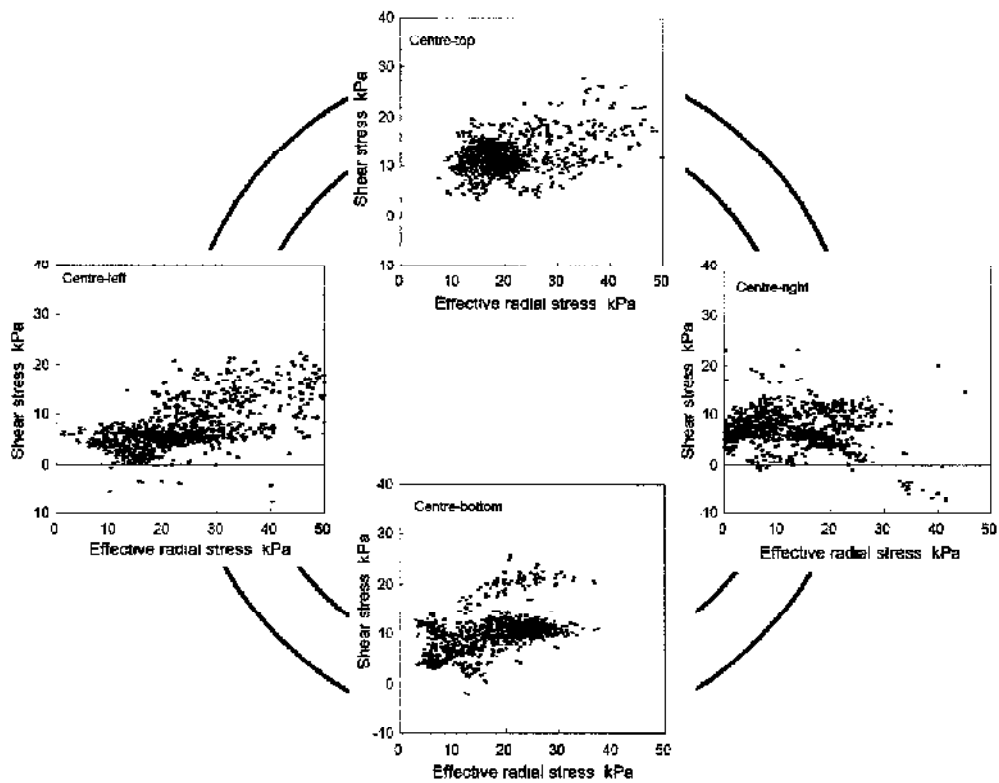


**Figure 6.40** Shear stress/effective radial stress relationship around the pipe in Scheme 9

## 6.4 EFFECTS OF STOPPAGES

### 6.4.1 Introduction

The delays between pushes (due to excavating, introducing new pipes, shift changeovers, evening and weekend breaks etc.) have been shown to routinely result in increased restart jacking forces in clay soils, section 5.3.3. This section will show how radial stresses and pore pressures (where data exist) can vary during stoppages to offer explanations for the 'stoppage effect'. Three types of clay are considered London clay of Schemes 3 and 6, stiff glacial clay of Schemes 1 and 8; and the soft peaty clay in Scheme 9

### 6.4.2 London clay

Total radial stresses at the start and end of stoppages during Scheme 3 are presented in Figure 6.41. The plot shows stresses decreasing during rest periods. It is not clear if this is a result of dissipating pore pressures as there were no reliable pore pressure data on this particular scheme (Norris 1992b).

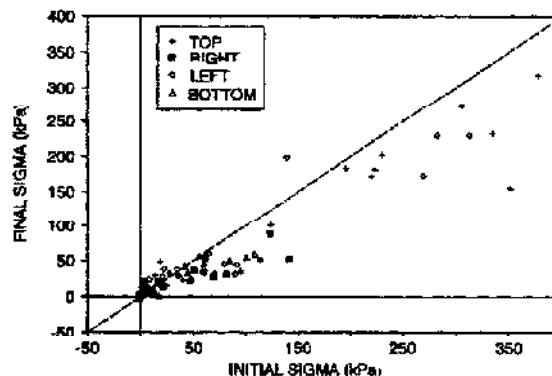


**Figure 6.41 Time dependent changes in total radial stresses during stoppages on Scheme 3 (after Norris 1992b).**

Total radial stresses, pore pressures and resulting effective stresses acting on the pipe bottom in Scheme 6 are presented in Figure 6.42 – data are taken from an entire Friday shift and the start of a Monday morning shift following the weekend stoppage.

As in Scheme 3, total radial stresses decrease with time during the stoppages. Figure 6.43 shows in detail the decrease for the eight stoppages together with jacking loads for the same period. Delays during the Friday shift (stoppages 1 to 7) range from 40 minutes to 100 minutes in duration –  $\ln$  time 3.7 to 4.6 in Figure 6.43(b) –

with a corresponding decrease in total stresses lying between 13% and 90%. The weekend break (stoppage 8 in Figure 6.43) resulted in stress reductions of 128% and 127% at the front and centre respectively. The restart jacking load following this long delay – a 67% increase – is unsurprisingly the largest recorded over the period of interest. The difference in magnitude between total stresses recorded at the two locations in the pipe is also notable. They generally differ by about 50kPa and only during stoppage 7 are the values similar. This suggests that the pipe's self-weight is unevenly distributed during most breaks, probably due to irregularities in the bore invert.

The pattern of pore pressure measurements during stoppages shown in Figure 6.42 is complex and difficult to interpret. Generally, upon cessation of shearing, there are negative pore pressures and as water flows through the boundary surface layer into the shear zone, pore pressures dissipate. This pattern occurs during stoppage 2 as shown in Figure 6.44, where a pore pressure of -39kPa was observed after an elapsed time of 60 min. Just prior to pushing, after an elapsed time of 100 min, a partial dissipation of 2kPa was measured. During the weekend break of stoppage 8, pore pressures dissipated fully but unfortunately logging could not continue over the weekend and therefore the rate of dissipation was missed. Effective radial stresses are also complex because of the pore pressure measurements, but the pattern is typically one of rapidly increasing stresses at the start of a break and then a decrease as negative pore pressures dissipate. The field data suggest stress and pore pressure characteristics as illustrated in Figure 6.45.

The soil through which the instrumented pipe, at pipe 11, was pushed along had been subject to numerous shearing/stoppage cycles and the resulting shear zone will have suffered some degree of structural deterioration, including the breaking of interparticle bonds, giving the clay fabric an opportunity to dilate and soften. Decreasing total radial stresses and corresponding decreases in pore pressures during the stoppages are consistent with the soil dilating. Shear strains and associated pressures in the stiff London clay can be very localised and pressure gradients between intact areas and the shear zone may account for the complex pattern of pore pressures observed. The increased jacking loads in London clay following stoppages may therefore be due to a combination of dilation and negative excess pore pressures.

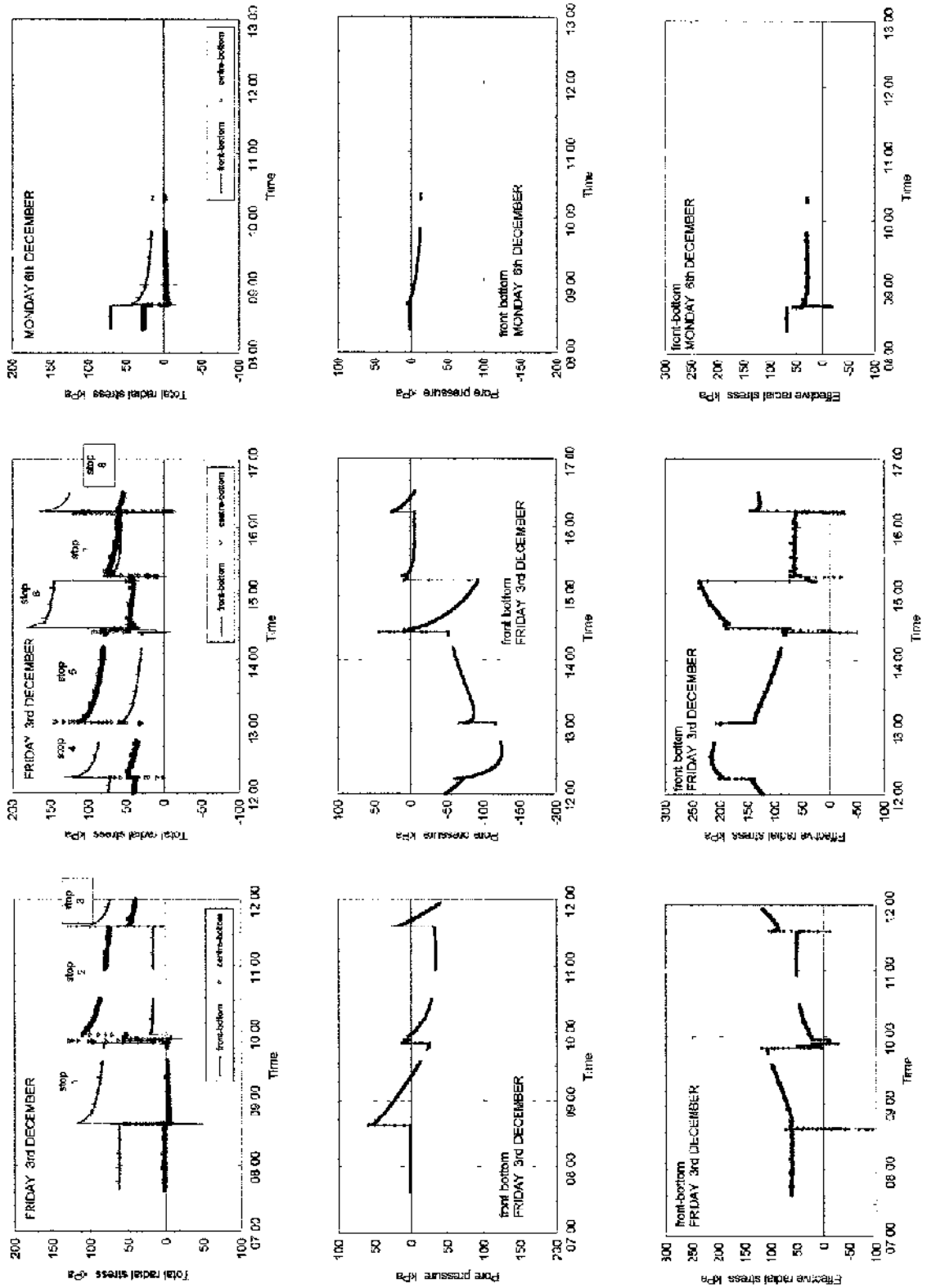
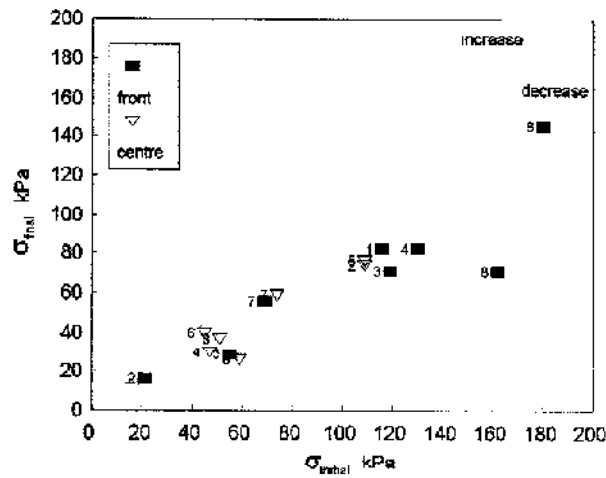
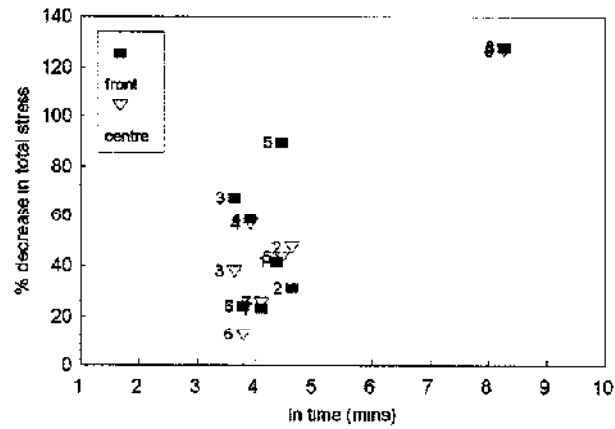


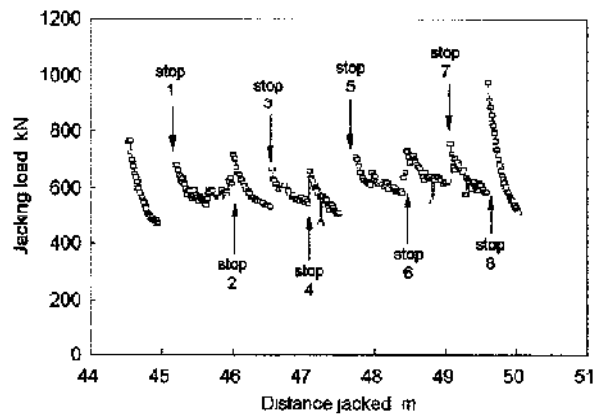
Figure 6.42 Variation in radial stresses and pore pressures on the pipe bottom during stoppages on Scheme 6.



a) Total radial stress on pipe bottom – initial v final



b) Total radial stress on pipe bottom - percentage decrease with time



c) Jacking load

Figure 6.43 Variation in interface stresses and jacking load during stoppages on Scheme 6.

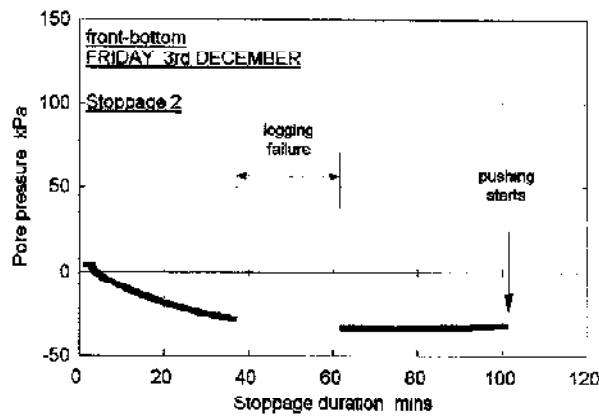


Figure 6.44 Variation in pore pressure during stoppage 2.

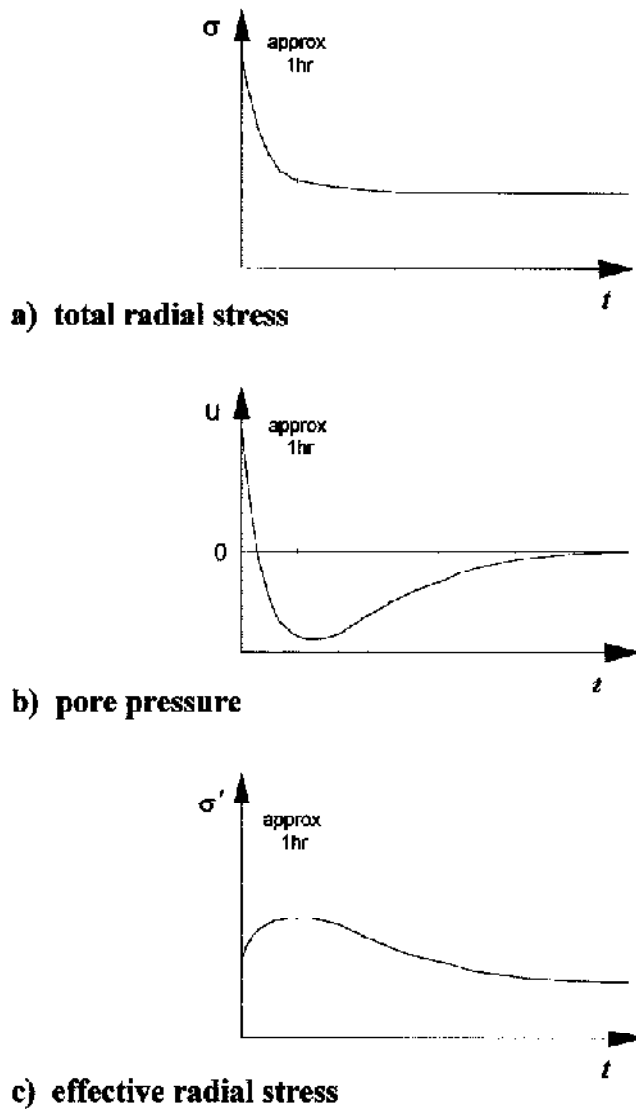
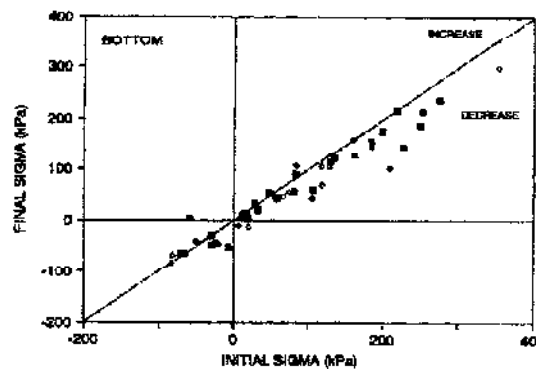


Figure 6.45 Assumed radial stress and pore pressure characteristics during a long stoppage in London clay.

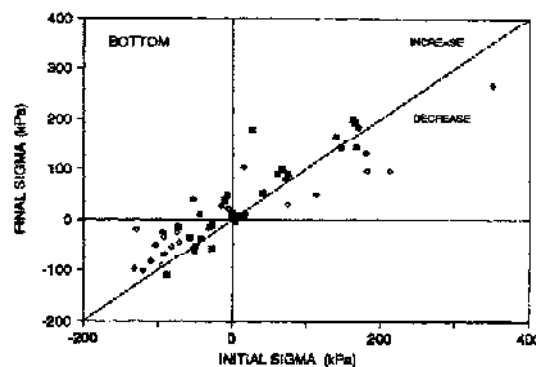


### 6.4.3 Stiff glacial clay

Total and effective radial stresses at the start and end of stoppages during Scheme 1 are presented in Figure 6.46. Total radial stresses decrease but effective stresses increase. Norris (1992b) suggested that shearing had generated excess pore pressures which then dissipated during the stoppages more rapidly than the decrease in total stress resulting in increased effective stresses and larger jacking loads.



a) total radial stresses



b) effective radial stresses

**Figure 6.46 Time dependent changes in radial stresses during stoppages on Scheme 1 (after Norris 1992b).**

During Scheme 8, only after weekend stoppages were significant increases in restart jacking loads observed – section 5.3.3.2. Radial stress and pore pressure measurements from before and after a weekend stoppage, together with corresponding jacking loads, are presented in Figure 6.47. Data are taken from the array of stress cells around the pipe rear. Pushing ceased at 15:10 hrs on the Friday afternoon and

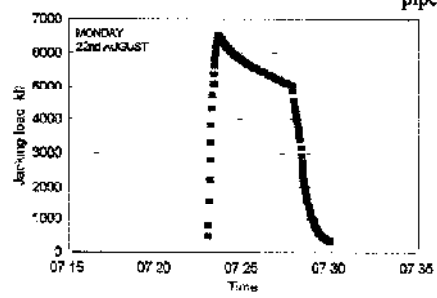
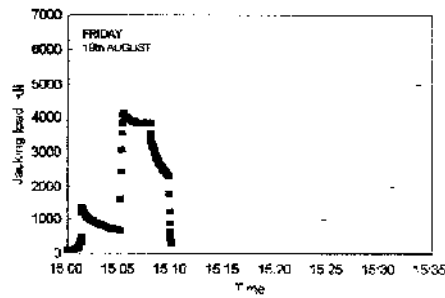
recommenced at 07:23 hrs on Monday. The stress and pore pressure measurements presented suggest a redistribution of lubricant pressure and loss of buoyancy. This could be due to some slurry leaching into any sand layers present in the glacial till.

At the left of the pipe total stress and pore pressure measurements are equal and both decrease by 30kPa over the weekend. A similar situation exists at the pipe top but at this location the measurements show an increase of 14kPa. Effective stress observations along the right indicate contact between pipe and soil, as opposed to pipe/lubricant gel contact. During the stoppage total stress increased by 30kPa, pore pressure increased by 57kPa with a resulting fall in effective stress of 27kPa. At the pipe bottom, total stresses and pore pressures reduced by 25kPa and 35kPa respectively, resulting in an increase of 10kPa in effective stress and loss of buoyancy. The increase in frictional resistance along the pipe bottom would account for the large restart forces observed on Monday mornings. Recharging the pressurised lubricant before attempting to recommence pushing would probably have resulted in restart jacking loads substantially lower than the measured values.

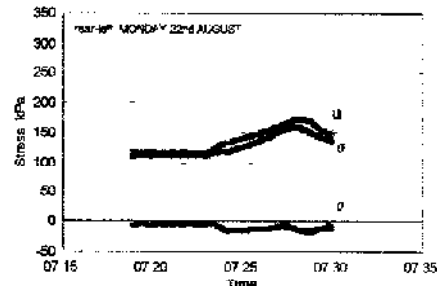
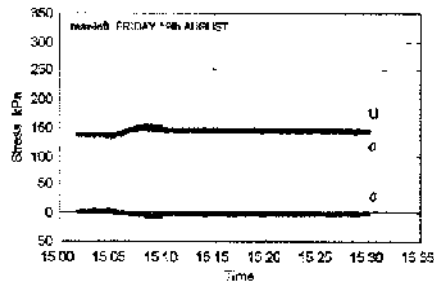
It has not been possible to study the geotechnical aspects of stoppages in the stiff glacial clay of Scheme 8 because the instrumented pipe was so placed that interface stresses were largely influenced by lubricant and lubrication procedures.

#### 6.4.4 Soft peaty clay

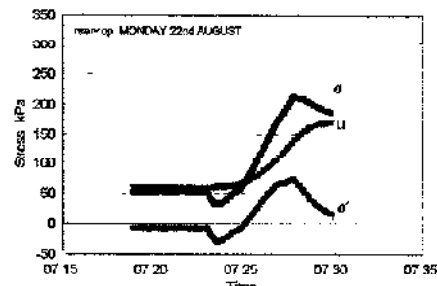
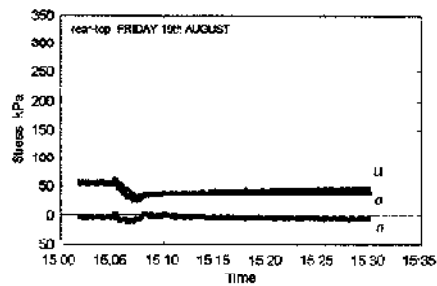
Changes in radial stresses around the centre of the pipe due to stoppages in the soft clay of Scheme 9 are presented in Figure 6.48. There is no clear pattern to the change in stresses during rest periods either pre- or post-lubrication, data points lie either side of the parity line and scatter in the effective stress plots is considerable. The change in stresses does not appear to result in increased jacking loads; with the exception of a weekend stoppage, the jacking record (Figure 5.4) does not show increased restart forces. Radial stresses and pore pressures measured around the pipe centre before and after the weekend are presented in Figure 6.49 (measurements after the break were recorded prior to lubricant introduction). Only at the top and left of the pipe do stresses and pore pressures change significantly during the break; total stresses decrease by 10kPa and 16kPa at the top and left respectively. Reductions in pore pressures, 27kPa (top) and 36kPa (left), are greater than the drop in total stresses,



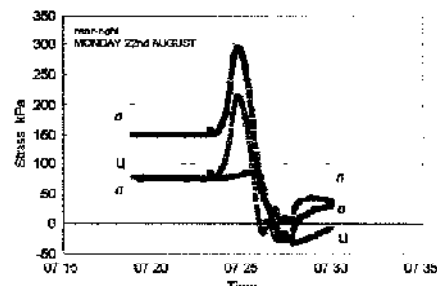
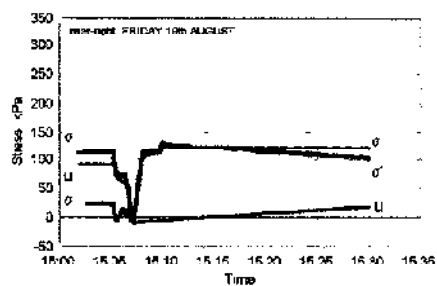
a) Jacking loads



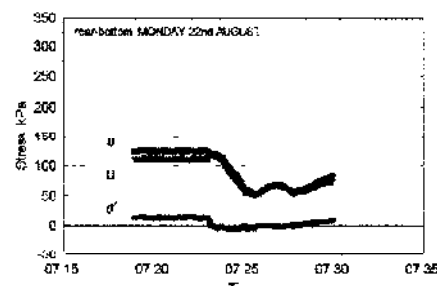
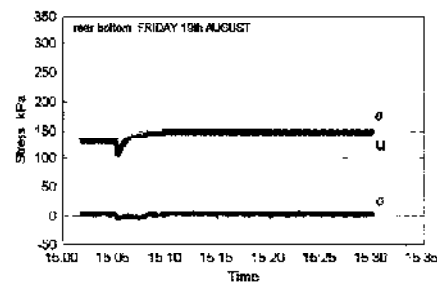
b) rear-left stresses



c) rear-top stresses



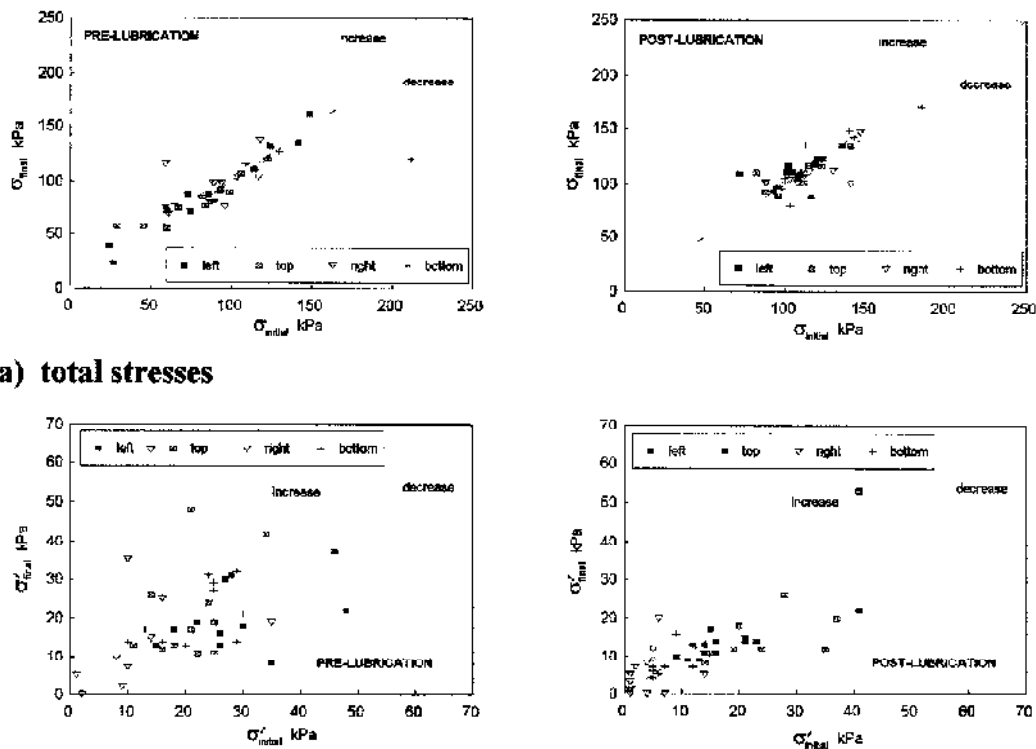
d) rear-right stresses



e) rear-bottom stresses

Figure 6.47 Time dependent changes in radial stresses and pore pressures after a weekend break during Scheme 8.

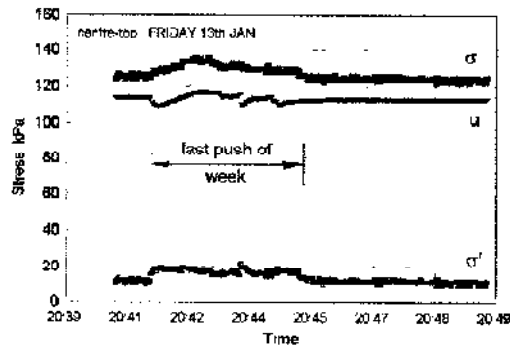
resulting in equal effective stress increases of 17kPa. Dissipation of shearing-induced excess pore pressures would probably show as reduced pressures all around the pipe since interface stress measurements during jacking are generally uniform (section 6.2.4) It is reasonable to assume therefore that these local pore pressure reductions are unlikely to be caused by the dissipation of shearing-induced excess pressures. The probable cause of decreasing pore pressures and corresponding increasing effective stresses is localised ground deformation. The reason for the observed response in radial stresses and pore pressures during the assumed deformation is not apparent. The mechanism of decreasing total stresses, pore pressure and corresponding increasing effective stresses is unlike that observed in London clay, where stresses and pore pressures change the instant pushing stops. In the soft clay of Scheme 9 the rate of change is much slower – there is no discernible change in stresses and pore pressures at the end of logging after the final push. Figure 6.50 illustrates the supposed stress and pore pressure characteristics at the pipe top and left during the weekend stoppage.



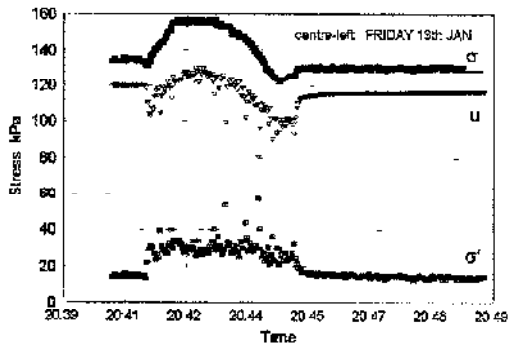
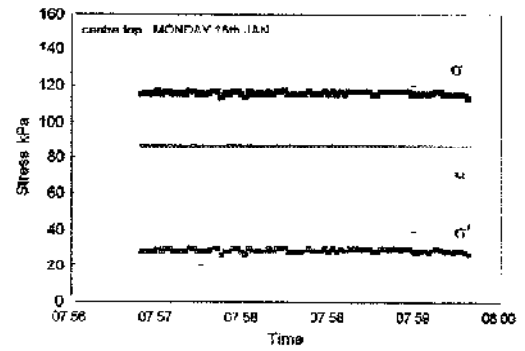
a) total stresses

b) effective stresses

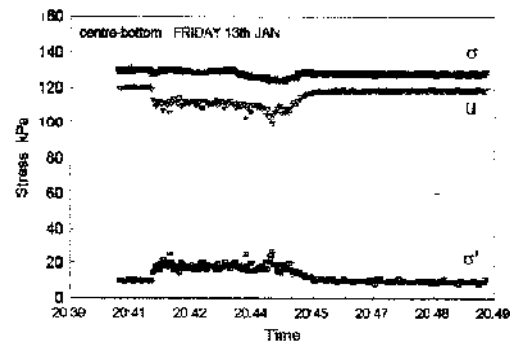
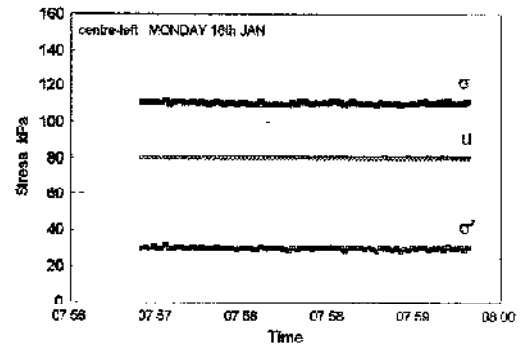
**Figure 6.48** Time dependent changes in radial stresses around the pipe centre during stoppages on Scheme 9.



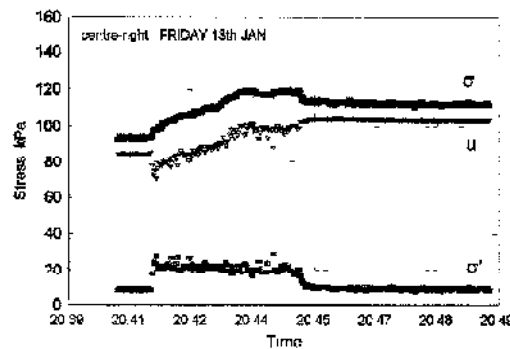
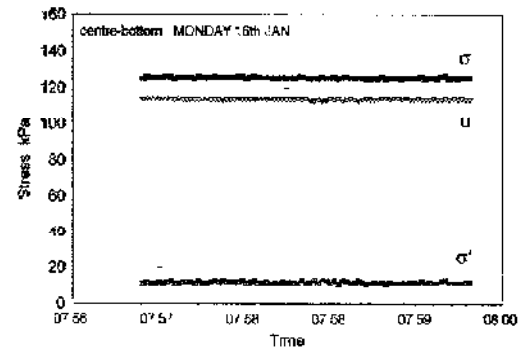
a) centre-top stresses



b) centre-left stresses



c) centre-bottom stresses



d) centre-right stresses

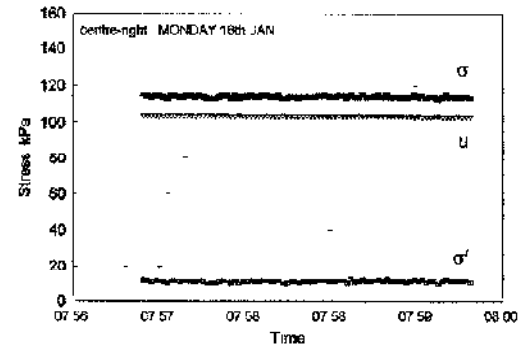
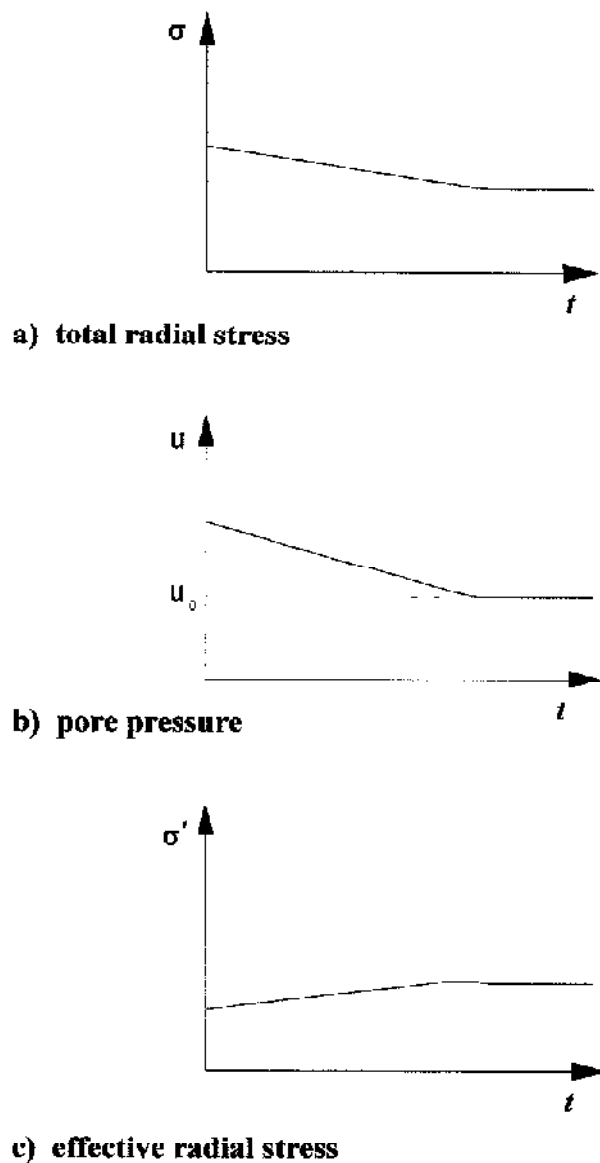


Figure 6.49 Time dependent changes in radial stresses and pore pressures after a weekend break during Scheme 9.



**Figure 6.50** Localised radial stress and pore pressure characteristics during a long stoppage in soft clay.

## 6.5 MISALIGNMENT EFFECTS

Tunnel excavation in pipe jacking inevitably deviates from the intended line and level. This typically results in the type of curvatures demonstrated by the alignment data of Figures 5.15 to 5.22. Previous authors (Haslem 1986, O'Reilly and Rogers 1987, Haslem 1996) assumed that increased contact stresses would be generated on the outside of such horizontal curves as illustrated in Figure 6.51. Field measurements from the Stage 2 research however, have shown the converse to be true in that ground reactions actually occur on the *inside* of horizontal curves.

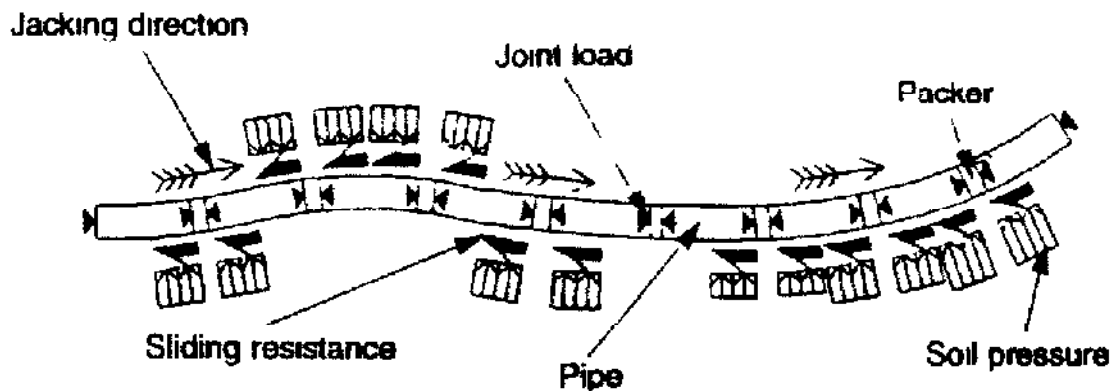


Figure 6.51 Haslem's flexible pipeline model (after Haslem 1996).

For Schemes 8 and 9 in Stage 3 research, deviations from the proposed line, though considerable in places, have not resulted in large angular misalignments. Comparison of alignment data and interface stress plots, Figures 6 52 and 6 53, are difficult to interpret in terms of misalignment but appear to show little clear evidence of increased contact stresses at points of maximum curvature. As discussed earlier in the chapter, pressurised lubricant greatly influenced interface stresses through most of Scheme 8 and the later section of Scheme 9 and lubricant may also have averted increased contact stresses due to misalignment

On Scheme 6 steering corrections occurred only in the horizontal plane, Figure 5 19. Excellent agreement between the position of maximum total stress, measured on the side of the pipeline, and the large horizontal deviation at chainage 20m is illustrated in Figure 6 54 Increased contact stresses on the left show the ground reaction on the inside of the curve. Along the right of the pipe (outside of the curve) there is no contact between ground and pipe as it passes through the deviation. At the curve's apex it is also notable that the maximum increase in stress occurs at the centre. At the front the increase is less than half that at the centre and there is no increase at the rear. This confirms that complex ground reaction distributions occur as pipes travel around curves. Figure 6.55 shows a plot of total radial stress at the pipe centre against angular deviation. As the centre of the pipe approaches the apex, increasing angular deviation gives rise to a larger ground reaction. When the pipe leaves the curve apex, angular deviation remains large but the ground reaction diminishes

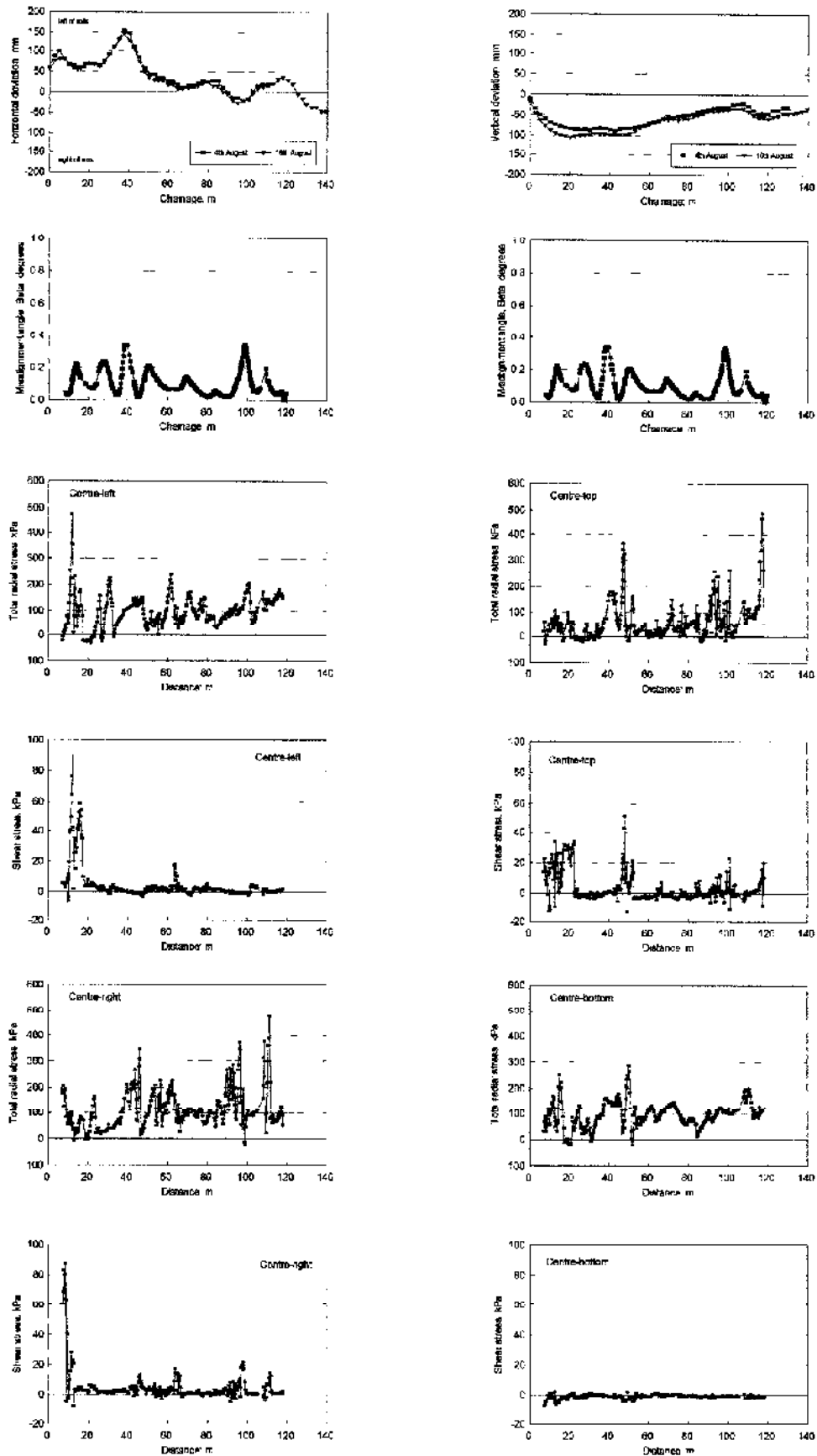


Figure 6.52 Comparison of tunnel alignment data and local interface stresses in Scheme 8.



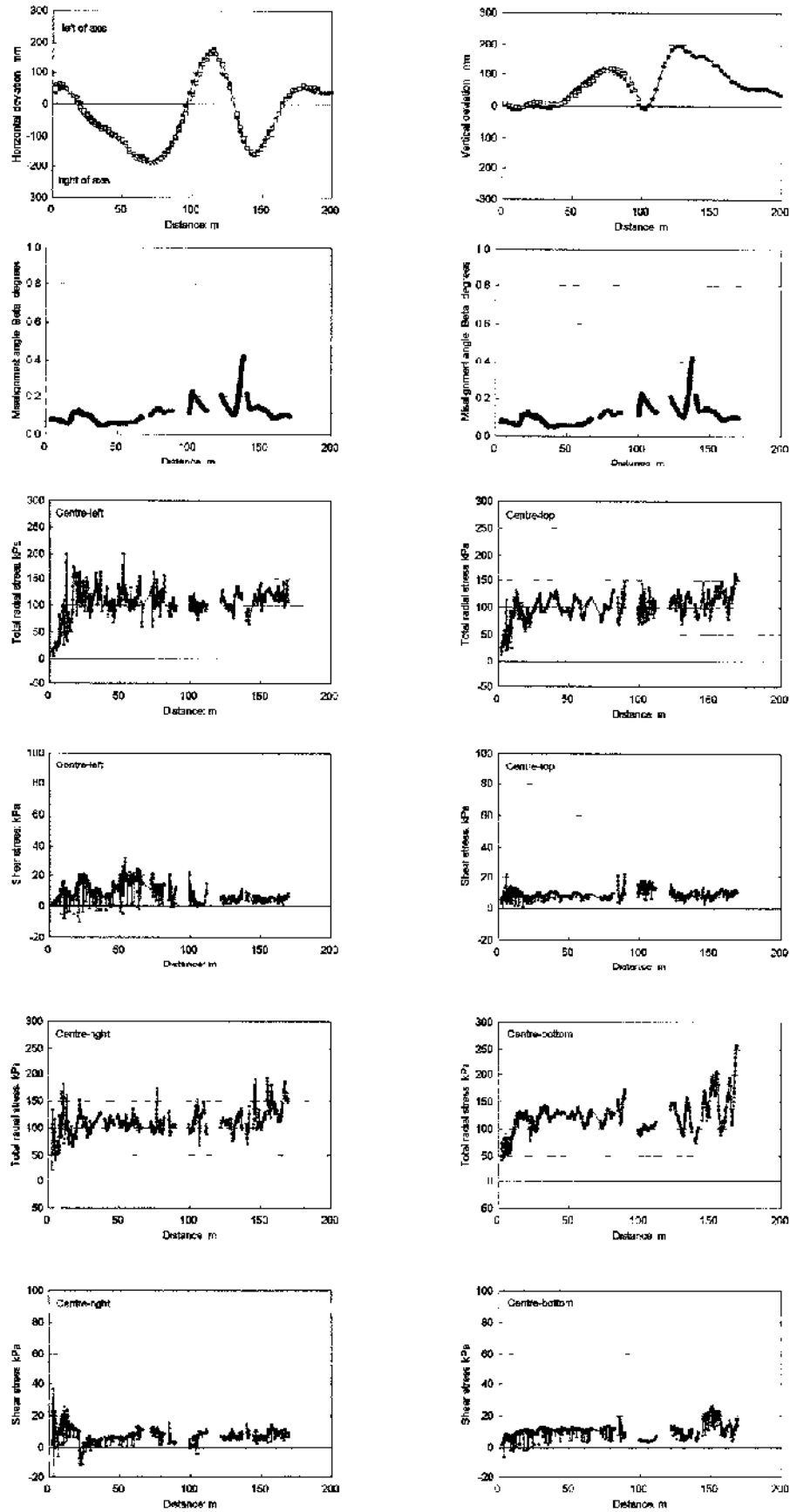


Figure 6.53 Comparison of tunnel alignment data and local interface stresses in Scheme 9.

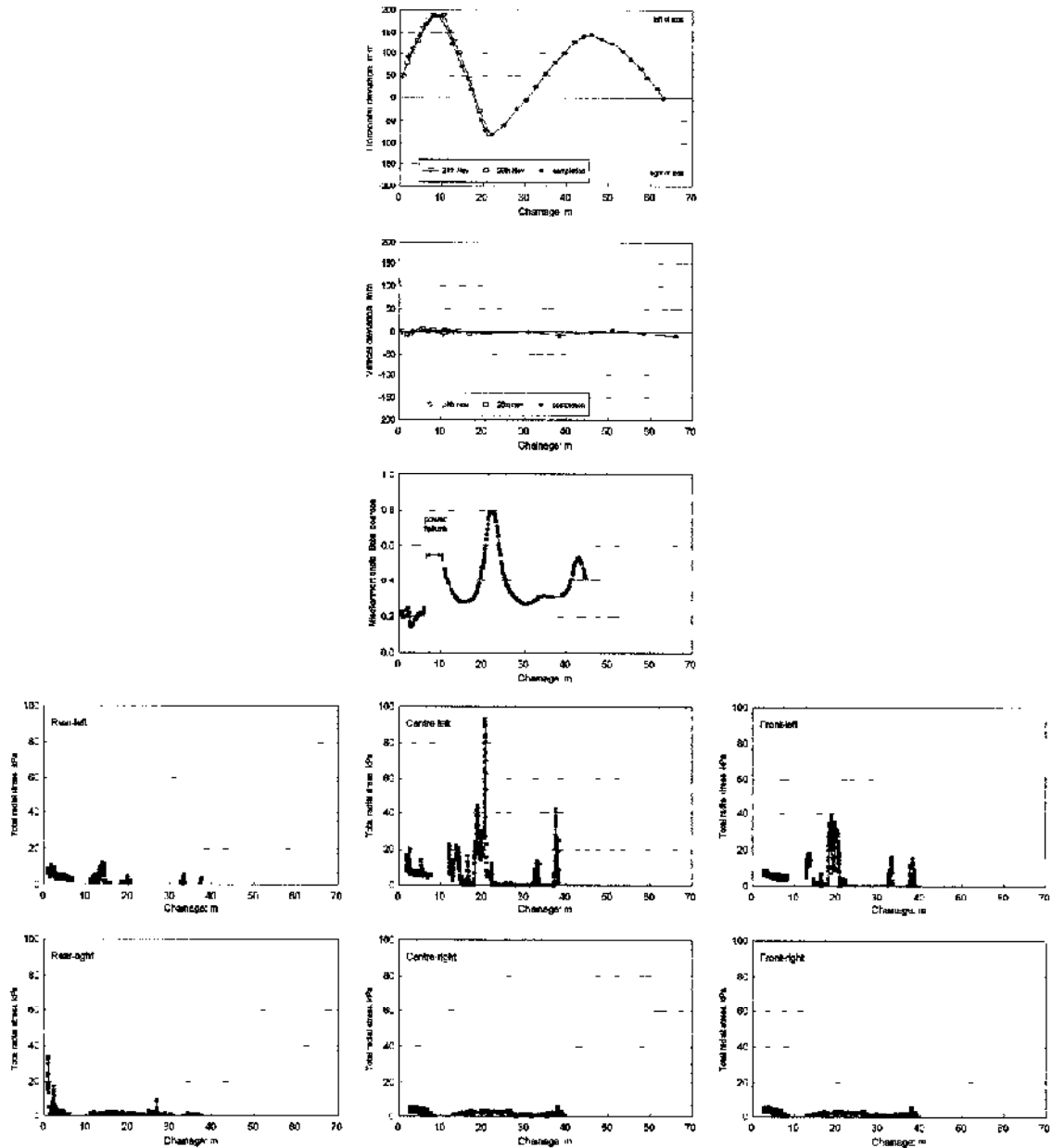


Figure 6.54 Comparison of tunnel alignment data and total radial stresses on the pipe side in Scheme 6.

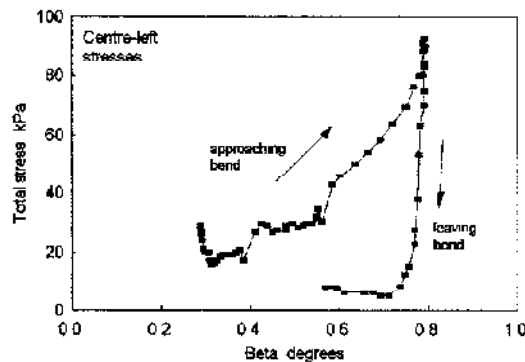


Figure 6.55 Relationship between angular misalignment and induced total radial stress in Scheme 6.

The ‘Oxford’ ground reaction model, based on field observations from Stages 2 and 3, Figure 6.56, assumes the pipeline acts as a prestressed segmental beam spanning between vertical and horizontal apices. Milligan and Norris (1998) have developed a simplified model, based on this theory, for forces acting on a half-wave length of pipeline – illustrated in Figure 6.57 and derived in Appendix D.  $P_1$  and  $P_2$  are the axial jacking forces and it can be shown that

$$P_2 = P_1 \frac{(l + D \tan \delta)}{(l - D \tan \delta)} + \frac{Wl^2 \tan \delta}{(l - D \tan \delta)} \quad (6.1)$$

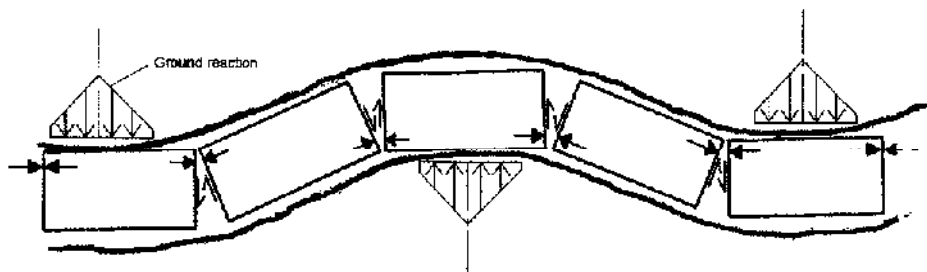


Figure 6.56 Oxford soil reaction model.

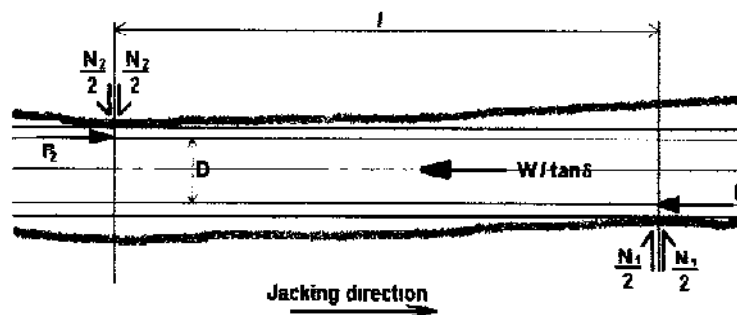


Figure 6.57 Theoretical half-wave model for pipe-soil interaction (after Milligan and Norris 1998).

Jacking loads from Scheme 1 have been compared to calculated values using this model. Calculated jacking loads at 17.5m and 35m are 235kN and 355kN respectively, compared with 227kN and 333kN for a perfectly straight pipeline and measured values of 246kN and 372kN. Agreement between calculated and measured values is reasonable but closer agreement could be achieved by refining the

distribution of reaction force  $N$  utilising Stage 3 observations. In Scheme 6 (London clay) there is at the start of the drive an almost perfect wave of about 18m in the horizontal alignment – jacking record and alignment survey are shown in Figure 5.19. The face load was zero, the interface friction angle  $13^\circ$ , the pipe internal diameter 1.5m, and the pipe weight 23.9kN/m. Jacking loads at 9m and 18m are calculated as 51kN and 107kN respectively compared with 50kN and 99kN from the self-weight model for a perfectly straight pipeline. Stoppage effects in the London clay, and a logging failure, prevent a direct comparison with measured jacking loads at 9m and 18m and therefore the average frictional resistance of 12.7kN/m and the lower bound of 6.7kN/m will be used. As a result measured average values are 114kN and 229kN; lower bound values are 60kN and 120kN. The ‘half-wave’ model values are far less than the average measured values but are comparable to the lower bound. The model appears to greatly underestimate jacking loads in London clay where the influence of stoppage effects will far outweigh that of any acceptable misalignment effects.

## 6.6 LUBRICATION EFFECTS

### 6.6.1 Introduction

Lubricant in the form of bentonite slurry was used on several of the monitored schemes from the start of the drives of Schemes 5 and 7; during the later stages of Schemes 4 and 9, and from early in the drive of Scheme 8. The purpose of this section is to gain a better understanding of how the bentonite-based lubricants functioned in the different ground conditions of Schemes 7, 8 and 9. Interface stress data presented are predominantly from Scheme 7, where the lubrication operation ceased for a significant time, and Scheme 9, where lubricant was introduced part way into the drive. Although lubricant was also introduced part way into the Scheme 8 drive, the instrumented pipe - inserted at pipe 74, about 180m behind the shield - was not in place and a contrast in interface stress behaviour, pre- and post-lubrication, cannot therefore be drawn. The effect of pumping and injecting lubricant on pore pressures around the instrumented pipe of the three schemes is discussed together with the effect on shear and effective radial stresses.

### 6.6.2 Scheme 7

The non-uniform arrangement of injection sockets in Scheme 7, described earlier in section 5.3.1.2, resulted in a lubricant zone more effective along the right of the instrumented pipe than along the left. The change in pore pressures when pumping the lubricant, typically resulting in increases of about 30kPa above hydrostatic pressure, were found to be influenced by the location of injection sockets. Figure 6.58 illustrates the localised change in pore pressures during a single push when the lubrication system was also operating. The push started just before 15:30hrs on the horizontal axes and continued until 15:38:40hrs. There was little change in pore pressures until pumping lubricant commenced at about 15:32hrs. At the bottom and right of the pipe pressures began to increase soon after pumping started and continued steadily up to about 80kPa – a pattern also seen at front-left location. At the centre-left, rear-left and top of the pipe, pressures increased to a steady-state very quickly following significant time lags – the length of time lag increased from front to rear of the pipe and around the left to the top. These data suggest a pressure wave effect, due to fresh slurry from the shield, locally moving easily along the bottom and right of the pipeline where there was probably an ‘open’ overbreak, albeit full of lubricant gel/bentonite filter cake.

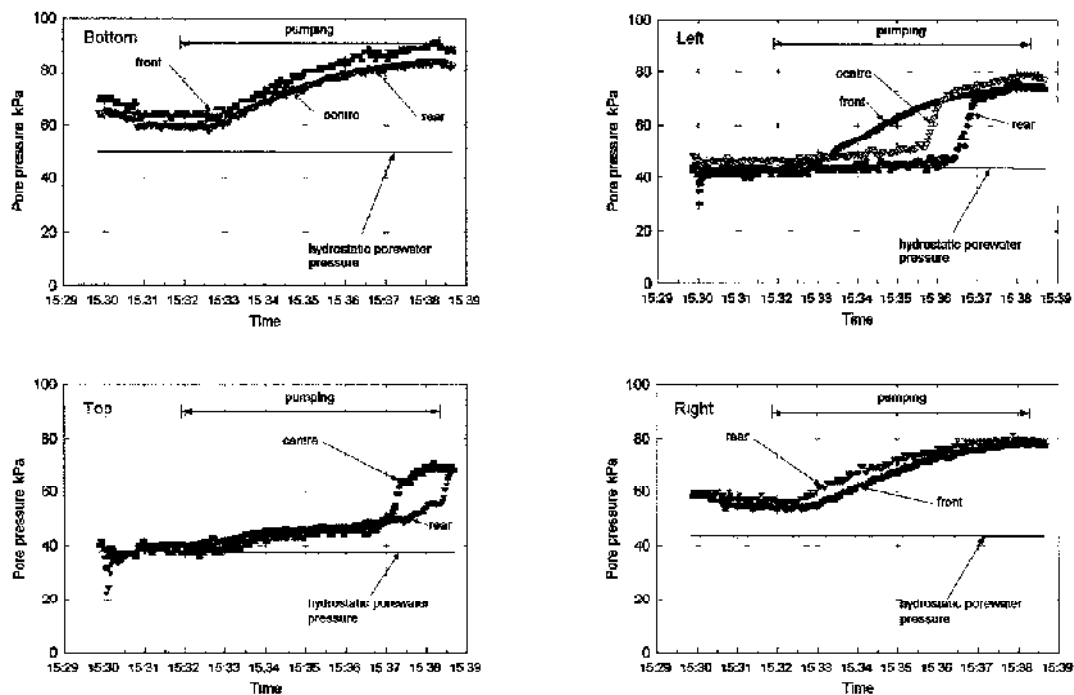
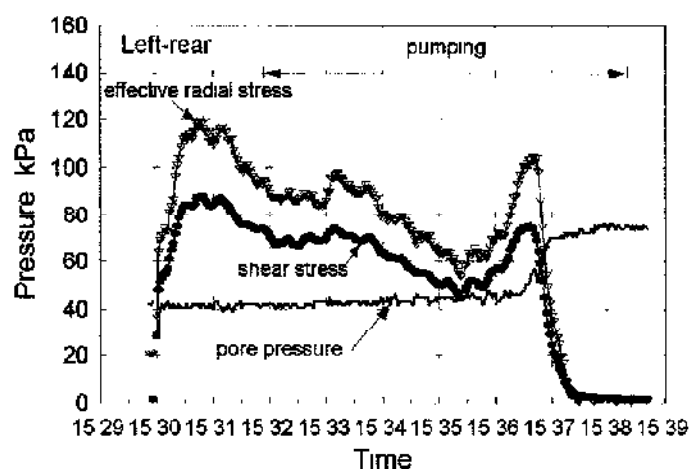
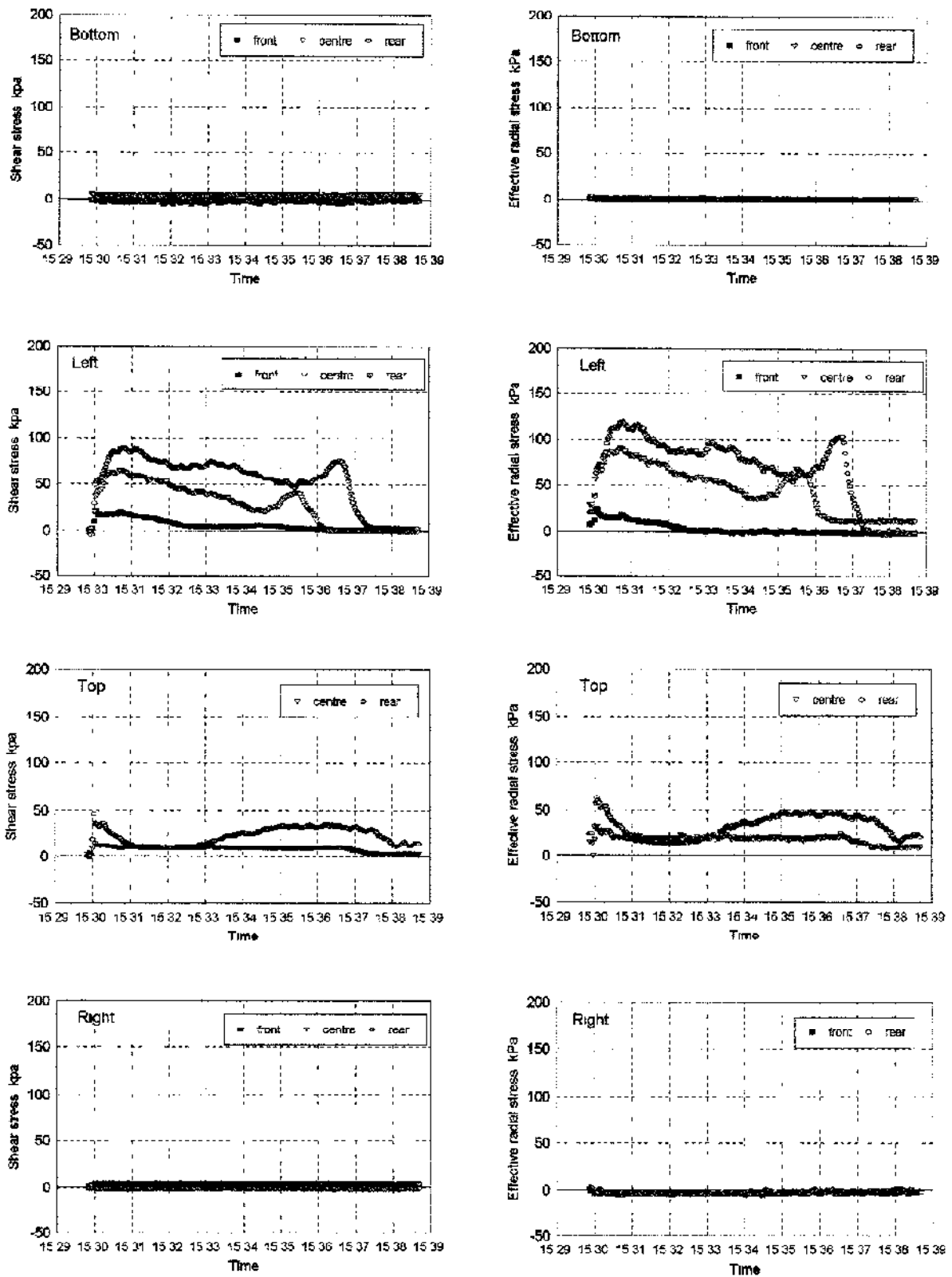


Figure 6.58 Variation in pore pressures during lubricant pumping on Scheme 7; push 61.97m to 63.42m.

Around the front-left to rear-top of the pipe the pressure wave had a difficult path where the overbreak had probably ‘closed’ and the pipe was in contact with the soil. Figure 6.59 shows interface stress and pore pressure data points from the left-rear cell for the same push. When pumping commenced the interface stresses decreased, somewhat erratically, until the increase at 15:35:30hrs - possibly due to lubricant pressure on the right pushing the pipe against the ground on the left. As pore pressures began to increase rapidly at 15:36:30hrs, stresses fall dramatically to zero. As the pore pressure reached a steady state of 65kPa, probably indicating the formation of an effective lubricant zone, there was clearly no contact between pipe and soil for the remainder of the push. Interface stresses from all contact stress cells for the same push are illustrated in Figure 6.60. Pore pressures have been omitted from the two columns of plots (shear stress on the left and effective radial stress on the right) for clarity. Along the bottom and right of the pipe interface stresses were very low or zero throughout the duration of the push - indicating sliding through an effective lubricant zone of bentonite slurry/gel. Plots representing stresses along the left and top of the pipe plainly illustrate pipe-soil contact, with magnitude increasing from the front to the rear of the pipe. Of particular interest are data from the left of the pipe where reductions in interface stresses, markedly abrupt at the centre and rear, correspond exactly to the increase in pore pressure at the same location. By the end of the push there was little contact between soil and the instrumented pipe.



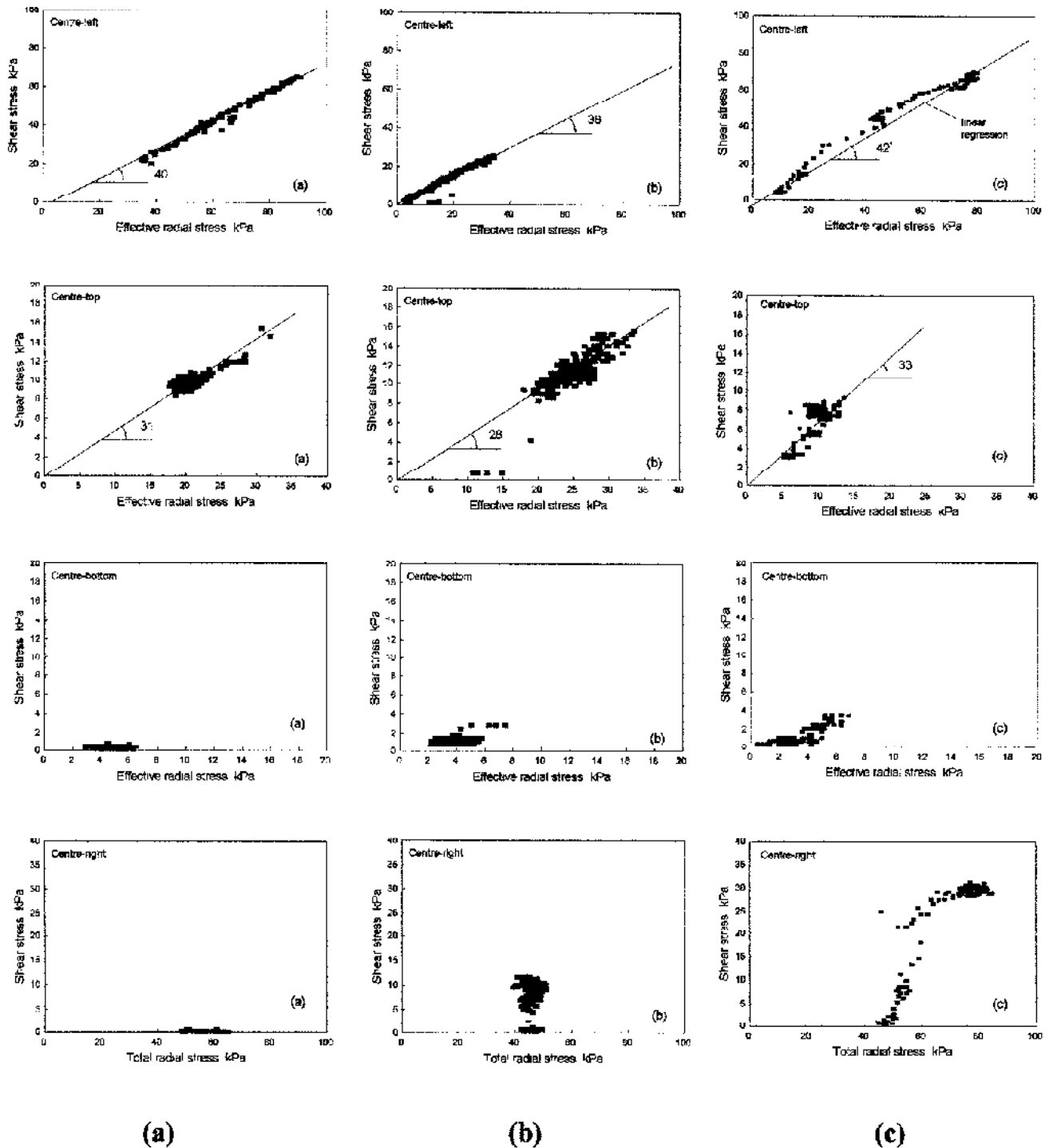
**Figure 6.59** Variation in left-rear interface stresses during lubricant pumping on Scheme 7; push 61.97m to 63.42m.



**Figure 6.60** Variation in interface stresses during lubricant pumping on Scheme 7; push 61.97m to 63.42m.

It was noted in chapter 5 that failure of the lubricating system during this scheme resulted in a significant increase in frictional resistance, Figure 5.2. The interface stress records however, Figures 6.5 to 6.8, show little indication of any change in behaviour due to cessation of lubricating. The compressed nature of the many data comprising the overall stress records make it difficult to determine any change in pattern, so data points of individual pushes from before, during and after the cessation have been examined. Figure 6.61 includes representative samples of the pushes, in this instance taking the form of shear stress/radial stress relationships from around the centre of the instrumented pipe. The plots are split into three phases (separated into columns): (a) day 4 of the drive during which lubricant was pumped; (b) day 5 where no pumping took place, and (c) day 7 when the lubrication system came back into operation. The linear relationship evident in the plots for the pipe left is a typical pattern found along that side of the pipe. During phase (a) the friction angle,  $\delta'$ , is  $40^\circ$ ; surprisingly, lubricant cessation, phase (b), results in a reduction in the friction angle of  $2^\circ$ . It is not clear whether this reduction is due to local variations in soil properties and/or a function of the lubricant gel becoming more effective following a period of pushing with no fresh slurry. In phase (c) (lubricant recommencement) the shear stress/radial stress relationship displays some non-linearity. Notwithstanding this apparent change in behaviour, a linear regression analysis results in a friction angle of  $42^\circ$ , an increase of  $2^\circ$  from that in phase (a). At the pipe top, where due to buoyancy, some contact with the tunnel crown is expected, the shear/radial stress relationship in all three phases is linear. The variation in friction angles seen in the plots of the pipe left is also found at the top with a  $3^\circ$  reduction between phases (a) and (b) and a  $5^\circ$  increase from (b) to (c). Buoyancy also results in the response shown in the plots for the pipe bottom, notably very low interface stresses indicating sliding along a low shear zone of bentonite lubricant. There is however, an emerging pattern of increasing shear stress from phases (a) to (c) suggesting the lubricant becoming less effective. Plots presenting data from the centre-right contact stress cell show total radial stress because the pore pressure transducer failed to respond correctly (noted in section 6.2.2) but pore pressures recorded at axis level on the left of the pipe are generally constant at about 40kPa.





(a) (b) (c)  
**Figure 6.61** Variation in shear stress/radial stress relationship during three phases of Scheme 7: (a) ineffective lubricating, (b) cessation of lubricant operation and (c) recommencement of lubricating.  
 (Note: Plots for the right of the pipe are in terms of total radial stress)

(Figure 6.7) Therefore a shift of 40kPa along the horizontal axes would reasonably represent effective radial stresses. The pattern of stresses along the right is: no pipe-soil contact during phase (a), increasing shear stresses through phases (b) to (c). The non-linear relationship of data points in phases (b) and (c) may represent contact between pipe and a depleted lubricant gel contaminated with soil grains.

During phase (b) when no lubricant was pumped, the tunnel was advanced by thirteen pipes, equivalent to approximately 33m length of new tunnel bore. Interface stress measurements suggest that soil in the new bore did not fully collapse onto the front of the pipe string (the instrumented pipe, inserted at pipe 2, was about 8m from the face) and that there was probably some adhering of lubricant gel to pipes entering the new bore. It is not apparent whether soil in the oldest part of the bore, nearest the thrust shaft, collapsed onto new pipes inserted during the two days of cessation of lubrication. When the lubrication system came back into operation, any closure or collapse of the tunnel bore could not be 'recovered', resulting in no reduction in previously established frictional resistance and a type II line in Figure 5.13. The fresh slurry was probably only effective in recharging lubricant in sections of the overbreak remaining open. The increase in pore pressures around the instrumented pipe while pumping lubricant during phase (a) has been demonstrated above. Pore pressure and total stress data from phase (c) show that pumping lubricant had no effect around the instrumented pipe; pore pressures remained constant, Figure 6.62. This suggests that soil had probably collapsed onto the front of the pipe string blocking any path for the fresh slurry.

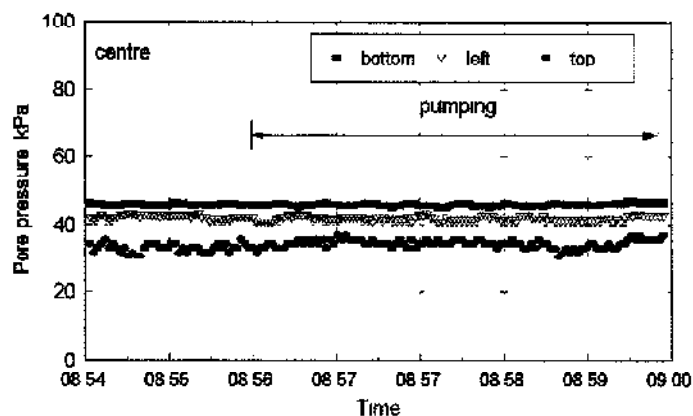
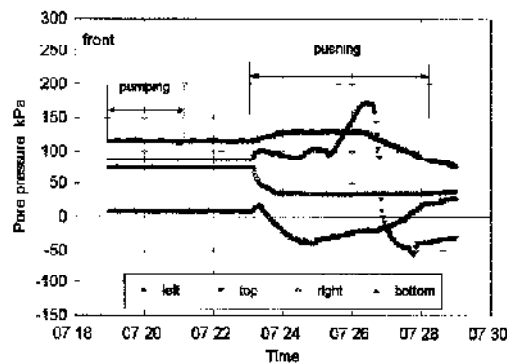


Figure 6.62 Variation in pore pressures during Scheme 7 following commencement of lubricating: day 7.

### 6.6.3 Scheme 8

In Scheme 8, an efficient lubrication operation using injection sockets at three locations in lubricant jacking pipes (Figure 5.3) spaced uniformly throughout the pipe string had the effect of keeping interface stresses around the instrumented pipe generally low throughout the drive, Figures 6.11 to 6.14. Shear stresses particularly, with the exception of marked peaks recorded at the pipe top, showed a very low average of 4kPa.

Many detailed interface stress data have been examined for periods in the drive when lubricant was being pumped – some typical results are illustrated in Figures 6.63 and 6.64. The data show that pumping lubricant had no influence on pore pressures and total stresses around the instrumented pipe (positioned about 180m behind the shield). This suggests that fresh slurry probably charged only sections of the overbreak in the new bore – around the shield and front of the pipe string. In the stiff glacial clay, the lubricant slurry appears to completely fill the overbreak resulting in a type I line in Figure 5.13.



**Figure 6.63** Variation in pore pressures during pumping lubricant in Scheme 8: front.

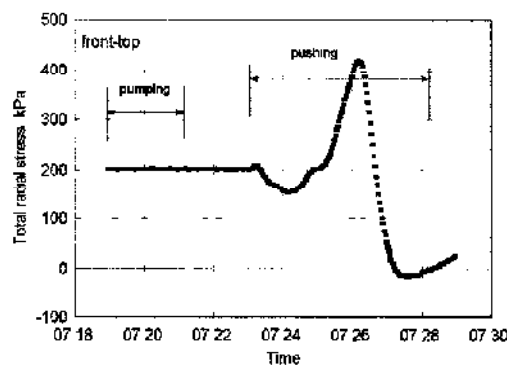


**Figure 6.64** Variation in total stress during pumping lubricant in Scheme 8: front-top.

#### 6.6.4 Scheme 9

Bentonite lubricant was introduced in the Scheme 9 drive following a weekend stoppage – at about 130m on the jacking record, Figure 5.4, and about chainage 85m on the horizontal axes of Figures 6.15 to 6.18. Due to noise restrictions in the residential area at the thrust shaft location, pumping lubricant was restricted to day shifts only, typically being pumped at the start and end of each shift. It has been previously noted that the instrumented pipe was inserted at pipe 19; the closest lubricant injection sockets were at axis level in pipes 18 and 17 on the right and left respectively. Introduction of the lubricant changed the interface stress behaviour, particularly pore pressures and total radial stresses.

Almost immediately after lubrication began, shear and effective radial stresses along the pipe bottom fell sharply and became more uniform, Figure 6.15. The reduction and uniformity of stresses was brief and after about chainage 120m, shear and effective radial stresses resume a pre-lubrication pattern and pore pressures became erratic and noticeably larger (resulting in corresponding increases in total radial stresses). The change in behaviour in post-lubrication pore pressures was evident all around the pipe but with different magnitudes. Along the pipe top for instance, post-lubrication pore pressures differed little in magnitude to those pre-lubrication, but they are much more erratic – Figure 6.16. Shear and effective radial stresses show an increase in magnitude indicating pipe buoyancy in the lubricant with a resulting increase in pipe-soil contact. Marked peaks in the effective stress plots correspond to the initial pushes of the first night shift after the lubricant was introduced. Along the right of the pipe the most noticeable changes in behaviour due to lubrication were in the effective radial stresses, Figure 6.17; after chainage 85m, average stresses fell but at the centre and front they were markedly peakier. At the pipe-left, Figure 6.18, there was a marked reduction in shear and effective radial stresses after lubricating – pore pressures and total radial stresses became a little less erratic. Table 6.5 includes average interface stress values from around the pipe centre for three distinct phases apparent in the interface stress records: (a) pre-lubrication; (b) soon after the lubricant was introduced, and (c) when the lubricant was well established.

Position (Centre)	Left				Top				Right				Bottom			
	$\sigma$ (kPa)	$u$ (kPa)	$\sigma'$ (kPa)	$\tau$ (kPa)	$\sigma$ (kPa)	$u$ (kPa)	$\sigma'$ (kPa)	$\tau$ (kPa)	$\sigma$ (kPa)	$u$ (kPa)	$\sigma'$ (kPa)	$\tau$ (kPa)	$\sigma$ (kPa)	$u$ (kPa)	$\sigma'$ (kPa)	$\tau$ (kPa)
Phase (a) (CH 0-85m)	107	72	35	11	94	73	21	11	106	88	18	7	115	93	22	10
Phase (b) (CH 85-120m)	99	67	32	6	99	69	32	18	109	105	5	5	113	105	8	6
Phase (c) (CH 120-170m)	113	94	19	5	114	93	21	13	122	115	8	8	141	125	15	13

**Table 6.5** Variation in average interface stresses (kPa) at the pipe centre during three phases in Scheme 9.

Values comprising Table 6.5 show increases in pore pressures (and a corresponding increases in total radial stresses) around the pipe between phase (a) and phase (c) ranging from 20kPa (top) to 32kPa (bottom). It is not yet fully understood why the bentonite-based lubricant caused these pressure increases. The change in average shear and effective radial stresses through the three phases is illustrated graphically in Figure 6.65. Along the right and bottom the variation in stresses is similar; phase (b) shows a relatively large decrease but phase (c) sees a recovery and average shear stresses become greater than pre-lubrication values. The reverse is true of the pattern at the pipe top where stresses rise during phase (b) but then fall back almost to pre-lubrication values in phase (c). The most beneficial effect of lubricating occurs along the pipe left: average stresses decrease during phase (b) and fall further to the values recorded during phase (c). The changes at the top and bottom may be a result of a greater buoyancy force during phase (b).

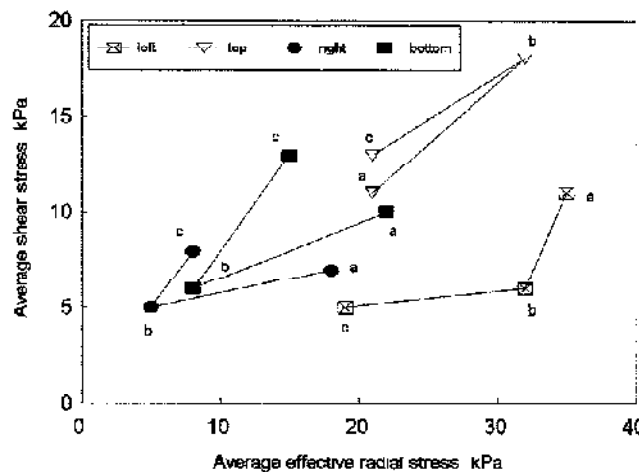


**Figure 6.65** Variation in average shear and effective radial stresses at the pipe centre during Scheme 9.

Stresses from several pushes have been extracted from the compressed data of the overall interface stress records and are presented in Figure 6.66. The plots are presented in three columns each representing one of the phases (a), (b) and (c). Along the left of the pipe, there was a small increase in effective radial stresses between phases (a) and (b) but during phase (c) they fell dramatically to around 10kPa. Shear stresses remained relatively constant throughout the three phases but were slightly lower, at about 10kPa, in the lubricated sections. Along the top of the pipe the introduction of lubricant, phase (b), resulted in an increase in shear and radial stresses that later, in phase (c), fell back to pre-lubrication values. The most notable effect of introducing lubricant occurred along the right of the pipe, where shear and radial stresses decreased to about zero. In phase (c) shear stresses increased and radial stresses became more erratic. Along the bottom of the pipe shear stresses remained relatively constant through all three phases; radial stresses remained low but fell by about 10kPa in the post-lubricant phases.

The effects of lubricant on shear stress/effective radial stress relationships are illustrated in Figure 6.67. Data in this figure again represent the same three phases described above. Before lubrication in phase (a), there was a similar pattern at the top, right and bottom of the pipe where shear stresses reached limiting values of 6kPa, 12kPa and 11kPa respectively. Values of undrained shear strength,  $s_u$ , at tunnel depth were typically 6kPa. Along the pipe left, data are very scattered but the effective radial stresses were greater than those at the other locations. Upon the introduction of lubricant, phase (b), stresses at the top and right became more erratic. Along the bottom of the pipe the shear/radial stress relationship was similar to that before lubrication but with a lower limiting shear stress of about 6kPa. During phase (c) stresses at the bottom of the pipe became more erratic, along the top and right of the pipe stresses became less erratic and moved closer to pre-lubricant limiting shear stresses. Along the left of the pipe during this final phase, the range of effective stresses became comparable to the other locations and the shear stress/effective stress relationship trend was toward a limiting shear stress of about 5kPa.

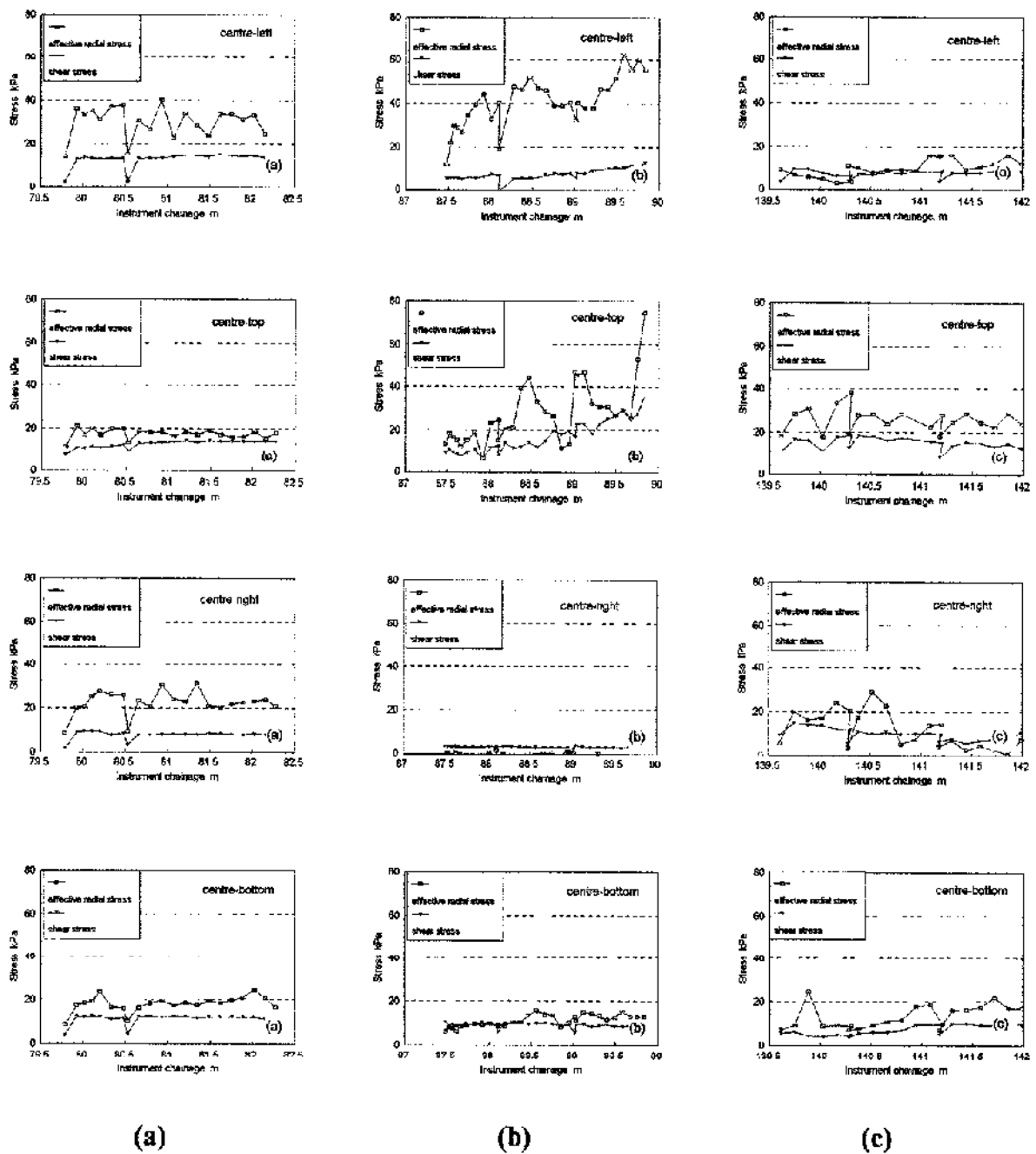


**Figure 6.66** Variation in shear and effective radial stresses during three phases of Scheme 9: (a) pre-lubrication, (b) soon after lubricating and (c) lubrication operation well established.

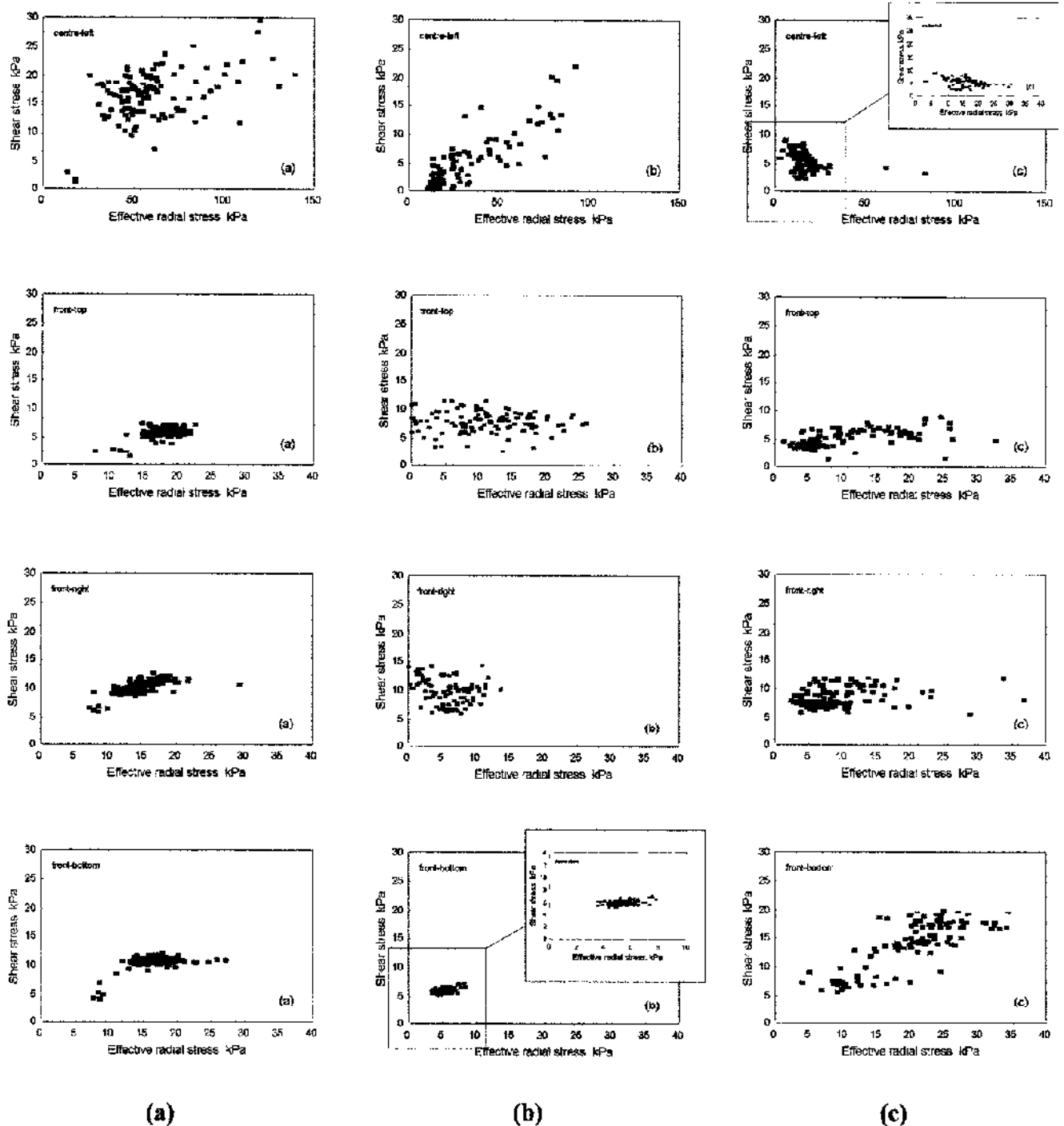


**Figure 6.67** Variation in shear stress/effective radial stress relationship during three phases of Scheme 9; (a) pre-lubrication, (b) soon after lubricating and (c) lubrication operation well established.



The effect of pumping lubricant on pore pressures during phase (b) is illustrated in Figure 6.68. The data are purposely taken from a period where the pipe string was stationary so as not to corrupt the effect with a push event, site records show lubricant pumping commencing at 17:11hrs and finishing at 17:22hrs. The effect on pore pressures along the pipe bottom was an almost immediate increase of about 5kPa. There was no variation in pressure at other locations around the pipe until completion of pumping where the response is most noticeable along the right. The variation and magnitude of pore pressure response around the pipe is not fully understood, but it is assumed that measurements at the right of the pipe are probably influenced by an injection socket on the right of the pipe 18 (immediately in front of the instrumented pipe)

In summary, pre-lubricant interface stresses are generally uniform around the right, top and bottom of the instrumented pipe, effective stresses at the left are notably greater. The introduction of lubricant in phase (b) has resulted in temporary localised effects around the pipe including a reduction in shear and effective radial stresses at the bottom and right, and increased, erratic stresses at the top. These effects can probably be attributed to the position on the right of the nearest lubricant socket and pipe uplift due to the pressurised slurry respectively. The stresses along the left after lubricating fell and did not increase during phase (c). Assuming these highly localised contact stresses are representative of all pipes within the string, then the summation of local reductions in shear and effective radial stresses results in the change in frictional resistance of the jacking record, Figure 5.4, from 25kN/m, pre-lubrication, to 14kN/m, post-lubrication.

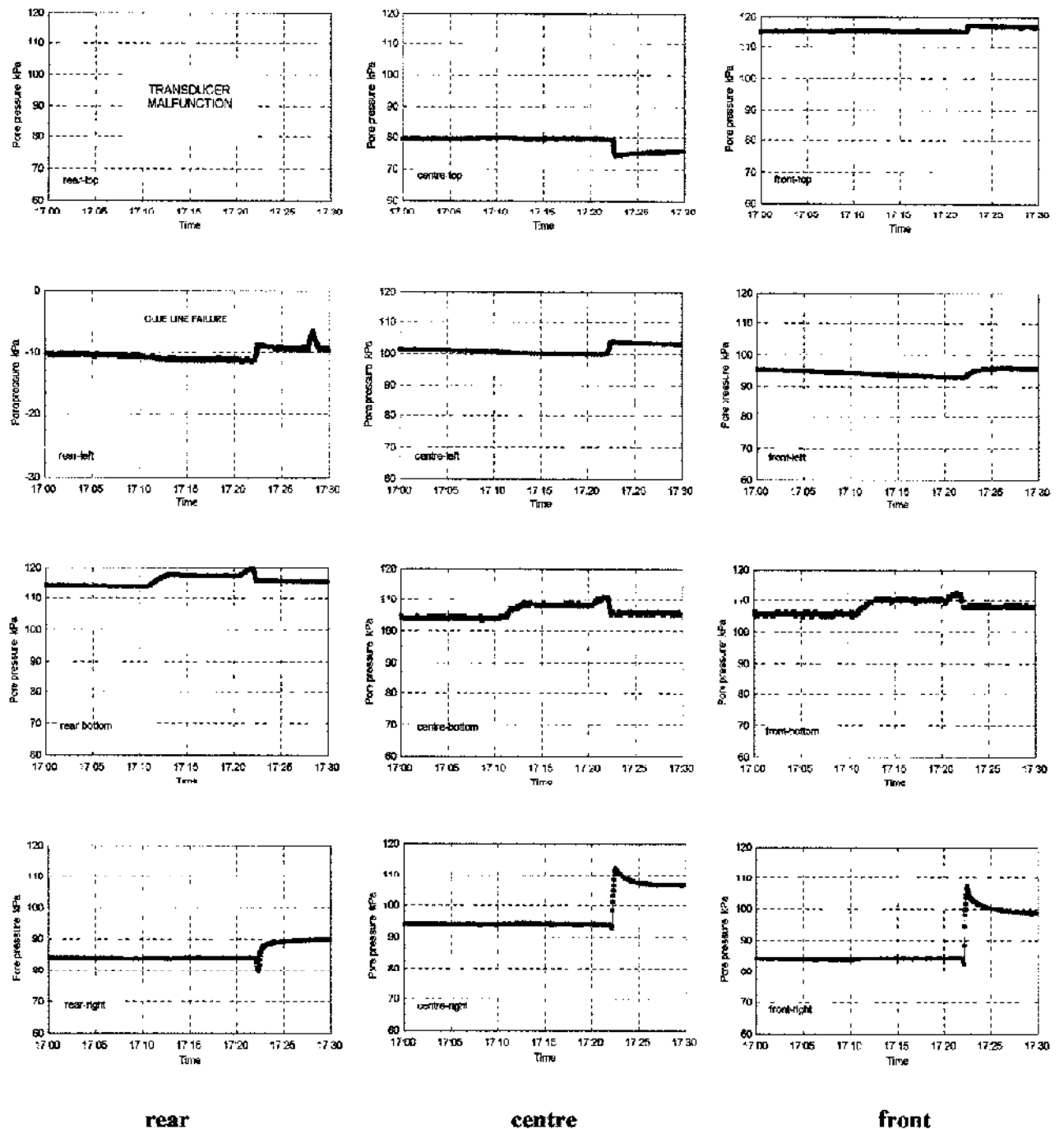


**Figure 6.68** Variation in pore pressures around the pipe during lubricant pumping on Scheme 9; phase (b) soon after lubricating.

## 6.7 CONCLUSIONS

### 6.7.1 Introduction

This chapter contains much detail on pipe-soil interaction and many data from the schemes monitored have been presented. The main observations and mechanisms described in the chapter have been extracted and are discussed below.

### 6.7.2 Interface stress records

Interface stress records were presented for the Stage 3 schemes. The data presented in these compressed plots were not adjusted for zero drift or instrument malfunction. As a result some effective radial stresses were often just below zero which must be erroneous. More significant negative peaks, in the range  $-10$  to  $-50$  kPa, particularly for Scheme 8, are not fully understood but are thought to be influenced by spikes in pore pressures due to lubricant injection.

At Scheme 6 in London clay, the interface stress records showed that contact between instrumented pipe and ground generally only occurred along the tunnel invert, indicating a condition of pipes sliding along the base of an open bore. The only other pipe-soil contact occurred at severe horizontal changes in bore alignment and also along a very small section of the tunnel soffit. The contact along the top of the pipe was attributed to an erratic hand-excavated bore.

In fine sand below the water table at Scheme 7, it appeared that the pipeline was buoyant in the bentonite lubricant and pipe-soil contact was shown to be non-uniform along and around the instrumented pipe. The reasons put forward for non-uniform contact were: arrangement of lubricant injection sockets; and position of the pipe relative to the microtunnelling machine (inserted as the second pipe behind the shield).

In the lubricated drive through glacial clay at Scheme 8, the pore pressure and total stress measurements were similar, and both very erratic; effective stresses were small and shear stresses very small. The picture here was of the pipeline largely buoyant in lubricant. Pressure within the lubricant varied rapidly, probably due to a function of injection procedures and the pipeline trying to straighten in a misaligned bore. Maximum shear stresses were recorded along the sides and top of the pipe along

a short section at the start of the drive. These relatively large shear stresses coincided with a section of drive where the clay was described as being noticeably wetter.

At Scheme 9 in soft clay, fairly uniform radial and shear stresses were measured around the instrumented pipe. Total radial stresses and pore pressures were almost equal, and effective radial stresses and shear stresses were low at about 20kPa and 10kPa respectively. The introduction of lubricant caused interface stresses along the top, bottom and right of the pipe to become more erratic, along the left of the pipe stresses became more consistent. The likely reason for this was a non-uniform distribution of lubricant slurry.

### 6.7.3 Ground related factors

Results relating local shear and radial stresses were examined and data presented for some of the Stage 2 schemes and all the Stage 3 schemes. In the cohesionless soils at Schemes 4, 5 and 7 the shear stress/radial stress relationships were clearly frictional, measured skin friction angles,  $\delta'$ , were in the range 20° to 43°

At the Stage 2 schemes in cohesive soils it was demonstrated that the relationship between shear and radial stresses also appeared to be frictional. In London clay at Scheme 3 however, there was evidence of a non-linear relationship; at higher radial stresses the shear stresses seemed to tend toward a limiting value. This type of non-linear relationship was also found at Scheme 6, also in the London clay, but at much lower shear stresses

Plots of interface stresses for individual pushes showed that contact stresses can be very localised and can vary rapidly as pipes advance. This was probably due to a relatively rigid pipe making contact with an irregular soil surface.

### 6.7.4 Effects of stoppages

For the schemes in London clay, total radial stresses were shown to decrease with time during stoppages. Unfortunately, changes in pore pressures were less clear and were very difficult to interpret. Consequently effective radial stresses were also highly complex. The many data examined showed a variety of responses during these stoppages and it was not possible to confirm a definitive mechanism. The general pattern appeared to be that shearing-induced excess pore pressures dissipate during

stoppages, so that the effective radial stresses increased even though total stresses decreased

At Scheme 8 (in stiff glacial clay) the interface stress measurements before and after weekend stoppages were consistent with a redistribution of lubricant pressure and loss of pipe buoyancy. For stoppages in the soft clay at Scheme 9 there was no detectable change in interface stresses during routine short delays. After the one significant stoppage of a weekend break, the decrease in pore pressures and corresponding increase in effective radial stresses suggested some closure of the tunnel bore.

#### **6.7.5 Misalignment effects**

Comparing tunnel alignment surveys and change in misalignment angles to interface stress records for horizontal misalignments, confirmed that increased contact stresses are generated on the inside of horizontal curves. Vertical misalignments in the monitored drives were not as severe as the horizontal deviations and it was not possible therefore to investigate the behaviour of a pipeline spanning between high points.

#### **6.7.6 Lubrication effects**

Detailed examination of interface stresses and fluid pressures during Scheme 7 demonstrated that a non-uniform distribution of lubricant slurry occurred. Interface stresses around the instrumented pipe showed very little pipe-soil contact along the right and bottom of the pipe, but significant contact on the top and left. Very low shear stresses (between zero and 5kPa) and zero skin friction angles were recorded along the bottom and right of the pipe, at the top and left, shear stresses of up to 50kPa were measured and the corresponding friction angles were 37° to 40°. During the pumping of lubricant it was notable that the time during which the pressure change occurred around the pipe varied significantly. The pressure change was influenced by the orientation of the pipe the tunnel bore; along the pipe left and at the top, where the pipe was in contact with the ground, the increase in pressure due to pumping fresh slurry was delayed the longest.

At Scheme 8, interface stresses around the instrumented pipe showed a much more even distribution of lubricant than that of Scheme 7. Effective radial stresses and shear stresses were very low (less than 5kPa) indicating negligible contact between the pipe and soil in the tunnel invert.

The results of introducing lubricant at Scheme 9 proved more difficult to interpret. The introduction of lubricant appeared to have only a temporary effect of reducing effective radial stresses and shear stresses along the right and bottom of the pipe; and increasing contact stresses along the left and top of the pipe. The non-uniform stress change was again attributed to the position of a lubricant injection socket, but the temporary nature of the effects is yet not fully understood.

## **chapter seven**

### **ground response**

---

#### **7.1 INTRODUCTION**

Like other methods of tunnelling, pipe jacking inevitably causes disturbance in the surrounding ground, and resulting deformation may result in damage to adjacent services, structures and pavements. One of the advantages pipe jacking has over other methods is that the tunnel behind the shield is immediately lined with pipes of sufficient strength and stiffness to withstand jacking forces. Deformation of the lining due to ground loading will be negligible and the technique should therefore minimise ground movements, provided no large displacements occur due to instability at the tunnel face or stress relief. Increasing use of pipe jacking in urban areas, where the concentration of existing services is high, therefore requires a greater understanding of the form and magnitude of resulting ground deformation.

This chapter aims to review how pipe jacking affects ground movements in a variety of grounds by drawing on observations from the monitoring work of Stage 3 and other relevant published data. Stage 3 fieldwork included measuring ground movements and change in ground stresses where possible. Inclinometers, settlement plates and surface settlement points were employed in the monitoring of transverse ground movements. On Scheme 8 longitudinal subsurface settlements close to the tunnel crown were accurately measured using electro-levels. Push-in pressure cells and piezometers were installed above and to the side of two of the monitored tunnels to measure in-situ stresses. Changes in ground stresses due to construction of the tunnel will be presented, and measured ground movements compared to current empirical predictive methods. Detailed information on the instrumentation used is included in Chapter 3.

#### **7.2 PREDICTION OF SETTLEMENTS**

The extent of transverse and longitudinal surface settlement above an advancing tunnel is illustrated in Figure 7.1. Following much research and analysis of tunnel settlement data, it is now widely accepted that the shape of the transverse

settlement profile immediately behind a tunnel is well described by an error function curve of the form shown in Figure 7.2. Surface settlement,  $S_v$ , is defined as

$$S_v = S_{\max} \exp\left[\frac{-y^2}{2i^2}\right] \quad (7.1)$$

where  $S_{\max}$  is the maximum settlement (at  $y = 0$ ) and  $i$  is the standard deviation of the curve. The width of the settlement profile is conveniently defined by  $i$ , which is the distance from the tunnel centre line to the point of inflexion. O'Reilly and New (1982) reviewed settlement data from tunnels in the UK to show that  $i$  was an approximately linear function of depth  $z_0$  and for most practical purposes can be simplified to

$$i = Kz_0 \quad (7.2)$$

where  $K$  is dependent on the type of soil and for tunnels in clays, and sands or gravels, may be taken as 0.5 and 0.25 respectively.

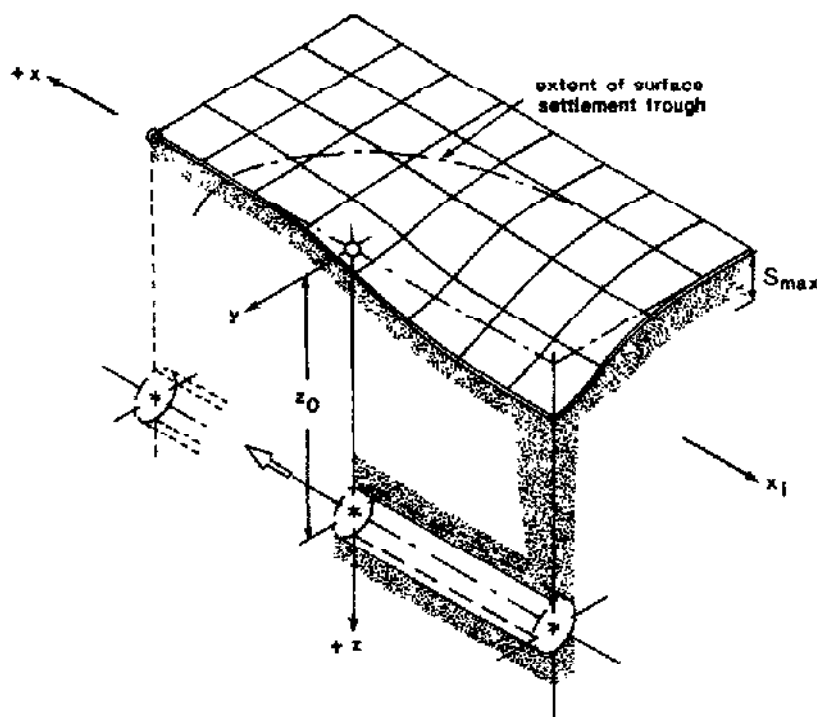
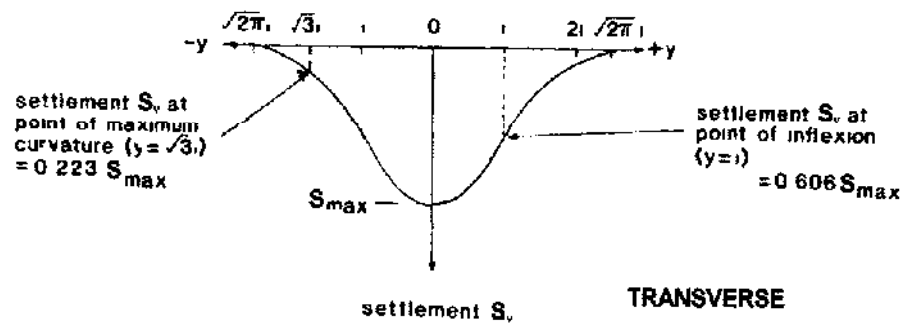


Figure 7.1 Settlement above an advancing tunnel (after Attewell et al, 1986).





**Figure 7.2** Idealised transverse settlement profile (after Attewell et al, 1986).

For subsurface settlements the trough width parameter  $i$  can be expressed as

$$i = K(z_0 - z) \quad (7.3)$$

Mair et al (1993) have shown that the ratio  $i/(z_0 - z)$  increases with depth (Figure 7.3) and

$$K = \left( \frac{0.175 + 0.325 \left( 1 - \frac{z}{z_0} \right)}{1 - \frac{z}{z_0}} \right) \quad (7.4)$$

The value of  $S_{\max}$  may be obtained by equating the volume of the settlement trough  $V_s$  to the volume of estimated ground loss. Integrating equation (7.1) gives

$$V_s = S_{\max} i \sqrt{2\pi} \quad (7.5)$$

rearranging,

$$S_{\max} = \frac{V_s}{i \sqrt{2\pi}} \quad (7.6)$$

There are two main source contributions comprising ground loss in tunnelling face loss (axial loss at the tunnel face) and closure of the ground between shield and

the tunnel lining. Ground loss is usually expressed as a percentage fraction,  $V_b$ , of the excavated area of the tunnel face.

For a circular tunnel

$$V_s = V_i \frac{\pi D^2}{4} \quad (7.7)$$

In pipe jacking ground loss due to movement at the face can be assumed to be negligible either because the face is continually supported by slurry pressure or because the excavation is in stiff clay. Tunnel diameters using the technique are relatively small and an open face in stiff clay should be highly stable with only very small movements due to elastic unloading occurring. Closure of the overbreak – extent of ground excavated between the bore diameter,  $D_e$ , and pipe diameter,  $D_p$  – should therefore be the only significant contribution to ground loss. For a circular pipe jack it is assumed

$$V_s = \frac{\pi}{4} (D_e^2 - D_p^2) \quad (7.8)$$

The idealised shape of the longitudinal settlement profile is shown in Figure 7.4. Settlement begins to show at the surface at a distance of about  $z_0$  or  $2z_0$  ahead of the face and initial displacement is normally 80% to 90% complete at a similar distance behind the face – Lake et al (1992).

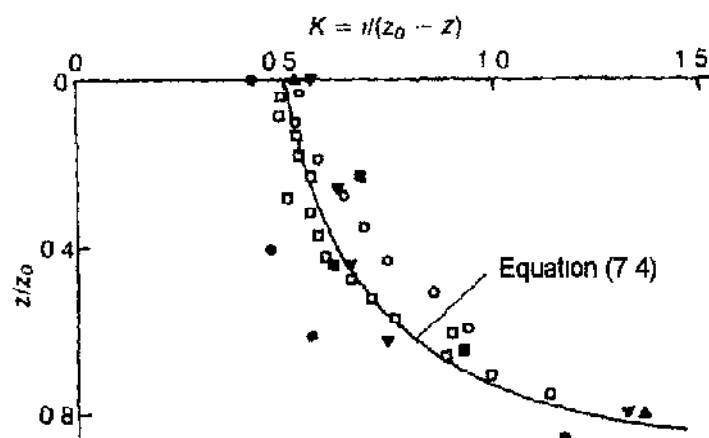


**Figure 7.3** Variation of  $K$  with depth for subsurface settlements above tunnels in clays (after Mair et al 1993).

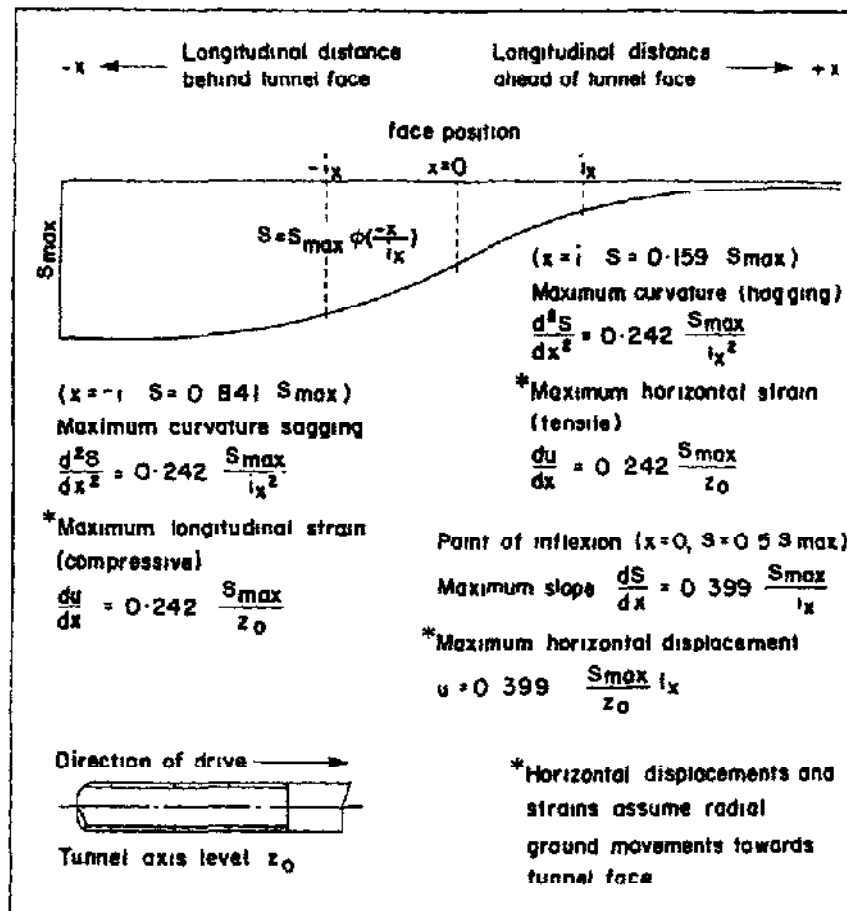


Figure 7.4 Idealised longitudinal surface settlement profile (after Lake et al 1992).

The longitudinal settlement trough is assumed to correspond to a cumulative probability curve, Attewell and Woodman (1982), and can be expressed as

$$S_v = \frac{V_s}{\sqrt{2\pi} i} \cdot e^{\left(\frac{y^2}{2i^2}\right)} \cdot \left[ G\left(\frac{x-x_i}{i}\right) - G\left(\frac{x-x_f}{i}\right) \right] \quad (7.9)$$

where  $x$  and  $y$  are tunnel co-ordinates and

$$G(s) = \frac{1}{\sqrt{2\pi}} \int_{-\infty}^s \exp\left(-\frac{t^2}{2}\right) dt \quad (7.10)$$

The value of the cumulative normal distribution function,  $G$ , can be evaluated by numerical integration or found in statistical tables.

## 7.3 FIELD MEASUREMENTS

### 7.3.1 Pressure cell readings

Horizontal stress and pore pressure measurements from the push-in pressure cells on Scheme 6 are shown in Figures 7.5 and 7.6. Cell A was installed over the tunnel centre line and cell B offset by 1.5m – Figure 4.5. The pore pressure response in both cells did not stabilise after installation and will not be discussed further. Total horizontal stress readings stabilised at approximately 400kPa – about 70kPa greater than the total horizontal stresses from the pressuremeter tests at the same depths (Table 4.5). In stiff clays Teddl et al (1984) suggest push-in pressure cells may over-read by approximately  $0.5s_u$ , whereas more recent work by Ryley and Carder (1995) recommend  $0.8s_u$  as a best-fit correction. The undrained strength of the London clay in Scheme 6 was about 90 - 100kPa (Table 4.5) and the over-read correction of  $0.8s_u$  gives good agreement between the pressure cell readings and pressuremeter tests. Cell A, intended to be just above the crown of the tunnel, was exposed at the face having been installed at the incorrect level (Figure 4.5) - it recorded a drop of about 240kPa to a final reading of 160kPa. As the shield approached, both cells showed a small increase in stress of about 18kPa which may be due to the soil arching in front of the tunnel excavation. Readings from cell B – offset by 1.5m – showed an immediate reduction in stress of 60kPa as the face passed. Stress decreased further with time to 215kPa at the final set of readings – about half the pre-tunnelling values. Elastic analysis of the stresses around an open bore - Poulos and Davies (1991) - with initial vertical and horizontal stresses of 190kPa and 330kPa respectively, predicts a drop in horizontal stress at the location of the cell of 167kPa. The greater drop recorded in practice may be the result of local plastic yielding around the opening.

The push-in pressure cells were also used in the soft clay of Scheme 9. Results are shown in Figure 7.7. Cell A was installed over the centre line just above the crown at a depth of 5m. Cell B, at 6.5m deep, and the piezometer were offset by 1.5m on opposite sides of the centre line – Figure 4.16. Generally cell and piezometer readings were reasonably stable soon after installation. At cell A, total horizontal stress,  $\sigma_h$ , was 160kPa prior to tunnelling, the corresponding pore pressure,  $u$ , 43kPa and resulting effective stress,  $\sigma'_h$ , 117kPa. Cell B at about 6.5m depth, gave pre-tunnelling readings  $\sigma_h$  of 200kPa,  $u$  at 35kPa and  $\sigma'_h$ , 165kPa.

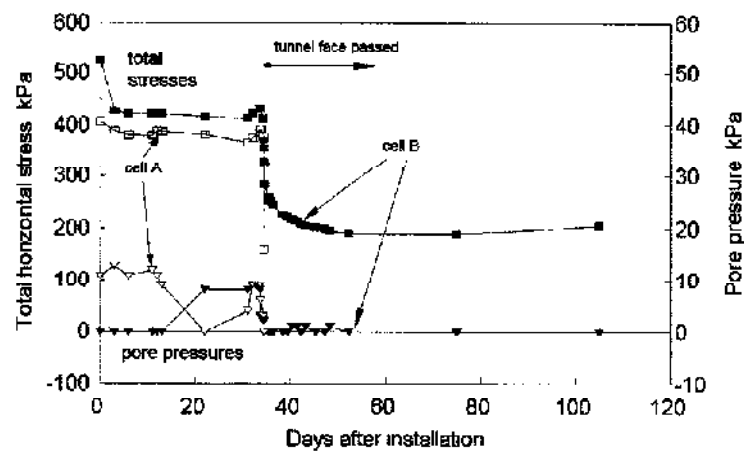


**Figure 7.5 Pressure cell readings during Scheme 6.**

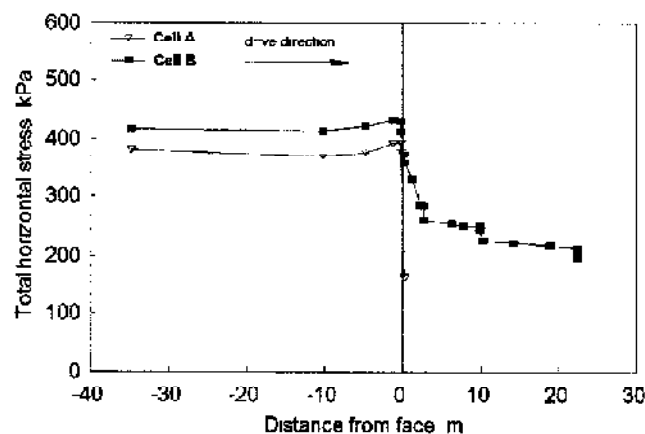


**Figure 7.6 Variation in total horizontal stresses against approximate distance from face during Scheme 6.**

Overconsolidation ratios (OCRs) of natural soft clays are typically in the range of 1 to 3.5. In the soft clay at nearby Tilbury, De Moor and Taylor (1991) found  $K_0$  varied from about 0.5 to 1.0 for the above range of OCRs in similar ground at a similar depth. The variation of pre-tunnelling  $\sigma'_h$  with depth recorded by the pressure cells is compared with the  $K_0=1$  line (based on overburden stress) in Figure 7.8. The overburden stress was calculated using an average bulk unit weight of  $13.3 \text{ kN/m}^3$  measured in the clay between 3m and 8m depth during triaxial testing of 100mm diameter samples. Densities recorded over this depth varied between  $1.15 \text{ Mg/m}^3$  to  $1.63 \text{ Mg/m}^3$ . Measured values of  $\sigma'_h$  in the lightly overconsolidated soil indicate  $K_0$  values far greater than unity and it is suggested therefore that the spade cells were

over-reading horizontal stresses in the soft clay. There are no data to compare the values to stresses measured using other techniques such as self-boring pressuremeters and empirical corrections cannot be made. It is suggested that these readings are best interpreted as change in stresses (i.e.  $\sigma_h/\sigma_{h,0}$ , where  $\sigma_{h,0}$  is the initial stabilised value), Figure 7.9. Just over the crown, cell A, there was a significant increase in total horizontal stress as the machine approached and passed the instrumented section, due to excess pore pressures. There were small increases in effective horizontal stress as the face passed which persisted until the end of construction. Adjacent to the tunnel at about axis level, cell B, positive pore pressures were small and as the machine passed, total and effective horizontal stress readings show an immediate and permanent reduction. The 22kPa decrease in  $\sigma'_h$  may be an over response as suggested above.

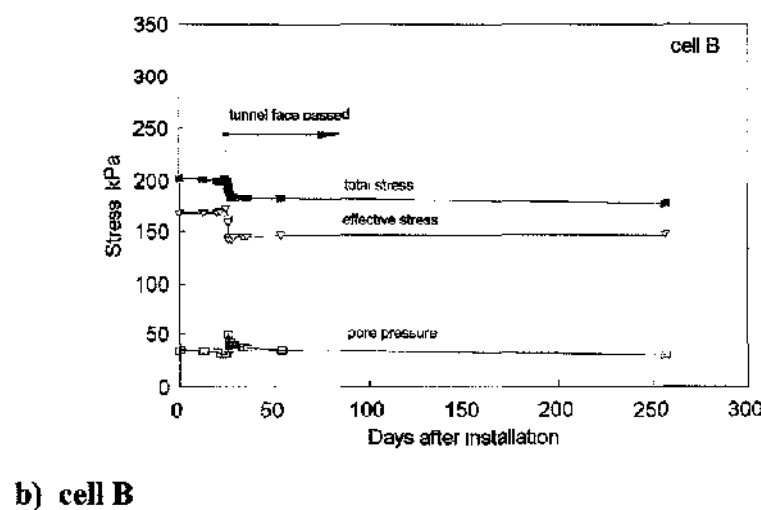
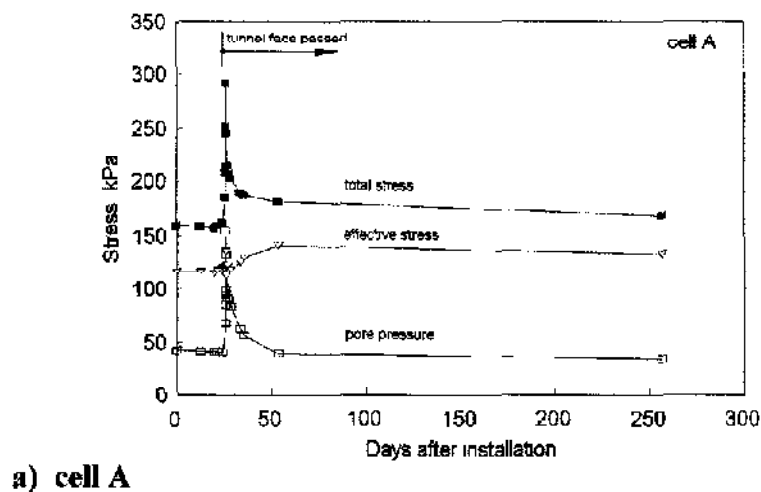
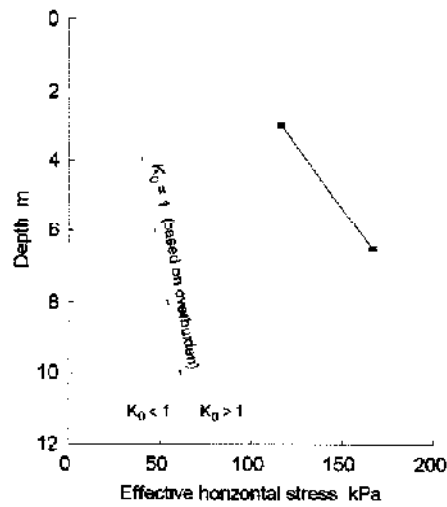
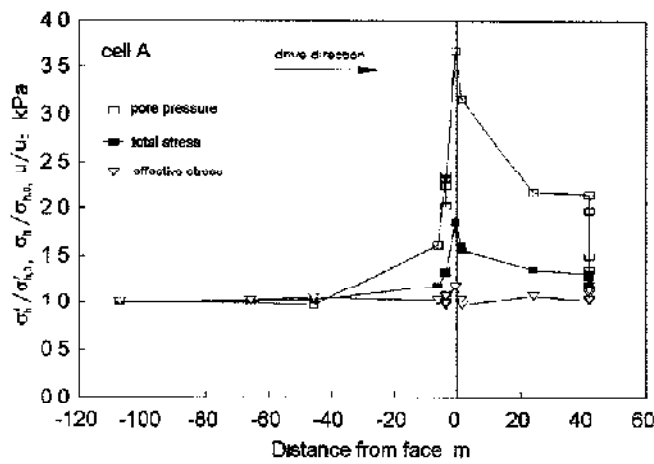


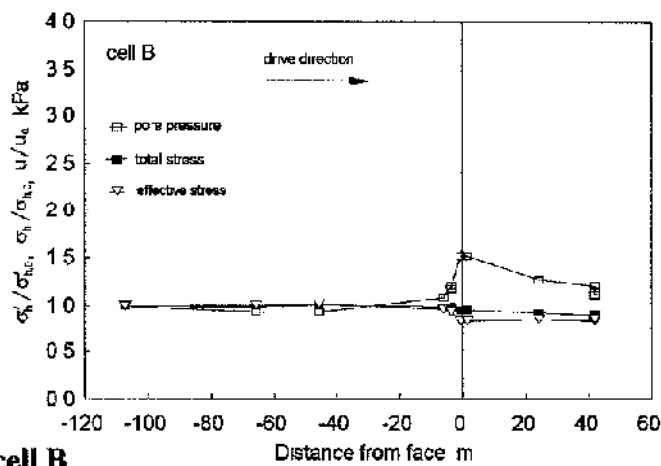
Figure 7.7 Pressure cell readings during Scheme 9.



**Figure 7.8** Effective horizontal stress variation with depth – pre-tunnelling, Scheme 9.



**a) cell A**



**b) cell B**

**Figure 7.9** Variation in pressure cell readings with tunnel progress in Scheme 9.

Fluctuations in pore pressure, brought about by tunnelling activities, gave rise to stress changes around the face. Figure 7.10 illustrates the development of excess pore pressures as the tunnel progressed. The largest increase of 115kPa was measured above the crown; piezometers adjacent to the tunnel recorded excess pressures of between 10kPa to 20kPa. Figure 7.11 shows the pore pressure variation with depth. Pre-tunnelling pore pressures at axis level and below the tunnel were close to hydrostatic pressures. Above the tunnel readings indicate pressures greater than the hydrostatic distribution, perhaps due to a perched water table in the clay. The final set of readings show dissipation of the excess pore pressures was fully complete seven months after construction, Figure 7.12.

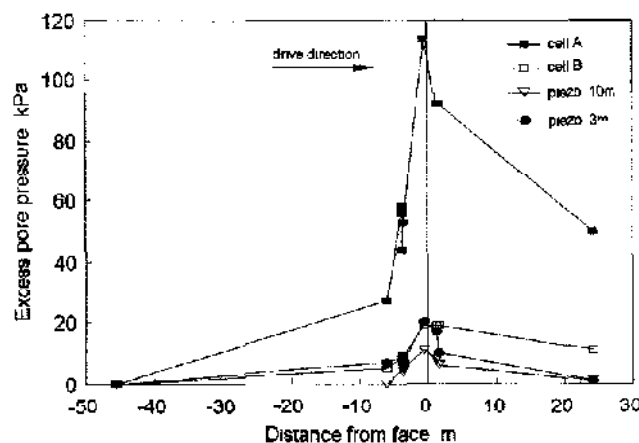


**Figure 7.10** Variation of excess pore pressure with tunnel progress in Scheme 9.

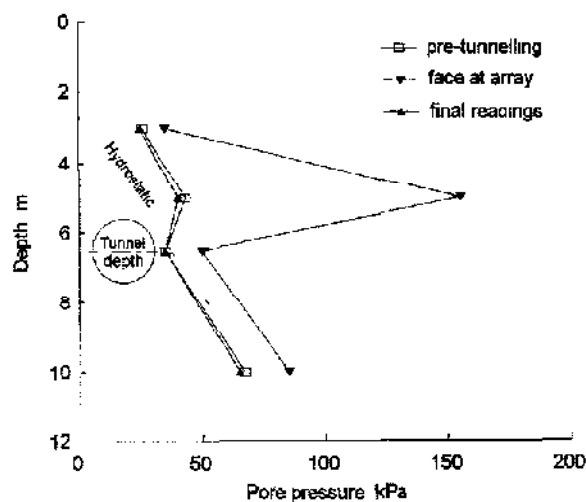


**Figure 7.11** Variation of total pore pressure with depth in Scheme 9.



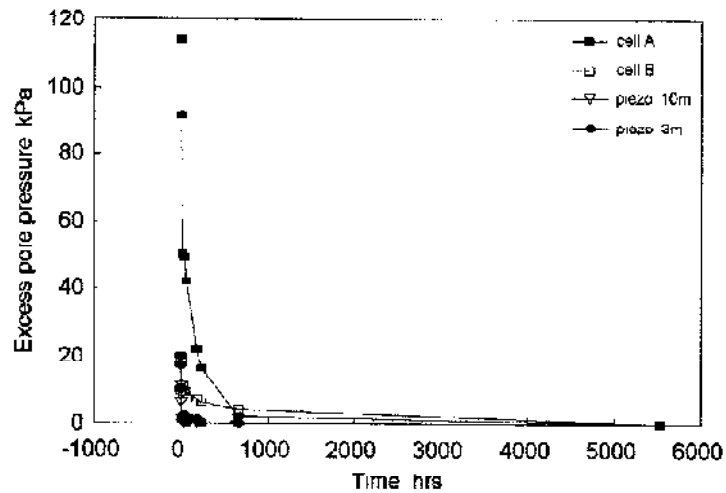


**Figure 7.12 Pore pressure dissipation in Scheme 9.**

### 7.3.2 Surface settlements

#### 7.3.2.1 Scheme 6

Surface settlement measurements in Scheme 6 were made by precise levelling of studs driven into the road pavement as it was not possible to install the ground movement monitoring stations shown in Figure 2 18. The surface settlements shown in Figure 7 13 therefore show movement of the road pavement. The settlements probably do not represent true ground movement since the stiff pavement may, to some degree, span over the actual settlement trough.

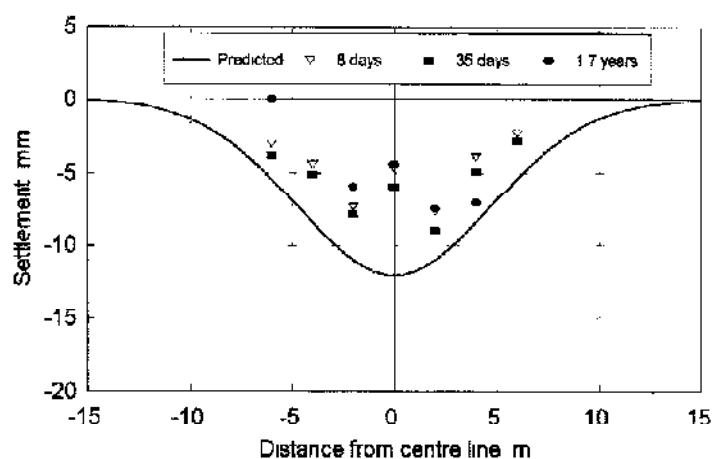


**Figure 7.13 Predicted and measured surface settlements after construction on Scheme 6.**

The overbreak in this scheme was provided by the miner excavating a clearance around the shield varying from about 10mm at the crown to a maximum of about 50mm

at the shoulder and zero at the invert. The average overbreak value is taken as 25mm. Using equations (7.1) to (7.8) gives the predicted profile shown in Figure 7.13. The value of  $t$  at the surface is 4.76m, assuming the ground to be cohesive (there is in practice a significant layer of sandy gravel above the London Clay), and the maximum predicted settlement is 12mm. Measured values taken eight days after completion of the tunnel indicate a similar settlement profile, except that the centre line value is rather less than those either side, though all lie within the calculated settlement profile. The final set of measurements - taken almost two years after completion - show a consistent profile but with levels slightly higher than expected. This can probably be attributed to local movements in the road pavement, either by traffic damage or temperature and seasonal movement.

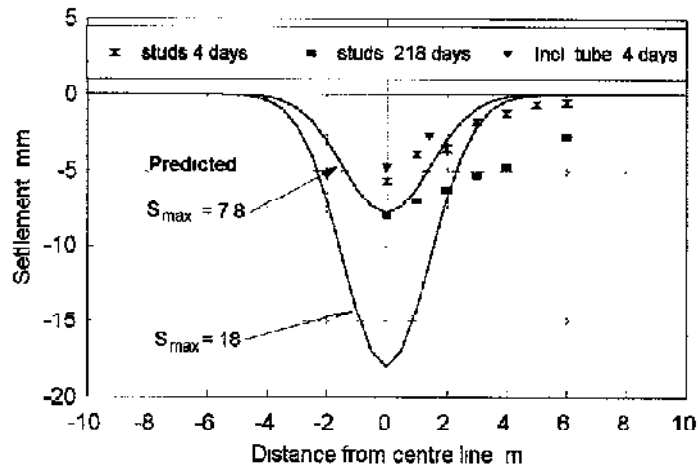
### 7.3.2.2 Scheme 7

Figure 7.14 shows the measured surface settlements and two predicted profiles. As in Scheme 6 measurements were made on studs (road nails) and not settlement stations due to the pipe jack location. The profile with  $S_{\max} = 18\text{mm}$  assumes that the full overbreak volume between cutter diameter and pipe outer diameter is converted into settlement. Observed movements four days after tunnel completion show a maximum settlement of only 6mm over the centre line but a distance to the point of inflexion close to the predicted value of 1.45m. There are two probable factors accounting for the discrepancy in magnitude of settlement:

- i) Shearing of the soil during settlement will cause some dilation of the dense sand resulting in the volume of the settlement trough being less than the overbreak volume.
- ii) The bentonite slurry gel - used as a lubricant - prevents the ground completely collapsing onto the pipes.

An alternative calculation, giving  $S_{\max} = 7.8\text{mm}$ , assumes that the difference in diameter between cutter and shield gives the overbreak volume. Allowing for some dilation, this alternative predicted profile is in reasonable agreement with the observations made four days after completion. However, the calculation leaves some doubt over whether settlements continue as the bentonite/soil gel consolidates under

pressure from the surrounding soil. In this case, observations made two hundred and eighteen days after completion show a further settlement over the centre line of about 2mm. The profile however, is much flatter than predicted probably due to the stiff road pavement. More recent measurements indicate no further increase in settlement.



**Figure 7.14** Predicted and measured surface settlements after construction on Scheme 7.

### 7.3.2.3 Scheme 8

Surface settlement profiles from Scheme 3 are plotted in Figure 7.15 with two predicted profiles. Measurements were taken on both road nails and settlement stations.

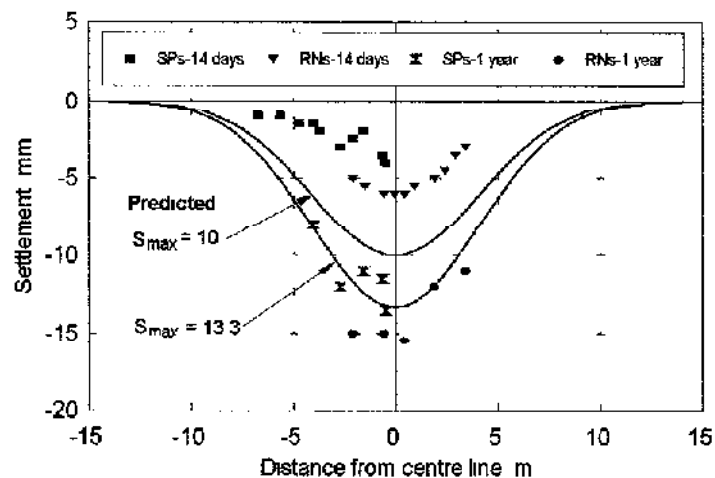


**Figure 7.15** Predicted and measured surface settlements after construction on Scheme 8.

The value of  $S_{max} = 13.3\text{mm}$  assumes full closure of the overbreak between cutter and pipes whereas the value of  $S_{max} = 10\text{mm}$  results from closure between cutter and shield, assuming that the remaining annulus is held open by bentonite slurry pressure. Both profiles are larger than early measurements, though the shape of the settlement trough is well predicted. Surprisingly, the settlements on the road nails were greater than on the settlement monitoring stations founded beneath the pavement. A more recent set of measurements show a less well defined trough pattern with settlements close to the predicted profile where full overbreak closure is assumed

#### 7.3.2.4 Scheme 9

Observed surface settlements with predicted profiles are shown in Figure 7.16. Erroneous readings and difficulties in accessing the settlement stations (located within a fenced off plot) has unfortunately resulted in only one set of reliable measurements. As with the calculations for Schemes 7 and 8, the deeper profile, where  $S_{max} = 11.5\text{mm}$ , assumes full overbreak closure. With partial closure,  $S_{max} = 5.8\text{mm}$ , the predicted profile matches almost exactly the observed settlements which might suggest the presence of pressurised slurry is preventing full short-term closure of the overbreak.

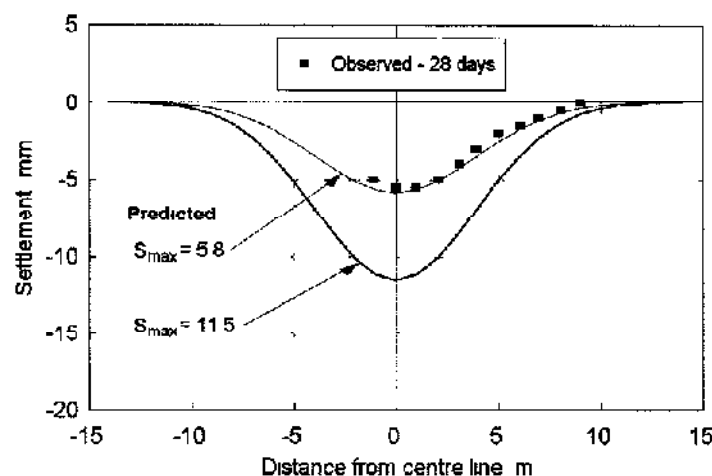


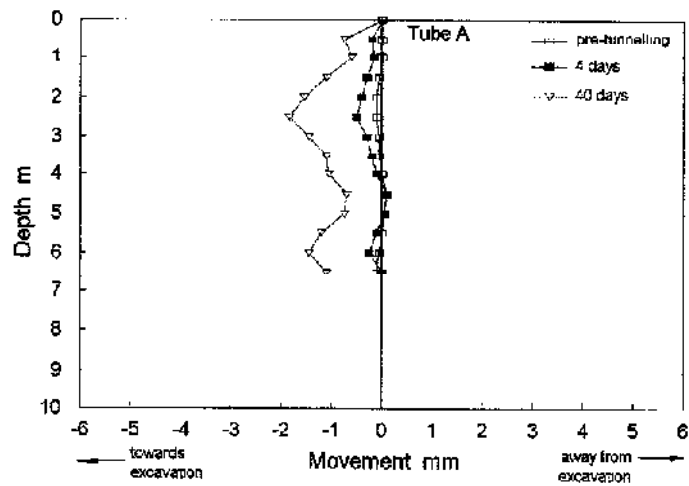
**Figure 7.16** Predicted and measured surface settlements after construction on Scheme 9.

### 7.3.3 Subsurface movements

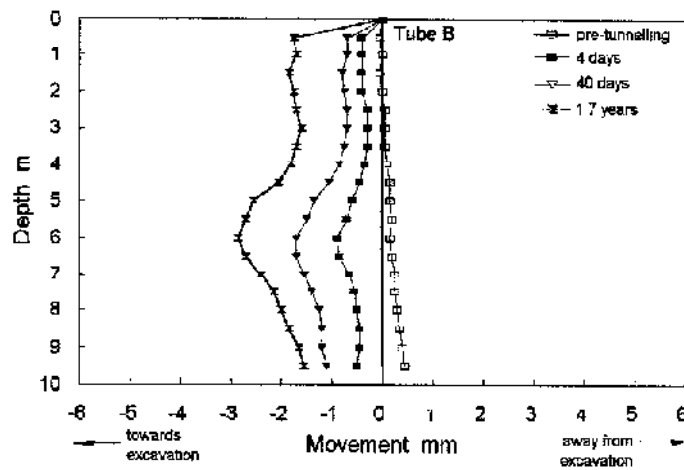
#### 7.3.3.1 Scheme 6

Longitudinal and transverse inclinometer access tube profiles are plotted in Figures 7.17 and 7.18 respectively. It should be noted that due to financial constraints, access tubes (in all four schemes) were not adequately embedded into strata sufficiently deep to prevent translation and/or rotation – all profiles are taken relative to the top of the tubes (restrained by grout and pavements). Maximum longitudinal displacements of about 3mm into the excavation were recorded 1.7 years after construction at approximately one tunnel diameter above the crown. Transverse movements are small, the maximum displacement of 5mm was observed just above the tunnel crown, Figure 7.19. Data from the access tube profiles and movement of the magnetic settlement plates have been combined to give the transverse displacement vectors shown in Figure 7.20. Maximum settlements of 11mm were measured above the tunnel crown.

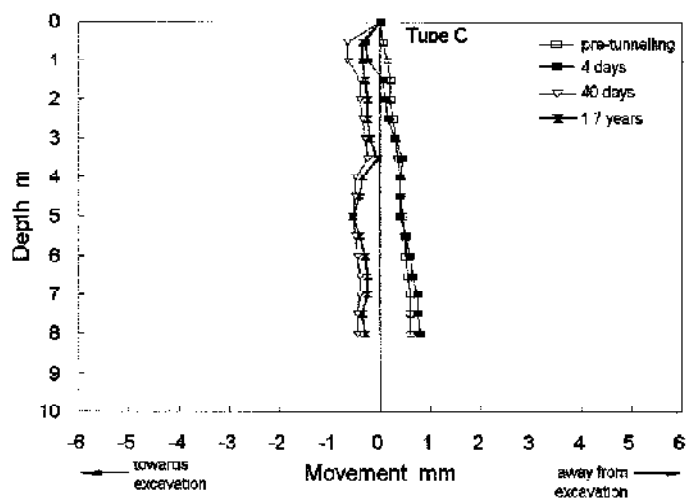
Measurements of subsurface ground movements during construction of five London Underground tunnels of approximately 4m in diameter, at depths of 20-29m, in London Clay were presented in dimensionless form by Mair and Taylor (1993), Figure 7.21. Vertical ground movements were measured at different distances above the tunnel centre line and horizontal movements were measured at various positions at tunnel axis level. Data are reasonably consistent and are in general agreement with linear plots. The gradient of the lines, which are almost parallel, is consistent with a  $G/s_u$  ratio of about 100, thus assumes idealised linear elastic-perfectly plastic soil behaviour. Figure 7.22 shows Scheme 6 subsurface movements plotted in the same dimensionless form. The gradient of lines through these data is similar to those for the deeper and larger tunnels. Assuming an undrained shear strength of about 100kPa at the depth of the pipe jack, the stability ratio  $\gamma z/s_u$  is 1.7, compared with an average value of about 2.5 for the deeper tunnels. Taking this into account, and assuming a complete unloading of the cylindrical cavity in the case of the pipe jack, a  $G/s_u$  ratio of about 80 is implied by the data in Figure 7.22. This compares favourably with the  $G/s_u$  ratio of 100 deduced from the movements around larger and deeper tunnels in London Clay.



a) Tube A

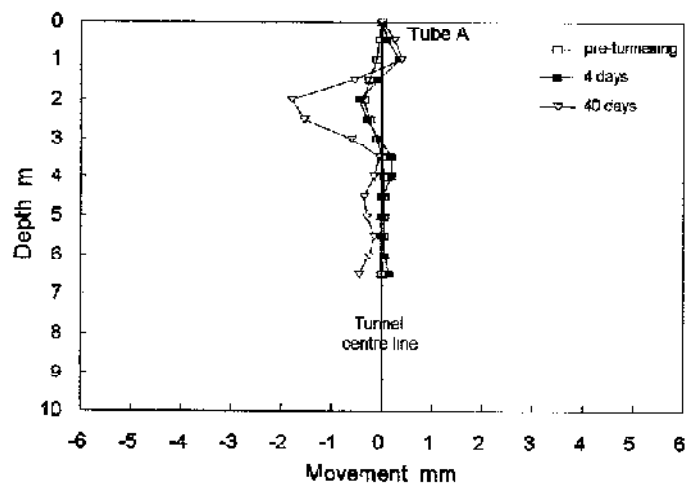


b) Tube B

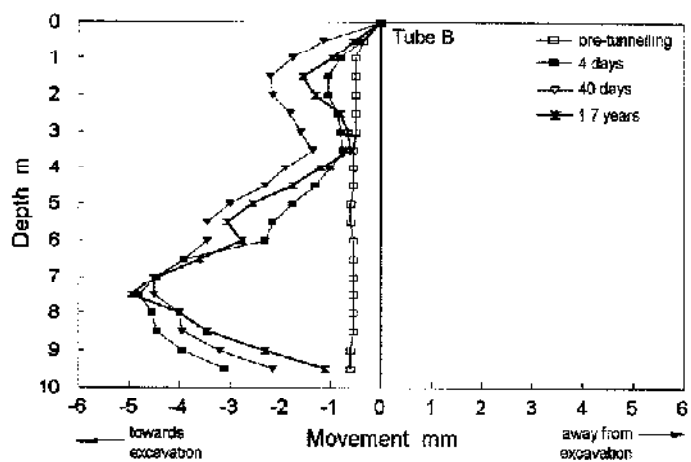


c) Tube C

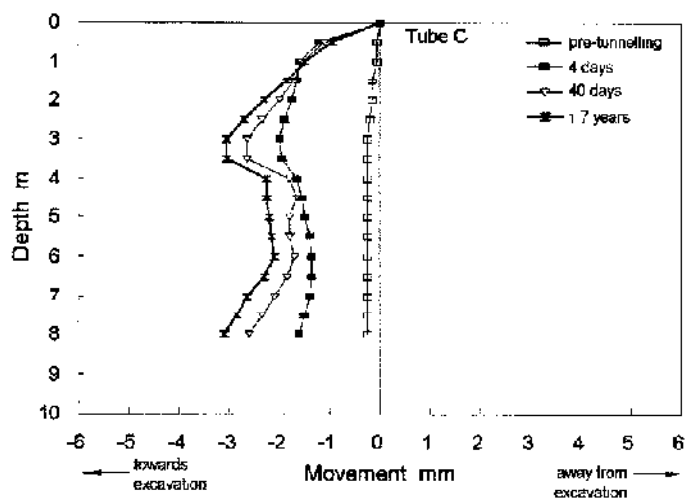
Figure 7.17 Longitudinal inclinometer access tube profiles on Scheme 6.



a) Tube A



b) Tube B



c) Tube C

Figure 7.18 Transverse inclinometer access tube profiles on Scheme 6.

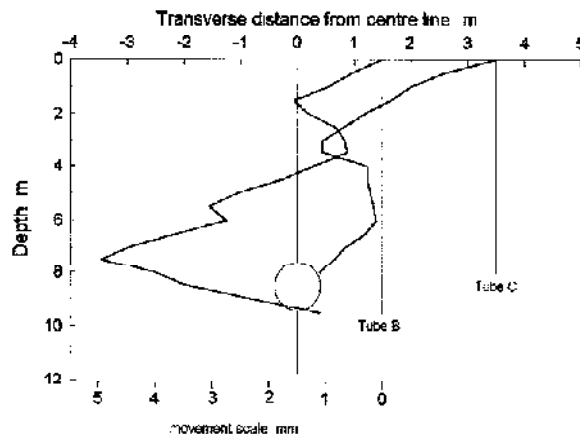


Figure 7.19 Maximum transverse access tube deformation at Scheme 6.

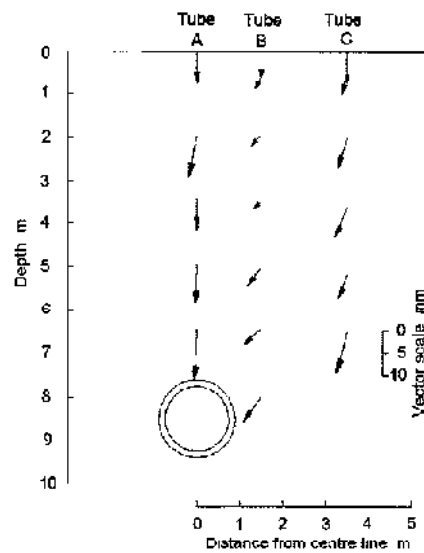


Figure 7.20 Displacement vectors 40 days after construction at Scheme 6.

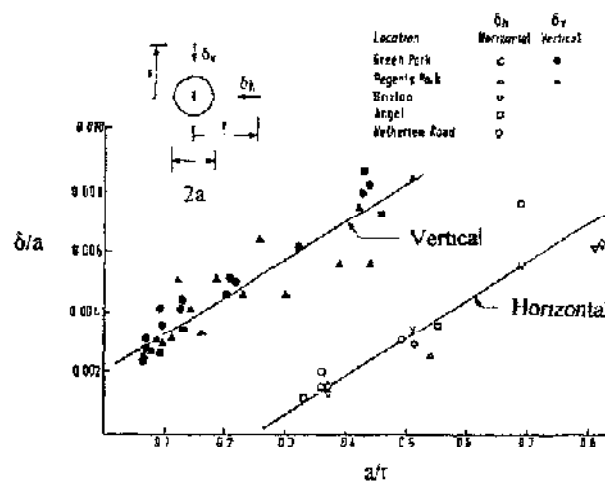
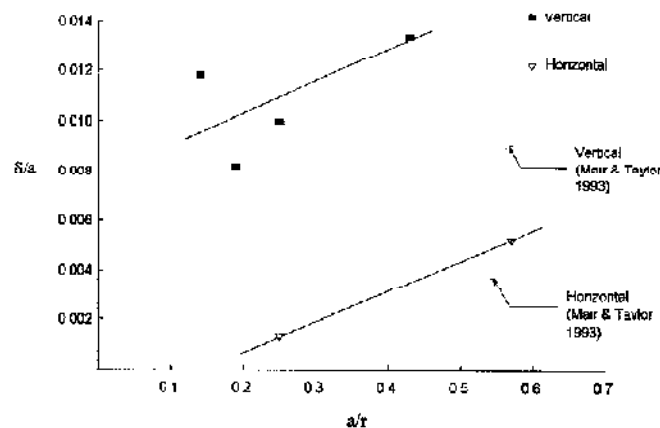


Figure 7.21 Vertical and horizontal subsurface movements in the vicinity of 4m diameter tunnels in London Clay at depths of 20-29m (after Mair and Taylor, 1993).





**Figure 7.22 Comparison of vertical and horizontal subsurface movements around the Scheme 6 drive with deeper 4m diameter tunnels in London clay.**

### 7.3.3.2 Scheme 7

Deformation of the inclinometer access tubes at Scheme 7 was negligible – typically less than 1mm – and showed no consistent pattern, Figures 7.23 and 7.24. Movements of the magnetic settlement plates are shown as displacement vectors in Figure 7.25. A considerable variation in plate movement was measured along the access tubes from 2mm (about the acceptable limit of accuracy for this type of measurement) to 8mm. The vertical displacement vectors are consistent with a relatively narrow displacement zone in the sand that can be attributed to a loosening of soil above the tunnel crown.

### 7.3.3.3 Scheme 8

Access tube profiles at Scheme 8 are plotted in Figures 7.26 and 7.27. It is suggested that the maximum longitudinal measurements indicated at tube C, Figure 7.26(c), are erroneous due to movement of the tube top. A translation of 2 to 3mm would probably reflect more realistic displacements of 0-1mm towards the excavation. Longitudinal displacement at tubes A and B is small, reaching a maximum of about 1.5mm at the tunnel axis level. Maximum transverse displacement is illustrated in Figure 7.28. Transverse movement is small and reaches a maximum of about 3mm at the level of the tunnel. Displacement vectors are shown in Figure 7.29: settlement magnets closest to the tunnel typically settle by about 5mm. It is not clear if movements were complete by the final set of readings. During a visit to the scheme one year after construction it was discovered that the tubes had been damaged during site clearance preventing longer term measurements being made.

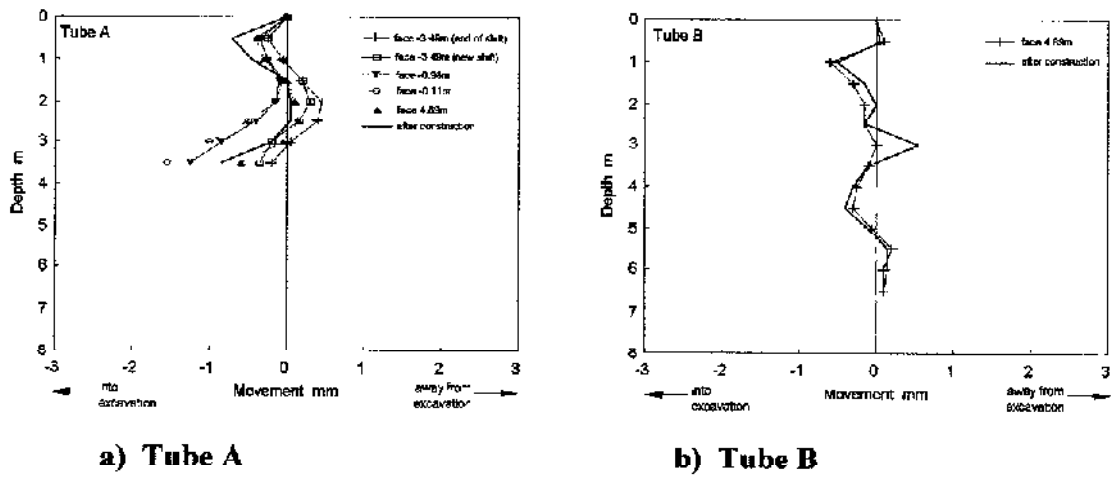


Figure 7.23 Longitudinal inclinometer access tube profiles on Scheme 7.

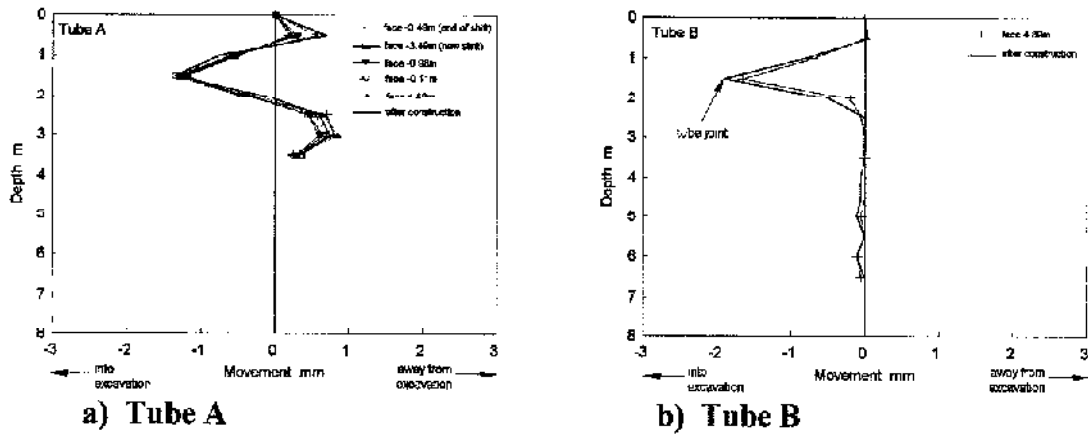


Figure 7.24 Transverse inclinometer access tube profiles on Scheme 7.

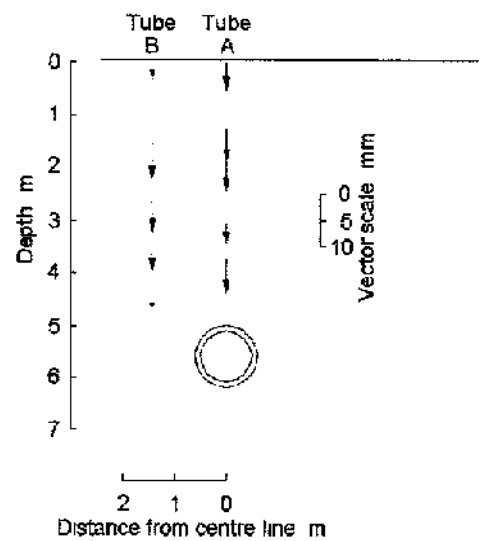


Figure 7.25 Displacement vectors after construction at Scheme 7.

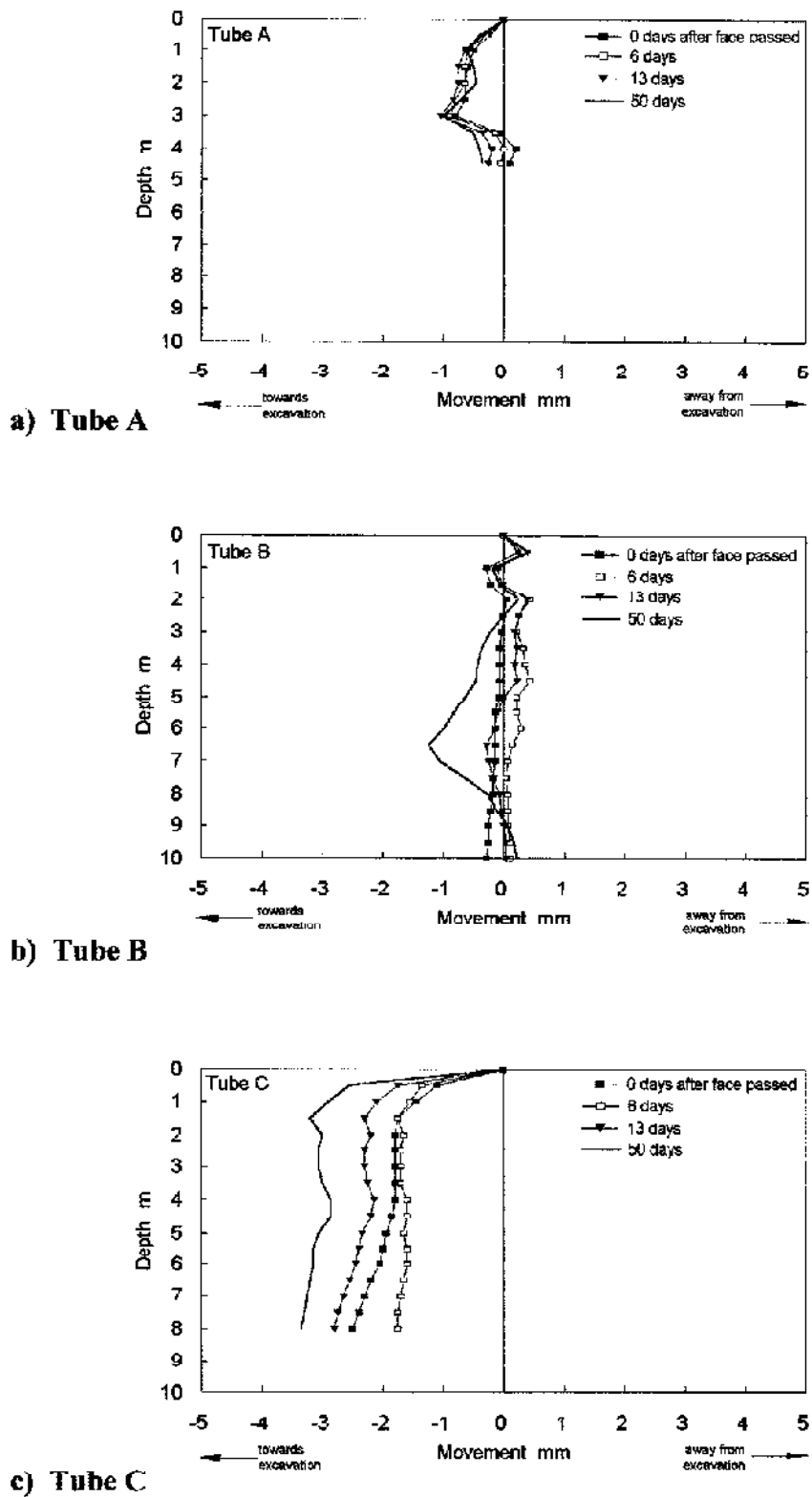
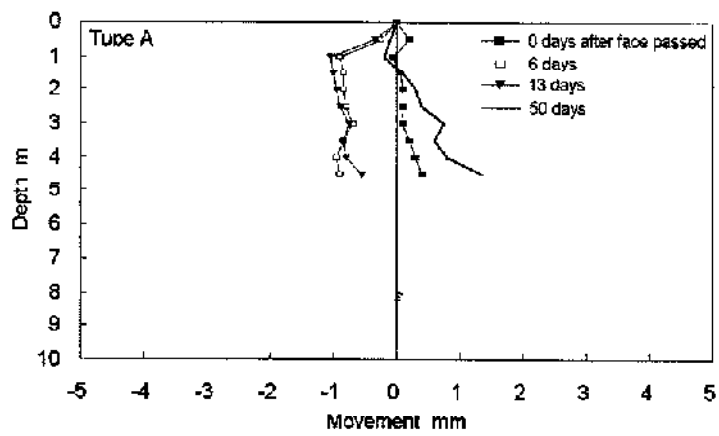
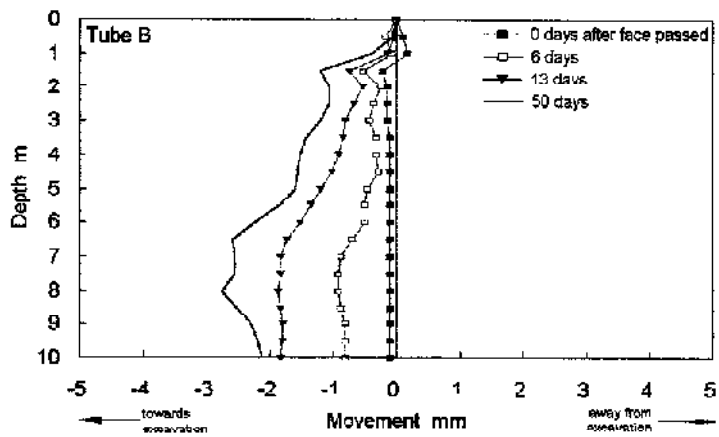


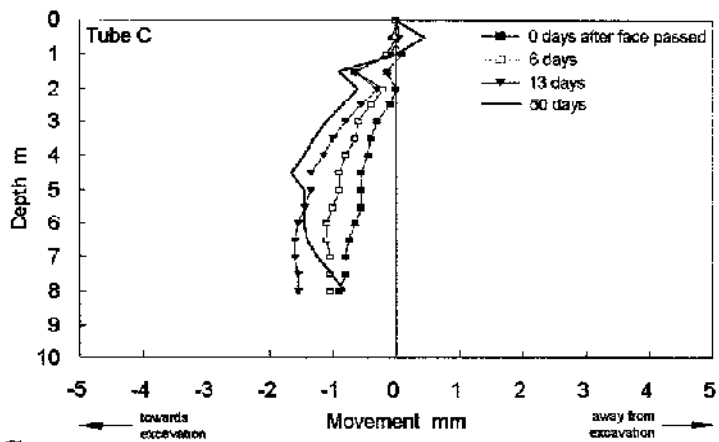
Figure 7.26 Longitudinal inclinometer access tube profiles on Scheme 8.



a) Tube A



b) Tube B



c) Tube C

Figure 7.27 Transverse inclinometer access tube profiles on Scheme 8.

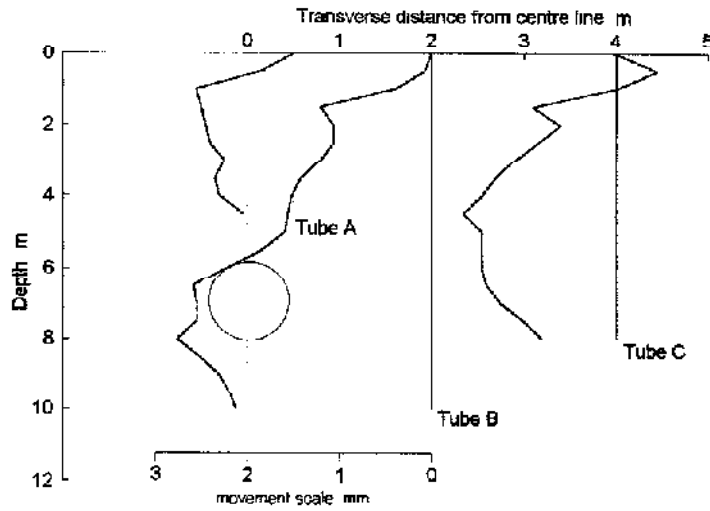


**Figure 7.28** Maximum transverse access tube deformation at Scheme 8.

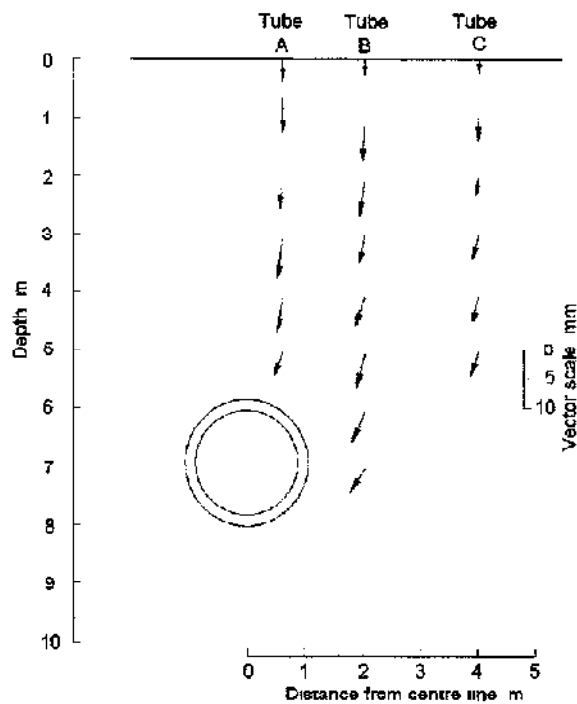


**Figure 7.29** Displacement vectors after construction at Scheme 8.

Detailed measurements of longitudinal subsurface movements were made using an inclinometer access tube containing ten electro-levels, Figure 4 13. The 10m

long tube was installed over the centre line of the 1800mm pipe jack at a depth of about 6m, from 0.5 to 1.0m above the crown. Datum readings were taken seven days after the electro-levels were installed with the face about 40m from the tube. Continuous measurements were made throughout the remaining excavation period and for seventeen days after drive completion; contractual and logistical problems prevented a further period of monitoring for long-term deformation. By integrating the electro-level readings, the continuous change in tube profile has been calculated. A selection of tube profiles as the tunnel advanced are plotted and compared to predicted profiles – using equations (7.9) and (7.10) – in Figure 7.30. The predicted profile assumes closure between cutter and shield, the remaining annulus being held open by bentonite slurry pressure, and is equivalent to a face loss of 1.5-2.0%. Agreement between the predicted profile and measurements is generally very good in shape and magnitude particularly as the trough begins to develop at the tube location, Figures 7.30(c) to (e). As the face approaches the shaft measured settlements are between 2-4mm less than the predicted profile, Figures 7.30(h) to (k), and a two-stage profile appears to have developed. There is a kink in the profile at about 7m from the shaft which can be attributed to consolidation settlement over the weekend 2-5 September. Figure 7.31 shows the consolidation settlement measured between 4:00p.m. on 2 September and 7:00a.m. on 5 September. The face was 8.8m from the shaft and consolidation has increased settlements at 8, 9 and 10m over those that would have occurred had excavation continued at the normal rate. During the excavation standstill settlements above the shield increased by

- i) 1.3mm at the tube end,
- ii) 0.7mm at 9m from the shaft; and
- iii) 0.1mm at 8m from the shaft.

Following completion of the pipe jack, settlement continued and at the final set of readings, taken 17 days after construction, measured settlements agree well with those predicted, Figure 7.30(l).

The longitudinal subsurface settlements show a mechanism largely following four phases of ground displacement: initial displacement, shield passing displacement, tail void displacement and consolidation settlement.

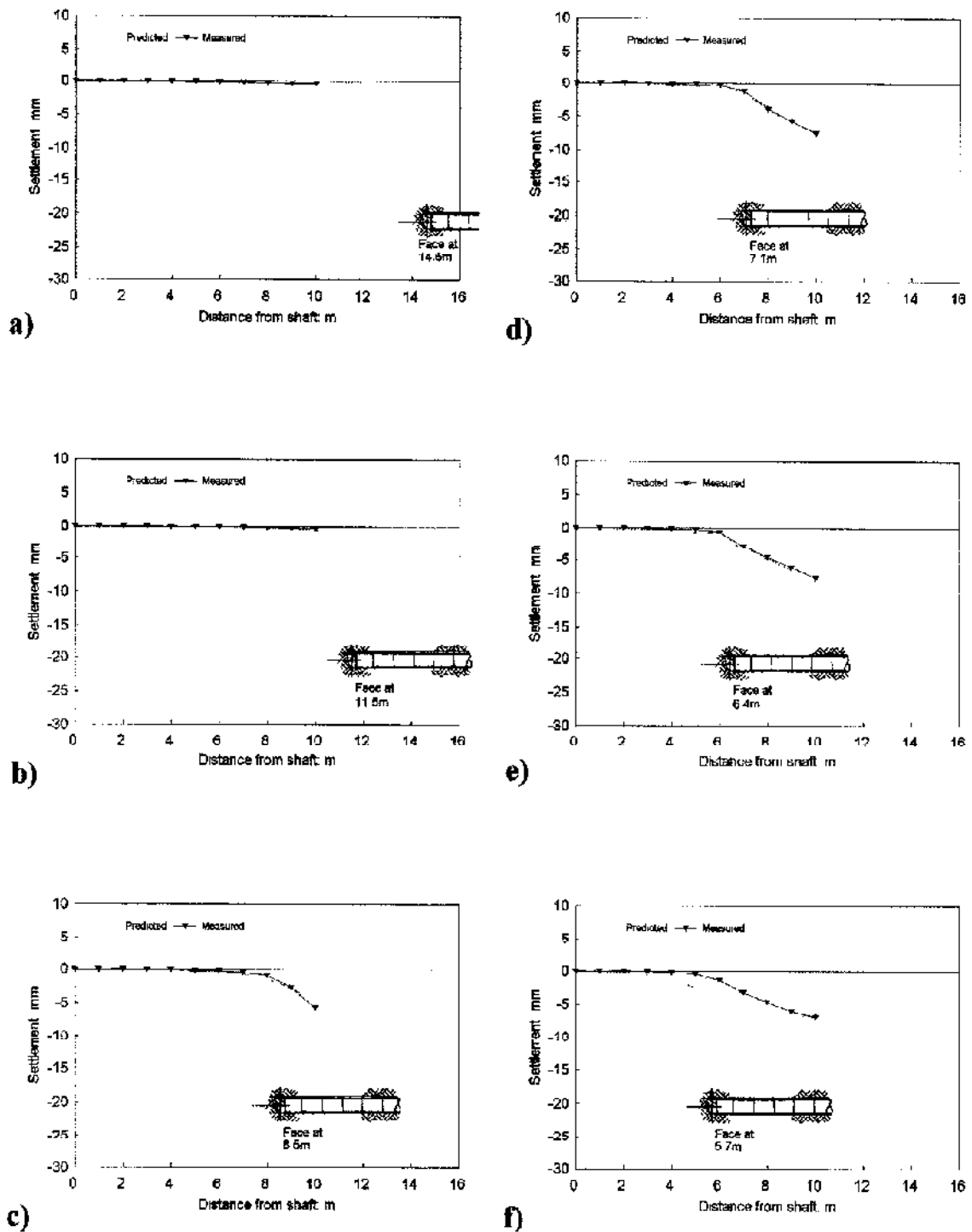


Figure 7.30 Sub-surface longitudinal settlement profiles at Scheme 8 – (a) to (f).

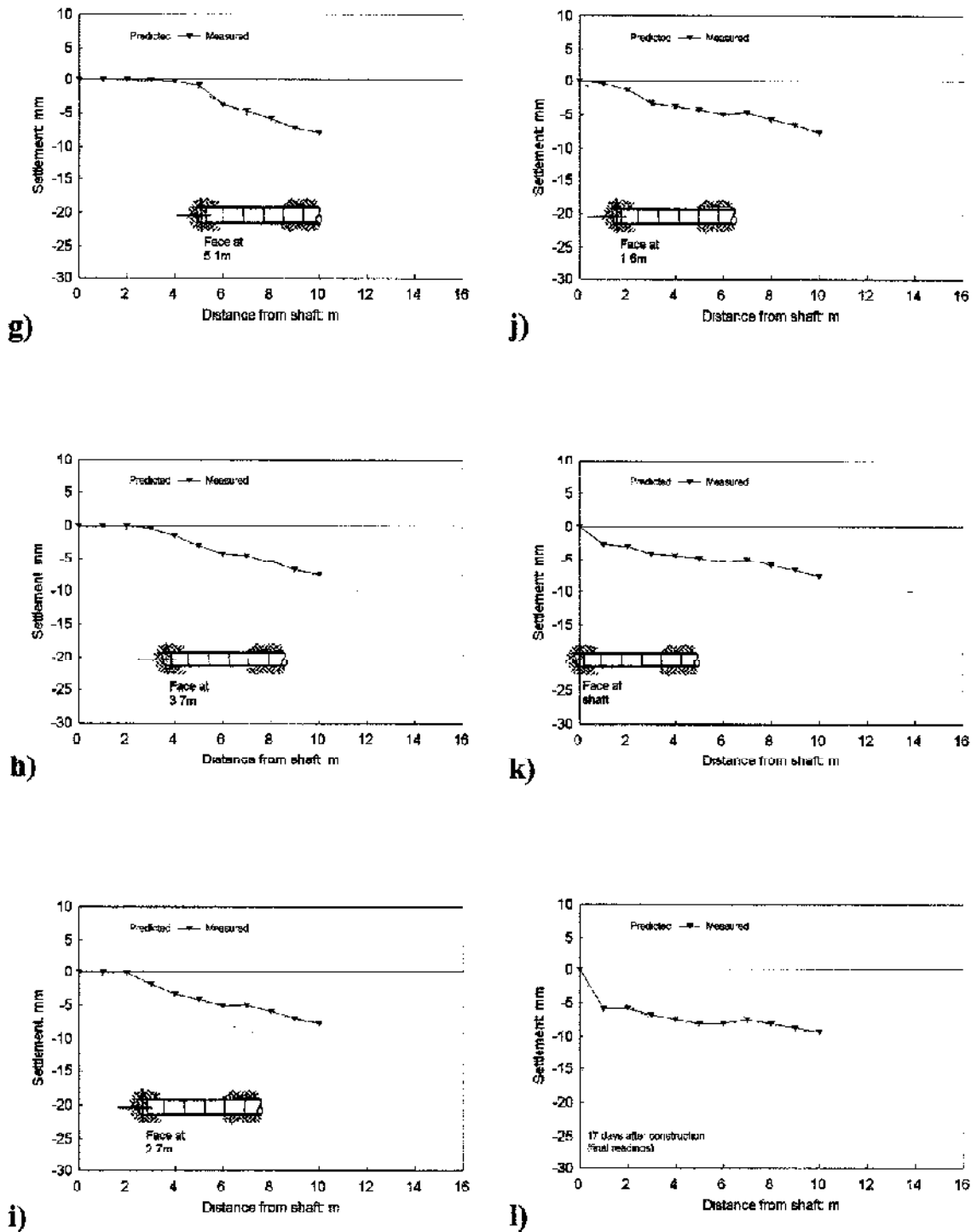
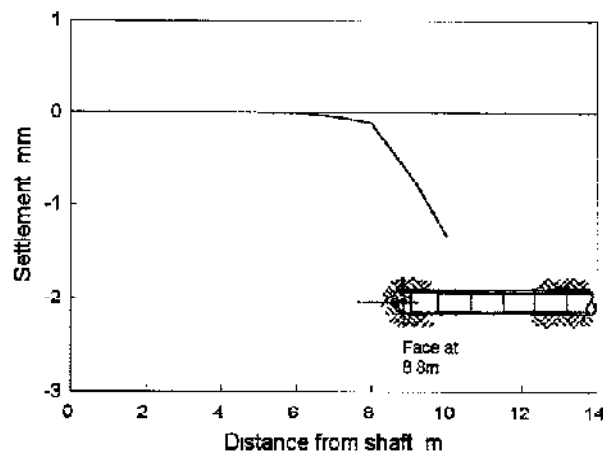


Figure 7.30 Sub-surface longitudinal settlement profiles at Scheme 8 – (g) to (l).





**Figure 7.31 Consolidation settlement of the electro-level tube during the weekend of 2-5 September at Scheme 8.**

#### I Initial displacement

Where the face of the shield machine has not reached the instrument location, displacements due to elastic unloading of stresses near the excavation can occur. Ground loss due to movement at the open-type shield here was negligible because the stiff to very stiff boulder clay at the face was highly stable. Initial settlements therefore were insignificant at 0.5mm or less - Figures 7.30(a) and (b)

#### II Shield passing displacement

The second phase is where excavation is taking place and the shield is passing the instruments or monitoring station in question. During this phase a void or overbreak is created between the surrounding ground and the shield. Settlements occurring during this phase in Scheme 8 are taken as those immediately above the shield and are typically 2 to 7mm

#### III Loss behind the shield

The third phase is where the shield has passed the location of interest and a greater void is created between the surrounding soil and the tunnel lining. The jacking pipes were 20mm smaller in diameter than the shield resulting in an overbreak between tunnel bore and pipes of 10mm on radius. During the jacking process bentonite slurry was injected into the void to prevent ground closure and reduce skin

friction. The shield was about 6m long, therefore once the cutterhead was 4m or less from the shaft wall – Figures 7.30(h) to (k) – settlements due to the additional ground loss behind the machine might be expected. There does not however appear to be any settlement of this type, probably due the bentonite slurry filling the void

#### IV Consolidation

The end of excavation marks the commencement of the final settlement phase where creep deformation or consolidation of cohesive soil occurs. Figure 7.32 shows continued settlements of 2 to 3mm between the period of cessation of excavation on 5 September and the final readings taken on 22 September. Consolidation settlements at individual electro-levels are presented in Figure 7.33. The smaller consolidation settlements at the end section of the tube (8, 9 and 10m) can be attributed to the consolidation that occurred during the weekend standstill of 2-5 September. The settlements are 0.5 to 1mm less than elsewhere along the tube which is about the same magnitude as the weekend consolidation settlement, confirming that settlements at all points are tending towards the same long-term value. Consolidation settlement variation with logarithm time is shown in Figure 7.34, and indicates a linear relationship. Extrapolation of the log-linear relation from 10hrs to above 100yrs suggests maximum further settlements of only 3 to 4mm

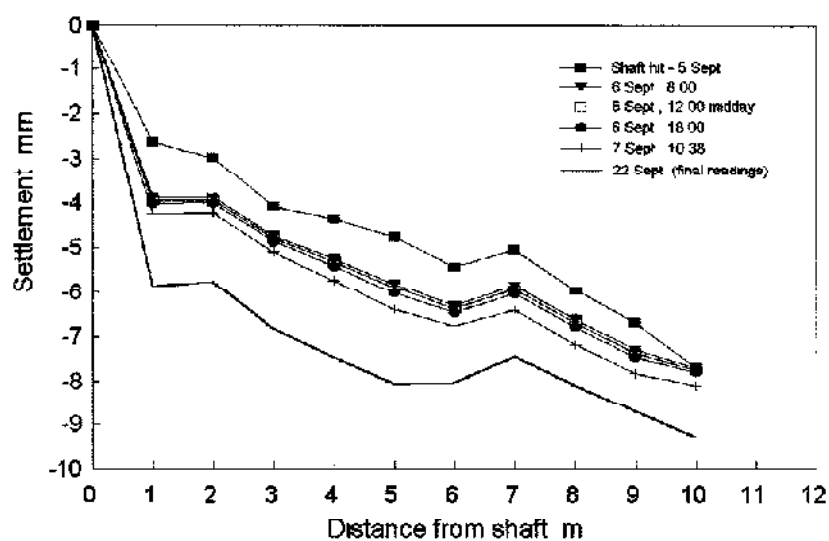


Figure 7.32 Settlement of the electro-level tube after construction at Scheme 8.

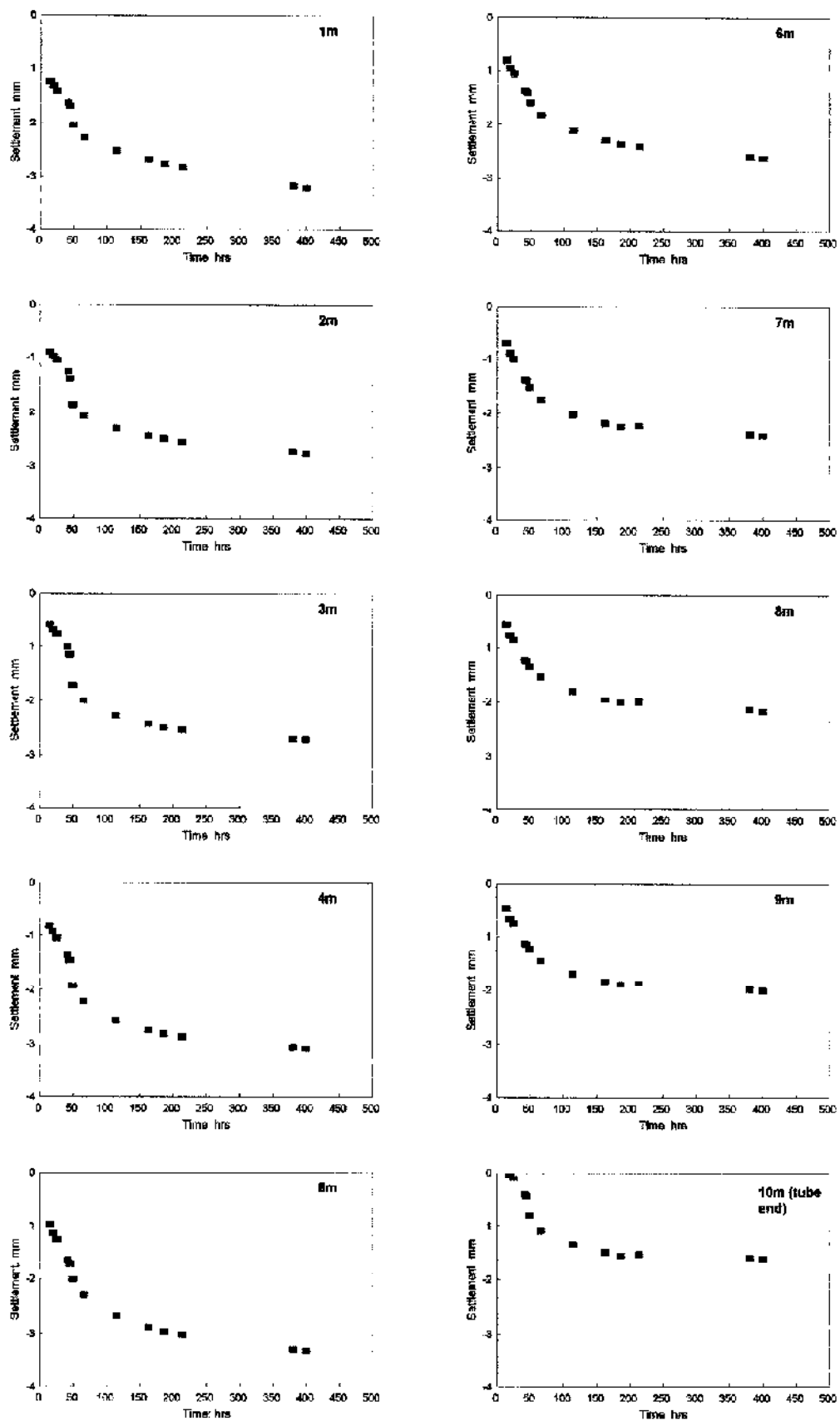
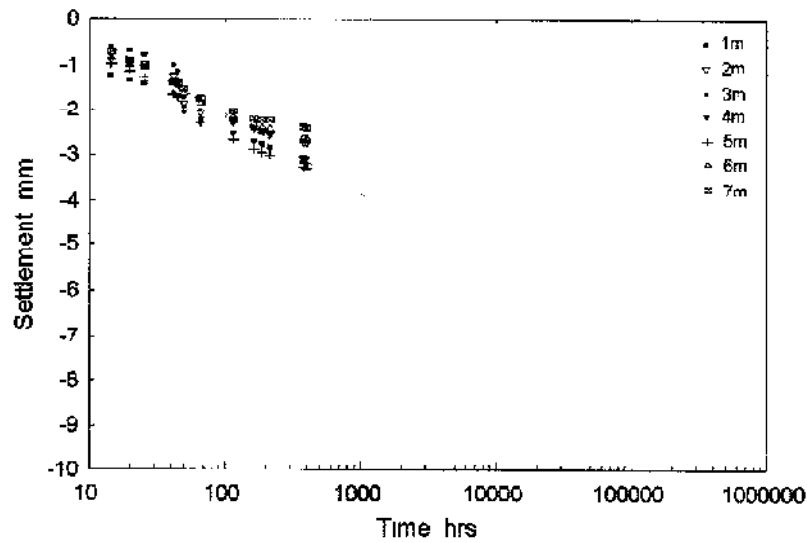
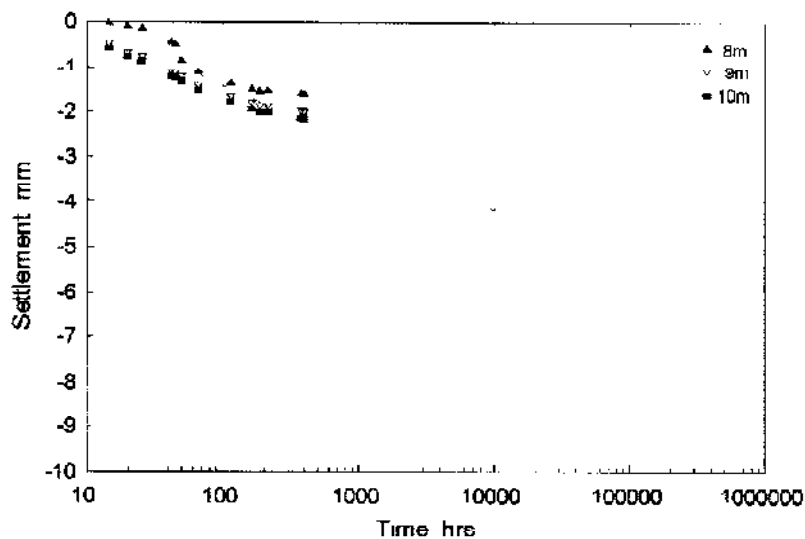


Figure 7.33 Consolidation settlements of the electro-levels at Scheme 8.



a) 1 to 7m

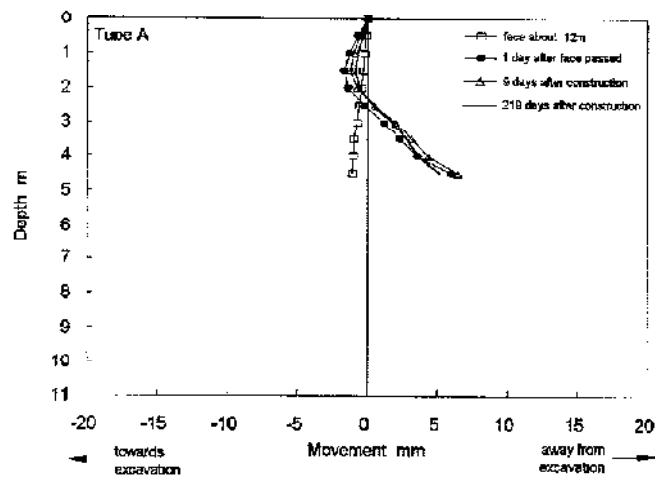


b) 8 to 10m

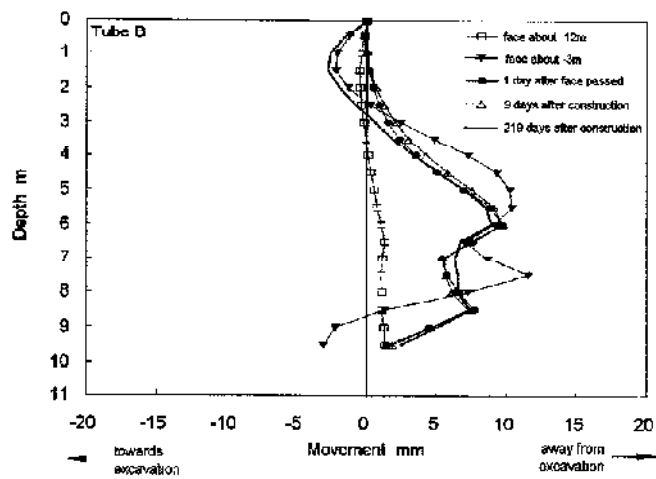
**Figure 7.34** Plot of consolidation settlement against logarithm of time at Scheme 8.

### 7.3 3.4 Scheme 9

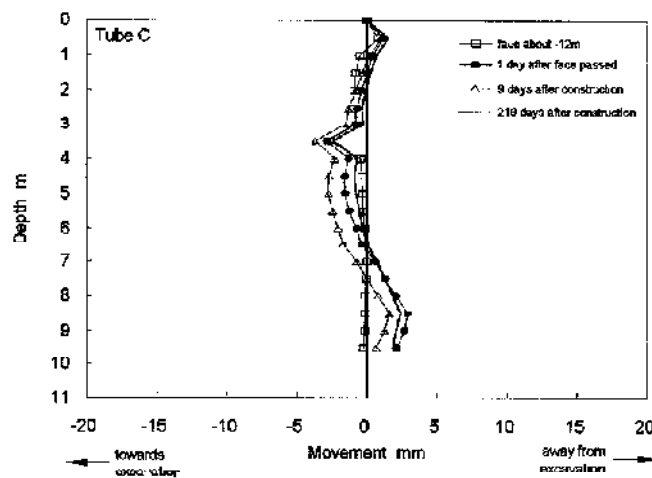
The largest measured subsurface movements occurred at Scheme 9 and are an order of magnitude greater than those measured at Schemes 6 to 8. Access tube profiles are shown in Figures 7.35 and 7.36. In the longitudinal direction a maximum displacement of 12mm was measured 1.5m from the tunnel centre line, Tube B, at about the level of the crown above the tunnel centre line, Tube A, movements of 7mm were measured in the direction of the drive.



a) Tube A

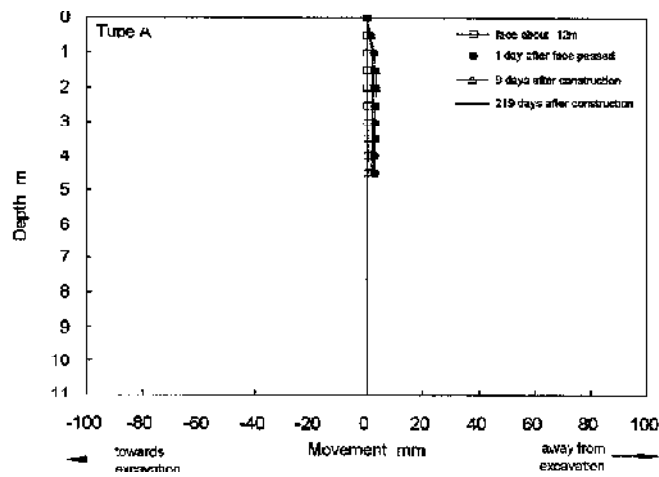


b) Tube B

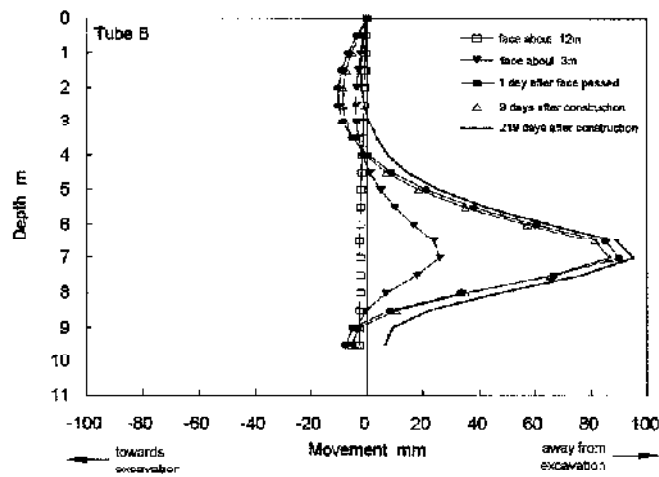


c) Tube C

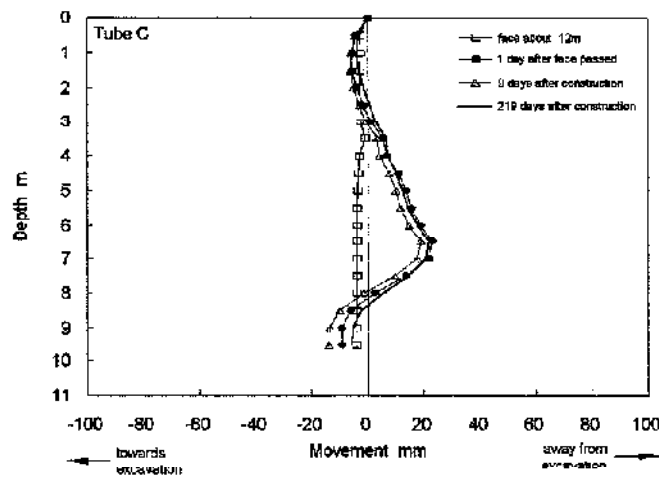
Figure 7.35 Longitudinal inclinometer access tube profiles on Scheme 9.



a) Tube A



b) Tube B



c) Tube C

Figure 7.36 Transverse inclinometer access tube profiles on Scheme 9.

In the transverse direction, large horizontal displacements in a perpendicular direction away from the excavation were observed close to the level of the tunnel axis, Figures 7.36 and 7.37. Above the tunnel centre line in Tube A only small transverse displacements, 2 to 3mm, were measured. A significant displacement of 25mm was measured at Tube B with the face about 3m from the instrumentation. After the face had passed the maximum displacement increased to 86mm just above the axis level. At Tube C, 3.5m from the tunnel centre line, a maximum displacement of 22mm was observed.

De Moor and Taylor (1989) measured movements due to a 2.1m diameter pipe jacked tunnel in similar ground at nearby Tilbury. Profiles of the largest transverse tube deformations at various distances from the tunnel centre line are presented in Figure 7.38. Displacements at Tilbury are similar in shape, direction and magnitude to Scheme 9 measurements: the maximum displacement of 107mm was observed at about 2m from centre line and was just above the level of the tunnel crown. Figure 7.39 shows measurements of horizontal movements at the level of the tunnel axis from the two different soft clay sites. Measurements are reasonably consistent and are in general agreement with the linear plot

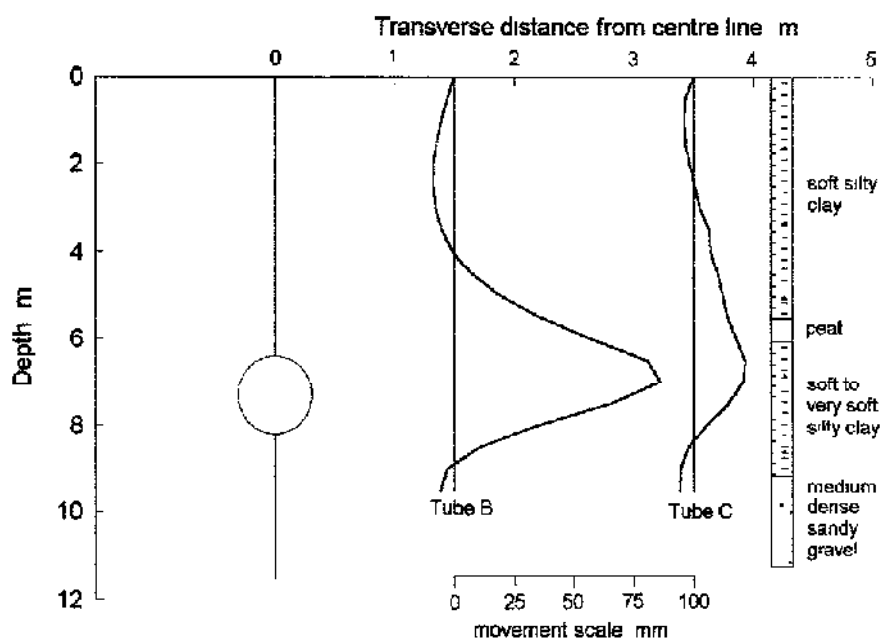


Figure 7.37 Maximum transverse access tube deformation at Scheme 9.

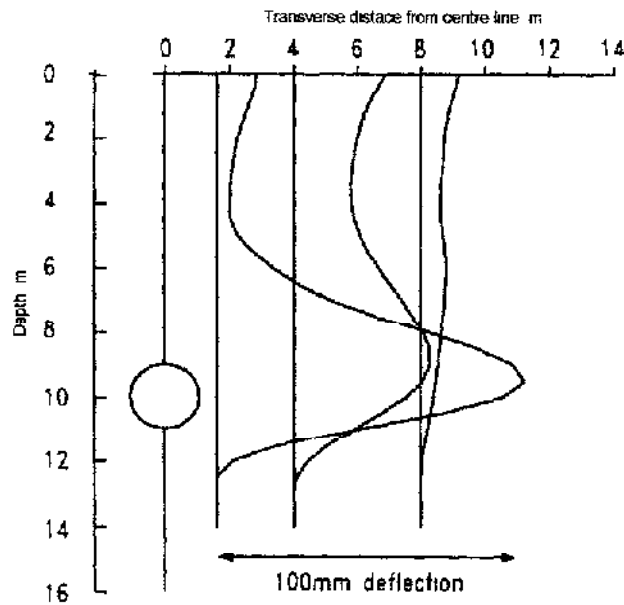


Figure 7.38 Maximum transverse access tube deformation at Tilbury (after De Moor and Taylor, 1989).

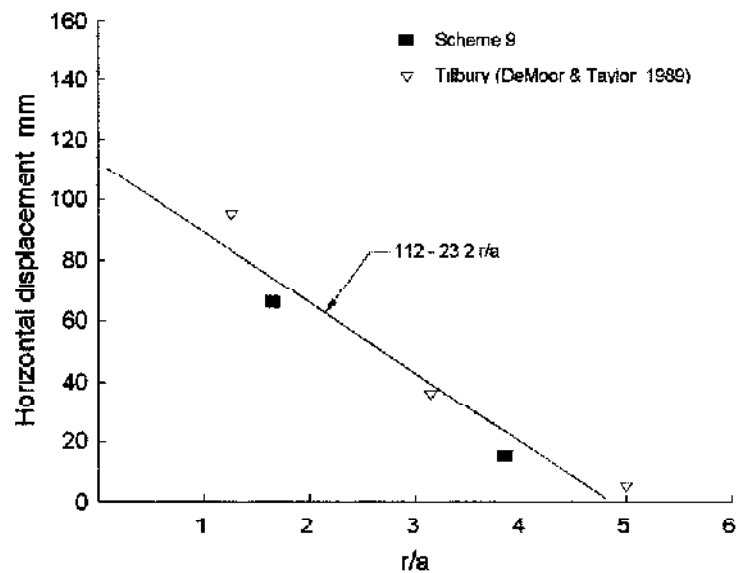


Figure 7.39 Horizontal subsurface displacement at tunnel axis level in the vicinity of pipe jacked tunnels in very soft clay.



As the tunnel advanced very large pore pressures were measured, reflecting high pressures generated at the face by the advancing slurry machine. As a result of this most of the subsurface displacements are significant and in a direction away from the excavation. It is not yet fully understood why the large subsurface movements did not translate to greater surface movements. With hindsight, it would have been preferable to have increased surface settlement instrumentation at a more accessible location and to have increased the frequency of readings. Installation of the electro-levels at this scheme, as had been originally planned, would have produced some very useful measurements and assisted in understanding the very large subsurface displacements.

Although magnetic settlement plates were installed around the access tubes, due to 24hr shift working measurements were made by three individuals, each using a slightly different datum. It has proved difficult to interpret the inconsistent sets of measurements and displacement vectors can not therefore be considered here.

#### 7.4 CONCLUSIONS

The principal conclusions are:

- i Surface settlements are consistent with expected profiles but measurements are somewhat smaller than predicted because ground losses appear to have been less than the full overbreak volume
- ii Subsurface movements in London clay were found to be in good agreement with the pattern of behaviour for deeper and larger tunnels.
- iii. Subsurface displacements were very small at Schemes 6, 7 and 8 and barely detectable using magnetic settlement plates
- iv. Electro-levels have been used very successfully to obtain very accurate measurements of a developing subsurface longitudinal profile
- v The slurry machine tunnelling method used in the soft clay at Scheme 9 has generated large forces at the tunnel face resulting in very large subsurface displacements that could potentially have been damaging to nearby services had any been sufficiently close to the tunnel

## **chapter eight**

### **conclusions and recommendations**

#### **8.1 FIELDWORK**

The site-based research was very difficult to organise and undertake successfully within the contract period due to few suitable sites being available for the fieldwork. The search for sites within the areas of each participating water company was unsuccessful. In practice, the main variables in choosing sites were start dates and ground type, length and depth of drives and to some extent, pipe size, were in the end immaterial. It was very unfortunate that delays at the fifth site earmarked for Stage 3 monitoring (in gravel and chalk), resulted in the intended work there being abandoned. Bentonite lubricant was used in varying degrees on the four sites chosen and the effectiveness (discussed in Section 8.3) varied greatly.

Sophisticated jacking rigs, with integral thrust rings, on two of the four monitored schemes precluded the use of heavy-duty load cells on the jack rams. Only by measuring hydraulic oil pressures at the rams and calibrating these pressures against load cell output were jacking loads determined at Schemes 7 and 8. Ideally, jacking forces should be measured using load cells on rams but during the course of this and the previous fieldwork, contractors indicated that the large cells were a hindrance to their normal operations. Any future work involving measuring jacking forces should, in addition to jack load cells, also consider alternative methods of measurement.

It proved satisfactory to record the position of the instrumented pipe using a linear displacement unit measuring forward movement of the pipe in the jacking pit. Using this system the author was able to predict the location of the instrumented pipe to within about  $\pm 150\text{mm}$ . However, it is recommended for any future work that the stainless steel wire (factory-fitted in the instruments) is replaced with heavy duty nylon fishing line, which is more robust and less prone to kinking. A second standby instrument would be advantageous as the jacking pit was found to be the harshest environment on site and any instrumentation placed there was prone to damage from many sources.

Gluing the contact stress cells into high tolerance holes (cast or bored) in the pipe wall should remain the preferred method so that the instrument is as far as possible an integral part of an otherwise standard jacking pipe. The method of retrieving the cells by overcoring from within the instrumented pipe was a straightforward operation at three of the four sites. Only at the Scheme 7 pipe jack, in sand below the water table, was the instrumented pipe (1000mm internal diameter) pushed through and raised to the surface for de-commissioning and instrument retrieval.

A two-second sampling rate for logging the pipe jacking data, though advantageous for capturing valuable information at the start of pushes, produced an amount of data too great for one researcher to deal with. The decision of the author to collect data at the two-second rate was with hindsight an error and contributed greatly to the late completion of this thesis. In future fieldwork the research team should adopt sampling rates quick enough to capture spikes at the start of pushes but should be careful not to generate excessive quantities of data that might never be analysed due to time constraints. A major problem faced by the author was the relatively low specification of personal computers available during the research period. Subsequent advances in personal computers and sophisticated multi-tasking software should now allow large amounts of raw data to be processed and converted to engineering units immediately and at source – although raw data should still be logged and also kept as a permanent record. The immediate conversion of raw data would cut down considerably on laboratory-based computing time.

The electro-levels at Scheme 8 provided large quantities of high quality ground movement data. It was intended that the instruments would be similarly used in the soft clay of Scheme 9 but regrettably a lack of clear communication between research staff and the Contractor's Agent, regarding installation requirements, prevented their further use. This situation could have been avoided by supplying the Agent with clear written instructions, including drawings, outlining the exact requirements.

Monitoring pipe jacking operations, taking readings from ground instrumentation and surveying surface settlement stations often proved too much work for one researcher and assistant. Future site-based work where jacking procedures and

ground response are monitored should include two or three people, in addition to the main researcher (primarily responsible for recording pipe jacking operations) to read the ground instrumentation and to survey settlement stations. In this way a greater number of ground response readings would be possible as the tunnel approaches and passes ground instruments.

## **8.2 JACKING LOADS**

### **8.2.1 Face loads**

The intercept of the line of average increase in jacking load at zero length has been assumed to represent the penetration force or 'face load'. In the stable bores in stiff cohesive soils at Schemes 1, 3 and 8 the penetration forces of 120-335kN are relatively small and are primarily due to friction on the shield and to a lesser extent, the inevitable trimming of some areas of the excavation. In the hand drive at Scheme 6, a generous overbreak was excavated by the miner resulting in zero face load. When a shield is used to substantially trim an excavation, the cutting edge resistance will cause significant increases in the total penetration force. At Scheme 4 the penetration resistance was very small when the miner excavated an overbreak but when the shield was used to trim the excavation, the resistance increased markedly by almost 800kN. At Scheme 2 the shield was also used to trim the excavation and resulted in a large face load of 950kN. In slurry support operations large penetration forces, comprising slurry support pressure and shield trimming resistance, may occur. In the machine-driven Schemes 5, 7 and 9 measured face loads varied between 600-1200kN.

This work has shown that zero face loads can be achieved in hand-driven pipe jacks where an overbreak is excavated. However, a generous overbreak may result in relatively large ground movements which may be less desirable than a large face load component of total jacking forces.

### **8.2.2 Lubrication**

The influence of lubrication on the pipe jacks monitored during Stage 3 was investigated by keeping a detailed log of lubricating procedures including start and finish times of lubricant pumping, approximate volumes pumped and the location of injection points in the pipeline. The fieldwork regrettably did not include a more

comprehensive study that with hindsight would have included: brand of bentonite, exact volumes pumped, pumping pressures and consistency of the slurry. The research into lubrication effects could have been improved with this additional information.

Bentonite slurry was used as the lubricant at all Stage 3 schemes and also at Scheme 5; polymer additives were used in the bentonite slurry at Scheme 4. The lubricating operations affected jacking resistances in a number of ways and measured reductions in resistance fall in the range 44 – 90%.

The partial lubrication used at Scheme 6 appeared to be ineffective in that the injection of slurry had no discernible effect in reducing jacking resistance. Only small volumes of slurry were pumped into a stable bore with a generous overbreak void, and the only injection sockets were located in the top and sides of the shield. Consequently, little of the unevenly distributed slurry had the desired effect of reducing friction between bottom of the pipe and tunnel invert. Had greater amounts of the aqueous slurry been pumped, swelling of the highly plastic clay soil might have been accelerated and caused the ground to close onto the pipeline leading to a higher jacking resistance. The stable bore at Scheme 4 is reported as also being partially lubricated. Here bentonite slurry with polymer additives was introduced towards the end of the drive and though it did not completely fill the overbreak void, it was very effective in producing a 59% reduction in frictional resistance.

Schemes 5 and 7, in granular soils below the water table, were fully lubricated by filling the overbreak void with bentonite slurry and pressurising it to overcome groundwater pressure, form a filter cake, and support the tunnel bore. In Scheme 5 the introduction of full bentonite support and lubrication was very effective in reducing frictional resistance from 100kN/m to 10kN/m – a 90% reduction. At Scheme 7, although classified as being fully lubricated, the situation is more complex because the lubricating system, in use from the start, was only fully operational at the beginning and end of the drive, and consequently periods of full lubrication were interspersed with sections of little lubrication. However, as in Scheme 5, there was a factor of ten or more between fully lubricated and partially lubricated resistances.

In the cohesive soils at Schemes 8 and 9 initial unlubricated lengths were followed by the introduction of full lubrication. In the stiff glacial clay at Scheme 8,

the tunnel bore was stable and during the unlubricated section, pipes slid along the base of the bore and the jacking resistance was relatively high. Introducing sufficient bentonite slurry to fill the overbreak void resulted in pipe buoyancy and a 69% reduction in resistance. Maintaining full lubrication effected a low frictional resistance for the remainder of the drive.

At Scheme 9, in very soft alluvial clay, the reduction from unlubricated to average lubricated resistance was 44%. It appears in this case of an unstable bore that the lubricant was able to displace soil, or natural clay slurry, in contact with unlubricated pipeline and become equally effective over both the unlubricated length and newly excavated bore.

This work has shown that in unstable ground, in particular cohesionless soils below the water table, it is preferable to start lubrication and ground support as soon as possible after the start of the drive, since it may not subsequently be possible to reduce the jacking resistance developed where the ground has collapsed. It has also been demonstrated that in stable ground, or in soft clay, the introduction of lubricant may be delayed until limiting jacking loads are approached, since it will be effective over the full length of pipeline soon after it is introduced.

### **8.2.3 Misalignment**

The absolute effect of misalignments on total jacking loads was not clear in the jacking records from the monitored schemes due to other influencing factors. To measure the effect, it would be necessary to compare jacking forces from pipe jacks in identical conditions, one driven perfectly straight and one purposely misaligned. This would only be feasible in a full-scale test bed operation, or at model scale in the laboratory. Misalignment effects have therefore been examined in this research programme through contact stresses between pipe and ground.

### **8.2.4 Stoppages**

A very important factor in highly plastic soils is the increase in jacking load following stoppages. The jacking records for Schemes 3 and 6 demonstrate the marked increase in forces associated with delays in London clay, where the force required to restart the jack can vary, depending on the length of delay, between 10-

55% greater than that required to sustain motion. Increases are detectable after delays of only a few minutes but the largest increases occur following stoppages of hours. It is recommended that designers use a 'stoppage factor' of 1.6 on calculated frictional resistances in London clay to allow for stoppage effects. During pipe jacks, increase in the jacking load due to a delay,  $t$  (hours), can be reasonably predicted using:

$$\delta P/P = 0.26 + 0.049 \ln(t).$$

It is suggested that after long delays in highly plastic clays, pressurising a non-aqueous lubricant filling the overbreak void before pushing may prevent large restart forces.

Increases in jacking load were also observed in the low plasticity clay of Scheme 1 but the magnitudes were much smaller than those observed in London clay. The maximum increase of 35% followed a weekend break. In the glacial clay at Scheme 8, large jacking loads following each weekend break were probably caused by the pipeline settling onto the tunnel invert over the weekend as some of the lubricating fluid dissipated into sand layers. These large restart forces may have been avoided by recharging the slurry before jacking. At Scheme 9, the one notable restart load also followed a weekend break but here was due to the ground closing onto the pipeline over the two-day period.

This thesis has shown that stoppage effects in unlubricated and partially lubricated pipe jacks through high plasticity clays can result in very large increases in jacking loads, fully lubricated behaviour in these soils requires further investigation. In stiff, low plasticity clays there may be jacking load increases due to stoppages and until the database for these clays is widened, a conservative 'stoppage factor' of 1.4 on calculated frictional resistances is recommended. In pipe jacks through soft clay and cohesionless soils there should be no noticeable increase in restart forces.

### **8.3 PIPE-SOIL INTERACTION**

#### **8.3.1 Pipe-soil contact**

The contact stress cells built into the wall of the instrumented pipes have provided valuable information on: the measure of interface friction between concrete

pipes and different ground types, interface stress variation during stoppages; the variation of stresses along pipes due to pipeline misalignment; and buoyancy and other lubrication effects. The quality of the effective radial stress measurements at Scheme 6 could have been improved had the author decided to use Druck pore pressure transducers in all the contact stress cells. The decision to use on a trial basis, a different type of transducer was a mistake. It is recommended that the reliable and stable Druck PDCR81 transducers are used for any similar fieldwork.

In the London clay at Scheme 6, the contact stress cells recorded data generally only along the pipe bottom indicating simple sliding along the base of an open bore, while at Scheme 9 in soft clay the contact stresses were almost equal all around the pipe. In the fully lubricated drives at Schemes 7 and 8 the bentonite slurry heavily influenced interface stresses.

The apparent frictional behaviour, in terms of total stresses, observed at the Stage 2 schemes through cohesive soils was not evident at Scheme 6. The lower range of stresses measured during the latter scheme appears to fall into two groups with non-linear shear-radial relations with limiting values of 15 and 40kPa respectively. This curvi-linear behaviour is more typical of London clay than is a purely frictional relationship. The limiting values are much lower than the undrained strength of the intact clay, of about 120kPa, giving ratios of undrained adhesion to undrained soil strength of 0.13 and 0.38. This probably represents the remoulded and softened shear zone in the tunnel bore.

Relations between shear and radial stresses during jacking through the cohesionless soil of Scheme 7, where substantial contact between pipe and soil occurred, have unsurprisingly shown the relationship to be frictional. As at Scheme 4, the relationship appears to be stress level dependent at stresses greater than 100kPa. At Scheme 7, the skin friction angle,  $\delta'$ , was  $37.5^\circ$  for substantial pipe-soil contact, comparing favourably with  $\delta'$  of  $38^\circ$  at Scheme 4. Partial lubrication generally had the effect of reducing the friction angle to about  $15^\circ$ , full lubrication resulted in friction angles close to zero.

On Scheme 9, relatively uniform shear stresses of 5-10kPa were measured all around the pipe, indicating undrained adhesive behaviour. There appeared to be little difference in behaviour in interface stress measurements from before and after



lubrication. It is suggested that the overbreak annulus remained open in the unlubricated length and filled with a natural clay slurry that was displaced by the bentonite slurry after lubrication.

This thesis has shown that contact between pipe and soil is essentially frictional in nature in cohesionless soils and stiff clays. It has also demonstrated that contact tends to be adhesive in softer clays and at higher stresses in stiff clays.

### 8.3.2 Stoppages

The delays between pushes in the London clay sites of Schemes 3 and 6 have been shown to result in significant increases in restart jacking loads. Only the interface stress measurements from Scheme 6, at the tunnel invert, have been available for detailed analysis relating to this phenomenon. It was unfortunate that at the time of monitoring only one of the three stress cells in the bottom of the pipe had been fully modified with a reliable pore pressure transducer. Readings from the two modified cells were generally dissimilar and also the repeatability of pore pressure measurements during stoppages was poor. There is therefore some doubt over the validity of pore pressures and effective radial stresses used in the analysis. Assuming that the pore pressure measurements presented for Scheme 6 are not erroneous, then the mechanism causing this stoppage effect is highly complex. Total stress measurements are repeatable and the data show stresses decreasing during the rest periods. Pore pressure data during the shorter delays show decreasing pressures (or increasing in a negative sense) causing suction, but during the longer breaks, overnight or weekends, pressures dissipate as groundwater drains towards the remoulded and softened shear zone. The resulting effective stresses during the short breaks generally increase and result in the increased restart force.

At Scheme 8 it was not possible to investigate the geotechnical aspects of any stoppage mechanism in stiff glacial clay because the instrumented pipe was inserted into a fully lubricated bore. The change in contact stresses around the Scheme 8 pipe showed that a redistribution of lubricant pressure and loss of buoyancy caused the increased jacking loads required to restart the drive after weekends. In the soft clay at Scheme 9 almost continuous progress resulted in few stoppages. A significant exception was the only weekend break that resulted in a large restart load.

Examination of the change in interface stresses during the weekend indicated the ground closing onto the pipeline

The understanding of geotechnical aspects of the stoppage mechanism in high plasticity clay could have been improved had a greater number of contact stress cells been placed in the bottom of the instrumented pipe at Scheme 6. The author should have anticipated a situation of pipes sliding along the base of an open bore at this particular scheme and should have designed a more appropriate distribution of cells. Placing one or two more cells in the pipe bottom, and offsetting them from the axis, would also have provided valuable information on the area of contact.

### **8.3.3 Misalignment**

The increased number of contact stress cells in this reported phase of fieldwork has allowed detailed observations on the complex variation of interface stresses along pipes travelling through misaligned bores. The tunnel at Scheme 7 was almost perfectly straight but at Schemes 6, 8 and 9 there were some significant deviations from line and/or level. The stress measurements have demonstrated that in pipe jacks deviating from line by typical amounts, contact between pipe and ground is made on the inside of bends: the misaligned pipelines appear to act as prestressed segmental beams spanning between points of maximum curvature. This information should allow the development or refinement of simple theoretical models for calculating the increase in jacking resistance due to misalignments.

### **8.3.4 Lubrication**

Interface stress measurements from this reported work have demonstrated beyond doubt that jacking pipes will become buoyant in full lubrication conditions. At Schemes 7 and 8, contact stress cells along the top of the pipes showed significant effective radial and shear stresses whereas cells in the bottom generally measured fluid pressure from the slurry and very low shear stresses, about the shear strength of the lubricating fluid. Contact stresses have also demonstrated the importance of arranging injection sockets to evenly distribute lubricant. At Scheme 7 the result of placing injection sockets along only the right side of pipes closest to the instrumented pipe, resulted in increased effective radial and shear stresses as the pipe was forced

against the left side of the tunnel bore. In contrast, the contact stresses measured around the instrumented pipe at Scheme 8 were relatively low all around the pipe because the arrangement of injection sockets ensured a more even distribution of slurry. If properly implemented, full lubrication can result in reducing the average shear resistance around a pipeline to about 5kPa

## **8.4 GROUND RESPONSE**

### **8.4.1 Ground movements**

Ground movements induced by the pipe jacking tunnelling technique have often been quoted as being negligible. Measurements at the reported schemes have generally shown very small movements in stiff clays and cohesionless soils. Using O'Reilly and New's (1982) model and the assumption that ground volume loss is only provided by closure of the overbreak annulus, surface settlements above pipe jacks can now be predicted with reasonable accuracy. It is recommended that in predicting surface settlements due to pipe jacking, equation (7.8) should be used for ground loss in place of a percentage face loss that may underestimate settlements.

The use of bentonite lubricants in overbreak voids appears to have prevented full overbreak closure in the short-term. On Scheme 6 and 8 longer-term measurements were taken but uncertainty in the size of the overbreak at the former scheme has led to inaccuracies in predicting settlement troughs. At the latter scheme the volume of the settlement trough is consistent with the full closure of the overbreak annulus.

Transverse subsurface movement at Schemes 6, 7 and 8 did not exceed 5mm. Subsurface movements in the London clay site (Scheme 6) though small were found to be in good agreement with the pattern of behaviour for larger and deeper tunnels. The large movements at tunnel axis level in the soft clay at Scheme 9, almost 90mm, were a result of large forces generated by the slurry machine. The longitudinal settlement profile measured by the electro-levels at Scheme 8 is consistent with closure of the overbreak annulus between cutterhead and shield. Development of the longitudinal profile with progress of the shield largely follows four phases of ground displacement: initial displacement, shield passing displacement, tail void

displacement and consolidation settlement. The largest settlements occurred immediately above the shield during the second phase.

#### 8.4.2 Ground stresses

The push-in pressure cells at Scheme 6 showed small increases in horizontal stresses as the shield approached, probably due to soil arching ahead of the tunnel excavation. As the shield passed, an immediate reduction in stress of 60kPa was measured. Stresses reduced further with time to approximately half the pre-tunnelling values at the final set of readings. The final reduction in stress was about 30% greater than that predicted by elastic analysis of stresses around an open bore and was probably due to local plastic yielding around the tunnel bore.

As the tunnel advanced through the soft clay at Scheme 9, the push-in pressure cells recorded large increases in pore pressures reflecting high pressures generated at the tunnel face. Driving records, requested from the contractor, including face support pressures (recorded by sensors in the shield) should allow a comparison between face loads and the measured lateral earth pressures.

### 8.5 FURTHER WORK

1. Craig's State-of-the-Art review (1983) should now be updated to include recent research and the wider database of jacking resistances now available.
2. Though bentonite lubricants have been used on several of the monitored schemes, their use and procedures was left entirely to the contractor's normal operation - brands, consistency, exact volume pumped and injection pressures were not noted or measured. A further fieldwork research stage should include instrumentation to monitor injection pressures at the pump and at injection points, suspension consistency and volumes of injected material. The use of non-aqueous lubricants on pipe jacks in heavily overconsolidated, highly plastic clays should be investigated. In particular the effect of pressuring the fluid prior to restarting the jack after long delays should be examined.
3. A detailed laboratory-based exercise should be undertaken to investigate the stoppage effect mechanism in low and high plasticity clays.

- 4 The direct effect of a misaligned bore on total jacking loads could be investigated further in pipe jacks through a full-scale test bed site, or at model scale in the laboratory, where lubrication and stoppage effects can be minimised or prevented completely. Jacking loads from a well-controlled 'straight' drive should be compared to those from a deliberately misaligned drive
5. In stiff clays, where the bore is stable and simple sliding along the tunnel invert is anticipated, contact areas along the pipe bottom should be investigated by offsetting one or more contact stress cells from the pipe axis
- 6 Interface stresses should be measured at a minimum of two locations within the pipe string – separated by a significant distance – to record changes in stress due to repeated shearing and stoppage cycles.
- 7 Long-term ground movement data around pipe jacks are few, further field monitoring should be carried out.
8. Electro-levels should be used again to measure ground movements, particularly in soft clays. Continuous measurements would provide detailed information on how ground movements develop ahead of an advancing tunnel in very soft ground

## 8.6 CONCLUDING REMARKS

This second phase of the site-based research was accomplished within the budget and was a very successful example of co-operation between industrial clients, contractors, academia and government. This is mainly due to the considerable management effort of the Pipe Jacking Research Management Group.

The work was successful in fully instrumenting a further four pipe jacks. Many data were collected, particularly interface stress measurements, and further analysis will continue for some time to come.

Information obtained from the reported work should allow the author and others to further develop and refine simple theoretical models for estimating likely jacking forces in different grounds. These models will be of great value to the specialised industry of pipe jacking and microtunnelling.

---

## references

---

Atkin, R., (1993) *Resewering Cambridge by Pipe Jacking*. Proc 2<sup>nd</sup> Int Conf on Pipe Jacking and Microtunnelling, London.

Atkinson, J.H. and Mair, R.J., (1981). *Soil mechanics aspects of soft ground tunnelling*. Ground Engineering, Vol. 14, No 5.

Attewell, P.B. and Woodman, J.P., (1982) *Predicting the dynamics of ground settlement and its derivatives caused by tunnelling in soil*. Ground Engineering, Vol 15, No 8, pp 13-36.

Attewell, P.B., Yeates, J, and Selby, A.R., (1986). *Soil Movements Induced by Tunnelling and their Effects on Pipelines and Structures* Blackie, Glasgow.

Auld, F.A., (1986). *Determination of pipe jacking loads*. Conference Proceedings. Pipe jacking Association, Manchester.

Bennett, D., Cording, E.J. and Isley, T., (1994) *Auger and slurry microtunnelling tests under controlled ground conditions*. Transportation Research Record 1431, TRB, National Research Council, Washington DC, pp. 75-82.

Bennett, D. and Taylor, P.A., (1993). *Construction of microtunnelling test facility at WES and preliminary test results* Proc. Advanced Technical Seminar: Trenchless Pipeline Rehabilitation, Horizontal Directional Drilling and Microtunnelling, Vicksburg, USA, pp 289-327

Bishop, A.W., Webb, D.L. and Lewin P.I., (1965) *Undisturbed samples of London clay from the Ashford Common shaft Strength-effective strength relationships*. Géotechnique Vol. 14, No 1, pp. 1-31

Bond, A.J. and Jardine, R J , (1989) *Instruments for measuring the effective stresses acting on a pile jacked into overconsolidated clay*. Conf. on Instrumentation in Geotechnical Engineering. ICE Nottingham Univ., April 3-5.

Chapman, D N , (1993). *Ground movements associated with trenchless pipelaying operations*. PhD Thesis, Loughborough University of Technology.

Chapman, D.N., (1996). *Ground movements associated with pipejacking operations*. Proc. Int Symp on Geotechnical Aspects of Underground Construction in Soft Ground, London, pp 665-670.

CIRIA Technical Note 112: see Craig (1983)

Clarkson, T.E. and Thompson, J.C., (1983) *Pipe Jacking State-of-the-Art in UK and Europe*. Journal of Transport Engineering Division, ASCE, Vol. 109(1)

Coller, P., Staheli, K., Bennett, D. and Post, R , (1996). *A review of jacking forces by both theoretical and empirical methods as compared with 20 years of practical experience*. Proc Int. No-Dig '96. New Orleans, pp 125-149.

Cooke, R.W and Price, G., (1973). *Horizontal inclinometers for the measurement of vertical displacement in the soil around experimental foundations*. Proc. BGS Symp on Field Instrumentation.

Cowan, S., (1993). *Ground movements associated with pipe jacking beneath an airport runway* Proc. 2<sup>nd</sup> Int. Conf. Pipe Jacking & Microtunnelling, London, Oct. 1993

Craig, R.N , (1983). *Pipe Jacking, a State-of-the-Art Review*. CIRIA Technical Note 112

Davies, E.H., Gunn, M.J., Mair, R.J. and Seneviratne, H.N., (1980). *The stability of shallow tunnels in underground openings in cohesive material* Géotechnique, Vol. 30, No. 4, pp 397-416.

De Moor, E.K. and Taylor, R.N., (1989). *Field studies of a shallow tunnel in very soft ground at Tilbury* Geotechnical Engineering Research Centre Report GE\89\22, City University, London

De Moor, E.K. and Taylor, R.N., (1991). *Ground response to construction of a sewer tunnel in very soft ground*. Proc 6<sup>th</sup> Int. Symp Tunnelling '91, Inst. Mining and Metallurgy, London, April 1991, pp. 43-54.

Dunnichiff, J., (1988) *Geotechnical instrumentation for monitoring field performance*. John Wiley & Sons Inc.

Dyer, M.R., Hutchinson, M.T. and Evans, N., (1996) *Sudden Valley Sewer A case history* Proc. Int. Symp on Geotechnical Aspects of Underground Construction in Soft Ground, London, pp. 671-676.

Hannah, T.H., (1985). *Field instrumentation in geotechnical engineering*. Trans Tech Publication

Haslem, R.F., (1983). *Ground resistance forces during tunnelling by pipe jacking* Internal paper, Dept. of Building and Civil Engineering, Liverpool Polytechnic.

Haslem, R.F., (1986). *Pipe jacking forces from theory to practice*. Proc. Infrastructure, Renovation and Waste Control Centenary Conference NorthWest Association, Instn. Civ. Engrs., London

Haslem, R.F., (1996). *Structural interaction at joints in pipe-jacked tunnels*. The Structural Engineer Vol 74, No 10, pp. 165-171



Holt, C C., Milligan, G W.E and Burd, H.J., (1997). *Prototype testing of improved microtunnelling pipes* OUEL Report No. 2151/97, University of Oxford.

Ishibashi, N., (1988) *Japan's recent small diameter pipe jacking construction methods* Proc. Int No-Dig '88, Washington DC, USA.

Kanari, H., Nagata, N , Kawaguchi, N and Shiomi, M., (1996). *Effect of stress absorbers on pipe splitting during jacking in curves*. Proc. Int. No-Dig '96. New Orleans, pp 278-289.

Kastner, R , Pellet, A-L., Ouvry, J-F. and Guilloux, A., (1996). *In-situ monitoring of microtunnelling*. Proc Int. No-Dig '96. New Orleans, pp 170-182.

Lake, L M., Rankin, W J., and Hawley, J , (1992) *Prediction and effects of ground movements caused by tunnelling in soft ground beneath urban areas* CIRIA Research Project 316, 1992

Loving, N W., (1938). *Concrete pipe in American sewerage practice*. Bulletin 17, American Concrete Pipe Association

Mair, R.J. and Taylor, R.N (1993) *Prediction of clay behaviour around tunnels using plasticity solutions* Predictive Soil Mechanics, Thomas Telford, London, pp. 449-463.

Mair, R.J., Taylor, R.N. and Bracegirdle, A (1993). *Subsurface settlement profiles above tunnels in clays* Géotechnique 43, No 2, pp. 315-320.

Marks (1987). *Standard handbook for mechanical engineers*. 9<sup>th</sup> Edition. Editor Avallone, E.A & Baumeister, T Mc Graw-Hill. pp. 5-44 & 45

Milligan, G.W E and Norris, P., (1994). *Pipe Jacking Research Results and Recommendations*. PJA, London, UK.

Milligan, G W E and Norris, P , (1998) *Pipe-soil interaction during pipe jacking*. Accepted for publication, Proc. Instn Civ. Engrs , Geotech. Engng , London

Milligan, G W.E and Ripley, K J , (1989). *Packing Materials in Jacked Pipe Joints*. Proc Int. No-Dig '89, London

Norris, P., (1992a) *Instrument design, manufacture and calibration for use in monitoring the field performance of jacked concrete pipes*. Report No OUEL 1919/92, Department of Engineering Science, Univ. of Oxford

Norris, P., (1992b). *The behaviour of jacked concrete pipes during site installation*. D.Phil Thesis, Univ. of Oxford

Norris, P and Milligan, G.W.E., (1991). *Field instrumentation for monitoring the performance of jacked concrete pipes*. FMGM 91, Proc 3<sup>rd</sup> Int. Symp. on Field Measurements in Geomechanics, Oslo

Norris, P. and Milligan, G.W E., (1992a). *Pipe end load transfer mechanisms during pipe jacking*. Proc. Int. Conf on Trenchless Construction, No-Dig 92, Washington

Norris, P. and Milligan, G W E., (1992b) *Frictional resistance of jacked concrete pipes at full scale*. Proc. Int. Conf. on Trenchless Construction, No-Dig 92, Paris.

O'Reilly, M.P. and Rogers, C.D F., (1987). *Pipe jacking forces* Proc Int. Conf on Foundations and Tunnels, Vol 2. Ed. M.C.Forde Edinburgh Engineering Technical Press.

O'Reilly, M.P. and New, B.M., (1982) *Settlements above tunnels in the United Kingdom - their magnitude and prediction*. Tunnelling '82, pp 173-187, London: IMM

Peck, R B , (1969) *Deep excavations and tunnelling in soft ground* Proc , 7th Int Conf Soil Mech , Mexico City, State of the art 3 pp 225-290.

Pipe Jacking Association, (1995a) *An introduction to pipe jacking and microtunnelling design*. PJA, London, UK.

Pipe Jacking Association, (1995b). *Guide to best practice for the installation of pipe jacks and microtunnels* PJA, London, UK.

Poulos, H.G. and Davies, E.H., (1991) *Elastic solutions for soil and rock mechanics*. Wiley, New York.

Price, G , and Wardle, I.F , (1983). *Recent developments in pipe/soil instrumentation systems*. Proc. of Field Measurements in Geomechanics, Zurich

Price, G., and Wardle, I.F and DeRossi, N., (1996). *Monitoring of tunnels, surrounding ground and adjacent structures*. Proc. Int Symp. on Geotechnical Aspects of Underground Construction in Soft Ground, London, pp. 737-743.

Ripley, K J , (1989). *The performance of jacked pipes*. D.Phil Thesis, Univ of Oxford

Roark, R.J. and Young, W.C., (1976). *Formulas for Stress and Strain* McGraw-Hill, New York

Rogers, C D.F , O'Reilly, M P and Atkin, R., (1989). *Pipe jacking beneath Burnham-on-Sea. a case history* Proc. Int. Conf on Foundations and Tunnels 89, Edinburgh, pp 51-56.

Rogers, C D.F. and Yonan, S.J., (1992) *Experimental Study of a Jacked Pipeline in Sand* Tunnels and Tunnelling, Vol 24, No 6, pp. 35-38.

Ryley, M.D. and Carder D R , (1995). *The performance of push-in spade cells installed in stiff clay* Géotechnique 45, No. 3, pp. 533-539

Shullock, S.H., (1982) *Problems in tunnelling by pipe jacking at Tilehurst*. Journal of the Institution of Water Engineers and Scientists, April, 1982

Stein, D., Mollers, K. and Bielecki, R., (1989). *Microtunnelling*. Ernst-sohn, Berlin, Germany.

Stevens, W.W., (1989) *Ductile Iron Jacking Pipes*. Proc. 4<sup>th</sup> Int Conf. on Trenchless Construction for Utilities, No-Dig 89, London

Taylor, M., (1994). Personal Communication. Assistant Resident Engineer (Scheme 7), North West Water.

Tedd, P., Chard, B.M., Charles, J.A. and Symons, I.F. (1984) *Behaviour of a propped embedded retaining wall in stiff clay at bell Common Tunnel*. Géotechnique, Vol. 34, No. 4, pp 513-532

Terzaghi, K., (1943). *Theoretical soil mechanics* John Wiley and Sons, New York.

Thompson, J.C., (1993) *Pipejacking and Microtunnelling* Chapman & Hall, London

Windle, D and Wroth, C P., (1977). *The use of a self-boring pressuremeter to determine the undrained properties of clays* Ground Engng Sept 1977 10(6), pp 37-46.

Zhou, J.Q., (1998). *Numerical Analysis and Laboratory Testing of Concrete Jacking Pipes*. D.Phil Thesis, University of Oxford.

## APPENDIX A – Australian CPA Analysis

The analysis presented by the Australian CPA is summarised below:

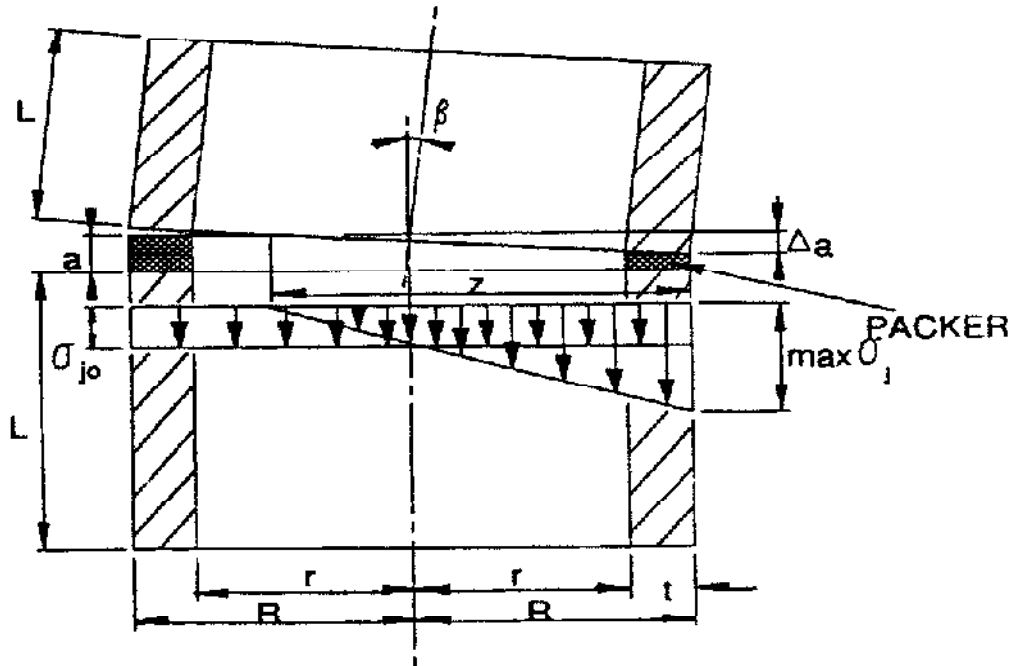


**Figure A.1 Australian Joint Stress Distribution**

Total packer and pipe deformation

$$\sum \Delta a = \Delta a + \Delta L$$

Deformations related to stress

$$\frac{\sigma_j a}{E_j} = \frac{\sigma_j a}{E_p} + \frac{\sigma L}{E_c}$$

but

$$\sigma = \frac{\sigma_j t_j}{t}$$

where  $t$  = wall thickness and  $t_j$  = wall thickness at joint

therefore

$$\frac{a}{E_j} = \frac{a}{E_p} + \frac{t_j L}{t E_c}$$

the corresponding joint elasticity coefficient  $E_j$  is given by

$$E_j = \frac{at E_p E_c}{at E_c + Lt_j E_p}$$

The problem reduces to the stress distribution in an annular cross-section where the tensile stresses are disregarded, Marks (1987)

From the diagram

$$\beta = \tan^{-1} \frac{\Delta a}{z} = \tan^{-1} \frac{a \max \sigma_j}{z E_j}$$

Rearranging

$$\beta = \tan^{-1} \frac{a}{E_j} \frac{\sigma_{j0}}{R} \frac{\max \frac{\sigma_j}{\sigma_{j0}}}{\frac{z}{R}}$$

where  $\frac{z}{R}$  can be found from tables, Marks (loc cit).

**APPENDIX B – Equipment Inventory**

Item Description	Quantity	Replacement cost at 1993 prices (£) (excluding VAT)	Total cost at 1993 prices (£) (excluding VAT)
1. Contact stress cells			
a) Housing	12	1200	14,400
b) Cambridge Transducer	12	1000	12,000
c) Druck PDCR81	10	350	3500
d) Keller 2Mi	2	200	400
2 Pipe Joint Pressure Cells	34	600	20,400
3 Tube Extensometers (including LVDTs)	6	900	5400
4 Pipe Joint Movement Indicators (including LVDTs)	6	400	2400
5 Jack Load Cells (including caps)	4	1800	7200
6 EDM unit	1	1950	<i>Returned at no cost</i>
7 Data logger equipment including purpose built power supply, steel containers and female connectors	10	Average 1350	13,500
8 Computers			
a) 386 Opus	1	1500	1500
b) 486 Opus	1	2300	2300
c) Notebook	1	2500	2500
d) Pentium 166	1	2500	2500
9 Cabling			
a) flexible power	400m	400	400
b) rigid power	100m	200	200
c) signal	500m	300	300
10 Male connectors/power supply plugs & sockets	Item	2500	2500
11 Instrument container	1	3500	3500
12 UPS power backup	1	800	800
		<b>Total</b>	<b>£95,700</b>

**APPENDIX C – Evaluation of joint angular deviation from line and level information.**

Figure C.1 illustrates an angular deviation  $\beta$  at their common joint.

Direction cosines of AB are  $l = \frac{x_2 - x_1}{L}, \quad m = \frac{y_2 - y_1}{L}, \quad n = \frac{z_2 - z_1}{L}$

(i.e.)  $l^2 + m^2 + n^2 = 1$

and direction cosines of BC are:  $l' = \frac{x_3 - x_2}{L}, \quad m' = \frac{y_3 - y_2}{L}, \quad n' = \frac{z_3 - z_2}{L}$

By definition the angular deviation  $\beta$  is given by:

$$\cos\beta = ll' + mm' + nn'$$

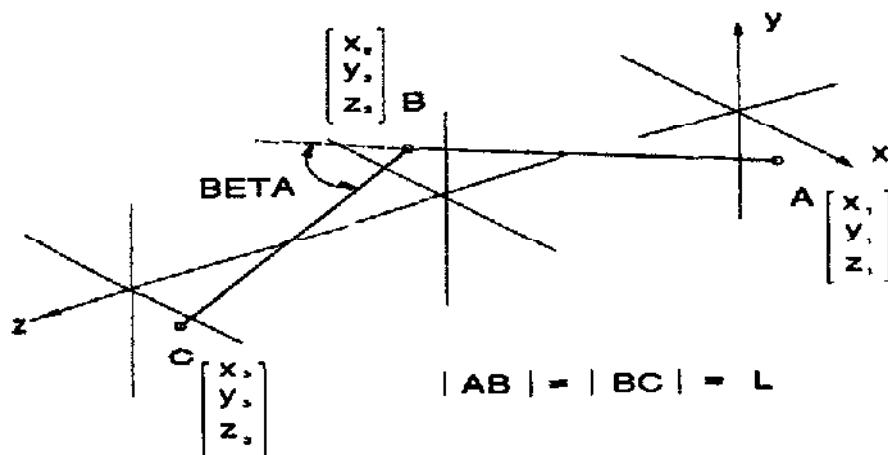


**Figure C.1 Coordinate system for determining  $\beta$  from line and level surveys.**



### APPENDIX D – Derivation of Milligan and Norris (1998) Half-wave Model

The simplified model for forces acting on a half-wave length ( $l$ ) of pipeline are illustrated in Figure D 1

$P_1$  and  $P_2$  are the axial jacking forces,  $N_1$  and  $N_2$  the additional contact forces between pipe and ground,  $W$  the self-weight per unit length,  $D$  the internal diameter of the pipes, and  $\delta$  the interface friction angle. At the points of maximum curvature the axial forces are assumed to act close to the edge of the pipe.

For lateral equilibrium 
$$N_1 = N_2 = N$$

For longitudinal equilibrium 
$$P_2 = P_1 + Wl \cdot \tan \delta + N \cdot \tan \delta$$

For moment equilibrium about point X 
$$P_1 D + Wl \cdot \tan \delta \frac{D}{2} = \frac{Nl}{2} - \frac{N}{2} \tan \delta \cdot D$$

Rearranging 
$$N = \frac{(2P_1 + Wl \cdot \tan \delta)D}{(l - D \cdot \tan \delta)}$$

therefore 
$$P_2 = (P_1 + Wl \cdot \tan \delta) + \frac{D \cdot \tan \delta (2P_1 + Wl \cdot \tan \delta)}{(l - D \tan \delta)}$$

and 
$$P_2 = P_1 \frac{(l + D \cdot \tan \delta)}{(l - D \cdot \tan \delta)} + \frac{Wl^2 \cdot \tan \delta}{(l - D \tan \delta)}$$

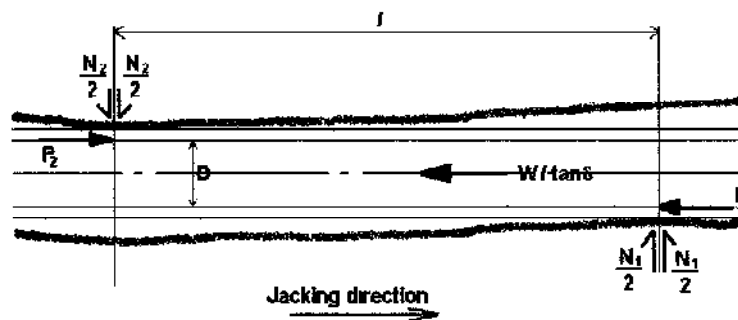


Figure D.1 Theoretical half-wave model for pipe-soil interaction.